SYNTHETIC and SPECTROSCOPIC STUDIES on HETEROMETALLIC CLUSTERS of PLATINUM

LIBRARY
DISPOSED
12 1 87
OXFORD

by

Malcolm Francis Hallam

Thesis submitted in part fulfilment of

the requirements for the degree of

Doctor of Philosophy

at the

University of Oxford

Wolfson College,

Oxford

June 1986

ABSTRACT

This Thesis describes the synthesis and structural characterisation of a range of heterometallic cluster compounds of platinum. **Chapter 1** reviews the current knowledge in this area and gives examples of the kinds of cluster compounds which have been characterised, with some emphasis on their mode of synthesis and their structural and spectroscopic characterisation. The structures of the cluster compounds are rationalised in terms of the triangular Pt_3 unit which dominates the cluster chemistry of platinum. The bonding in the simplest triplatinum cluster compounds is analysed and is used as a basis for understanding the interconversion of platinum cluster compounds and the formation of heterometallic platinum-gold cluster compounds.

Chapter 2 describes the synthesis and characterisation of the homometallic platinum cluster compounds which are convenient precursors for the formation of heterometallic cluster compounds. A general synthetic route to the platinum carbonyl phosphine clusters has been developed and the exchange of bridging CO and SO_2 ligands in this type of cluster was investigated. The synthesis of a new type of anionic 44 electron triplatinum cluster, $[Pt_3(\mu\text{-}SO_2)_2(\mu\text{-}X)(PR_3)_3]^-$, is described.

The syntheses of heterometallic clusters from the triangulo-platinum cluster compounds are reported in **Chapter 3.** The use of $[AuPR_3]$ as a capping fragment generates clusters with a tetrahedral Pt_3Au framework. The synthesis and characterisation of two novel "sandwich" compounds are reported in which a gold or copper atom is coordinated between two parallel triplatinum units. A full single

crystal X-ray crystallographic study has been carried out on each of these compounds and their geometric parameters contrasted.

Chapter 4 describes the reactions of the platinum-sulphido complex $[Pt_2(\mu\text{-}S)(CO)(PPh_3)_3]$. This compound is found to be chemically robust. The Pt-Pt bond has so far proved resistant to insertion reactions and only the ligands trans to the sulphur atom are readily exchanged. The bridging sulphido- group appears to have an extensive coordination chemistry which has lead to the synthesis of some heterometallic complexes. This property does not, as yet, provide a route into cluster formation but instead produces complexes which are aggregates of metal atoms.

The application of ^{31}P and ^{195}Pt NMR studies to the characterisation of platinum cluster compounds is discussed in **Chapter 5.** The solution NMR spectra of compounds synthesised in the course of this research are described and analysed in detail. A large amount of NMR data for homometallic triplatinum clusters has been gathered and it has been possible to characterise a number of such compounds having relatively low symmetry. The heterometallic complexes described in Chapters 3 and 4 have also been characterised using NMR spectroscopy by considering the extra MPR_3 fragments as perturbations on the spectra of the compounds from which they were derived. Analysis of the complex spectra obtained for such compounds was greatly assisted by the use of computer simulation techniques.

The work described in this Thesis was carried out in the Inorganic Chemistry Laboratory, Oxford, from October 1983 to May 1986, under the supervision of Dr D.M.P. Mingos. All the work is my own, unless stated to the contrary, and it has not previously been submitted for a degree at this or any other University.

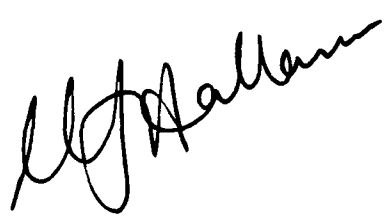

ACKNOWLEDGEMENTS

I would like to thank my supervisor, Dr D. Michael P. Mingos, for his ideas and encouragement during the course of my research. I am particularly grateful for his his help and advice which was always freely available.

I am grateful to a number of people for assistance with the characterisation of some compounds: to Dr Mary McPartlin for the X-ray crystallographic analyses described in Chapter 3, to Michael Luke for the X-ray crystallographic analyses described in Chapter 4 and to Dr Martin Grossel for obtaining the 162MHz ^{31}P NMR spectrum described in Chapter 5.

My thanks are also due to the various members of the research group, past and present, whose lively discussions were a constant stimulation. In particular, I would like to remember David Evans, Robert Wardle, David Gilmour and Michael Luke whose research in related areas offered much guidance in my earlier days.

Finally, I thank Sheila for assistance with the typing and printing and for putting up with my long absences during the preparation of this Thesis.

ABBREVIATIONS

GENERAL

atm	atmosphere
Bu^n	n-butyl
Bu^t	tertiary butyl
Bz	benzyl
cod	1,5-cyclooctadiene
Cy	cyclohexyl
dppe	bis(1,2 diphenylphosphino)ethane
dppm	bis(1,2 diphenylphosphino)methane
dppp	bis(1,2 diphenylphosphino)propane
ESCA	electron spectroscopy for chemical analysis
Et	ethyl
HOMO	highest occupied molecular orbital
LUMO	lowest unoccupied molecular orbital
Me	methyl
NMR	nuclear magnetic resonance
Ph	phenyl
PPN	bis(triphenylphosphoranylidene)ammonium
Pr^i	iso-propyl
R	alkyl
THF	tetrahydrofuran
TMNO	trimethylamine N-oxide
TMP	trimethyl phosphite
Tol	tolyl
UV	ultra-violet
Xyl	xylyl

INFRA-RED ABSORPTION BANDS

(v)s	(very)strong
m	medium
w	weak
sh	shoulder
br	broad

NMR DATA

δ	chemical shift
$\{^1H\}$	broad-band proton decoupled
^nJ	coupling constant over n bonds
ppm	parts per million
s	singlet
t	triplet

CONTENTS

CHAPTER 1 A SURVEY OF STRUCTURES AND METHODS IN PLATINUM CLUSTER CHEMISTRY

1.1 The study of cluster chemistry 1

1.2 Clusters and aggregates 3

1.3 Synthesis of cluster compounds 6

1.3.1 Homonuclear platinum cluster compounds

1.3.2 Heterometallic platinum-gold cluster compounds

1.3.3 Homometallic platinum sulphido- complexes

1.4 Characterisation of platinum cluster compounds 14

1.4.1 X-ray crystallography

1.4.2 Infra-red spectroscopy

1.4.3 Nuclear Magnetic Resonance studies

1.4.4 Other methods

1.5 Structures of platinum cluster compounds 19

1.5.1 Bonding in platinum cluster compounds

1.5.2 X-ray crystallographic studies

1.5.3 Steric and electronic effects

1.6 Structures and bonding in heterometallic platinum-gold clusters 32

1.6.1 Structures containing the Au-Au moiety

1.6.2 Structures based on Pt_3 triangular units

1.7 Structures of platinum sulphido- complexes 38

1.7.1 Complexes derived from $[Pt_2(\mu\text{-}S)_2(PPh_3)_4]$

1.7.2 Platinum sulphido- complexes with a Pt-Pt bond

1.8 Summary 42

CHAPTER 2 SYNTHESIS AND CHARACTERISATION OF HOMOMETALLIC TRIANGULO-CLUSTER COMPOUNDS OF PLATINUM

2.1 Introduction 43

2.1.1 Synthesis of carbonyl phosphine cluster compounds of platinum

2.1.2 Synthesis of platinum phosphine cluster compounds containing the bridging SO_2 ligand

2.1.3 42 versus 44 electron Pt_3 triangular clusters

2.1.4 Tetra- and pentanuclear cluster compounds

2.2 A general synthetic route to platinum carbonyl phosphine cluster compounds 51

2.2.1 The reducing agent

2.2.2 The mononuclear platinum precursor

2.2.3 Synthesis and characterisation of the cluster compounds

2.2.4 Factors affecting cluster nuclearity

2.3 Reactions of triangulo-triplatinum cluster compounds with unsaturated inorganic molecules 58

2.3.1 Reactions for which fragmentation of the platinum cluster is not required

2.3.2 Reactions involving fragmentation of the platinum cluster

2.3.3 Synthesis of a binuclear complex by cluster fragmentation

2.4 Amine oxide labilised ligand exchange 76

2.5 Synthesis of anionic triplatinum cluster compounds 79

2.6 Summary 82

CHAPTER 3 SYNTHESIS AND CHARACTERISATION OF SOME HETEROMETALLIC CLUSTER COMPOUNDS OF PLATINUM

3.1 Introduction 83

3.2 The reaction of $[Pt_3(\mu\text{-}CO)_3(PPh_3)_4]$ with $[AuPPh_3]^+$ 83

3.3 Gold-capping reactions of $[Pt_3(\mu\text{-}SO_2)_3(PPh_3)_3]$ 87

3.4 Sandwich-type cluster compounds 88

3.5 Synthesis and structural characterisation of the sandwich compound $[Pt_3(\mu\text{-}CO)_3(PPh_3)_3]_2Au^+\ PF_6^-$ 93

3.6 Synthesis and structural characterisation of the sandwich compound $[Pt_3(\mu\text{-}CO)_3(PPh_3)_4]_2Cu^+\ PF_6^-$ 98

3.7 Reaction of $[Pt_3(\mu\text{-}CO)_3(PCy_3)_3]$ with $[Au(CO)Cl]$ 100

3.8 Summary 103

CHAPTER 4 SYNTHETIC AND STRUCTURAL STUDIES OF $[Pt_2(\mu\text{-}S)(CO)(PPh_3)_3]$

4.1 Introduction 105

4.2 Synthesis and Structural characterisation of $[Pt_2(\mu\text{-}S)(CO)(PPh_3)_3]$ 107

4.2.1 X-ray structural analysis of $[Pt_2(\mu\text{-}S)(CO)(PPh_3)_3]$

4.3 The reaction of $[Pt_2(\mu\text{-}S)(CO)(PPh_3)_3]$ with the olefin complex $[(\eta\text{-}C_5H_5)Fe(CO)_2(C_2H_4)]^+$ 112

4.4 Heterometallic complexes derived from $[Pt_2(\mu\text{-}S)(CO)(PPh_3)_3]$ 113

4.4.1 Synthesis and structural characterisation of the complex $[Pt_2(\mu\text{-}S)(CO)(PPh_3)_3\ Au(PPh_3)]^+\ PF_6^-$

4.4.2 Silver and copper analogues of $[Pt_2(\mu\text{-}S)(CO)(PPh_3)_3\ Au(PPh_3)]^+$

4.4.3 The reaction of $[Pt_2(\mu\text{-}S)(CO)(PPh_3)_3]$ with $[Au(Me_2S)Cl]$

4.5 Summary 122

CHAPTER 5 $^{31}P\{^1H\}$ AND $^{195}Pt\{^1H\}$ NMR STUDIES ON PLATINUM CLUSTER COMPOUNDS

5.1 Introduction 124

5.2 NMR spectra of Pt_3 triangular clusters 125

5.3 Pt_3 triangular clusters of lower symmetry 127

5.4 Heterometallic clusters from triangulo- Pt_3 compounds and gold 134

5.5 Platinum μ-sulphido and related compounds 140

5.5.1 Structures with chemically equivalent phosphines

5.5.2 Structures based on $[Pt_2(\mu\text{-}S)(CO)(PPh_3)_3]$

5.6 Summary 157

CHAPTER 6 EXPERIMENTAL DETAILS

6.1 General 159

6.2 Experimental Details Relevant to Chapter 2 161

6.2.1 Synthesis of cis-$[Pt\{P(CH_2CH_2CN)_3\}(CO)Cl_2]$

6.2.2 Synthesis of $[dppmAuCl]_2$

6.2.3 Reaction of $[dppmAuCl]_2$ with $[Pt(cod)Cl_2]$

6.2.4 Synthesis of $[Pt_3(\mu\text{-}CO)_3(PBu^n{}_3)_3]$

6.2.5 Synthesis of $[Pt_3(\mu\text{-}CO)_3\{P(CH_2CH_2CN)_3\}_3]$

6.2.6 Synthesis of $[Pt_3(\mu\text{-}CO)_3(PCy_3)_3]$

6.2.7 Synthesis of $[Pt_4(\mu\text{-}CO)_5(PMe_2Ph)_4]$

6.2.8 Synthesis of $[Pt_5(CO)(\mu\text{-}CO)_5(PPh_3)_4]$

6.2.9 Synthesis of $[Pt_3(\mu\text{-}CO)_3(PPh_3)_4]$

6.2.10 Synthesis of $[Pt_3(\mu\text{-}SO_2)_3(PCy_3)_3]$

6.2.11 Synthesis of $[Pt_3(\mu\text{-}SO_2)_3(PPh_3)_3]$

6.2.12 Substitution by CO of SO_2 in $[Pt_3(\mu\text{-}SO_2)_3(PPh_3)_3]$

6.2.13 Reaction of $[Pt_3(\mu\text{-}SO_2)_3(PCy_3)_3]$ with CO

6.2.14 Conversion of $[Pt_3(\mu\text{-}SO_2)_3(PCy_3)_3]$ to $[Pt_3(\mu\text{-}CO)_3(PCy_3)_3]$

6.2.15 Reaction of $[Pt_3(\mu\text{-}CO)_3(PPh_3)_4]$ with CS_2

6.2.16 Reaction of $[Pt_3(\mu\text{-}CO)_3(PPh_3)_4]$ with COS

6.2.17 Synthesis of $[Pt_3(\mu\text{-}SO_2)_2(\mu\text{-}Cl)(PPh_3)_3]^-$ $BzEt_3N^+$

6.2.18 Synthesis of $[Pt_3(\mu\text{-}SO_2)_2(\mu\text{-}Cl)(PCy_3)_3]^-$ PPN^+

6.2.19 Synthesis of $[Pt_3(\mu\text{-}SO_2)_2(\mu\text{-}Br)(PCy_3)_3]^-$ Et_4N^+

6.2.20 Reactions of $[Pt_3(\mu\text{-}SO_2)_2(\mu\text{-}Cl)(PCy_3)_3]^-$ PPN^+ with different ratios of $[Au\{P(p\text{-}FC_6H_4)_3\}]^+$

6.3 Experimental Details Relevant to Chapter 3 171

6.3.1 Synthesis of $[Au(PPh_3)Cl]$

6.3.2 Synthesis of $[Pt_3(\mu\text{-}CO)_3(PPh_3)_5]^+$ PF_6^-

6.3.3 Synthesis of $[Pt_3Au(\mu\text{-}SO_2)_2(\mu\text{-}Cl)(PPh_3)_4]$

6.3.4 Synthesis of $[Pt_3(\mu\text{-}CO)_3(PPh_3)_3]_2Au^+$ PF_6^-

6.3.5 Synthesis of $[Pt_3(\mu\text{-}CO)_3(PPh_3)_3]_2Cu^+$ PF_6^-

6.4 Experimental Details Relevant to Chapter 4 174

6.4.1 Synthesis of $[Pt_2(\mu\text{-}S)(CO)(PPh_3)_3]$

6.4.2 Reaction of $[Pt_2(\mu\text{-}S)(CO)(PPh_3)_3]$ with $[Fe(\eta\text{-}C_5H_5)(CO)_2(C_2H_4)]^+$ BF_4^-

6.4.3 Synthesis of $[Pt_2(\mu\text{-}S)(CO)(PPh_3)_3Au(PPh_3)]^+$ PF_6^-

6.4.4 Synthesis of $[Pt_2(\mu\text{-}S)(CO)(PPh_3)_3Ag(PPh_3)]^+$ PF_6^-

6.4.5 Synthesis of $[Pt_2(\mu\text{-}S)(CO)(PPh_3)_3Cu(PPh_3)]^+$ PF_6^-

6.4.6 Synthesis of $[Pt_2(\mu\text{-}S)(CO)(PPh_3)_3]_2Au^+$ PF_6^-

REFERENCES 178

APPENDICES 185

Final fractional atomic coordinates and temperature factors for crystallographic structure determinations

A $[Pt_3(\mu\text{-}CO)_3(PPh_3)_3]_2Au^+$ PF_6^-

B $[Pt_3(\mu\text{-}CO)_3(PPh_3)_3]_2Cu^+$ PF_6^-

C $[Pt_2(\mu\text{-}S)(CO)(PPh_3)_3]$

D $[Pt_2(\mu\text{-}S)(CO)(PPh_3)_3Au(PPh_3)]^+$ PF_6^-

CHAPTER ONE

A SURVEY OF STRUCTURES AND METHODS IN PLATINUM CLUSTER CHEMISTRY

1.1 The study of cluster chemistry

Metal cluster chemistry is currently a particularly active area of research. Some of the interest derives from the aesthetic pleasure in predicting and then creating ever larger polyhedral clusters. A singularly satisfying example was the synthesis[1] of $[Au_{13}Cl_2(PMe_2Ph)_{10}]^{3+}$ since earlier molecular orbital calculations[2] had predicted the stoichiometry and structure for this molecular cluster. On a more practical level, the aim of this type of research is to understand the structure of metal surfaces and the catalytic processes which can occur on them. Most catalytic processes in chemical industries involve reactions on the surfaces of metals or their oxides or sulphides. Such reactions require the coordination of reactants at the surface and in terms of structure and stereochemistry this should bear some resemblance to the coordination of small molecules or ions to a metal atom or group of atoms in a discrete molecular cluster. This Thesis is concerned with the synthesis and structures of a narrow group of small cluster compounds and, to some degree, their reactivity. A detailed examination of the "Cluster - Surface Analogy" is outside the scope of this survey but can be found in reviews by Muetterties and others.[3,4] It is worth making a few comments on the relevance of the types of cluster compound which have been studied to the understanding of surface chemistry.

The surfaces of catalyst-type materials have exposed metal atoms, each of which is bound to a number of other exposed metal atoms. Therefore, it seems more realistic to model surface coordination

chemistry not so much on molecular complexes containing only one metal atom but rather on molecular cluster compounds which are based on polyhedral metal frameworks. There is no suggestion that clusters are fully analogous to metal surfaces - there are major electronic differences between bulk metals and molecular clusters. However, there are sufficient similarities for the clusters to be an adequate working model for surface catalysts. In the chemistry of platinum there is, in fact, one example where there is a strong similarity between cluster and bulk metal. The two largest of the characterised clusters, the Pt_{38} and Pt_{26} carbonyl anions, both have close-packed arrangements of metal atoms and the cubic structure of the Pt_{38} cluster is the same as in metallic platinum.[5] The average Pt-Pt bond distance in the latter cluster is 2.83Å compared with 2.77Å in the metal.

Cluster compounds serve not only as models for catalyst systems but can also act as selective and efficient catalysts in their own right. Of interest to this work is that some catalytic studies have been carried out on Pt_3 triangular cluster compounds. Specifically, the carbonyl anions $[Pt_3(\mu\text{-}CO)_3(CO)_3]_n^{2-}$ or the neutral $[Pt_3(\mu\text{-}CO)_3(PR_3)_4]$, each supported on alumina,[6] have been found to compare favourably with Pt or Pt-Sn metallic catalysts traditionally used for the isomerisation of hexanes. The latter type also showed a particular selectivity towards demethylation of methylpentanes. This was attributed to the phosphine ligands which block the formation of a cyclopentane intermediate, not for steric reasons but rather by changing the electronic environment on the metal.

The same carbonyl anions are also known to catalyse some

hydroformylation reactions.[7] For example, at 120° and under a pressure of 100atm of hydrogen and CO, 1-pentene is catalytically converted in the presence of $[Pt_3(\mu\text{-}CO)_3(CO)_3]_4^{2-}$ to a mixture of aldehydes. At the end of the reaction, the platinum is recovered as a mixture of $[Pt_3(\mu\text{-}CO)_3(CO)_3]_4^{2-}$ and $[Pt_3(\mu\text{-}CO)_3(CO)_3]_3^{2-}$.

1.2 Clusters and aggregates

A metal cluster may be defined as a molecular compound containing three or more metal atoms held together sufficiently closely that bonding interactions are considered to exist between them. Theoreticians may be able to calculate that the occupied multicentred molecular orbitals encompassing the metal atoms are bonding in nature and crystallographers may be able to show that inter-metal distances are short enough to say that metal-metal bonds exist. Thus the series of Pt_3 triangular compounds and the Pt_3Au tetrahedral compounds illustrated in Figure 1.1 are accepted as metal clusters.

P = tertary phosphine

X = CO, SO_2

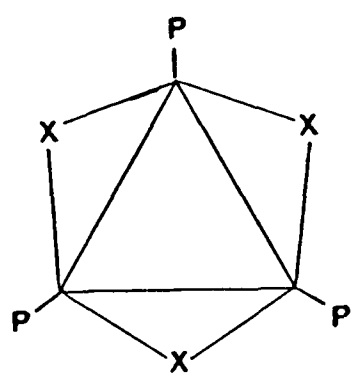

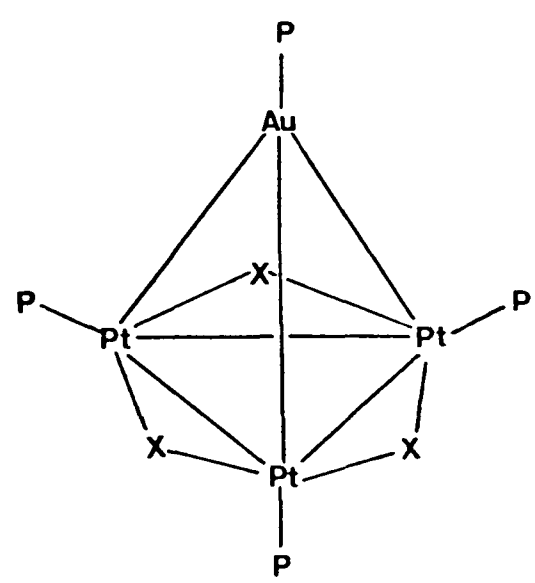

Typical distances: Pt-Pt 2.6-2.8Å[8] Pt-Pt 2.7Å[9] Pt-Au 2.8Å

Figure 1.1 Metal-metal bonded clusters

Transition metal-metal bonding is favoured by overlap of (n-1)d orbitals at intermolecular distances which are sufficiently long to avoid core-core and ligand-ligand repulsion. Elements on the left hand side of the second and third transition series form metal-metal bonded species with the help of good π-donor ligands such as halide, alkoxide and amido groups.[10] This Thesis is concerned with the cluster compounds of the heavier elements on the right hand side of the transition series. These metals rely on π-acid ligands such as CO, phosphines and cyclic aromatic organic ligands. The metal-metal bonding in such compounds may be attributed to a combination of low effective nuclear charge, leading to good overlap of d orbitals, and stabilisation of cluster molecular orbitals by interaction with unoccupied ligand π^* orbitals.

Molecular compounds are also found in which a number of metal atoms are held together by bridging ligands at separations greater than accepted metal-metal bonding distances. Such compounds may be described as aggregates and an example is illustrated in Figure 1.2 below.

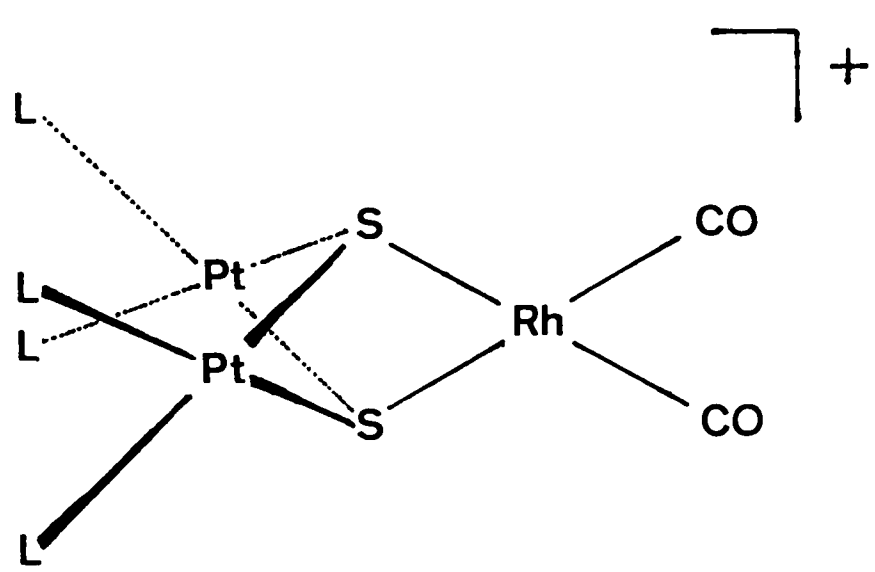

L = tertiary phosphine

Internuclear distances: Pt-Pt 3.27Å
Pt-Rh 3.03Å, 3.05Å[11]

Figure 1.2 A polynuclear metal aggregate

The difference between a cluster and an aggregate at first sight may be only in the distance separating the metal atoms since it is not always possible to be certain of the existence of a formal metal-metal bond simply on the basis of electron-counting. This is particularly true in cases such as platinum where the metal atoms readily adopt coordination geometries based on both 16 and 18 electron configurations.[12] The trinuclear complex $[Pt_3(\mu\text{-}PPh_2)_3(Ph)(PPh_3)_2]$,[13] shown below, illustrates this point.

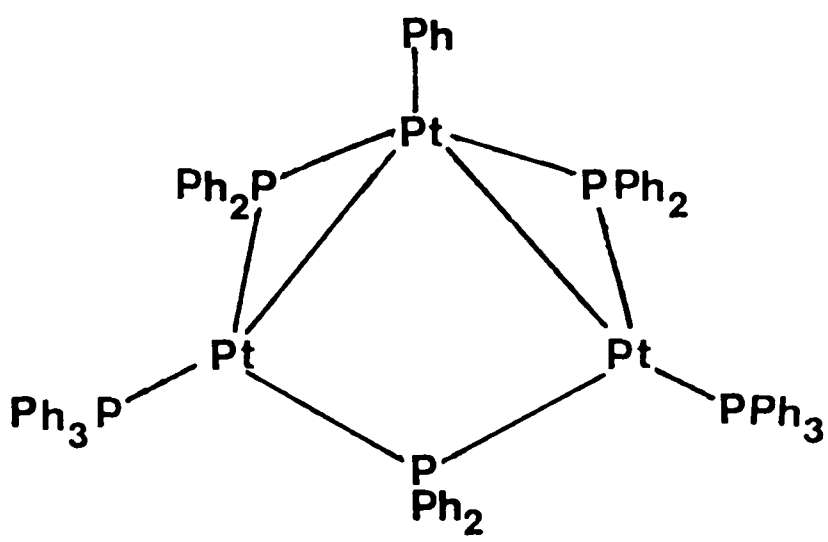

d(Pt-Pt) (Å)

2.785
2.785
3.630

This example of a 44 electron complex is unusual in that the extra pair of electrons over what is required for a Pt_3 triangle has been localised to the extent of separating two Pt atoms beyond what is normally considered to be a bonding distance. Many other 44 electron platinum triangles are known and in these cases, although there is some bond lengthening, the Pt-Pt distances remain in the range anticipated for metal-metal bonds.

The difference between bonded and non-bonded metal atoms can often be defined quite easily. $[Pt_2Au(\mu\text{-}S)(CO)_2(PPh_3)_4]^+$, which is discussed in Chapter 4, has a well defined Pt-Pt bond (2.65Å) and two non-bonding Pt-Au distances of more than 3.0Å. This is consistent

with the observed chemistry of this and a range of similar compounds in which changes are readily made in the coordinated ligands while the $Pt_2(\mu\text{-}S)$ core remains intact.

1.3 Synthesis of cluster compounds

The synthesis of metal cluster compounds has progressed greatly in the last two decades in that it is now possible to control reaction conditions in favour of cluster formation rather than waiting on good fortune. It is still very difficult to predict the precise nature of the cluster which will result from a given reaction. Indeed, the large number of bond breaking and bond forming steps in such reactions often lead to a complex mixture of products which must then be separated either by solvent extraction or by chromatographic methods.

1.3.1 Homonuclear platinum cluster compounds

The field of platinum cluster chemistry was pioneered by Chatt and his co-workers[12] who provided the first preparatively simple synthesis of trinuclear phosphine carbonyl cluster compounds by the hydrazine reduction of sodium tetrachloroplatinite in the presence of a tertiary phosphine and CO (Reactions 1.1 and 1.2).

$$Na_2PtCl_4 \xrightarrow[\text{2. } N_2H_4,\ KOH,\ CO]{\text{1. } PPh_3,\ EtOH} [Pt_3(\mu\text{-}CO)_3(PPh_3)_4] \qquad (1.1)$$

$$Na_2PtCl_4 \xrightarrow[\text{2. } N_2H_4,\ KOH,\ CO]{\text{1. } PMe_2Ph,\ MeOH} [Pt_4(\mu\text{-}CO)_5(PMe_2Ph)_4] \qquad (1.2)$$

The yields of these reactions were generally low and mononuclear by-

products had to be removed by Soxhlet extraction.

Chini and co-workers[7] found that the reduction of Na_2PtCl_6 in the presence of CO, but without phosphine, gave a series of carbonyl anions:

$$Na_2PtCl_6 \xrightarrow[\text{NaOH, MeOH}]{\text{CO}} [Pt_3(\mu\text{-CO})_3(\text{CO})_3]_n^{2-} \quad (n = 2\text{-}5,\ 10) \qquad (1.3)$$

These oligomers result from the stacking of Pt_3 triangles along the pseudo 3-fold axis and the nuclearity of the cluster formed is critically dependent on the stoichiometry and conditions of the reaction.

More recently, a strategy has been developed by which low-valent, coordinatively unsaturated species are generated from mononuclear starting materials and are then condensed to form clusters. In platinum cluster chemistry the required intermediate may have the form $[PtL_2X_2]$ where L = tertiary phosphine and X = CO or SO_2. It is thought that such species are intermediates in the following reactions.

$$[PtH_2(PCy_3)_2] \xrightarrow[C_6H_6]{\text{CO}} [Pt_3(\mu\text{-CO})_3(PCy_3)_3] \qquad (1.4)^{14,15}$$

$$[Pt(PPh_3)_2(C_2O_4)] \xrightarrow[\text{2. NaBF}_4]{\text{1. UV, H}_2\text{, EtOH}} [Pt_3(\mu\text{-PPh}_2)_3(\mu\text{-H})(PPh_3)_3]^+ \qquad (1.5)^{16}$$

Some mononuclear platinum(0) complexes can be isolated and these tend to be useful precursors for platinum cluster formation. This is particularly true of olefin complexes in which the olefin ligand is

quite labile:

$$[Pt(cod)_2] \xrightarrow[\text{petrol}]{CNBu^t} [Pt_3(\mu\text{-}CNBu^t)_3(CNBu^t)_3] \qquad (1.6)^{17}$$

$$[Pt(C_2H_4)_2(PCy_3)] \xrightarrow[\text{hexane}]{SO_2} [Pt_3(\mu\text{-}SO_2)_3(PCy_3)_3] \qquad (1.7)^{18}$$

Once formed, platinum cluster compounds are readily interconverted and become themselves sources of new clusters by means of ligand exchange and by degradation and aggregation reactions.

1.3.2 Heterometallic platinum-gold cluster compounds

No examples of structurally characterised platinum-gold cluster compounds had appeared in the literature until recently when Wardle, in this laboratory, reported that it was possible to cap Pt_3 triangular clusters with an $Au\text{-}PR_3$ fragment.[9] The products, like previously known mixed-metal gold clusters, depended for their synthesis on the isolobal relationship between $AuPR_3$ and the hydrido-ligand.[19,20] Lewis *et al*[21] had demonstrated the addition of the cation $[AuPPh_3]^+$ to the metal carbonyl cluster anions and Stone's group[22] had reported the elimination of methane from a metal carbonyl hydrido- cluster and $[MeAuPPh_3]$.

It has been found that the neutral *triangulo*- cluster $[Pt_3(\mu\text{-}CO)_3(PCy_3)_3]$, although unreactive towards $[AuCl(PR_3)]$, is sufficiently nucleophilic to react with $[AuPR_3]^+$ when formed *in situ* from $[AuCl(PR_3)]$ and $TlPF_6$. There is a precedence in the literature for a capping reaction of this type. Several platinum-mercury cluster compounds have recently been synthesised where a mercury atom caps the

Pt_3 unit. Such compounds are described in detail in Chapter 3. The product of the reaction with $[AuPR_3]^+$ is a tetrahedral cationic cluster in which the gold fragment has symmetrically capped the Pt_3 triangle.[23] It has also been found that the neutral SO_2 cluster $[Pt_3(\mu\text{-}SO_2)_3(PCy_3)_3]$ reacts with $[AuCl(PR_3)]$ in two ways. In the presence of $TlPF_6$, the tetrahedral, symmetrically capped structure is formed as with the carbonyl cluster. In the absence of $TlPF_6$, there is still a reaction in which the gold atom caps the Pt_3 triangle. In this case the product is neutral, with one of the bridging SO_2 ligands on the Pt_3 triangle replaced by a bridging chloride ligand.[24] These syntheses are illustrated in Figure 1.3 which also shows how SO_2 and CO ligands in the heterometallic Pt_3Au clusters may be exchanged to a limited degree.

Synthetic routes to mixed platinum-gold cluster compounds have also been found recently in which all the starting materials are mononuclear. Braunstein et al[25] have reported the synthesis and structural characterisation of a mixed triangular cluster, $[PtAu_2Cl(PEt_3)_2(PPh_3)_2]^+$:

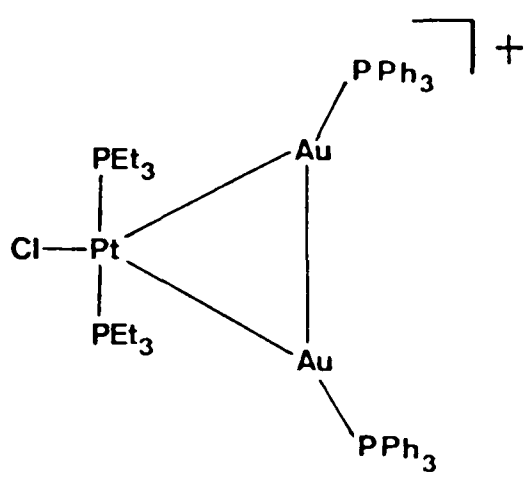

The starting materials for the synthesis were trans-$[PtHCl(PEt_3)_2]$ and $[Au(THF)(PPh_3)]^+$, the latter generated in THF solution from the reaction of $[AuCl(PPh_3)]$ and $AgCF_3SO_3$. Gilmour et al[26] have also

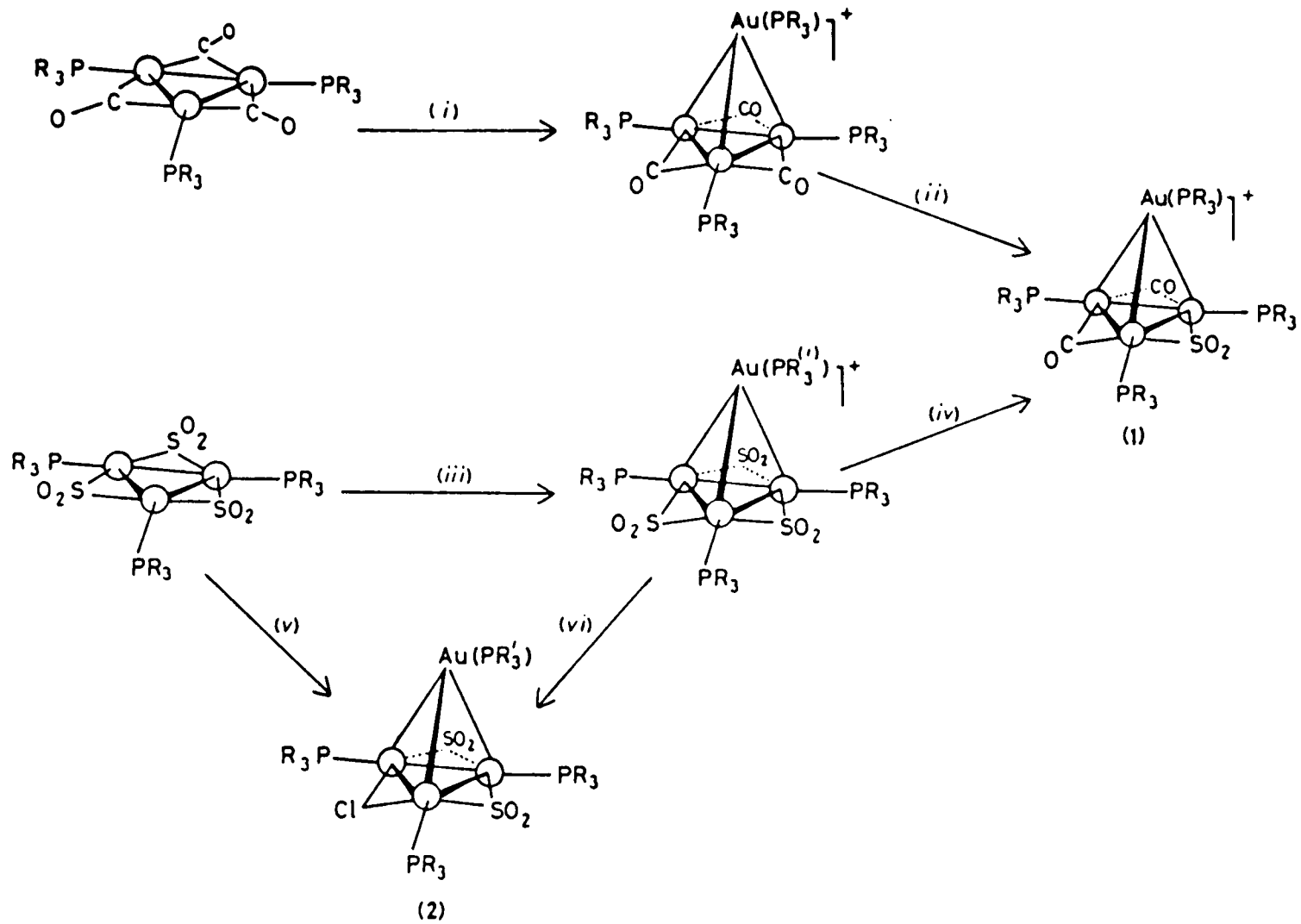

Scheme. ○, Pt; $PR_3 = P(C_6H_{11})_3$ and $PR'_3 = P(C_6H_4F\text{-}p)_3$. (*i*) $[Au(PR_3)]^+$, C_6H_6; (*ii*) SO_2, CH_2Cl_2; (*iii*) $[Au(PR_3)]^+$, thf; or $[Au(PR'_3)]^+$; (*iv*) CO, thf, 50 °C; (*v*) $[AuCl(PR'_3)]$, C_6H_6; (*vi*) NMe_4Cl, C_6H_6–EtOH

Figure 1.3 Synthesis and interconversion of some tetrahedral platinum-gold cluster compounds

reported the synthesis and characterisation of a mixed tetranuclear cluster which adopts a "flattened butterfly" structure:

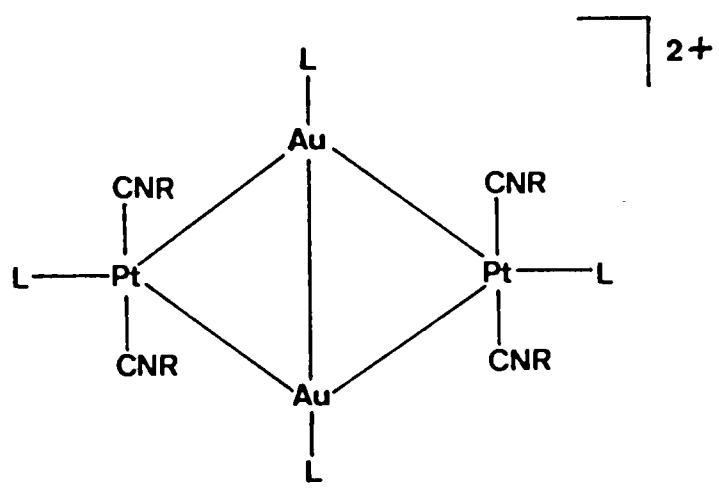

L = PPh_3

R = Xylyl

This compound was synthesised by adding $[Au(CN\text{-}Xylyl)_2]^+ X^-$ (X = BF_4 or PF_6) to a solution of $[Pt(PPh_3)_2(C_2H_4)]$ in acetone.

In Chapter 3 of this Thesis, the idea of capping Pt_3 triangles with mononuclear gold fragments is extended further in an attempt to develop the chemistry of the Pt_3 triangular clusters.

1.3.3 Homometallic platinum sulphido- complexes

Many homometallic sulphido- complexes of platinum have been isolated which can be classified into two groups. One type consists of two metal-metal bonded platinum atoms bridged by a single sulphur and is the basis of the work described in Chapter 4. The other type consists of two non-bonded platinum atoms held together by two sulphur ligands. In both cases the sulphur atoms have the capability to bond further to other metals.

Baird and Wilkinson first reported[27] that the reaction of $[Pt(PPh_3)_3]$ with COS yielded a product which they formulated as $[Pt(PPh_3)_2(COS)]$. They later reported[28] that on heating in chloroform, this complex gave an orange air-stable compound, which

they identified on the basis of infra-red spectroscopy and elemental analysis as $[Pt_2(\mu\text{-}S)(CO)_2(PPh_3)_3]$. Subsequently, Skapski and Troughton[29] showed by X-ray crystallography that the compound had only one CO ligand and the following structure.

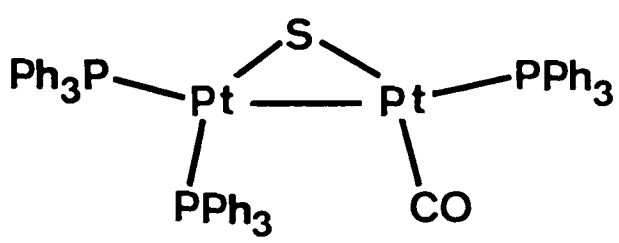

The platinum atoms in this compound have a nominal oxidation state of +1 which represents an oxidation by COS from the $[Pt(PPh_3)_3]$ starting material.

An analogous synthesis has been reported[30] which uses CS_2 instead of COS. The reaction of $[Pt(dppe)(CS_2)]$ with $[Pt(PPh_3)_2(C_2H_4)]$ gives the complex shown below.

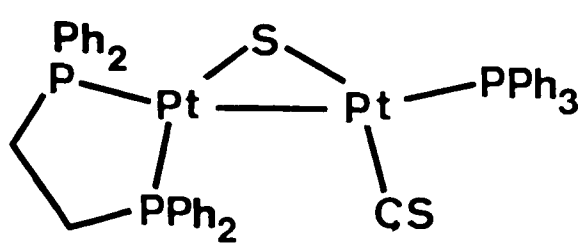

A similar complex, $[Pt_2(\mu\text{-}S)(PPh_3)_4]$, has been produced by the reaction of <u>cis</u>-$[Pt(PPh_3)_2Cl_2]$ with Na_2S in NH_3-EtOH. In this case the Pt(II) starting material was reduced, probably by the ammoniacal ethanol solvent.

Two compounds based on the $Pt_2(\mu\text{-}S)_2$ unit were isolated from the reaction in ethanol of <u>cis</u>-$[Pt(PMe_2Ph)_2Cl_2]$ with Na_2S.[31] One was white, water soluble and ionic and, on the basis of infra-red and analytical evidence, was assigned the following structure:

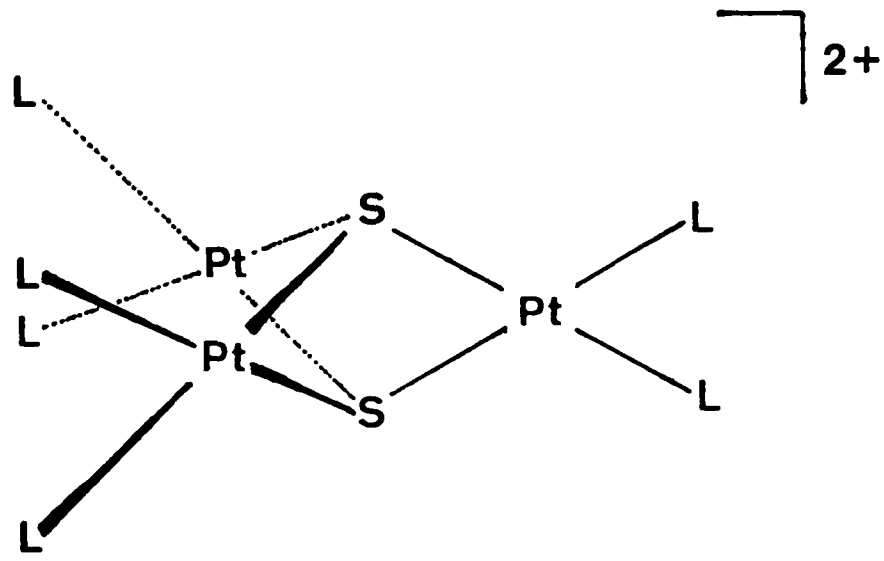

L = PMe_2Ph

The other compound was yellow, non-conducting and was shown by X-ray crystallography to have the stucture below:

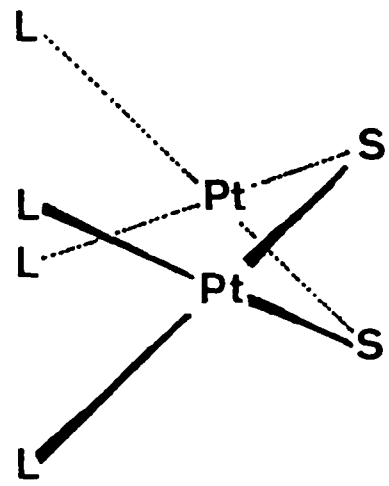

The latter compound contains two approximately square-planar platinum centres linked by two bridging sulphido- ligands. The former product is derived from this compound by further coordinating the sulphur atoms to a PtL_2 unit and this has been confirmed by reacting $[Pt_2(\mu\text{-}S)_2(PMe_2Ph)_4]$ with one mole-equivalent of <u>cis</u>-$[Pt(PMe_2Ph)_2Cl_2]$ to give $[Pt_3(\mu\text{-}S)_2(PMe_2Ph)_6]^{2+}$ in high yield.

Ugo[32] has reported the compound $[Pt_2(\mu\text{-}S)_2(PPh_3)_4]$, isostructural with $[Pt_2(\mu\text{-}S)_2(PMe_2Ph)_4]$, and synthesised by reacting $[Pt(PPh_3)_2(SH_2)]$ with O_2 or sodium ethoxide. This particular platinum-sulphido complex has been the subject of many studies on

heterometallic aggregates[11,33,34] since both sulphur atoms readily coordinate to other metals.

1.4 Characterisation of platinum cluster compounds

A range of techniques are available for the structural characterisation of platinum cluster compounds. In the solid state, the most definitive is the method of single crystal X-ray crystallography. A number of forms of spectroscopy are utilised for identifying cluster compounds in solution and in the solid state. In the course of this work infra-red, ultra-violet(UV) and NMR spectroscopy have been widely used, the last of these being developed as a means of determining structure in solution. Elemental analyses are routinely carried out on new products but the results are used with reservation since a number of factors, such as solvation, can give misleading results.

1.4.1 X-ray cystallography

Sometimes the use of X-ray crystallography is the only means of elucidating the structure of a cluster compound. This applies particularly to high nuclearity and complex structures. In this work X-ray crystallography has been used to determine the structure of a complex heterometallic cluster for which spectroscopic evidence is deceptively simple (see Chapter 4) and has also been used to compare solid state structures with solution structures as determined by NMR spectroscopy (see Chapter 5). The main strength of the technique is in determining the metal atom framework which makes up the cluster and in placing on the framework the principal heavier ligands. It is sometimes difficult, however, to locate small ligands, particularly in

high nuclearity clusters. For example, in the Pt_{38} cluster,[5] the number and distribution of CO ligands is uncertain and chemical analysis has been needed to provide an estimate of about 44 ligands.

1.4.2 Infra-red spectroscopy

The carbonyl region of infra-red spectra is useful for identifying cluster species and for the Pt_3 triangular clusters it is often possible to distinguish between the compounds $[Pt_3(\mu\text{-}CO)_3L_3]$ (D_{3h}) and $[Pt_3(\mu\text{-}CO)_3L_4]$ (C_{2v}). The former D_{3h} structure is characterised by one strong band in the bridging carbonyl region (1750 - 1950cm^{-1}) whereas the latter C_{2v} structure shows two strong bands. The pentanuclear cluster $[Pt_5(CO)(\mu\text{-}CO)_5(PPh_3)_4]$ is also readily identified by its infra-red spectrum since it is one of the few platinum phosphine carbonyl clusters having a terminal carbonyl ligand (1990cm^{-1}).

Sulphur dioxide always occupies a bridging position in cluster compounds[35,36] and two bands in the region 1000 - 1300cm^{-1} correspond to symmetric and asymmetric (S-O) stretching vibrations.

Other ligands which are found in terminal and bridging positions and which may be detected by infra-red spectroscopy are isocyanides and hydride ligands. In the terminal bonding mode, absorption bands are found for both at about 2100cm^{-1}. Bridging hydrides give bands in the region 1500 - 1800cm^{-1} and bridging isocyanides at about 1700cm^{-1}.

Infra-red spectral data for a large number of platinum cluster compounds containing ligands such as those described above are collected together in a recent review by Mingos and Wardle.[8]

1.4.3 Nuclear Magnetic Resonance studies

The platinum cluster compounds which are the subject of this Thesis contain a number of easily observed NMR nuclei: ^{1}H, ^{13}C, ^{31}P and ^{195}Pt - all with nuclear spin $I = \frac{1}{2}$.

Proton NMR has not proved to be very instructive for the compounds described in this Thesis since it gives information mostly about the internal structure of the phosphine ligands. It has, however, come into its own in locating hydride ligands in compounds for which crystallography has failed.[37,38] For example, in $[Pt_5(\mu\text{-}H)_6H_2(PBu^t{}_2Ph)_5]$ the relative integrated intensities of the two signals at $\delta = -5.45$ and -14.13ppm in the ^{1}H NMR spectrum indicated the presence of 6 bridging and 2 terminal hydride ligands as shown in the structure below.

$L = PBu^t{}_2Ph$

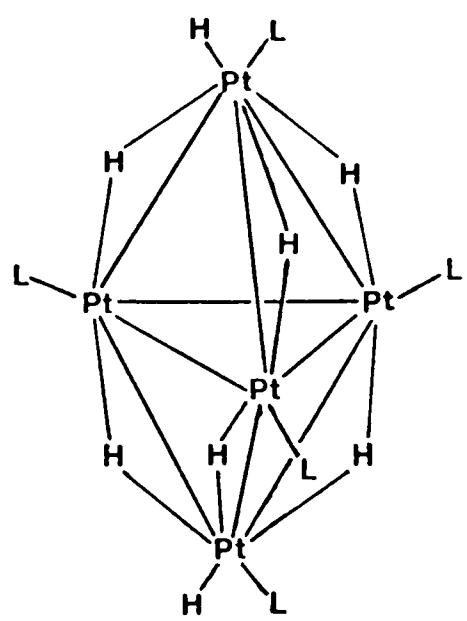

^{13}C NMR has not been exploited in this work for a number of reasons. As for proton NMR, most information derived would relate to the internal structure of organic ligands. There would be some interest in probing the ^{13}C of carbonyl ligands but these have long relaxation times and in practice are difficult to observe, particularly in the presence of other organic ligands. Chini and

others[39] have made use of ^{13}C NMR to examine the carbonyl ligands of the stacked anionic clusters $[Pt_3(\mu\text{-}CO)_3(CO)_3]_n^{2-}$ and have shown unambiguously that, over the temperature range studied, there is no terminal/bridge intramolecular exchange.

Long relaxation times are a general problem with ^{13}C NMR and they result in the need for long delays between pulses on Fourier Transform spectrometers. This difficulty is compounded by the low natural abundance of ^{13}C (1.1%) which means that long accumulation times are also required.

On the other hand, $^{31}P\{^1H\}$ and $^{195}Pt\{^1H\}$ NMR are very informative about the number, type and structural relationship of these two nuclei in the cluster compounds under consideration. Both nuclei are easy to observe as indicated by the data in Table 1.1 and the ability of modern Fourier Transform spectrometers to accumulate spectra rapidly means that even for fairly complex structures, $^{31}P\{^1H\}$ spectra with good signal to noise ratios are produced in 15 - 20 minutes. For platinum, tens of thousands of pulses are often required to produce a satisfactory spectrum and the technique is only feasible because ^{195}Pt relaxation times are usually quite short (small fractions of a second). This means that little or no delay is needed between pulses which can therefore, be made at a rate of up to 200 per minute. Hence $^{195}Pt\{^1H\}$ spectra with acceptable signal to noise ratios are possible in only a few hours.

	Relative abundance (%)	Observation frequency (MHz) scaled to ^{1}H = 100	Relative sensitivity	Absolute sensitivity
^{1}H	100	100	1.00	1.00
^{13}C	1.1	25.1	1.59×10^{-2}	1.76×10^{-4}
^{31}P	100	40.4	6.63×10^{-2}	6.63×10^{-2}
^{195}Pt	33.7	21.4	9.94×10^{-3}	3.36×10^{-3}

Table 1.1 NMR parameters for some common nuclei

The application of $^{31}P\{^{1}H\}$ and $^{195}Pt\{^{1}H\}$ NMR spectroscopy in this work as a means of structure determination is described in detail in Chapter 5. Besides this use, the NMR technique in solution has been applied to the observation of dynamic situations. ^{195}Pt studies on the carbonyl anions $[Pt_3(\mu\text{-}CO)_3(CO)_3]_n^{2-}$ have demonstrated the free rotation of Pt_3 triangles within clusters and the facile exchange of Pt_3 triangles between clusters which occurred when a trace of a cluster with n>3 was present.

In contrast to the crystallographic studies[40,41] on $[Pt_4(\mu\text{-}CO)_5(PMe_2Ph)_4]$ which show a "butterfly" structure with approximate C_{2v} symmetry, the $^{31}P\{^{1}H\}$ and $^{195}Pt\{^{1}H\}$ NMR data[40] reveal equivalent ^{31}P and ^{195}Pt spins which describe a tetrahedral arrangement of platinum atoms. The interpretation given for this is that the solution NMR observes a time averaging of all possible edge-opened tetrahedra as shown below:

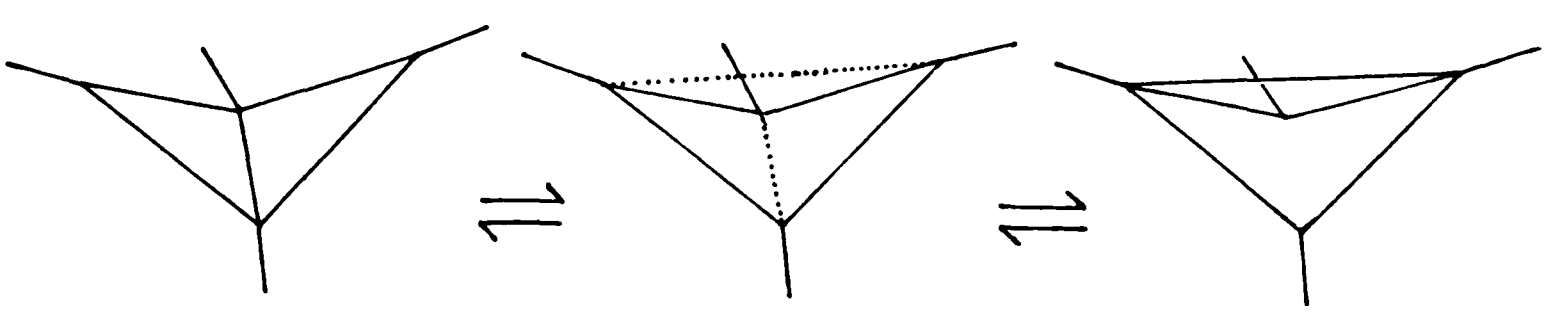

1.4.4 Other methods

Electron spin resonance (ESR) data have been recorded for $[Pt_3\{\mu\text{-}Fe(CO)_4\}_3(CO)_3]^-$ in solution and in the solid state,[42] confirming that this compound, which is a rare example of a 43 electron Pt_3 cluster, has a single unpaired electron. The stability of the paramagnetic cluster probably derives from the unpaired electron being localised mostly on the platinum atoms, and from the steric properties of the μ-$Fe(CO)_4$ groups which hinder spin-pairing by dimerisation. ESR spectroscopy has not been put to use in this work because the more usual 42 and 44 electron Pt_3 triangles are diamagnetic.

UV spectroscopy has found good use in the cluster chemistry of gold[43]. The high nuclearity clusters (Au_6 - Au_{13}) generally show absorption bands at between 300 - 500nm of the UV spectrum which are very characteristic of the gold framework but vary little with small changes in the ligands. In this work UV spectroscopy has only been used to monitor the course of a reaction in which the product shows a characteristic absorption band which is absent in the starting material (see Chapter 2).

1.5 Structures of platinum cluster compounds

A dominant feature of platinum cluster chemistry, which is also a central feature of this work, is the prevalence of the Pt_3 triangular unit. Not only is there a large family of Pt_3 triangulo- clusters but there is also a growing number of higher nuclearity clusters whose structures may be derived from the fusion of triangles. The pattern of metal frameworks observed in the structures of platinum clusters seems not to depend for its existence on the ligands in use other than that suitable ligands are necessary for cluster formation in the first

place.

The order which exists among these structures becomes apparent when the clusters are organised according to the total number of valence electrons which they contain. Figure 1.4 shows a number of platinum cluster compounds, containing 3, 5 or 7 metal atoms, with their skeletal electron counts. Tetranuclear clusters of platinum show a greater variation in their electron counts and some examples are shown in Figure 1.5.

The simple $[Pt_3(\mu\text{-}X)_3L_3]$ cluster has 42 skeletal electrons to which may be added two further electrons if an extra phosphine ligand can be incorporated or if an anionic bridging ligand is introduced. The pentanuclear clusters with a trigonal bipyramidal framework have 68 electrons. If a suitable bond in such a structure is broken then an edge-bridged tetrahedral structure is obtained for which the electron count is 70. It is difficult to generalise as well about the tetranuclear structures except to say that lower numbers of cluster bonding electrons tend to give tetrahedral geometries whereas the addition of more electron pairs leads to localised bond breaking and the "butterfly" geometry.

The Pt_7 cluster shown in Figure 1.4 is interesting because it demonstrates how a high nuclearity cluster is built up from a Pt_3 triangle, first by capping on each side to form a trigonal bipyramid and then by bridging two pyramid edges. In addition to the expected 11 terminal and bridging isocyanide ligands, this cluster also has an extra isocyanide ligand coordinating in an unusual fashion through the C=N group to three Pt atoms with four electrons. The effect of this is to produce in the structure a planar cyclic $CNPt_3$ unit.

L = tertiary phosphine

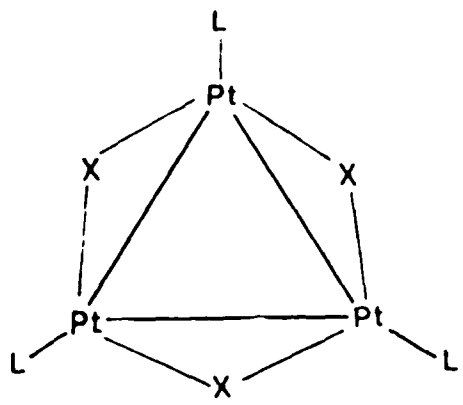

$Pt_3(CO)_3L_3$ 42e

X = CO, SO_2

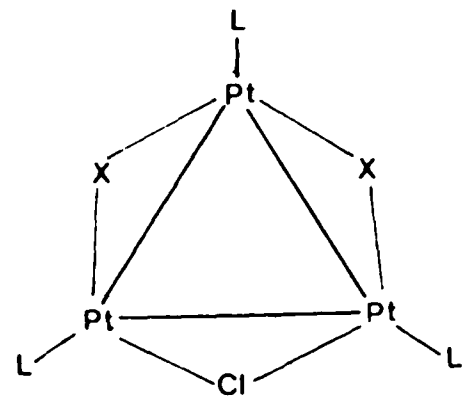

$Pt_3(SO_2)_2(Cl)L_3$ 44e

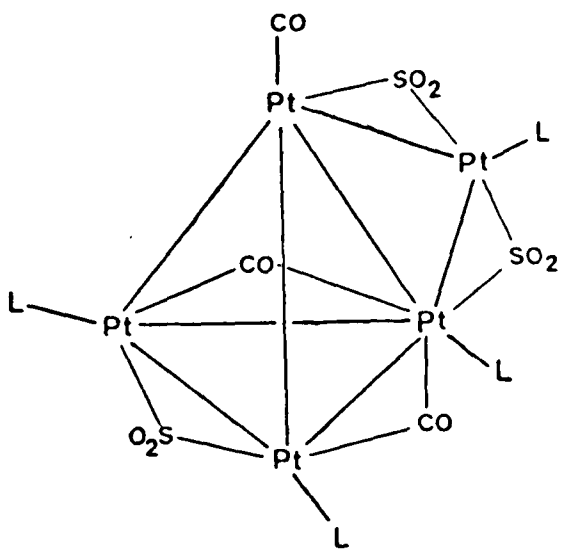

$Pt_5(CO)_3(SO_2)_3(PPh_3)_4$ 70e

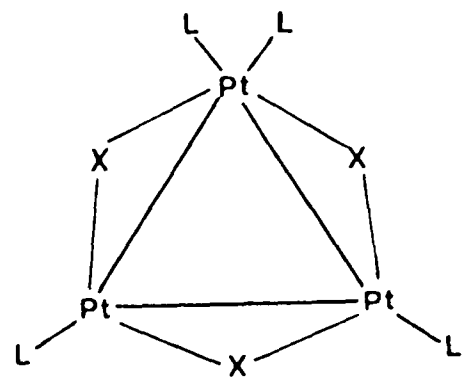

$Pt_3(CO)_3L_4$ 44e

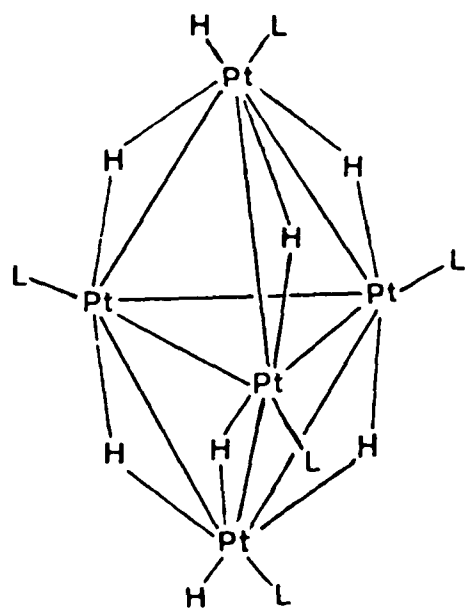

$Pt_5(H)_8(PBu^t_2Ph)_5$ 68e

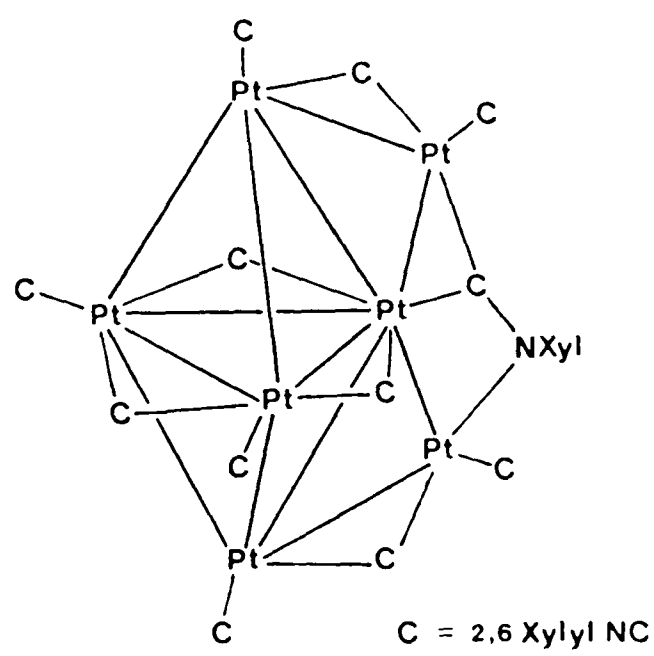

$Pt_7(2,6\ Me_2C_6H_3NC)_{12}$ 96e

Figure 1.4 Polyhedral electron counting in platinum cluster compounds

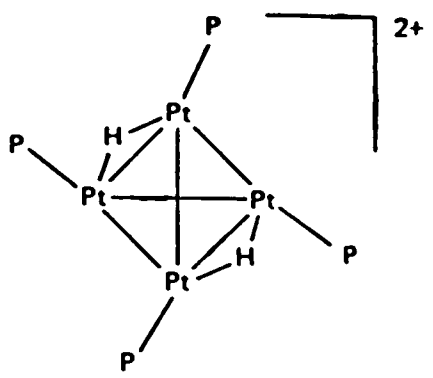

$[Pt_4(\mu\text{-}H)_2(PBu^t_3)_4](BF_4)_2$
48 electrons, average d(Pt–Pt) 2.68(5) Å

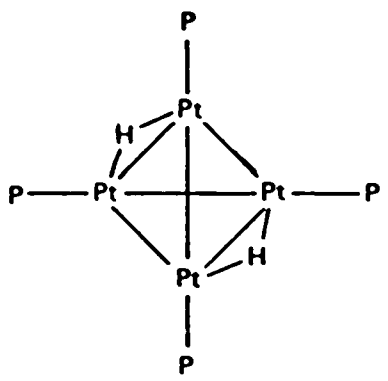

$[Pt_4(\mu\text{-}H)_2(PBu^t_3)_4]$
50 electrons, average d(Pt–Pt) 2.74(3) Å

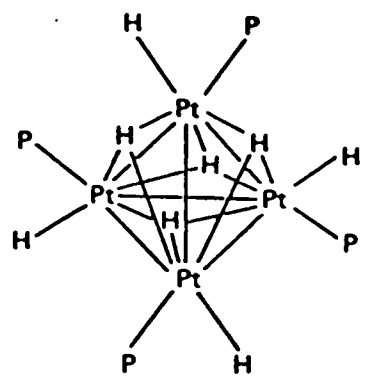

$[Pt_4(\mu_3\text{-}H)_4H_4(PPr^i_2Ph)_4$
56 electrons, average d(Pt–Pt) 2.94(5) Å

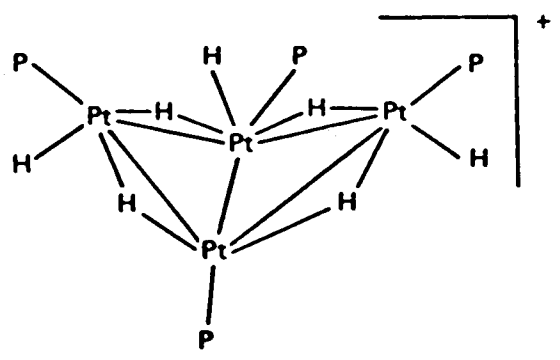

$[Pt_4(\mu\text{-}H)_4H_3(PBu^t_3)_4](BPh_4)$
54 electrons, average d(Pt–Pt) 2.78(4) Å

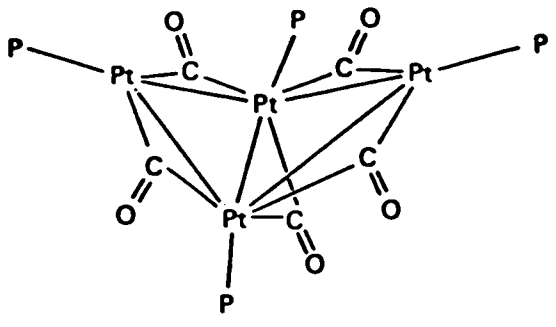

$[Pt_4(\mu\text{-}CO)_5(PMe_2Ph)_4]$
58 electrons, average d(Pt–Pt)
2.760(8) Å (orthorhombic)
2.735(9) Å (monoclinic)

Figure 1.5 Some tetranuclear platinum cluster compounds

1.5.1 Bonding in platinum cluster compounds

In order to rationalise the structures observed in platinum cluster compounds molecular orbital calculations have been performed on triangular Pt_3L_6 (L = tertiary phosphine) complexes.[45] By considering the triangle in terms of three angular PtL_2 fragments, two possible conformations are found, having skeletal molecular orbitals as shown in Figure 1.6. The calculations and theoretical basis for this and similar results are beyond the scope of this work, but it is instructive to note that while the latitudinal conformer (ligands in the Pt_3 plane) has three bonding skeletal orbitals, the longitudinal conformer (ligands out of the Pt_3 plane) has only two. Occupation of these molecular orbitals leads to the prediction of a 42 electron count for the latitudinal conformer and a 40 electron count for the longitudinal conformer, that is Pt_3L_6 and $Pt_3L_6^{2+}$ respectively. Since the former has an additional electron pair involved in skeletal bonding, it can be expected to be the preferred structure.

The frontier orbitals of the angular PtL(CO) fragment are very similar to those of PtL_2 except that the CO ligand provides extra low-lying π-acceptor orbitals. It is not surprising, therefore, that the molecular orbitals of the cluster $[Pt_3(CO)_3L_3]$, in the latitudinal conformation, are directly analogous to those of Pt_3L_6. In the context of this work the next step is to rearrange the CO ligands into bridging positions to generate the cluster $[Pt_3(\mu\text{-}CO)_3L_3]$. This is possible because CO has in plane π^* orbitals. Further calculations demonstrate that if each μ_2-CO ligand is treated as two one-electron σ-donor ligands there is little change in the frontier orbitals except to allow a greater proportion of d character in some of them (see Figure 1.7). The overall effect is that the bridging carbonyl

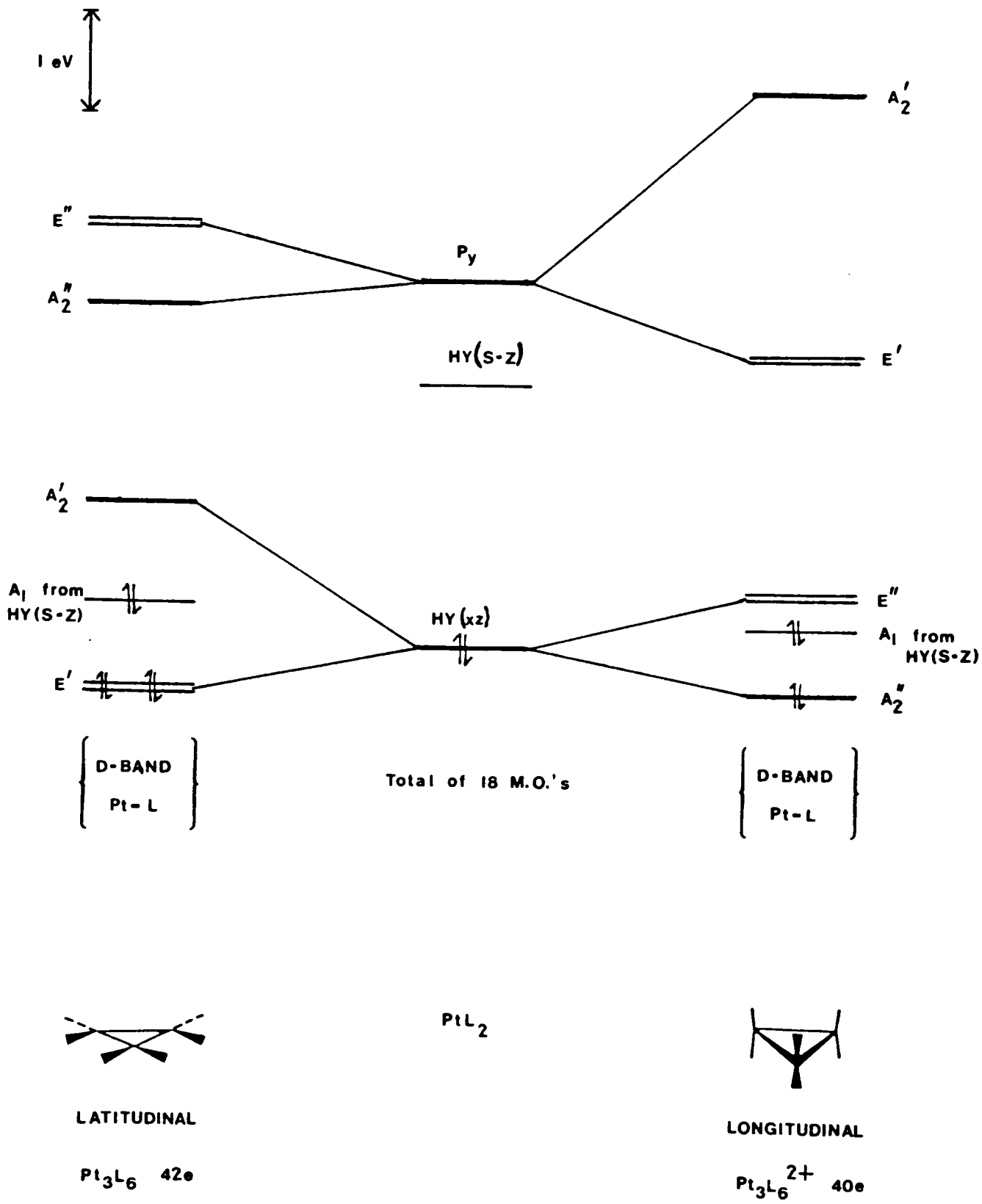

Figure 1.6 Schematic representation of the skeletal molecular orbitals for latitudinal and longitudinal conformers of $Pt_3(PH_3)_6$.

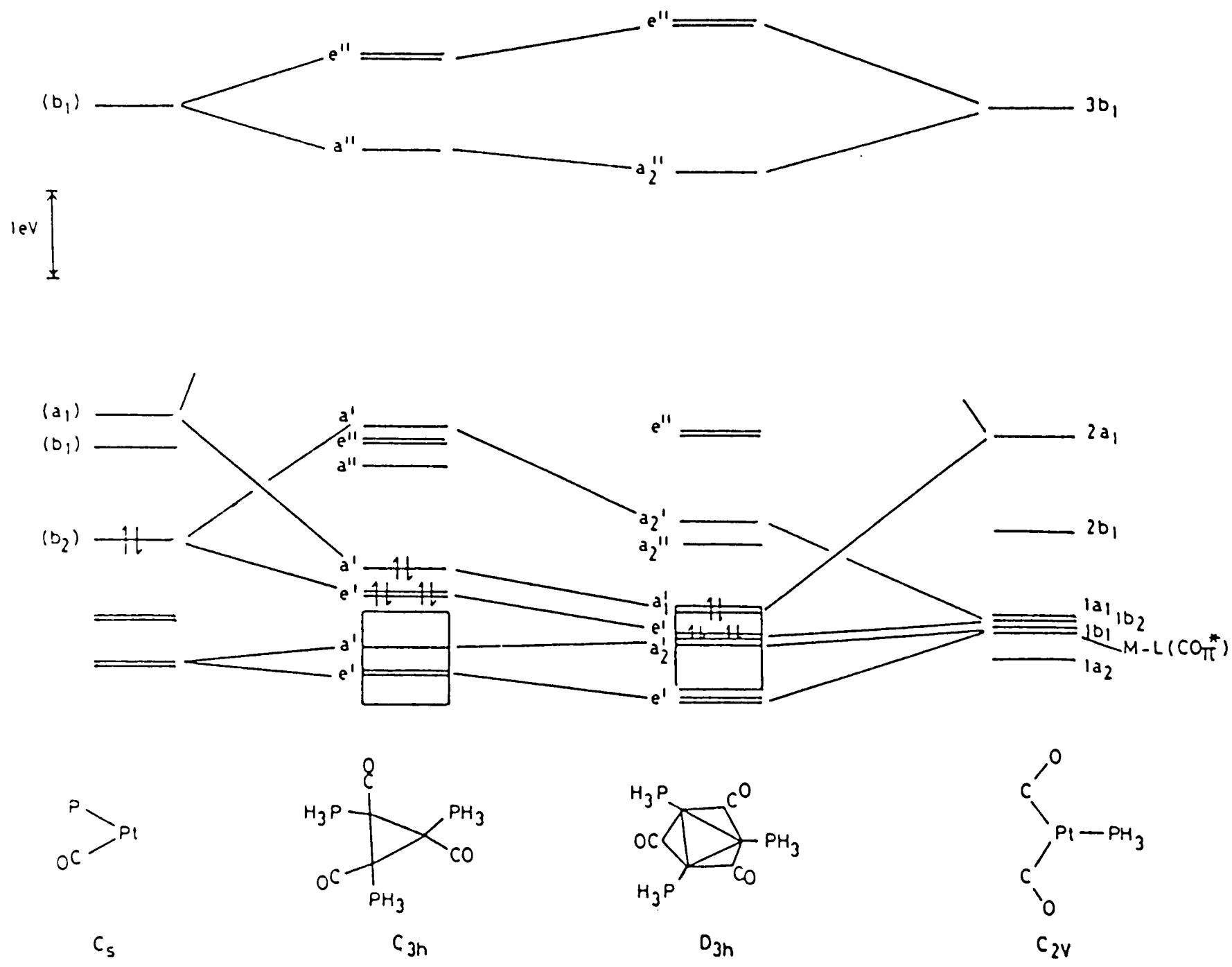

Figure 1.7 A comparison of the cluster MO's of $[Pt_3(CO)_3(PH_3)_3]$ and $[Pt_3(\mu\text{-}CO)_3(PH_3)_3]$

geometry is more stable than the latitudinal Pt_3L_6 structure, to the extent that all known cluster compounds of this type adopt the bridging geometry. This, then, is the rationale behind the 42 electron Pt_3 triangular cluster from which the other sructures are derived.

A number of Pt_3 triangular clusters are known which have 44 skeletal electrons. These fall into two groups. One type has the same arrangement of ligands , three terminal and three bridging, as the 42 electron compounds except that one or more of the bridging ligands provide the two extra electrons. The other type owes its extra electrons to a fourth terminal ligand. The familiar examples of this type of compound are the clusters $[Pt_3(\mu\text{-}CO)_3L_4]$ in which one of the platinum atoms is formally an 18 electron centre compared with the usual 16 electrons.

The key to the occurrence of 44 electron Pt_3 triangles is the LUMO of the $[Pt_3(\mu\text{-}X)_3L_3]$ species.[46] If X has suitable π^* orbitals perpendicular to the Pt_3 plane, then the a_2'' orbital is the LUMO and can often be stabilised for occupation (see Figure 1.7). The existence of a number of compounds has been rationalised on this basis. The anion $[Pt_3(\mu\text{-}CO)_3(CO)_3]^{2-}$ (identified in solution at least[39]) has the extra electron pair in this a_2'' orbital, which plays an important role in the formation of the stacked carbonyl anion clusters.[47] The neutral tetrakis-phosphine clusters, $[Pt_3(\mu\text{-}CO)_3L_4]$, are also accounted for on the basis that the fourth phosphine can interact at a platinum centre via the a_2'' orbital.

For bridging ligands such as SO_2, the a_2'' orbital is not stabilised. The 44 electron triangles can be formed by the use of the a_2' orbital (see Figure 1.7). This orbital is stabilised by certain bridging ligands to the extent that it becomes the LUMO with an energy

low enough for occupation. The a_2 orbital lies in the plane of the Pt_3 triangle and this fact is exploited in Chapter 2 for the synthesis of the chloride bridged Pt_3 anions. With regard to neutral clusters, it is possible to achieve a 44 electron cluster without occupation of the a_2 orbital. In Section 1.2 it was observed that in $[Pt_3(\mu\text{-}PPh_2)_3(Ph)(PPh_3)_2]$, there is a change of geometry from a closed to an open triangle. The extra electron pair appears to be localised between two platinum centres with concomitant increase in their separation to a non-bonding distance.

1.5.2 X-ray crystallographic studies

As the discussion in Section 1.4 has indicated, the use of X-ray crystallography is the final authority in the determination of solid state structures, especially for high nuclearity clusters where it is often difficult to gain much structural information by other means. A large number of Pt_3 triangular clusters have been characterised in the solid state and some representative examples are shown in Table 1.2 together with their Pt-Pt bond distances.

The triangular clusters with 42 skeletal electrons are all approximately equilateral and their Pt-Pt distances generally lie at the lower end of the observed range. Larger Pt-Pt distances are associated with bulkier bridging ligands such as SO_2. For $[Pt_3(\mu\text{-}Ph)(\mu\text{-}PPh_2)(\mu\text{-}SO_2)(PPh_3)_3]$, the Pt-Pt bond lengths reflect the number of electrons contributed by each bridging ligand (see Table 1.3).

	d(Pt-Pt)/Å	reference
<u>42 electron compounds</u>		
$[Pt_3(\mu\text{-}CO)_3(PCy_3)_3]$	2.656, 2.656, 2.653	48
$[Pt_3(\mu\text{-}SO_2)_3(PPh_3)_3]$	2.695, 2.695, 2.712	49
$[Pt_3(\mu\text{-}Ph)(\mu\text{-}PPh_2)(\mu\text{-}SO_2)(PPh_3)_3]$	2.781, 2.696, 2.816	50
$[Pt_3(\mu\text{-}CNBu^t)_3(CNBu^t)_3]$	2.629, 2.637, 2.629	17
$[Pt_3(\mu\text{-}H)(\mu\text{-}PPh_2)_2(PPh_3)_3]^+$	2.82 average	37
$[Pt_3(\mu\text{-}H)(\mu\text{-}PPh_2)_2(PPh_3)_3]^+$	2.796, 2.795, 2.638	16
<u>43 electron compound</u>		
$[Pt_3\{\mu\text{-}Fe(CO)_4\}_3(CO)_3]^-$	2.66 average	51
<u>44 electron compounds</u>		
$[Pt_3(\mu\text{-}CO)_3(PCy_3)_4]$	2.675, 2.736, 2.714	52
$[Pt_3(cod)_3(SnCl_3)_2]$	2.58 average	53
$[Pt_3\{\mu\text{-}Fe(CO)_4\}_3(CO)_3]^{2-}$	2.75 average	51
$[Pt_3(\mu\text{-}PPh_2)_3(Ph)(PPh_3)_2]$	2.785, 2.785, 3.630	54
$[Pt_3(\mu\text{-}SO_2)_3(PCy_3)_2(dppp)]$	2.753, 2.826, 2.811	55

<u>Table 1.2</u> Bond lengths in some triangulo- platinum cluster compounds

ligand	No. of electrons donated to cluster	d(Pt-Pt) (Å)
μ-Ph	1	2.70
μ-SO_2	2	2.78
μ-PPh_2	3	2.82

Table 1.3 Correlation of bond length with ligand electron count in $[Pt_3(\mu\text{-Ph})(\mu\text{-PPh}_2)(\mu\text{-SO}_2)(PPh_3)_3]$

An increase in the number of skeletal electrons tends to give a corresponding increase in Pt-Pt bond lengths whether localised into one bond as in $[Pt_3(\mu\text{-PPh}_2)_3(Ph)(PPh_3)_2]$, or shared over all bonds as in $[Pt_3(\mu\text{-SO}_2)_3(PCy_3)_2(dppp)]$. This same phenomenon is found in the tetranuclear clusters illustrated in Figure 1.5. A comparison of the four clusters based on phosphine and bridging hydride ligands reveals a steady increase in d(Pt-Pt) as the electron count rises from 48 to 56.

From the few structurally characterised pentanuclear clusters, a comparison of $[Pt_5(CO)(\mu\text{-CO})_2(\mu\text{-SO}_2)_3(PPh_3)_4]$ and $[Pt_5(CO)(\mu\text{-CO})_5(PPh_3)_4]$, both 70 electron clusters, highlights the question: At what metal-metal separation does a bond cease to exist? In the former compound the unbridged Pt-Pt distances (see Figure 1.4) have been measured at about 2.81Å and 2.88Å and are sufficiently similar to the other Pt-Pt distances (2.75 - 2.83Å) to justify a description of the cluster as edge-bridged tetrahedral. In the latter compound the unbridged Pt-Pt distances are quite long (average 2.92Å) and it has been suggested that the cluster is better described in terms of two vertex sharing triangles.

X-ray crystallographic data on higher nuclearity cluster

compounds goes further to support the idea of platinum cluster chemistry based on the Pt_3 unit. The carbonyl anions of Chini[47] are made up from familiar Pt_3 triangles stacked at separations greater than accepted Pt-Pt bonding distances. There are also high nuclearity three dimensional networks based on Pt_3 triangles which lead to the close packed structures observed for Pt_{26} and Pt_{38} clusters.[5]

A triplatinum cluster has been characterised which does not have a triangular structure. The compound $[Pt_3(PPh_3)_2(2,6\text{-CNXylyl})_6](PF_6)_2$, which has been synthesised in two different ways,[56,57] has a linear structure with the two P atoms and the three Pt atoms making up a five atom chain:

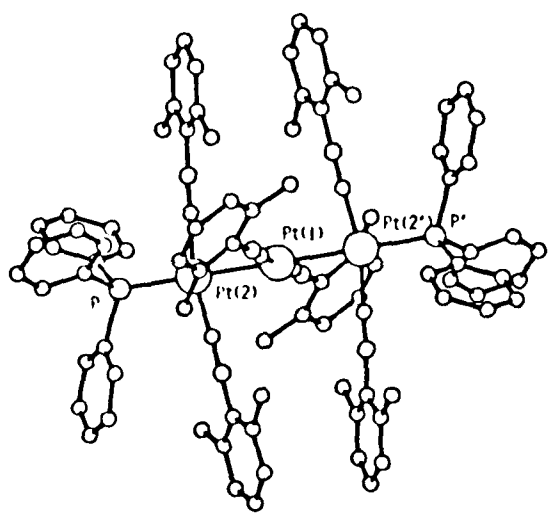

Each Pt atom exhibits approximate square planar geometry and the square planes are twisted away from each other such that neighbouring five atom planes are 81 apart. The Pt-Pt distance of (2.64Å) is similar to those found in the triangular clusters. The linear cluster reacts with dppm to give an A-frame complex:

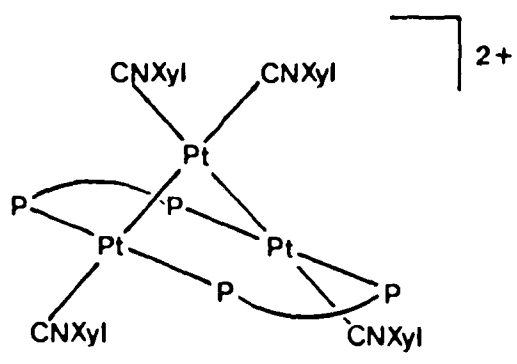

The Pt atoms retain their square planar geometry but the dppm ligand bridges the ends of the Pt_3 unit to give a Pt-Pt-Pt bond angle of 80°. This compound, therefore, resembles the edge-opened triangular cluster $[Pt_3(\mu\text{-}PPh_2)_3(Ph)(PPh_3)_2]$ (see Section 1.2). Both complexes have 44 skeletal electrons and both have two Pt-Pt bonds and one long non-bonded Pt-Pt distance. In the A-frame complex the non-bonded distance is 3.30Å which is shorter than that in the phosphido- complex (3.63Å).

1.5.3 Steric and electronic effects

The emphasis in this Section placed on bonding in platinum cluster compounds might suggest that electronic effects tend to dominate the course of cluster forming reactions. Support for this suggestion lies in the observation that the bridging ligands in the clusters $[Pt_3(\mu\text{-}X)_3(PR_3)_3]$ are coplanar with the metal triangle, irrespective of the phosphine, giving maximum overlap of cluster orbitals. In contrast, the SO_2 and PCy_3 ligands in $[Pt_3(\mu\text{-}SO_2)_3(PCy_3)_2(dppp)]$ are all bent out of the plane of the metal triangle. The long Pt-Pt bonds in this compound also suggest a strong steric influence by the ligands.[55]

Steric effects have been cited as the reason for the incomplete substitution of CO by SO_2 in $[Pt_5(CO)(\mu\text{-}CO)_5(PPh_3)_4]$[58] as well as being a major influence on the course of the reaction of $[Pt_3(\mu\text{-}CO)_3(PCy_3)_3]$ with 2,6-xylyl isocyanide.[59] In most platinum cluster compounds it is found that the disposition of the bridging ligands relative to the metal skeleton can be described in terms of idealised fragments derived from the trigonal bipyramid or square pyramid,[8] as would be expected from consideration of electronic factors alone.

1.6 Structures and bonding in hetermetallic platinum-gold clusters

Heterometallic platinum-gold clusters are a recent discovery and few examples have been structurally characterised. X-ray crystallographic analyses have been carried out on six such cluster compounds, the syntheses of which were described in Section 1.3. The structures of these compounds, as shown in Figure 1.8, bear a strong resemblance to the structures described in the previous Section for homometallic platinum clusters. All of the compounds are based on triangular units and have similar skeletal electron counts to their homometallic platinum counterparts.

1.6.1 Structures containing the Au-Au moiety

Structures I and II in Figure 1.8 may be seen as a combination of T-shaped PtL_3 fragments and Au_2L_2 fragments.[60] The PtL_3 fragment is isolobal with $AuPR_3$, CH_3 and similar fragments[19] and is capable of forming either localised or multicentred bonding as illustrated below.

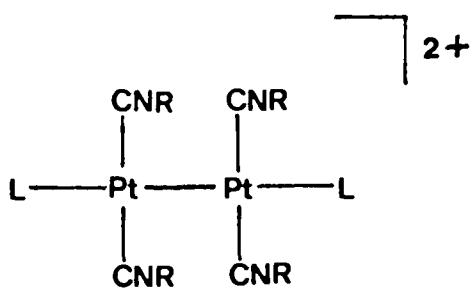

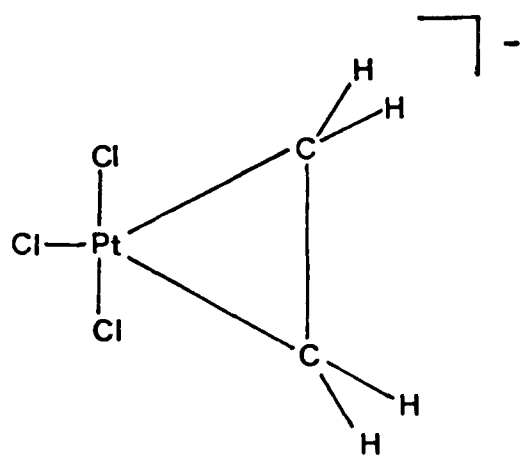

In I, the PtL_3 unit symmetrically bridges the $Au_2(PPh_3)_2$ moiety giving a distorted trigonal bipyramidal geometry about platinum and is structurally analogous to the olefin complex above. The main bonding interaction between the PtL_3 and Au_2L_2 units arises from the formation

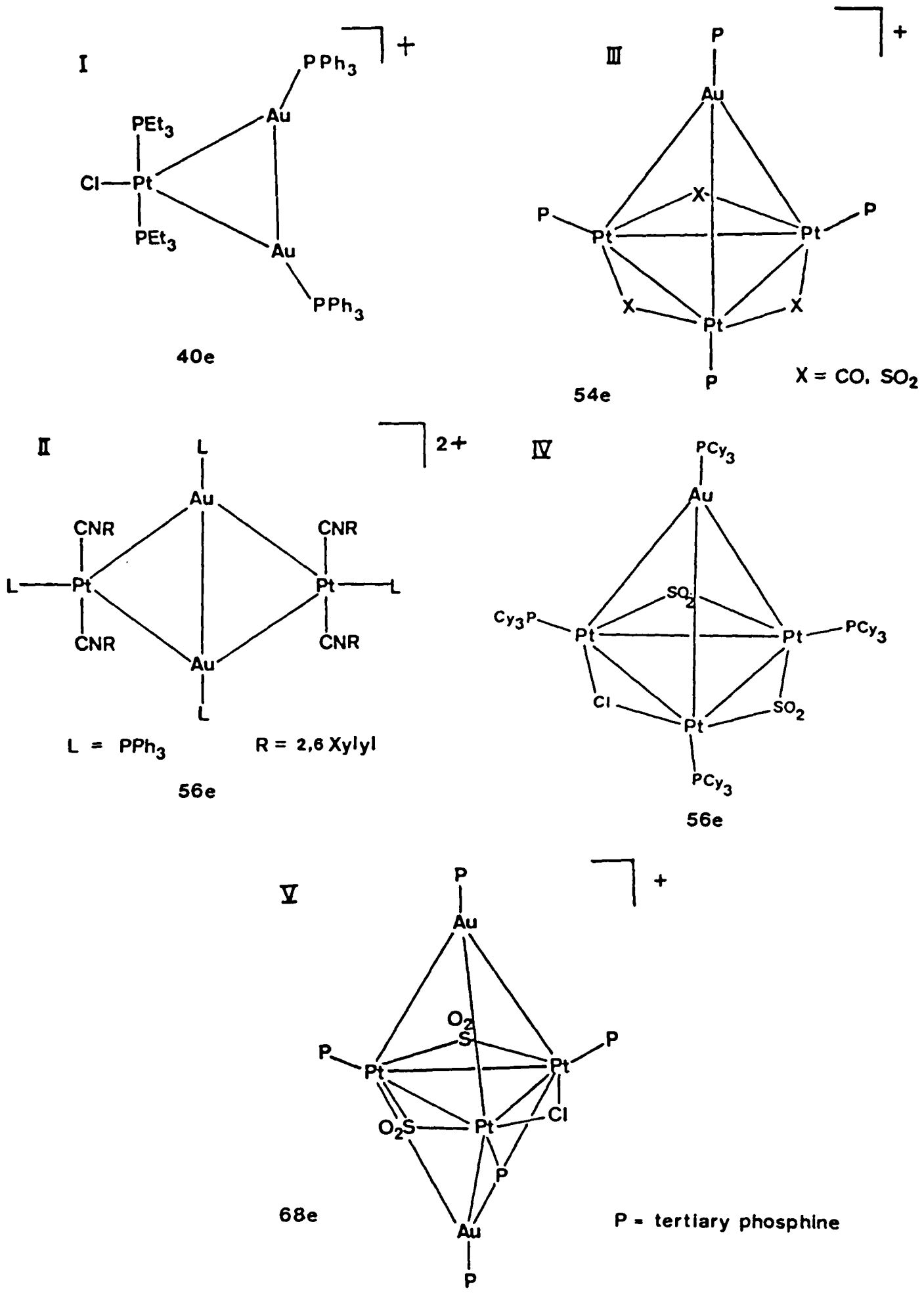

Figure 1.8 Some heterometallic platinum-gold cluster compounds

of a 3-centre 2-electron bond which is stabilised by bending the Au_2L_2 fragment such that the Au-L bonds point towards the centre of the $PtAu_2$ triangle. This is demonstrated by the bond data for $[PtAu_2(PEt_3)_2Cl]^+$ given in Table 1.4.

In II two PtL_3 fragments are coordinated to a linear Au_2L_2 fragment. The X-ray crystallographic analysis[26] of $[Pt_2Au_2(PPh_3)_4(CNXyl)_4]^{2+}$ has revealed that this coordination is not symmetric and that the platinum atoms are displaced towards one of the gold atoms. The extent of this distortion is shown by the bond data given in Table 1.4. The Au-Pt distances for one gold atom are at least 0.2Å shorter than those for the other which are at the limits of distances for recognised metal-metal bonding. In contrast, the Au-Au distance (2.59Å) is particularly short. This is because the two Au-L bonds are constrained to lie in a plane between the two $PtAu_2$ triangles.

1.6.2 Structures based on Pt_3 triangular units

The platinum-gold clusters III - V in Figure 1.8 are all based on triangular $[Pt_3(\mu\text{-}X)_3(PR_3)_3]$ units which have either been capped by one $AuPR_3^+$ fragment leading to 54 or 56 valence electron tetrahedral clusters or alternatively by two $AuPR_3^+$ fragments leading to a 68 valence electron trigonal bipyramidal cluster. The bonding in the Pt_3 triangular unit was discussed in Section 1.5.1. Figure 1.7 in that Section showed that the frontier orbitals are of a_1 (HOMO) and a_2 (LUMO) symmetry. In a capping reaction between a Pt_3 triangular cluster and an AuL^+ moiety bonding interactions arise between the a_1 orbitals of each component.[60] These interactions are stronger if the ligands on the Pt_3 triangle are bent away from the capping gold atom

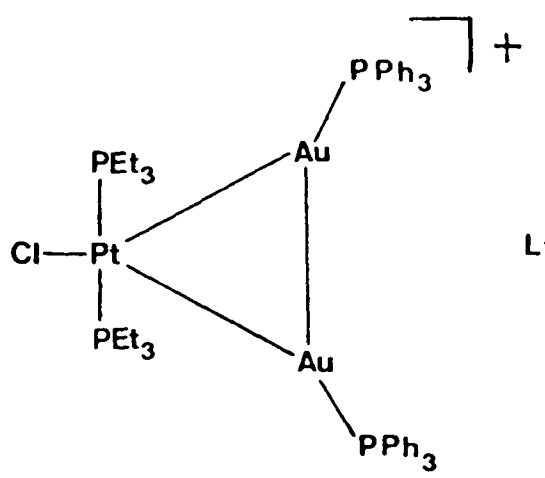

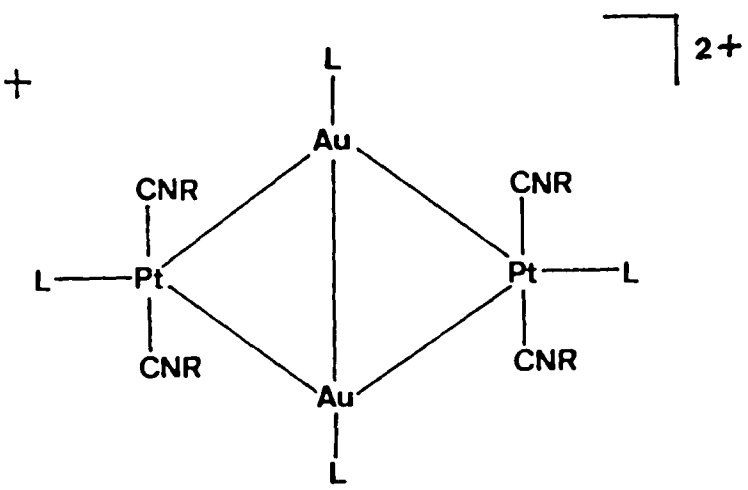

d(Pt-Au)	2.601, 2.600Å	2.717, 2.711Å 3.026, 2.922
d(Au-Au)	2.737Å	2.590Å
Au Pt Pt	58.2°	69.5, 58.3° 57.2, 66.9
Pt Au Au	63.5°	53.3, 64.6°
Au Pt Pt	—	135.0, 114.9°

Table 1.4 Metal-metal bond data for two clusters containing the Au-Au moiety

to allow greater orbital overlap. Such distortions are observed in the solid state for $[Pt_3(\mu\text{-}CO)_3(PCy_3)_3AuPCy_3]^+$ and the related clusters.[23] Since there is little interaction between the a_1 orbital of the AuL^+ fragment with either a_2 orbital of the Pt_3 triangle, the cluster bonding in these compounds is based on a 4-centre 2-electron bond involving only the a_1 orbitals.

The a_2 orbitals of the Pt_3 triangle are unaffected by AuL^+ capping and so retain the bonding characteristics described in Section 1.5.1. Therefore, the stabilisation of the a_2' orbital by substitution of one bridging SO_2 ligand by Cl^- allows the formation of the 56 electron cluster IV which parallels the 44 electron Pt_3 clusters. It is perhaps surprising that both the 54 and 56 electron Pt_3Au clusters should have tetrahedral geometries since generally the addition of an electron pair to a tetrahedral structure results in a skeletal rearrangment to the "butterfly" structure.

Table 1.5 summarises bond length data for the known platinum-gold clusters and related triangulo- Pt_3 clusters. The data confirm that the Pt_3Au clusters have tetrahedral structures with Pt-Au bonds slightly longer than Pt-Pt bonds. Capping of the 42 electron $[Pt_3(\mu\text{-}X)_3L_3]$ cluster by AuL^+ to generate $[Pt_3Au(\mu\text{-}X)_3L_4]^+$ leads to a lengthening of the Pt-Pt bonds. Further lengthening is caused by addition of another electron pair into the a_2' orbital which is Pt-Pt antibonding.

Besides forming 54 and 56 electron Pt_3Au clusters it is also possible to cap the Pt_3 triangle on both sides with AuL^+ fragments to generate the trigonal bipyramidal Pt_3Au_2 cluster (V). The major bonding interactions occur between the a_1' in-phase combination of hybrid orbitals from the two AuL^+ fragments and the same a_1 orbital

	Pt-Pt (Å)	Pt-Au (Å)	reference
42 electrons			
$[Pt_3(SO_2)_3(PPh_3)_3]$	2.695(1) - 2.712(1)	—	49
$[Pt_3(CO)_3(PCy_3)_3]$	2.653(2) - 2.656(2)	—	48
54 electrons			
$[Pt_3Au(CO)_2(SO_2)(PCy_3)_4]^+$	2.667(4) - 2.746(1)	2.755(1) - 2.759(5)	24
$[Pt_3Au(CO)_3(PCy_3)_4]^+$	2.696(9) average	2.758(5) average	23
56 electrons			
$[Pt_3Au(SO_2)_2(Cl)(PCy_3)_3\{P(p\text{-}FC_6H_4)_3\}]$	2.851(1) - 2.869(1)	2.766(1) - 2.771(1)	60
68 electrons			
$[Pt_3Au_2(SO_2)_2(Cl)(PCy_3)_3\{P(p\text{-}FC_6H_4)_3\}_2]^+$	2.884(2) - 2.887(2)	2.772(2) - 2.803(2)	60

Table 1.5 Metal-metal bond lengths in platinum-gold clusters

(HOMO) of the Pt_3 triangle descibed above. There is additionally a small interaction between the a_2'' combination of the AuL^+ fragments and the high lying a_2'' molecular orbital of the Pt_3 triangle. The Pt_3Au_2 cluster bonding has 4 skeletal electron pairs, the fourth being provided by substitution of a bridging SO_2 ligand by Cl^-. The delocalisation of the a_1 cluster orbital over five metal atoms compared with four in the tetrahedral Pt_3Au clusters causes a further lengthening of the metal-metal bond distances (see Table 1.5).

1.7 Structures of platinum sulphido- complexes

Platinum does not form any simple mononuclear sulphido- complexes containing the unit Pt=S. The existence of such compounds would require the formation of d_π-p_π bonds between the sulphur and the metal atoms which is prevented by the almost complete d shell in platinum. Consequently, the sulphido- ligand uses its electron pairs in forming bridges, usually to other metal atoms. There are also a number of platinum polysulphido- complexes in which sulphur demonstrates its tendency to catenate and X-ray crystallography has been used to confirm the existence of the platinum metallocycles shown in Figure 1.9 below. The $[PtS_{15}]^{2-}$ anion contains three PtS_5 rings[61] and a PtS_4 ring has been found in the complex $[(dppe)PtS_4]$.[62]

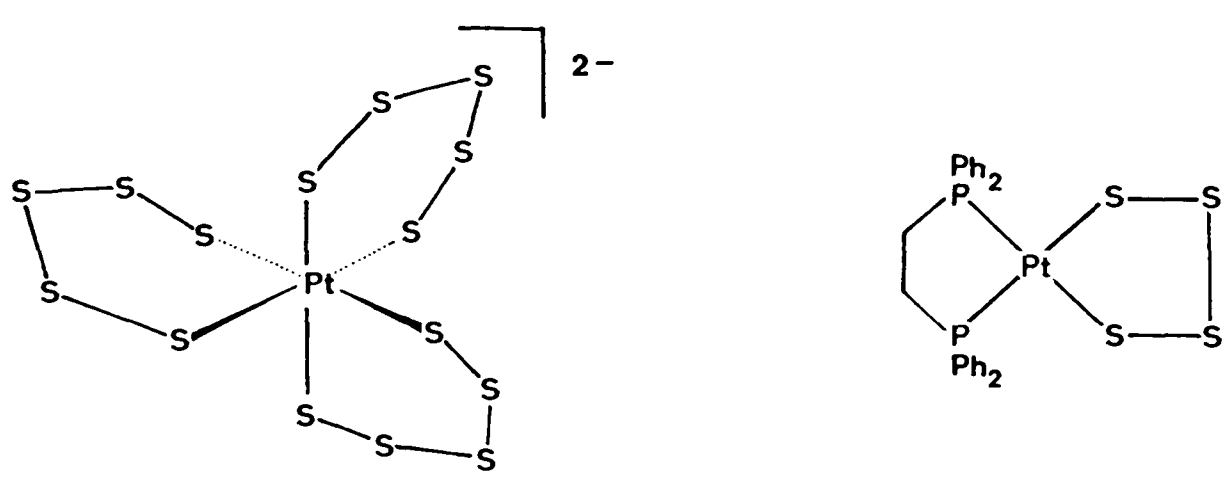

Figure 1.9 Platinum polysulphido- complexes

1.7.1 Complexes derived from $[Pt_2(\mu\text{-}S)_2(PPh_3)_4]$

The synthesis of $[Pt_2(\mu\text{-}S)_2(PPh_3)_4]$ was described in Section 1.3.3 as an important example of a compound with the potential for generating a wide range of heterometallic aggregates through coordination to its two sulphur atoms. The structure of this complex consists of two approximately square planar PtL_2S_2 moieties "hinged" at the bridging sulphur atoms. The angle between the planes is approximately 125° and the separation of the sulphur atoms is approximately 3.04Å. This arrangement allows the sulphur atoms to act either as separate ligands or together as a bidentate ligand. A number of heterometallic complexes have been characterised in which $[Pt_2(\mu\text{-}S)_2(PPh_3)_4]$ coordinates to other metals in a variety of ways. It is often found that a second $[Pt_2(\mu\text{-}S)_2(PPh_3)_4]$ molecule can be coordinated to the same metal, resulting in aggregates of up to six metal atoms. Figure 1.10 shows some examples in which the platinum complex acts as a bidentate ligand. The geometry about the sulphur atoms in all cases is approximately pyramidal. The metal atoms attached to the chelating sulphido- ligands exhibit both square planar [for Pd(II) and Rh(I)] and tetrahedral [for Hg(II)] geometries. The separations of the metal atoms, typically 3.1 - 3.2Å, are all sufficiently large to preclude the existence of metal-metal bonding. The structure of the hexanuclear complex (III) is noteworthy because it resembles a range of binuclear chloro- bridged complexes:

M = Pt, Pd
$L_1 = PR_3$; L_2 = Cl

M = Rh
$L_1 = L_2 = CO, C_2H_4, \frac{1}{2}(cod)$

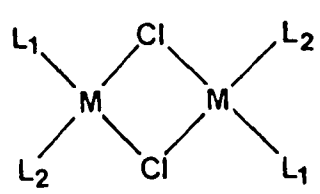

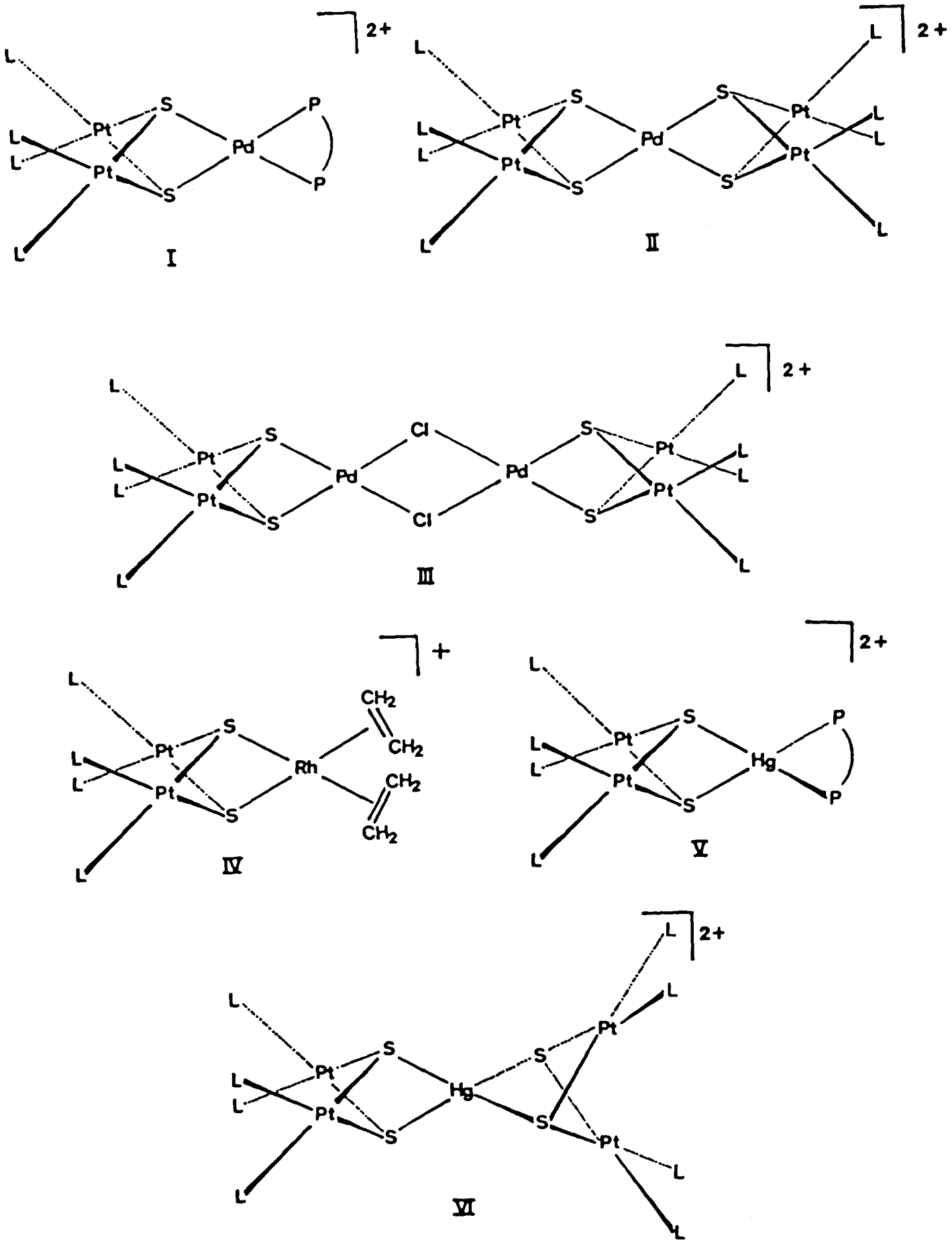

Figure 1.10 Some heterometallic derivatives of $[Pt_2(\mu\text{-}S)_2(PPh_3)_4]$

The M_2Cl_2 bridges of such complexes are readily cleaved by donor molecules.

$[Pt_2(\mu\text{-}S)_2(PPh_3)_4]$ has been reacted with $AgBF_4$ resulting in the formation of the complex illustrated below.[33]

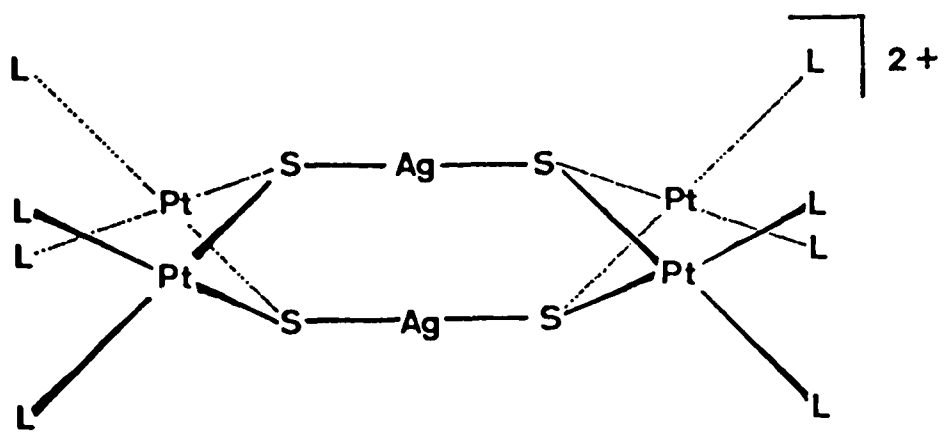

In this complex the μ_3-sulphido ligands from the same $Pt_2(\mu\text{-}S)_2$ unit are coordinated to separate silver atoms in contrast to the complexes shown in Figure 1.10. This allows Ag(I), a d^{10} system, approximately to retain its preferred linear geometry. In consequence, the geometry about the sulphido- ligands is distorted away from pyramidal. A striking feature of the structure is the Ag-Ag distance of 2.82Å which is significantly shorter than the metal-metal distance in elemental silver (2.89Å) and suggests the existence of metal-metal bonding. The Pt-Ag distances are particularly long (3.5 - 3.9Å) and so Pt-Ag bonds can be discounted.

1.7.2 Platinum sulphido complexes with a Pt-Pt bond

The chemistry of the complex $[Pt_2(\mu\text{-}S)(CO)(PPh_3)_3]$ is the subject of the investigations described in Chapter 4 and so the detailed structure of this compound has been given some attention. An X-ray crystallographic analysis of the structure is discussed in Chapter 4 from which only the main points will be mentioned here.

The complex $[Pt_2(\mu\text{-}S)(CO)(PPh_3)_3]$ is an example of a small but

growing number of compounds containing the $Pt_2(\mu\text{-}S)$ triangular unit. The Pt-Pt distance is 2.65Å which is typical of a Pt-Pt bond. The Pt-S distances are 2.26 and 2.27Å with the slightly shorter bond lying trans to the carbonyl group. The molecule is approximately planar but the coordination geometry at the metal atoms is necessarily distorted from square planar (see Section 1.3.3).

The structure of a related complex $[Pt_2(\mu\text{-}S)(2,4,6\text{-}Bu^t{}_3C_6H_2NC)_4]$ has recently been reported.[63] This compound also contains the $Pt_2(\mu\text{-}S)$ triangular unit with a Pt-Pt bond of 2.60Å which is shorter than that found in $[Pt_2(\mu\text{-}S)(CO)(PPh_3)_3]$. The isocyanide ligands used in this compound are particularly bulky but the C-N-C bond angles are still approximately linear.

1.8 Summary

It is clear that some structural and chemical relationships exist between transition metal cluster compounds and the coordination of molecular species on metal surfaces. The need to understand better the nature of cluster compounds has prompted much research into both synthetic methods and the determination of structures. Sufficient information is becoming available for rational syntheses of platinum cluster compounds to be devised and this idea is taken up in this Thesis. A variety of methods are available for characterising cluster compounds and it is often possible to make an unambiguous structure determination without having to resort to single crystal X-ray crystallography. Much progress has also been made towards understanding the bonding in cluster compounds and there is good agreement between recent theoretical proposals and the available structural data.

CHAPTER TWO

SYNTHESIS AND CHARACTERISATION OF HOMOMETALLIC TRIANGULO-CLUSTER COMPOUNDS OF PLATINUM

2.1 Introduction

A large number of homonuclear cluster compounds of platinum are now known, of which the most abundant group is that with three metal atoms in a triangular arrangement. A growing number of higher nuclearity cluster compounds have been characterised containing from four up to 52 platinum atoms. A recent review[8] describes the structures of some of these compounds. The interesting feature common to all these structures is the occurrence of the Pt_3 triangular unit. In the first instance, platinum shows a strong tendency to form Pt_3 triangular clusters and secondly, when higher nuclearity clusters are formed, they seem to be built up from triangular units. Examples illustrating this point are given in Figure 2.1. The Pt_4 "butterfly" cluster is built from two edge sharing triangles and the Pt_5 cluster can be viewed either as an edge bridged tetrahedron or as a pair of triangles sharing a common vertex. Specific examples lend themselves to one or other of these descriptions according to the Pt-Pt distance on the two unbridged edges. Shorter distances give structures which more closely fit the tetrahedral description whereas longer distances give structures which resemble more closely a pair of triangles.

This Chapter describes the synthesis and properties of a range of homonuclear cluster compounds of platinum which are based on the Pt_3 triangular unit. The particular compounds of interest to this Thesis are those which are stabilised by tertiary phosphine ligands and by unsaturated bridging ligands such as CO or SO_2.

$Pt_4(CO)_5(PPh_3)_4$

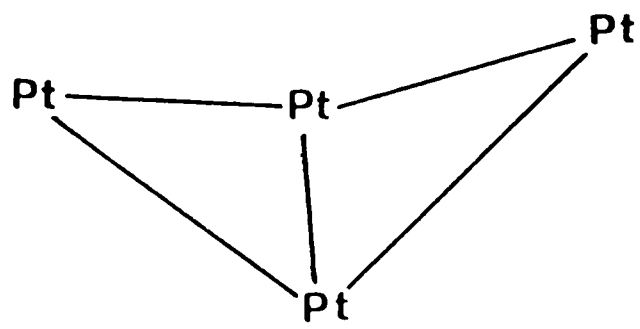

$Pt_5(CO)_6(PPh_3)_4$

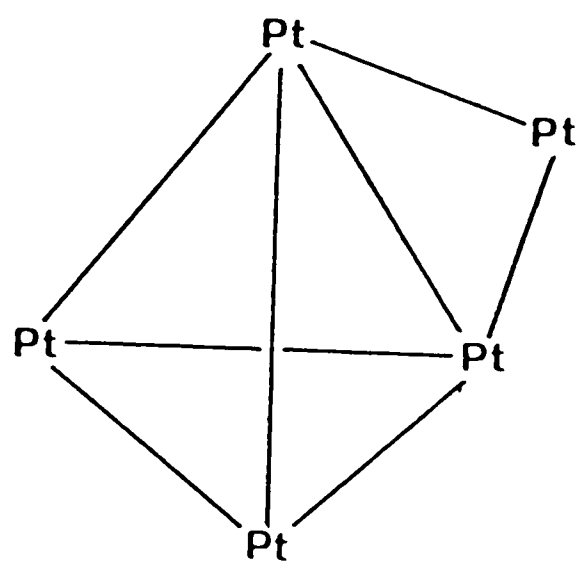

$Pt_7(2,6\ Me_2C_6H_3NC)_{12}$

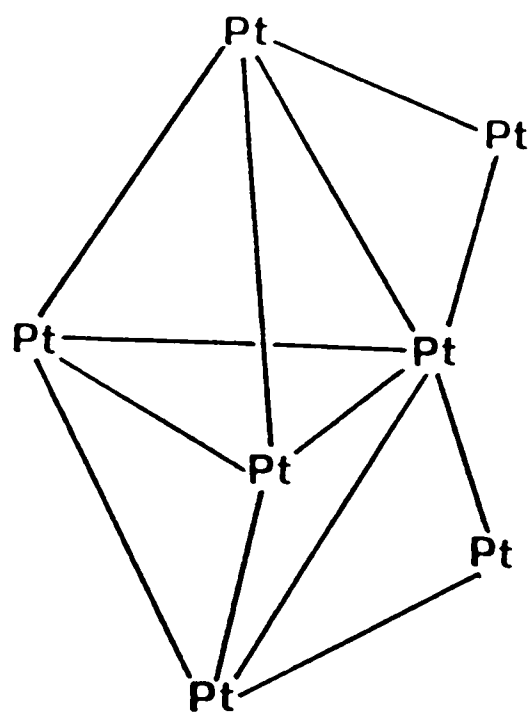

Figure 2.1 Cluster compounds of platinum based on the Pt_3 triangular unit.

2.1.1 Synthesis of carbonyl phosphine cluster compounds of platinum

A number of clusters of the type $[Pt_3(\mu\text{-}CO)_3(PR_3)_n]$ (n = 3 or 4) have been prepared and structurally characterised[12,48,52] as well as higher nuclearity clusters of the type $[Pt_4(\mu\text{-}CO)_5(PR_3)_4]$[12,40,41,64] and $[Pt_5(CO)(\mu\text{-}CO)_5(PR_3)_4]$.[65,66] The chemical properties of these cluster species have not been widely reported, although Braunstein et al[67] have investigated their interconversion on chromatographic columns. To some extent the study of these compounds has been hampered by the lack of a convenient high yield general synthetic route. The reported syntheses generally start with mononuclear platinum compounds which have two coordinated phosphines per platinum. Some representative examples are shown below:

$$3(PR_3)_2PtH_2 \xrightarrow[C_6H_6]{CO} [Pt_3(\mu\text{-}CO)_3(PR_3)_3] + 3H_2 + 3PR_3 \qquad (2.1)$$

$$5(PR_3)_2Pt(CO)_2 \xrightarrow[EtOH]{heat} [Pt_3(\mu\text{-}CO)_3(PR_3)_4] + 2Pt(PR_3)_3 + 7CO \qquad (2.2)$$

$$(PR_3)_2PtCl_2 + 2NaMn(CO)_5 \longrightarrow [Pt_5(CO)(\mu\text{-}CO)_5(PR_3)_4] + [Mn_2(CO)_{10-x}(PR_3)_x] \quad (x = 0\text{-}2) \qquad (2.3)$$

All of these routes have certain disadvantages. Reactions of type (2.1)[14] are restricted to complexes of bulky phosphines, which are good σ-donors (eg R = Cy, Bu^t) for which the dihydride complex is known. In addition, the reaction is accompanied by the formation of mononuclear side products, which are difficult to separate from the cluster.[68] Reactions of the type (2.2)[12] employ platinum itself as a

phosphine scavenger, leading to low yields of the cluster which must be separated from the mononuclear by-product. Reactions of the type (2.3)[65,66] utilise air-sensitive and expensive carbonyl anions as both reducing agents and phosphine scavengers and again the platinum cluster must be separated from the phosphine substituted metal carbonyls by chromatography which can cause cluster interconversion.[67]

In Section 2.2 the development of a high yield synthetic route to platinum carbonyl phosphine cluster compounds is described. The method uses mononuclear platinum precursors with only a single phosphine ligand. This effectively eliminates many of the problems referred to above and is also economic in the use of the phosphine, an important factor when the phosphine is either expensive or difficult to obtain.

2.1.2 Synthesis of platinum phosphine cluster compounds containing the bridging SO_2 ligand

Until recently, only two cluster compounds of platinum were known which contained coordinated SO_2. A few crystals of $[Pt_3(\mu\text{-}SO_2)_3(PPh_3)_3]$ were isolated when solutions of $[Pt(SO_2)_2(PPh_3)_2]$ were allowed to stand for several months[49] and $[Pt_3(\mu\text{-}Ph)(\mu\text{-}PPh_2)(\mu\text{-}SO_2)(PPh_3)_3]$ was discovered from the thermolysis reaction of $[Pt(\eta^2\text{-}C_4H_6)(SO_2)(PPh_3)_2]$.[50] Since then, it has been found in this laboratory[46,58] that a range of compounds of the former type may be prepared by passing SO_2 gas through through warm (60°) toluene or acetone solutions of preformed carbonyl clusters. Cluster compounds of the type $[Pt_3(\mu\text{-}SO_2)_3(PR_3)_3]$ are now routinely prepared by this method:

$$\left.\begin{array}{l}[Pt_3(\mu\text{-}CO)_3(PR_3)_3] \\ \quad R = Cy,\ Bu^n,\ CH_2CH_2CN \\ [Pt_3(\mu\text{-}CO)_3(PPh_3)_4] \\ \\ [Pt_4(\mu\text{-}CO)_5(PMe_2Ph)_4]\end{array}\right\} \xrightarrow[60^\circ,\ \text{toluene or acetone}]{SO_2} [Pt_3(\mu\text{-}SO_2)_3(PR_3)_3] \qquad (2.4)$$

Yields are usually 70-80% based on Pt and the products are readily characterised by means of analytical, infra-red[35] and, most conclusively, $^{31}P\{^1H\}$ NMR data. The analysis of their NMR spectra is discussed fully in Chapter 5.

More recently, Ritchey and Moody[18] have reported the synthesis of $[Pt_3(\mu\text{-}SO_2)_3(PCy_3)_3]$ from the reaction of $[Pt(C_2H_4)_2(PCy_3)]$ with SO_2. It is not yet known whether this reaction will prove to be a convenient high yield general synthetic route.

Some pentanuclear clusters containing the bridging SO_2 ligand have also been prepared by the reaction of SO_2 gas with preformed clusters[46,58]:

$$[Pt_5(CO)(\mu\text{-}CO)_5L_4] \xrightarrow[60^\circ\ \text{toluene}]{SO_2\ (1\ \text{atm})} [Pt_5(CO)(\mu\text{-}CO)_2(\mu\text{-}SO_2)_3L_4] \qquad L = PPh_3,\ AsPh_3 \qquad (2.5)$$

In this case there is only partial replacement of the bridging carbonyl ligands. X-ray crystallographic studies on $[Pt_5(CO)(\mu\text{-}CO)_2(\mu\text{-}SO_2)_3(PPh_3)_4]$ (see Figure 2.2) show that only the least hindered carbonyl ligands are replaced and so steric factors are likely to be important in this reaction.

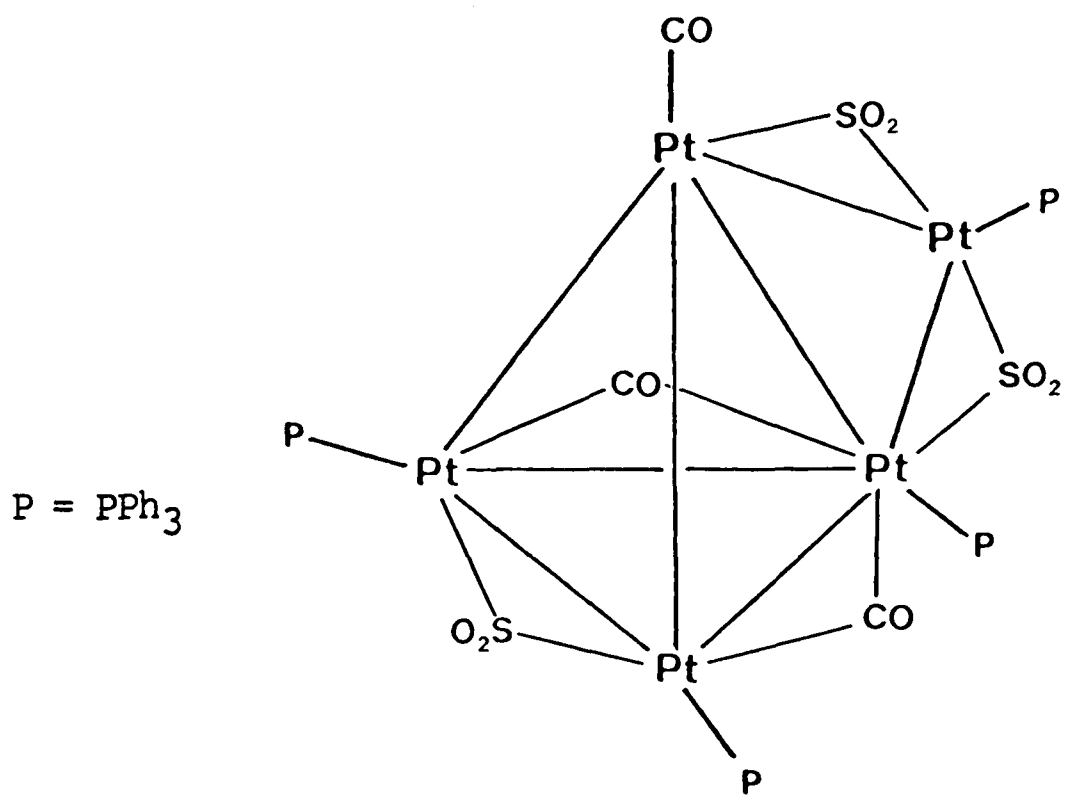

Figure 2.2 Structure of $[Pt_5(CO)(\mu\text{-}CO)_2(\mu\text{-}SO_2)_3(PPh_3)_4]$

2.1.3 42 versus 44 electron Pt_3 triangular clusters

In the case of the simple triplatinum clusters, two series of compounds have been synthesised which differ in their skeletal electron counts. Clusters of the type $[Pt_3(\mu\text{-}X)_3(PR_3)_3]$ (X = CO or SO_2) all have 42 skeletal electrons whereas those of the type $[Pt_3(\mu\text{-}X)_3(PR_3)_4]$ have 44 electrons. The electronic differences between the two types were discussed in Chapter 1. It is found that the observed structures can be rationalised by considering the frontier orbitals of the Pt_3 triangle. It is apparent that both steric and electronic factors are responsible for discriminating between the alternative electron counts. In a few instances it has proved possible to isolate both the 42 and 44 electron clusters. For example, some preliminary crystallographic data have been reported[48,52] for the compounds $[Pt_3(\mu\text{-}CO)_3(PCy_3)_n]$, where n = 3 and 4. Molecular orbital calculations have suggested that the π-acceptor qualities of the bridging and terminal ligands play an important role in influencing

the relative stabilities of the 42 and 44 electron species.[69,70] In clusters with PPh_3 as a terminal ligand, the 44 electron species, $[Pt_3(\mu\text{-}CO)_3(PPh_3)_4]$, is found with bridging CO and the 42 electron species, $[Pt_3(\mu\text{-}SO_2)_3(PPh_3)_3]$, is found with bridging SO_2. This may be attributed to the weaker π-acceptor properties of SO_2 compared with CO. In molecular orbital terms, the fourth phosphine in $[Pt_3(\mu\text{-}CO)_3(PPh_3)_4]$ puts two extra electrons into the unoccupied cluster a_2'' orbital. This orbital is suitable because it derives from the μ-CO π^* orbitals which lie out of the cluster plane:

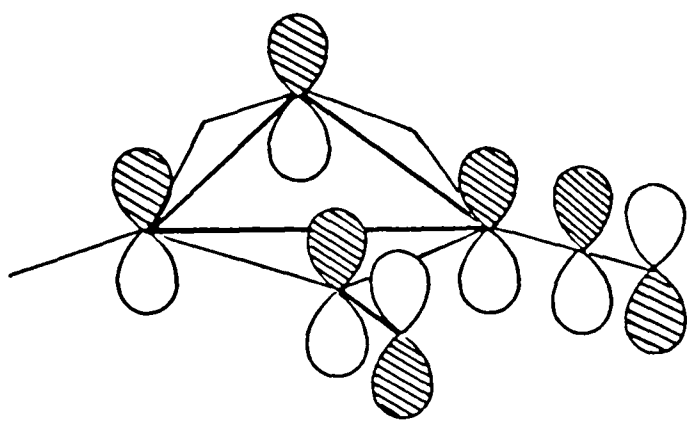

The incidence of the 44 electron cluster $[Pt_3(\mu\text{-}CO)_3(PR_3)_4]$ does not simply correlate with the electronic properties of the phosphine and so other factors must be involved. However, the absence of analogous 44 electron clusters containing bridging SO_2 instead of CO is neatly explained by this same electronic argument. Hoffmann <u>et al</u>[71] have shown that changing the bridging ligand in $[Pt_3(\mu\text{-}X)_3(CO)_3]$ from CO to SO_2 destabilises the a_2'' orbital and so it is reasonable that that addition of a fourth phosphine to $[Pt_3(\mu\text{-}SO_2)_3(PR_3)_3]$ is disfavoured.

The possibility of using a chelating diphosphine ligand to stabilise the 44 electron species relative to the 42 has recently been examined.[55] The reactions of dppp with the cluster compounds $[Pt_3(\mu\text{-}X)_3(PCy_3)_3]$ (X = CO, SO_2) are summarised in Figure 2.3 below:

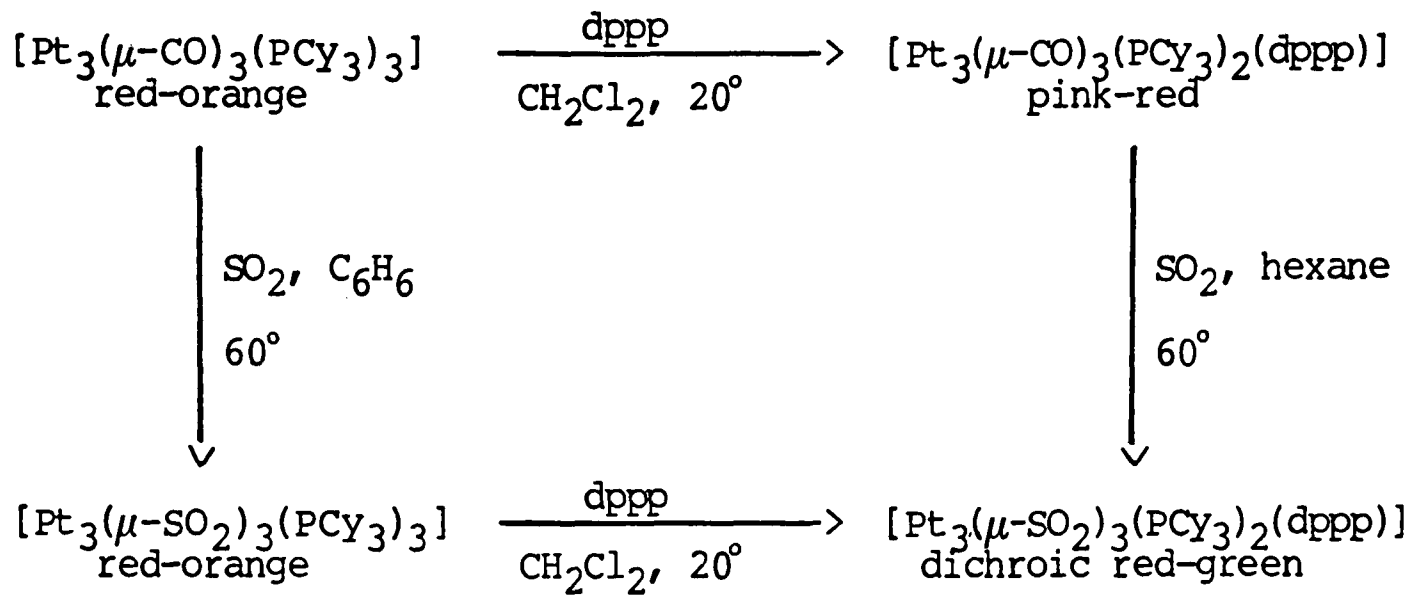

Figure 2.3 Routes to 44 electron cluster compounds using dppp

NMR and crystallographic studies on the products, $[Pt_3(\mu\text{-}X)_3(PCy_3)_2(dppp)]$, showed that the chelating dppp ligand bonds in a symmetrical manner when X = CO. When X = SO_2, the dppp ligand chelates in such a manner that one Pt-P bond is almost in the plane of the Pt_3 triangle and the other is well out of this plane. This structural difference has been attributed to the larger steric repulsions which are generated in the SO_2 cluster.

2.1.4 Tetra- and pentanuclear cluster compounds.

With some phosphine ligands the preference for the 44 electron species in the neutral Pt_3 cluster is so strong that the 42 electron species can not easily be isolated. Examples of this are $[Pt_3(\mu\text{-}CO)_3(PR_3)_4]$ where PR_3 = PPh_3 or PMe_2Ph. The compounds $[Pt_3(\mu\text{-}CO)_3(PR_3)_4]$ contain $\frac{4}{3}$ molecule of phosphine per platinum centre and so can not be formed by simple reduction of $[Pt(PR_3)(CO)Cl_2]$ which has only one phosphine per platinum. It is found that if this reduction is carried out in the absence of additional phosphine, then higher

nuclearity clusters are formed in which there is no more than one phosphine per platinum centre. In the case where $PR_3 = PMe_2Ph$, the product is the tetranuclear cluster $[Pt_4(\mu\text{-}CO)_5(PMe_2Ph)_4]$ and when $PR_3 = PPh_3$, the product is the pentanuclear cluster $[Pt_5(CO)(\mu\text{-}CO)_5(PPh_3)_4]$.

2.2 A general synthetic route to platinum carbonyl phosphine cluster compounds.

In this laboratory, Evans[46] found that the compounds *cis*-$[Pt(PR_3)(CO)Cl_2]$ can be reduced under mild conditions (one atmosphere of carbon monoxide) to give cluster compounds in good yields (60-80%). From this work a general method has been established and is described below by which cluster compounds of platinum which contain only phosphine and carbonyl ligands can be synthesised reliably and efficiently.

Such is the success of this method that it was hoped that it might also be extended to provide a route to more complex compounds and possibly to mixed metal compounds. Unfortunately attempts in this direction have so far not met with success.

2.2.1 The reducing agent

A variety of reducing agents were examined and the best results were obtained with either zinc dust (in THF or acetone as solvent) or sodium borohydride (with methanol as solvent). Both of these reducing agents have previously proved to be effective in the synthesis of mononuclear platinum(0) compounds when the phosphine is present in excess, as shown in (2.6)[72] and (2.7)[73]:

$$(PR_3)_2PtCl_2 \xrightarrow[THF]{CO/Zn} (PR_3)_2Pt(CO)_2 \qquad (2.6)$$

$$(PR_3)_2PtCl_2 + 2PR_3 \xrightarrow[EtOH]{NaBH_4} Pt(PR_3)_4 \qquad (2.7)$$

The BH_3.THF complex also proved to be a satisfactory reducing agent for cluster formation, but sodium amalgam was too powerful a reducing agent and brought about reduction to the metal. Both zinc dust and $NaBH_4$ are used as reducing agents in the syntheses described below. The choice between them is generally based on the comparative solubilities of starting material and product in methanol (preferred for $NaBH_4$) against acetone or THF (preferred for zinc dust). In one case, the reduction of cis-$[Pt(PCy_3)(CO)Cl_2]$, it is shown that virtually identical yields of the same cluster product can be obtained using either reducing agent.

2.2.2 The mononuclear platinum precursor

This method has now been developed to give an efficient and reliable synthetic route to platinum carbonyl phosphine cluster compounds. The first step was to ensure that the mononuclear precursors, cis-$[Pt(PR_3)(CO)Cl_2]$ could be easily and efficiently prepared for a wide range of phosphines. A number of methods are available, for example:

$$Pt(cod)Cl_2 + CO + PR_3 \xrightarrow[(ii)\ Et_2O]{(i)\ CHCl_3} Pt(PR_3)(CO)Cl_2 \qquad (2.8)^{74}$$

$$K^+[PtCl_3(C_2H_4)]^- + CO + PR_3 \xrightarrow{Me_2CO/PhH} Pt(PR_3)(CO)Cl_2 \qquad (2.9)^{75}$$

$$Pt_2(PR_3)_2Cl_4 + CO \xrightarrow{C_6H_6} Pt(PR_3)(CO)Cl_2 \qquad (2.10)^{76}$$

$$Pt(PR_3)_2Cl_2 + CO \xrightarrow[CH_2Cl_2]{SOCl_2} Pt(PR_3)(CO)Cl_2 \qquad (2.11)^{77}$$

Reaction (2.8) was found to be the most convenient and effective route, being straightforward and reliable for a wide range of phosphines of the type PR_3. Care was sometimes needed in isolating the product. For example, in the synthesis of $Pt(PCy_3)(CO)Cl_2$, if most or all of the solvent was removed before the product was isolated from the 1,5-cyclooctadiene which is liberated in the reaction, then the product reverted to the starting material, $Pt(cod)Cl_2$. The known compounds <u>cis</u>-$[Pt(PR_3)(CO)Cl_2]$, where $PR_3 = PPh_3$, PMe_2Ph, $PBu^n{}_3$ and PCy_3, were prepared in this manner and identified on the basis of analytical, infra-red and melting point data.[75,76] (See Chapter 6) In addition the compound <u>cis</u>-$[Pt\{P(CH_2CH_2CN)_3\}(CO)Cl_2]$, which was first prepared in this laboratory[78] was synthesised and characterised by analytical and infra-red data.

Attempts have also been made to prepare compounds of the type <u>cis</u>-$[Pt(P)(CO)Cl_2]$ where (P) is a diphosphine type ligand which is coordinated to platinum at only one end so that another metal such as gold could coordinate at the other. The intention was to see whether reduction of such compounds might be a possible route into mixed platinum-gold cluster compounds. Reaction (2.8) seemed a promising method for this idea since there had been only one reported[74] failure to synthesise $Pt(PR_3)(CO)Cl_2$ using a conventional phosphine - with R = o-tolyl. This was ascribed to steric factors which inhibit

nucleophilic attack by the bulky phosphine. Evans[46] has also tried unsuccessfully to prepare $Pt[P(OPh)_3](CO)Cl_2$, both from $Pt(cod)Cl_2$ as in (2.8) and by the method of (2.9). In each case the only product to be isolated which contained $P(OPh)_3$ was $Pt[P(OPh)_3]_2Cl_2$. Steric factors can not be responsible in this case since the Tolman cone angle[79] for $P(OPh)_3$ is only 128° compared with 145° for PPh_3 and 194° for P(o-tolyl)$_3$. The failure to isolate $Pt[P(OPh)_3](CO)Cl_2$ is probably due to the low basicity of the phosphite which prevents coordination of CO to Pt(II) in the presence of free $P(OPh)_3$.

In this work, a third type of failure was found with the diphosphine ligands dppm and dppp. Both preferred to chelate on the platinum and no CO could be incorporated even with a thorough saturation of the gas:

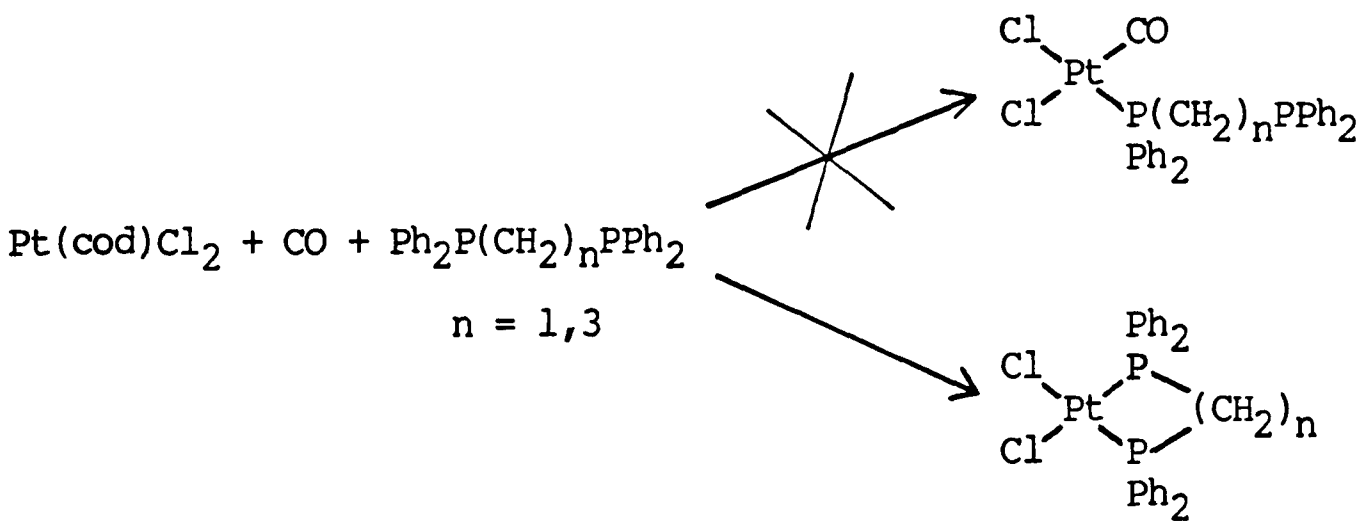

(2.12)

In an alternative approach, the diphosphine ligand was first reacted in 1:1 mole ratio with $Au(Me_2S)Cl$ to produce a compound which could generate the $P(CH_2)_nP$-Au-Cl unit:

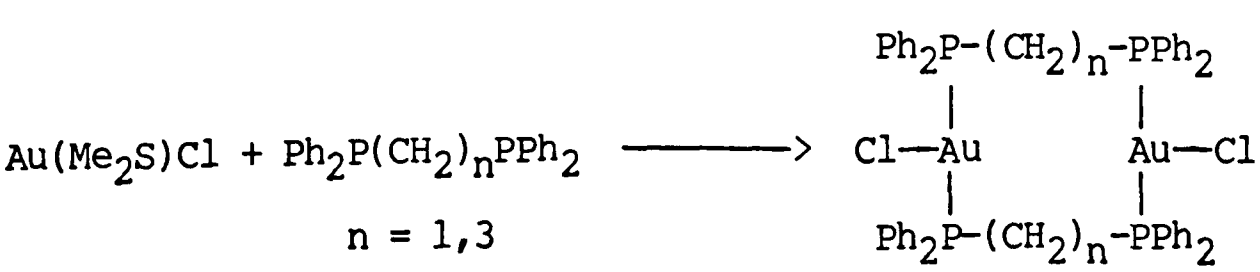

(2.13)

The dimeric nature of the product in (2.13) has been reported by Schmidbaur[80] and both the analytical and $^{31}P\{^{1}H\}$ NMR data support the structure shown.

The compounds $[Au(dppm)Cl]_2$ and $[Au(dppp)Cl]_2$ were then reacted with $Pt(cod)Cl_2$ and CO according to the method of reaction (2.8). Unfortunately, it was again not possible to isolate the compound with both CO and P coordinated to Pt(II). The products obtained, as identified by elemental analysis and $^{31}P\{^{1}H\}$ and $^{195}Pt\{^{1}H\}$ NMR, were $Pt(P)_2Cl_2$ (where P = $Ph_2P(CH_2)_nPPh_2AuCl$) and the starting material $Pt(cod)Cl_2$:

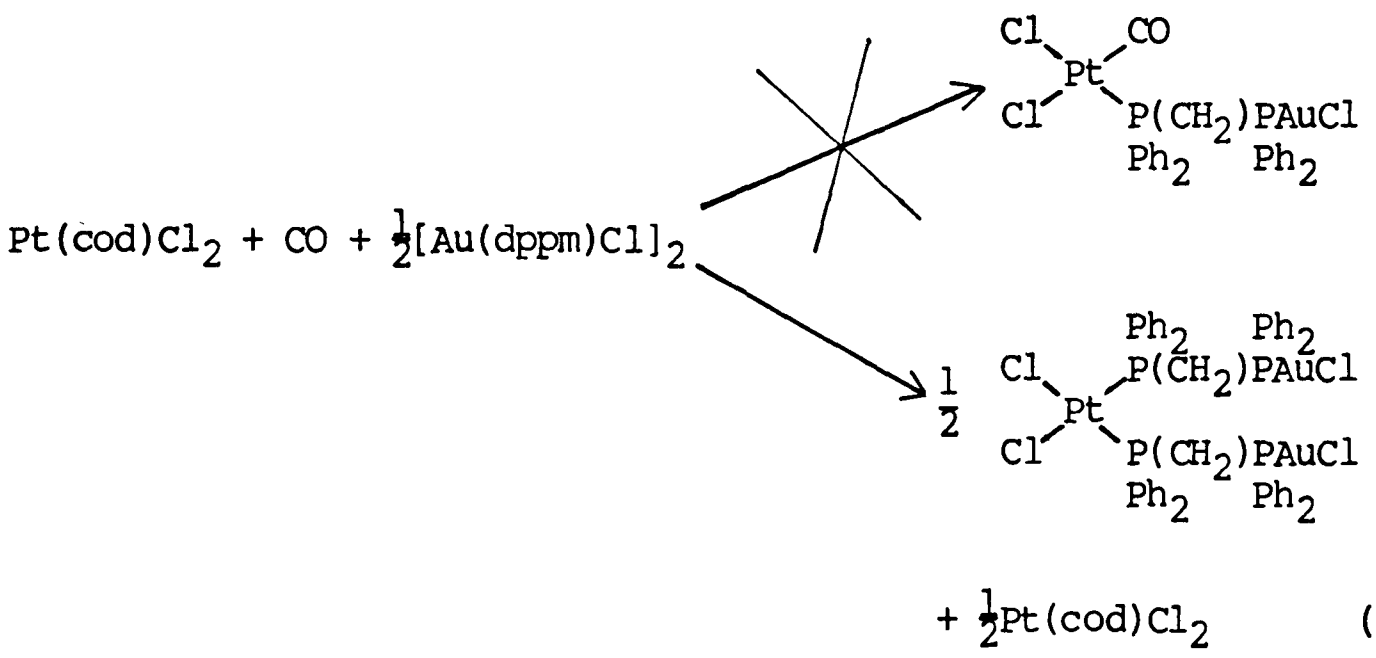

(2.14)

2.2.3 Synthesis and characterisation of the cluster compounds

Having established the potential of a general synthetic route to platinum carbonyl phosphine cluster compounds starting from cis-$[Pt(PR_3)(CO)Cl_2]$, a series of specific reactions were carried out to establish the conditions necessary for isolating the products in good yield. Full experimental details are given in Chapter 6.

Sodium borohydride was used to reduce CO saturated methanol solutions of the compounds cis-$[Pt(PR_3)(CO)Cl_2]$, where $PR_3 = PBu^n_3$,

PCy_3 and PMe_2Ph. In the case of PCy_3 and PBu^n_3, the product obtained, in better than 60% yield, was the triangulo-Pt_3 cluster $[Pt_3(\mu\text{-}CO)_3(PR_3)_3]$. These two clusters were characterised on the basis of analytical and infra-red evidence and in particular by measurement of their characteristic[81,82] $^{31}P\{^1H\}$ and $^{195}Pt\{^1H\}$ NMR spectra. The coupling constants obtained from these NMR spectra are given in Table 5.2 (Chapter 5), together with those of some related clusters.

Reduction of cis-$[Pt(PMe_2Ph)(CO)Cl_2]$ by this method gave the tetranuclear cluster $[Pt_4(\mu\text{-}CO)_5(PMe_2Ph)_4]$ in 80% yield. The product was characterised by analytical, infra-red and $^{31}P\{^1H\}$ NMR data. In particular the very distinctive NMR spectrum matched that reported by Pregosin[40] for the cluster obtained by allowing $[Pt_3(\mu\text{-}CO)_3(PMe_2Ph)_4]$ to decompose under an atmosphere of CO. The structure of the tetranuclear product from the latter reaction has been determined by X-ray crystallography.[40,41]

Zinc dust was used to reduce CO saturated solutions of cis-$[Pt(PR_3)(CO)Cl_2]$ where $PR_3 = P(CH_2CH_2CN)_3$, PCy_3 and PPh_3. The product isolated after reacting $[Pt\{P(CH_2CH_2CN)_3\}(CO)Cl_2]$ for 18 hours was the triangulo-Pt_3 cluster $[Pt_3(\mu\text{-}CO)_3\{P(CH_2CH_2CN)_3\}_3]$ (73% yield), which was characterised on the basis of analytical, infra-red and $^{31}P\{^1H\}$ NMR data. The relevant coupling constants are given in Table 5.2. $[Pt(PCy_3)(CO)Cl_2]$ gave the same cluster product as was obtained by the $NaBH_4$ reduction above. However, the reaction was much slower, requiring four days to achieve a 60% yield at ambient temperature.

$[Pt(PPh_3)(CO)Cl_2]$ was reduced quite quickly (within six hours) but in this case the product, in 76% yield, was the pentanuclear cluster $[Pt_5(CO)(\mu\text{-}CO)_5(PPh_3)_4]$. This compound was identified on the basis of analytical data and its very characteristic[66] infra-red

spectrum.

The reaction of $Pt(PPh_3)(CO)Cl_2$ was repeated in the presence of a one-third mole equivalent of free PPh_3. In this instance the trinuclear cluster $[Pt_3(\mu\text{-}CO)_3(PPh_3)_4]$ was isolated in 80% yield. This, too, could be identified on the basis of infra-red[12] and analytical data. In agreement with the observations of Chatt and Chini, this cluster was found to convert to the tetranuclear $[Pt_4(\mu\text{-}CO)_5(PPh_3)_4]$ on standing for a period of days in acetone solution under an atmosphere of CO.

2.2.4 Factors affecting cluster nuclearity

The results described above have demonstrated that the nuclearity of the cluster obtained by the reduction of cis-$[Pt(PR_3(CO)Cl_2]$ is sensitive to the steric and/or electronic requirements of the tertiary phosphine. The other synthetic routes to platinum clusters have also resulted in clusters of differing nuclearity depending on the phosphine used.[12,41,48,52,65,66]

Consider first the case of the trinuclear $[Pt_3(\mu\text{-}CO)_3(PR_3)_3]$ clusters. Previously it has been suggested[14,82] that such clusters are only stable with phosphines which have a large cone angle[79,83] such as PCy_3 (170°) or PBu^t_3 (182°). This work indicates, however, that this is primarily a reflection of the mode of synthesis employed since the dihydride precursors involved (reaction 2.1) are only available for such bulky phosphines as discussed above. Thus both PBu^n_3 and $P(CH_2CH_2CN)_3$ which have relatively small cone angles (132° in each case[79]) have been shown to form stable clusters of the type $[Pt_3(\mu\text{-}CO)_3(PR_3)_3]$. It is not clear exactly what factors favour the

formation of such clusters since although PCy_3, PBu^t_3 and PBu^n_3 are strong σ-donor and poor π-acceptor ligands, $P(CH_2CH_2CN)_3$ is anomalous in this respect in that it has an extremely low basicity arising from the electron-withdrawing character of the cyano groups[84].

Use of phosphines such as PPh_3 and PMe_2Ph with intermediate cone angles and electronic parameters destabilises clusters of the type $[Pt_3(\mu\text{-}CO)_3(PR_3)_3]$. Traces of $[Pt_3(\mu\text{-}CO)_3(PPh_3)_3]$ have been identified[85] as minor products of the reaction of $[Pt(C_2H_4)_2(PPh_3)]$ with $[Rh(CO)_2(C_5Me_5)]$ and the $^{31}P\{^1H\}$ NMR spectrum at room temperature was indicative of rapid phosphine exchange. This phenomenon is not observed for the other examples of $[Pt_3(\mu\text{-}CO)_3(PR_3)_3]$ reported above and elsewhere[81,82] but is consistent with the fact that the stable trinuclear cluster compounds formed with these two phosphines are $[Pt_3(\mu\text{-}CO)_3(PR_3)_4]$.[12]

In the absence of excess ligand, these phosphines appear to favour the formation of $[Pt_5(CO)(\mu\text{-}CO)_5(PPh_3)_4]$ and $[Pt_4(\mu\text{-}CO)_5(PMe_2Ph)_4]$ respectively, an observation common to this and other[12,40,65,66] synthetic methods.

2.3 Reactions of triangulo-triplatinum cluster compounds with unsaturated inorganic molecules.

It has been seen that platinum in the zerovalent state has a strong tendency to from triangular trinuclear cluster compounds[8] and even higher clusters are still based on the triangular Pt_3 unit. It is also becoming apparent that interconversion between different platinum triangles is quite easy and consequently the family of triangular platinum cluster compounds is getting very large and diverse. Bearing in mind the long term interest in platinum cluster

compounds as models for metal surfaces and as potential catalysts, it is now becoming important to gain some understanding of the reactivity of these compounds. The methods used to synthesise the cluster compounds suggest that the first area which needs investigation is the reactivity of the Pt_3 triangular unit towards the small molecules which are themselves used as ligands.

The Pt_3 cluster compounds owe their stability to a suitable combination of π-acceptor ligands and clusters with various phosphines, isocyanides, CO and SO_2 in terminal and/or bridging modes of bonding have been isolated (see Figure 2.4). In their pioneering work on the synthesis of carbonyl phosphine clusters, Chatt and Chini[12] observed that some of the clusters reacted further with free phosphine and CO, for example, reactions 2.15 and 2.16 below.

$$[Pt_3(\mu\text{-}CO)_3L_4] + 5L \longrightarrow 3[Pt(CO)L_3] \qquad L = PEt_3,\ PPh_2Me,\ PPh_3 \tag{2.15}$$

$$2[Pt_3(\mu\text{-}CO)_3(PPh_3)_4] + 3CO \longrightarrow [Pt_4(\mu\text{-}CO)_5(PPh_3)_4] + 2Pt(PPh_3)_2(CO)_2 \tag{2.16}$$

It was apparent from these and other similar observations that some unsaturated inorganic molecules can promote interconversion of platinum clusters which may or may not require fragmentation of the cluster. Therefore, it was of interest to investigate a number of reactions with such molecules to determine some of the factors which influence the stability of platinum clusters towards fragmentation.

$X = CO, SO_2$

$Pt_3(\mu\text{-}X)_3(PR_3)_3$

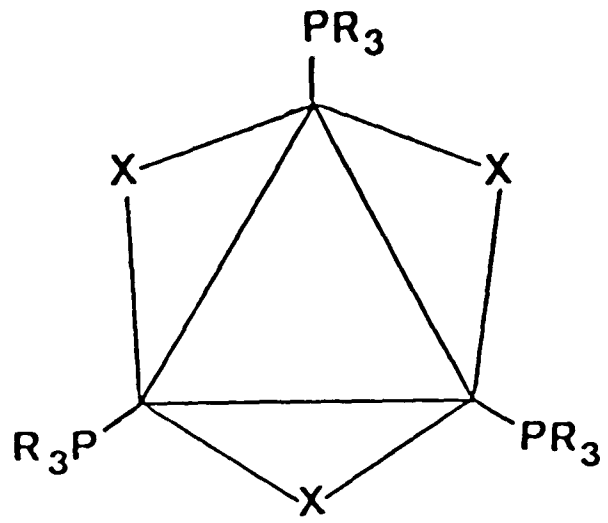

$Pt_3(\mu\text{-}Ph)(\mu\text{-}PPh_2)(\mu\text{-}SO_2)(PPh_3)_3$[50]

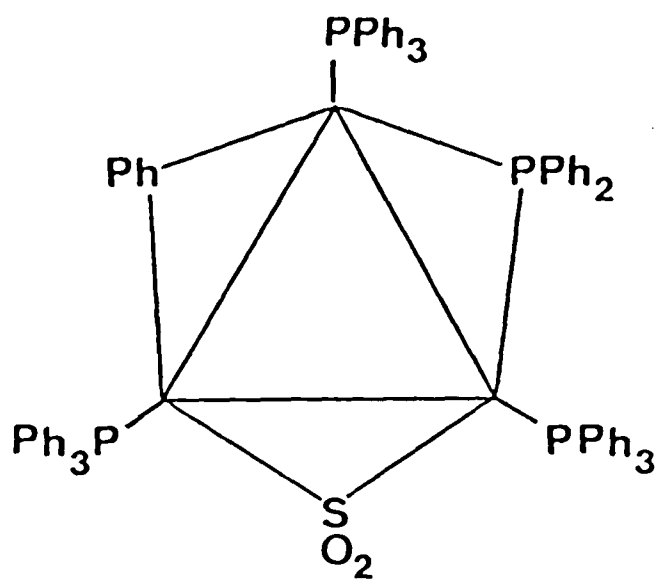

$Pt_3(\mu\text{-}CNC_8H_9)_3(CNC_8H_9)_2(PCy_3)$[59]

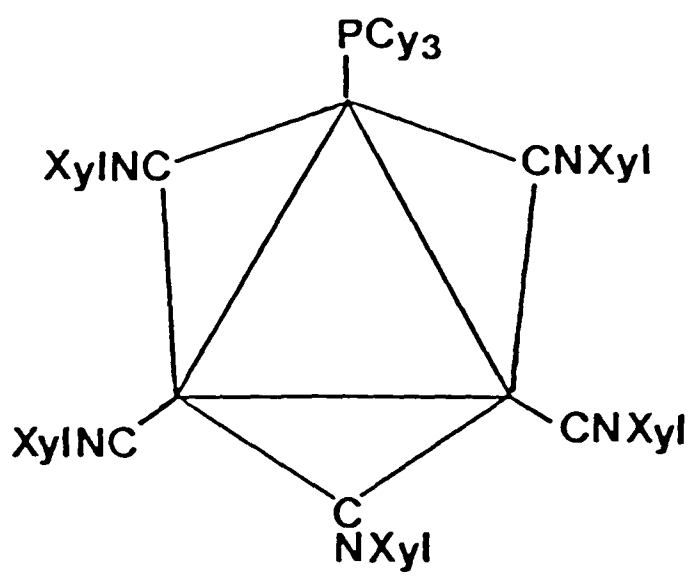

Figure 2.4 The use of different π-acceptor ligands to stabilise Pt_3 triangles.

2.3.1 Reactions for which fragmentation of the cluster is not required

Farrar and coworkers[86] have investigated the exchange of phosphine ligands in the compounds $[Pt_3(\mu\text{-}CO)_3L_3]$ where L is a bulky phosphine such as PCy_3, PPr^i_3 or PBu^t_3. They found that the phosphines L readily and quickly exchange with a less bulky phosphine L′ and, depending on how much of the free phosphine L′ is used, various amounts of mixed-phosphine triangles are formed. On the other hand if two or more triangles $[Pt_3(\mu\text{-}CO)_3L_3]$, with different phosphines and ^{13}CO labelling, are mixed in the absence of free ligands, then scrambling of both ^{13}CO and phosphine ligands is found to take place, but quite slowly. It seems that phosphine exchange occurs via an associative mechanism and does not involve breaking the Pt_3 triangle:

$$[Pt_3(CO)_3L_3] + L' \longrightarrow [Pt_3(CO)_3L_3L'] \longrightarrow [Pt_3(CO)_3L_2L'] + L \qquad (2.17)$$

Such a mechanism is reasonable in view of the known compounds $[Pt_3(\mu\text{-}CO)_3L_4]$. The slower, general scrambling reaction between different Pt_3 triangles is likely to involve fragmentation and evidence for this will be discussed later. It should be remembered that Farrar's observations apply to very bulky phosphines. His Pt_3 cluster compounds were all stable to fragmentation in the presence of a large excess of free phosphine and no mononuclear platinum compounds were detected, in contrast to the results of Chatt and Chini with the smaller phosphine PPh_3.[12]

Secondly, Briant et al[59] have found that $[Pt_3(\mu\text{-}CO)_3(PCy_3)_3]$ reacts readily with 2,6-xylyl isocyanide (CNC_8H_9) as shown in Figure

2.5 below:

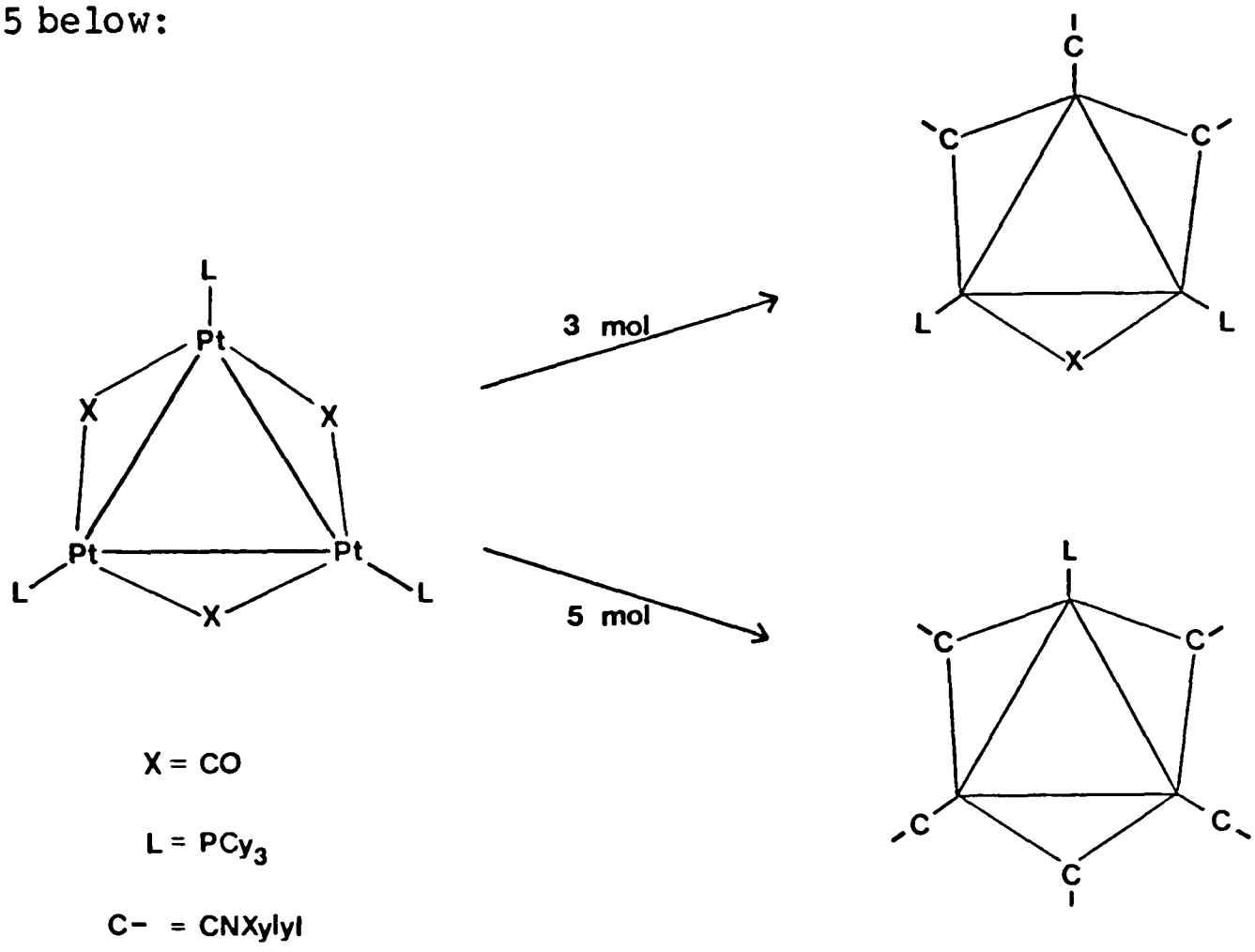

Figure 2.5 Reaction of $[Pt_3(\mu\text{-}CO)_3(PCy_3)_3]$ with CNC_8H_9

The notable features of these reactions are that they occur very rapidly and they involve substitution of both terminal phosphine and bridging CO ligands. The two products shown are the only two products obtained from reacting $[Pt_3(\mu\text{-}CO)_3(PCy_3)_3]$ with CNC_8H_9 and their structures suggest that the isocyanide ligands are quite demanding in their steric requirements. It seems, therefore, that these reactions proceed by successive substitution around the Pt_3 triangle and do not involve fragmentation.

The third case has already been described in Section 2.1.2 and is the reaction of carbonyl phosphine cluster compounds with SO_2. This reaction is used as a facile synthetic route to SO_2 cluster compounds of platinum and involves the apparently simple replacement of carbonyl ligands by SO_2. In all the syntheses reported so far, no intermediate

or alternative products have been detected and there is no evidence to suggest that the Pt_3 triangle is broken at all in the reaction. This is true not only for the simple Pt_3 triangles, but also for the few known examples in higher clusters. In fact, in the reaction of SO_2 with $[Pt_5(CO)(\mu\text{-}CO)_5(PPh_3)_4]$ (reaction 2.5), the precise substitution of only the three least hindered carbonyl ligands with no change in the Pt_5 framework is evidence against a fragmentation mechanism.

A related SO_2 cluster of palladium has recently been studied in this laboratory.[87] A benzene solution of $[Pd_3(\mu\text{-}SO_2)_3(PCy_3)_3]$ was reacted with CO and found to give a mixture of substituted products which were characterised on the basis of the $^{31}P\{^1H\}$ NMR spectrum shown in Figure 2.6. The spectrum indicates only triangular Pd_3 compounds and, in contrast to observations to be made in the next Section, provides no evidence for fragmentation of the triangular structure in the course of ligand exchange. The absence of any band due to terminal CO ligands in the infra-red spectrum of the product supports this assertion. The complexes identified in the NMR spectrum are listed below in Table 2.2 together with their NMR parameters. The chemical shift of $[Pd_3(\mu\text{-}SO_2)_3(PCy_3)_3]$, not present in the spectrum, is added for comparison. The chemical shifts of the simple, symmetrical Pd_3 compounds, containing <u>either</u> CO <u>or</u> SO_2 but not both, were measured from separate authenticated[87] samples.

The assignment of the two mixed structures $[Pd_3(\mu\text{-}CO)_x(\mu\text{-}SO_2)_y(PCy_3)_3]$ is not conclusive. However, the chemical shifts have been assigned on the basis that in related clusters of platinum, bridging SO_2 ligands give smaller $^3J(P\text{-}P)$ values than analogous bridging CO ligands (see Tables 5.1 and 5.2). As with the platinum

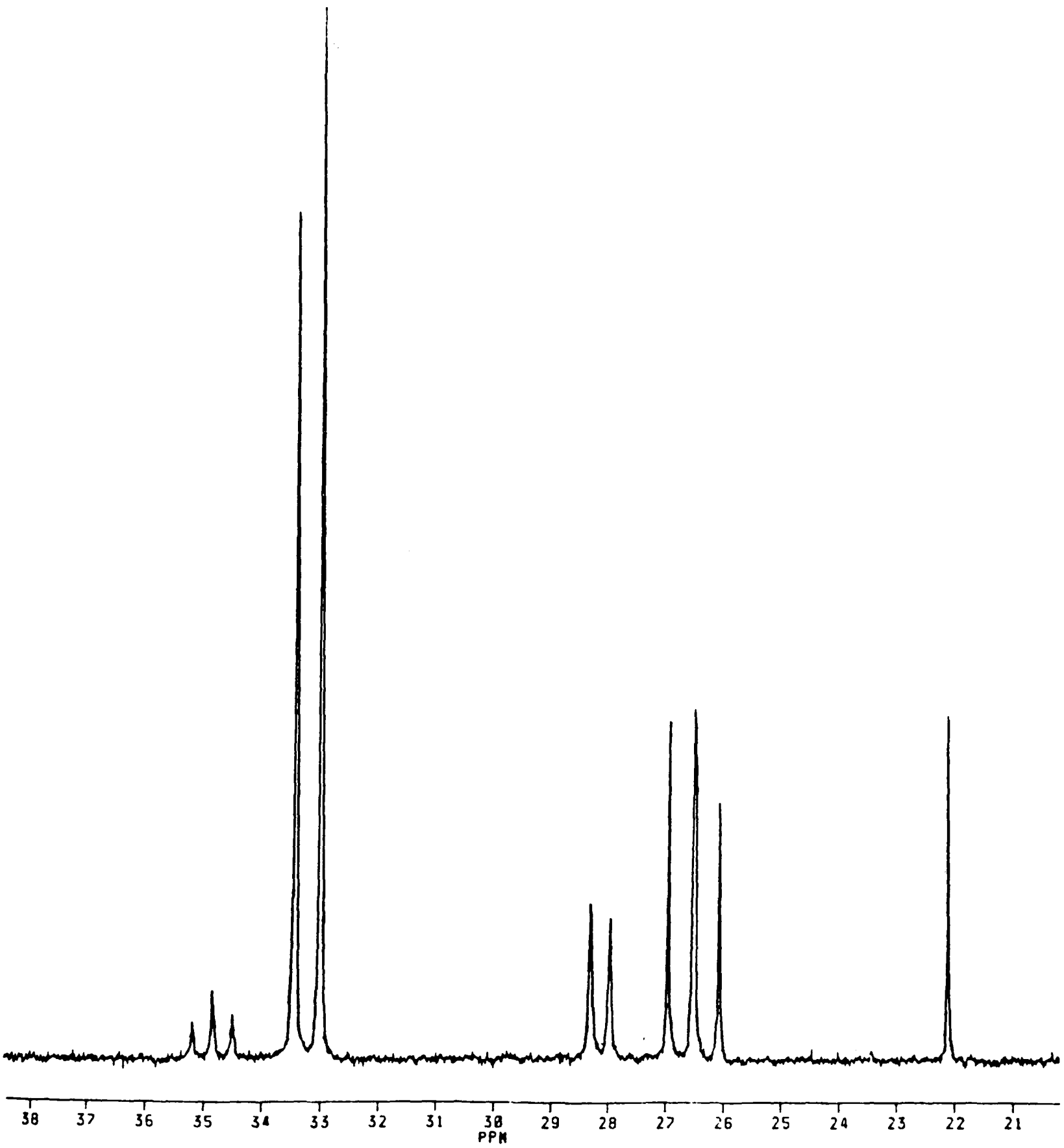

Figure 2.6 Products from reacting $Pd_3(SO_2)_3(PCy_3)_3$ with CO $^{31}P\{^1H\}$ NMR spectrum in benzene solution

clusters, the major product is the mixed trinuclear cluster with two CO ligands and one SO_2.

	$\delta(^{31}P)$ (ppm)	$^3J(P,P)$ (Hz)	approximate proportion
$[Pd_3(CO)_3(PCy_3)_3]$	22.1	-	9%
$[Pd_3(CO)_2(SO_2)(PCy_3)_3]$	26.5(t) 33.2(d)	44	80%
$[Pd_3(CO)(SO_2)_2(PCy_3)_3]$	28.1(d) 34.8(t)	35	11%
$[Pd_3(SO_2)_3(PCy_3)_3]$	35.0	(for comparison)	

Table 2.1 Products from reacting $[Pd_3(\mu\text{-}SO_2)_3(PCy_3)_3]$ with CO
Data from analysis of the $^{31}P\{^1H\}$ NMR spectrum

2.3.2 Reactions involving fragmentation of the platinum cluster

It is thought that, as bridging ligands, CO and SO_2 have quite similar electronic properties. SO_2 is the better σ-donor but CO is the better π-acceptor.[36] Therefore, it was logical to see if the conversion of CO bridged Pt_3 triangular clusters to their SO_2 bridged equivalents could be reversed by treating the SO_2 clusters with CO gas. Evans[46] has carried out the reaction of $[Pt_3(\mu\text{-}SO_2)_3(PPh_3)_3]$ with CO. This is a peculiar example since the original carbonyl compound, $[Pt_3(\mu\text{-}CO)_3(PPh_3)_4]$, contains four phosphine ligands and, therefore, can not be regenerated by this method. The obvious product, $[Pt_3(\mu\text{-}CO)_3(PPh_3)_3]$, is electron deficient and is not easily isolated. The product obtained in good yield (80% on Pt) from this reaction was the pentanuclear cluster $[Pt_5(CO)(\mu\text{-}CO)_5(PPh_3)_4]$, which

is the same as that usually synthesised in the presence of limited triphenylphosphine (Section 2.2.3). Such conversion of a Pt_3 cluster to a Pt_5 cluster necessarily involves fragmentation of the Pt_3 triangle. In this case the cause is the relatively low basicity of the triphenylphosphine. Little else can be deduced about the reaction since the only platinum containing compounds observed were the pentanuclear cluster and a mixture of unidentified mononuclear breakdown products.

In Section 2.2.3 it was shown that $[Pt_3(\mu\text{-}CO)_3(PPh_3)_4]$ can be synthesised from $[Pt(CO)(PPh_3)Cl_2]$ if an extra one third mole of phosphine per mole of platinum is added. Therefore, it was decided to repeat the reaction of $[Pt_3(\mu\text{-}SO_2)_3(PPh_3)_3]$ with CO in the presence of an additional one third mole of PPh_3. In this case there was a rapid colour change from dark to pale orange and spectroscopic evidence (infra red and $^{31}P\{^1H\}$ NMR) indicated that the only significant product is the mixed SO_2/CO triangular cluster shown below:

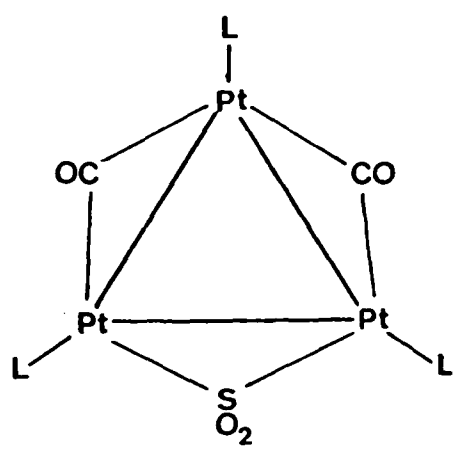

No product was observed which contained the extra phosphine. Nor was there any suggestion of either a pentanuclear cluster or a binuclear complex. It seems, therefore, that the presence of the free phosphine in this reaction may suppress total fragmentation of the Pt_3 triangle.

In order to make a better judgement on the interconversion of CO and SO_2 cluster compounds, the reaction of $[Pt_3(\mu\text{-}SO_2)_3(PCy_3)_3]$ with CO was investigated. PCy_3 is a bulky and relatively basic phosphine and it readily allows the isolation of the 42 electron carbonyl cluster $[Pt_3(\mu\text{-}CO)_3(PCy_3)_3]$. CO gas was bubbled through a benzene solution of $[Pt_3(\mu\text{-}SO_2)_3(PCy_3)_3]$ for 15 minutes. There was an immediate colour change from orange to yellow. A yellow crystalline solid was isolated, the infra-red spectrum of which contained bands due to terminal and bridging CO as well as SO_2. The $^{31}P\{^1H\}$ NMR spectrum of this product showed it to be a mixture of two compounds. On the basis of the spectral analysis described in Chapter 5, one of these compounds was shown to have a platinum triangle with three phosphine ligands, two in one chemical environment and one in another. The other compound, however, contains only two symmetrically arranged platinum-phosphine units and the magnitudes of the coupling constants indicate that the compound is based on the linear P-Pt-Pt-P moiety. On the basis of the spectroscopic and analytical evidence, the triangular compound was characterised as $[Pt_3(\mu\text{-}CO)_2(\mu\text{-}SO_2)(PCy_3)_3]$.

Evidently, this attempt at reversing the conversion of a carbonyl cluster to its SO_2 equivalent has not gone to completion. Even with prolonged exposure to CO and warming to 60°, replacement of the final SO_2 could not be achieved. Additionally a binuclear species was observed. This compound was not isolated but, in view of the spectroscopic evidence, the most probable structure is:

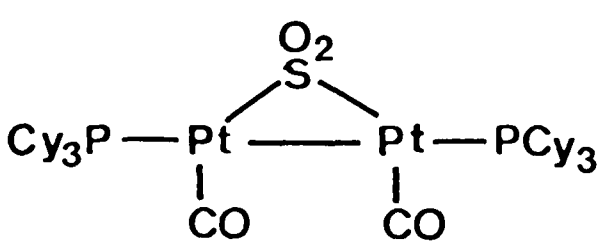

The reaction of $[Pt_3(\mu\text{-}SO_2)_3(PCy_3)_3]$ with CO was repeated with the exposure to CO limited to two minutes. A bright yellow crystalline solid, soluble in benzene, ethanol and diethyl ether, was isolated. The infra-red spectrum showed that, apart from a very small trace of a compound containing terminal CO (presumably the binuclear species), the yellow product was entirely $[Pt_3(\mu\text{-}CO)_2(\mu\text{-}SO_2)(PCy_3)_3]$. Both of the above reactions were reversed on treatment with SO_2, giving $[Pt_3(\mu\text{-}SO_2)_3(PCy_3)_3]$ as the only isolable product. These results suggest the following sequence of reactions.

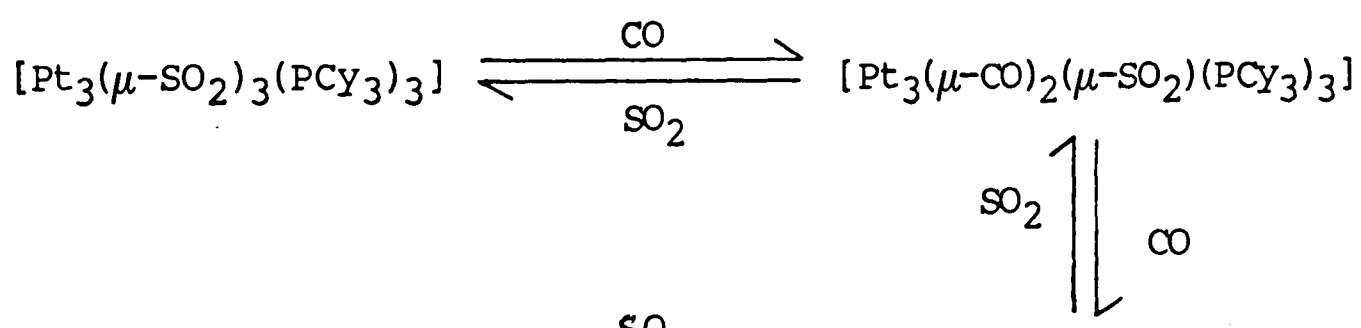

Recently Farrar and co-workers[86] have investigated the reaction of SO_2 with $[Pt_3(\mu\text{-}CO)_3(PBu^t{}_2Ph)_3]$, a carbonyl cluster with a particularly bulky phosphine which is also a good σ-donor. They observed a similar sequence of reactions which are summarised in the scheme below.

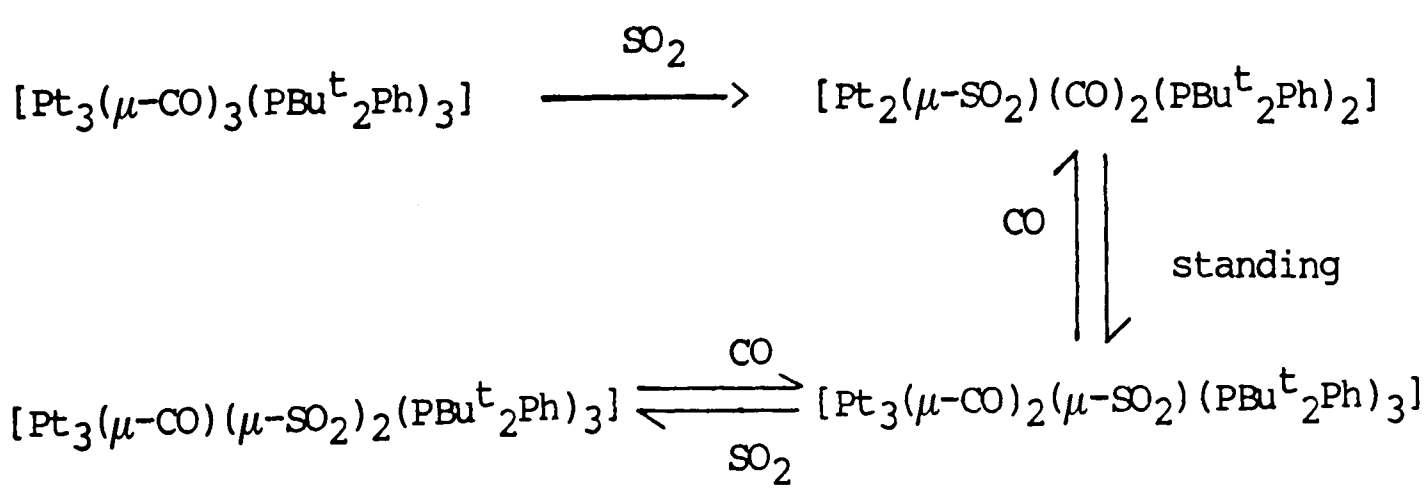

The main difference between these two schemes is that with PCy_3 the fully CO - substituted cluster could not be obtained whereas for

$P(Bu^t{}_2Ph)$ the fully SO_2 - substituted cluster was not obtained. Farrar was also able to observe both of the mixed triangular clusters $[Pt_3(\mu\text{-}CO)_x(\mu\text{-}SO_2)_y(PBu^t{}_2Ph)_3]$. It is probable that neither of the schemes gives all of the intermediate compounds and that each interconversion of triangular clusters occurs via a binuclear species.

Interconversion of the various observed complexes involving fragmentation and aggregation reactions is easily achieved with modest changes in conditions because the CO and SO_2 ligands react at similar rates and give products of comparable stabilities. The influence of the phosphine appears to be such that the smaller, less basic phosphines allow fast and complete reaction with CO or SO_2 gas to maximum substitution, possibly without the need for fragmentation. The bulky phosphines, such as PCy_3 and $PBu^t{}_2Ph$, which are also better σ-donors favour fragmentation of the Pt_3 triangle, giving both trinuclear and binuclear products but without easily reacting to completion. In particular, reactions of these compounds have revealed no mononuclear products. On the other hand, in the case of PPh_3, provided there is sufficient phosphine present fragmentation of the Pt_3 triangle is not necessary and, in the presence of excess phosphine, degradation to mononuclear species is quite likely.

$[Pt_3(\mu\text{-}SO_2)_3(PCy_3)_3]$ has also been reacted with 2,6-xylyl isocyanide, in a 1:3 mole ratio. In contrast to the reaction of the carbonyl cluster, described in the previous Section, this reaction yielded a mixture of products of which one had a binuclear structure. The products of the reaction were characterised on the basis of the $^{31}P\{^1H\}$ NMR spectrum shown in Figure 2.7. This apparently complex spectrum can be explained in terms of a mixture of two compounds. One

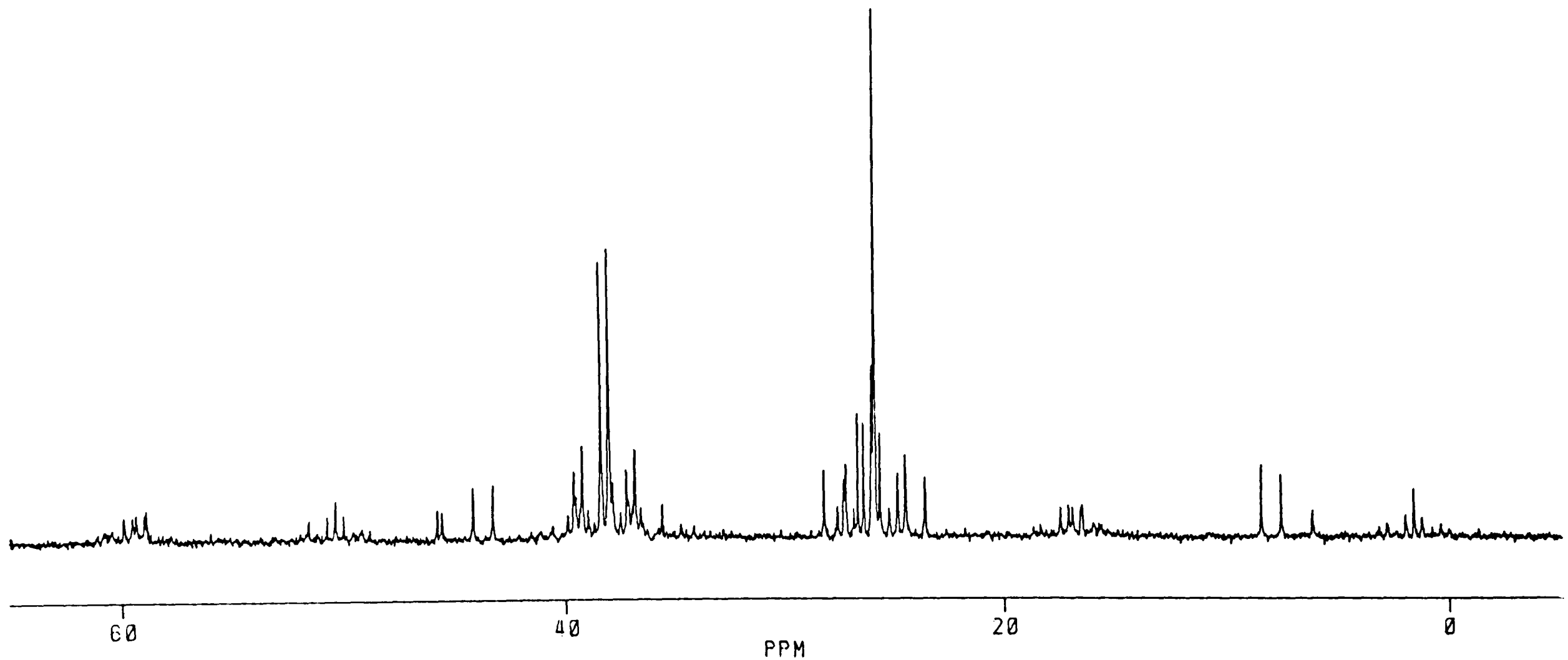

Figure 2.7 Reaction of $Pt_3(SO_2)_3(PCy_3)_3$ with three moles of 2,6-xylyl isocyanide: $^{31}P\{^1H\}$ NMR spectrum of product mixture

compound shows a strong line at 25.9ppm with associated pairs of doublets recognisable as belonging to a near linear, symmetrical P-Pt-Pt-P system. The coupling constants calculated from this part of the spectrum are given in Table 2.2 and a computer simulation of the spectrum is shown in Figure 2.8. The infra-red spectrum of the mixture shows terminal isocyanide bands[88] at least one of which is thought likely to belong to this binuclear compound and so its structure is probably:

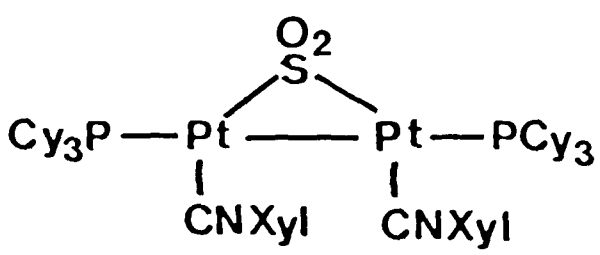

The remaining lines in the $^{31}P\{^{1}H\}$ spectrum form a pattern which has already been seen for the triangular species $[Pt_3(\mu\text{-}X)_2(\mu\text{-}Y)(PR_3)_3]$ described earlier in this Section. Therefore, the second compound in this mixture still contains exactly three phosphines in terminal positions on a Pt_3 triangle. Whether any of the bridging SO_2 ligands has been replaced by the isocyanide is uncertain, since there are two possible structures for the compound, shown below, which could reasonably fit the data as well as being consistent with known related compounds:

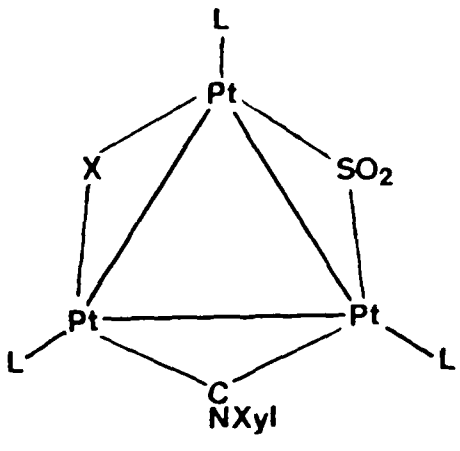

X = CNXyl or SO_2

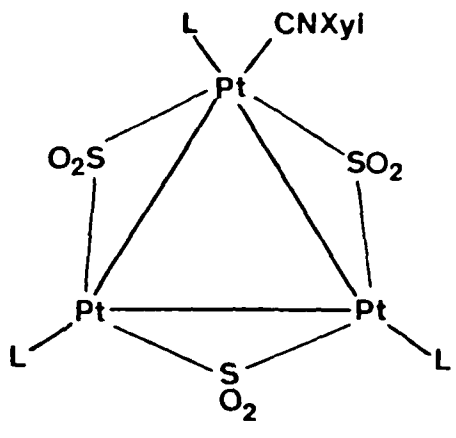

Proposed structure:

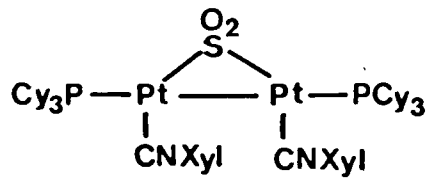

$\delta(^{31}P)$	25.9ppm
$^{1}J(Pt-P)$	3631Hz
$^{2}J(Pt-P)$	377Hz
$^{3}J(P-P)$	91Hz

Table 2.2 Reaction of $Pt_3(SO_2)_3(PCy_3)_3$ with isocyanide: $^{31}P\{^{1}H\}$ NMR data for the binuclear product

Proposed structure:

(non-phosphine ligands uncertain)

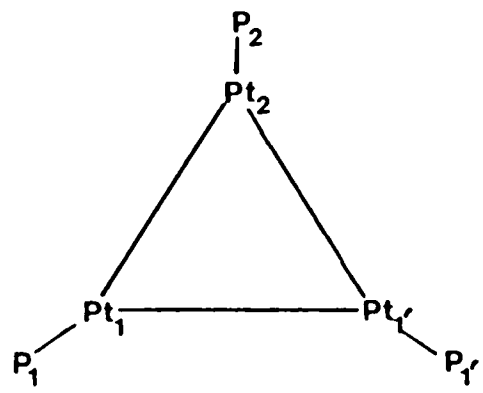

Chemical shifts (ppm):

$\delta(^{31}P)$:	P_1	38.2;	P_2	26.0

Coupling constants (Hz):

$^{1}J(Pt-P)$:	Pt_1-P_1	4358;	Pt_2-P_2	4953
$^{2}J(Pt-P)$:	Pt_1-P_1'	271;	Pt_1-P_2	243;
	Pt_2-P_1	230		
$^{3}J(P-P)$:	P_1-P_1'	20;	P_1-P_2	38

Table 2.3 Reaction of $Pt_3(SO_2)_3(PCy_3)_3$ with isocyanide: $^{31}P\{^{1}H\}$ NMR data for the trinuclear product

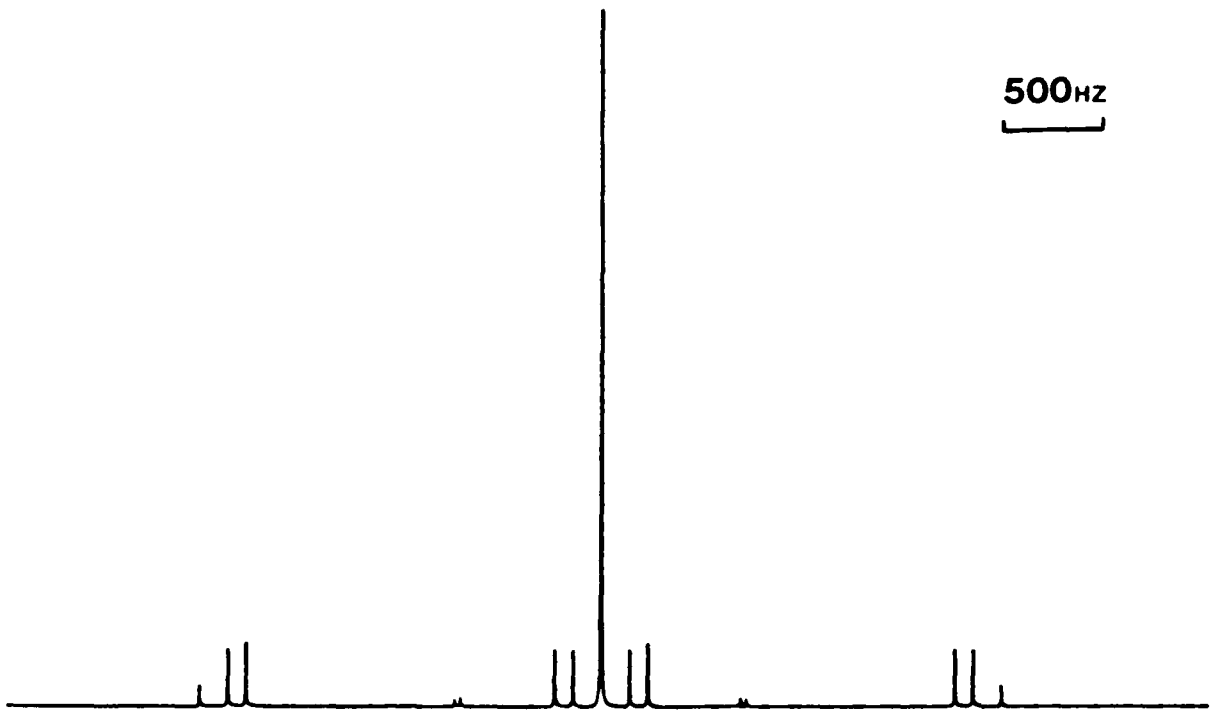

Figure 2.8 Reaction of $Pt_3(SO_2)_3(PCy_3)_3$ with isocyanide: Simulation of $^{31}P\{^1H\}$ NMR spectrum for the binuclear product

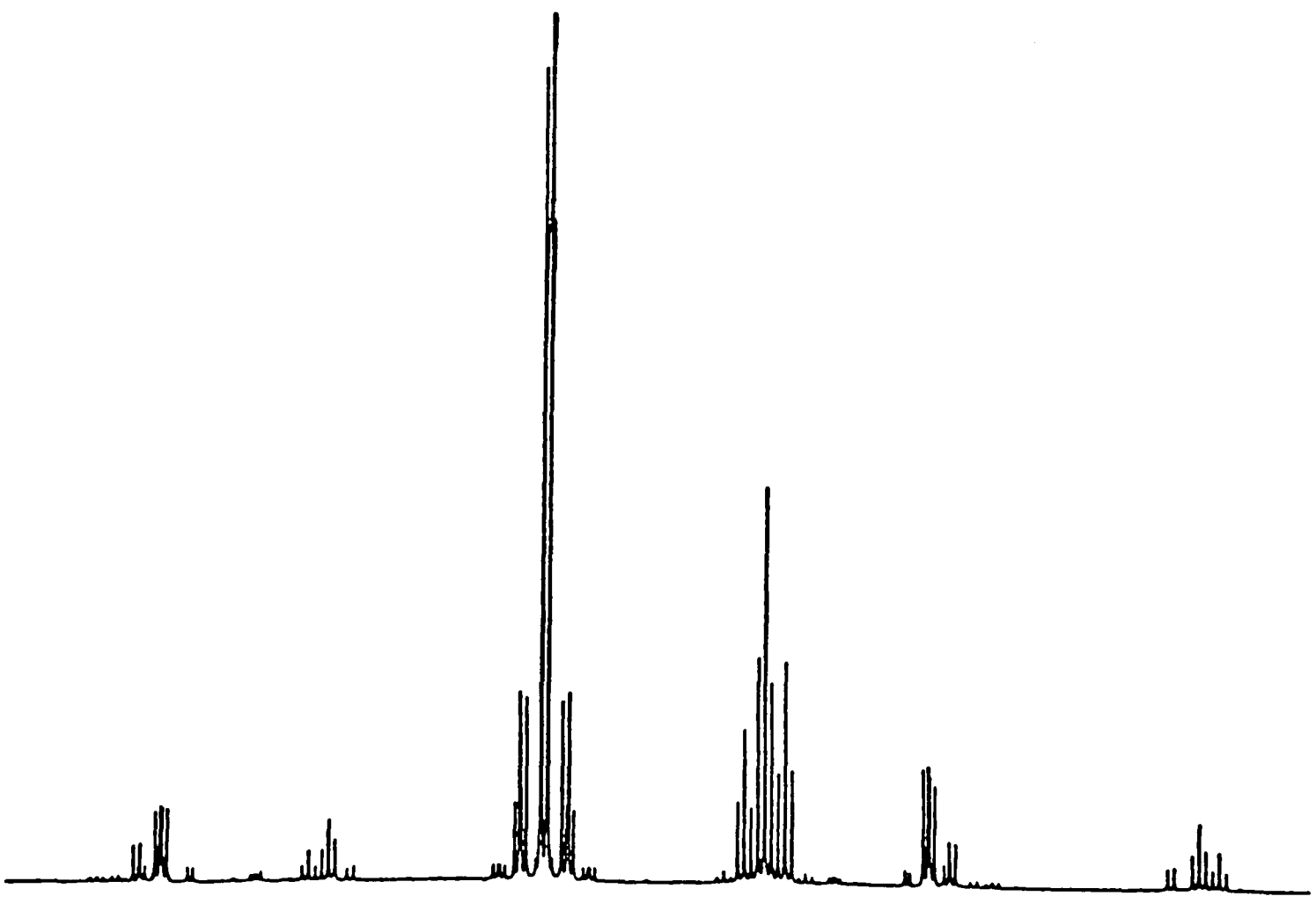

Figure 2.9 Reaction of $Pt_3(SO_2)_3(PCy_3)_3$ with isocyanide: Simulation of $^{31}P\{^1H\}$ NMR spectrum for the trinuclear product

The 42 electron cluster on the left seems the simpler and more obvious product but the phosphine ligands are probably too bulky to allow substitution without first fragmenting the triangle. In view of the observed binuclear product discussed above, this is a reasonable product. The 44 electron cluster on the right is an interesting prospect because it has so far been impossible to coordinate a fourth terminal ligand to an SO_2 bridged triangle without using a chelating diphosphine.[55]

The NMR parameters for this compounds are given in Table 2.3 and a computer simulation for the $^{31}P\{^1H\}$ spectrum is given in Figure 2.9.

2.3.3 Synthesis of a binuclear complex by cluster fragmentation

In addition to their observations on the reaction of $[Pt_3(\mu\text{-}CO)_3(PBu^t{}_2Ph)_3]$ with SO_2, Farrar *et al* have reported that the same carbonyl cluster reacts readily with CS_2 and COS to give complexes of lower nuclearity.[86] Their findings are summarised in Figure 2.10.

Much of the work in this Thesis has centred on clusters containing PPh_3. Additionally another part of this work, described in Chapter 4, is concerned with the chemistry of sulphur bridged binuclear complexes of platinum. Therefore, it was of interest to link these areas together by investigating the reaction of $[Pt_3(\mu\text{-}CO)_3(PPh_3)_4]$ with CS_2 and COS. The reaction with CS_2 proceeded rapidly even at -10°. The only cluster compound isolated was the now familiar pentanuclear cluster $[Pt_5(CO)(\mu\text{-}CO)_5(PPh_3)_4]$, identified on the basis of its characteristic infra red spectrum. Additionally small amounts of some mononuclear breakdown products were observed. The reaction with COS at room temperature eventually (after about 24 hours) gave in good yield (84%) the binuclear complex $[Pt_2(\mu\text{-}S)(CO)_2(PPh_3)_2]$, in

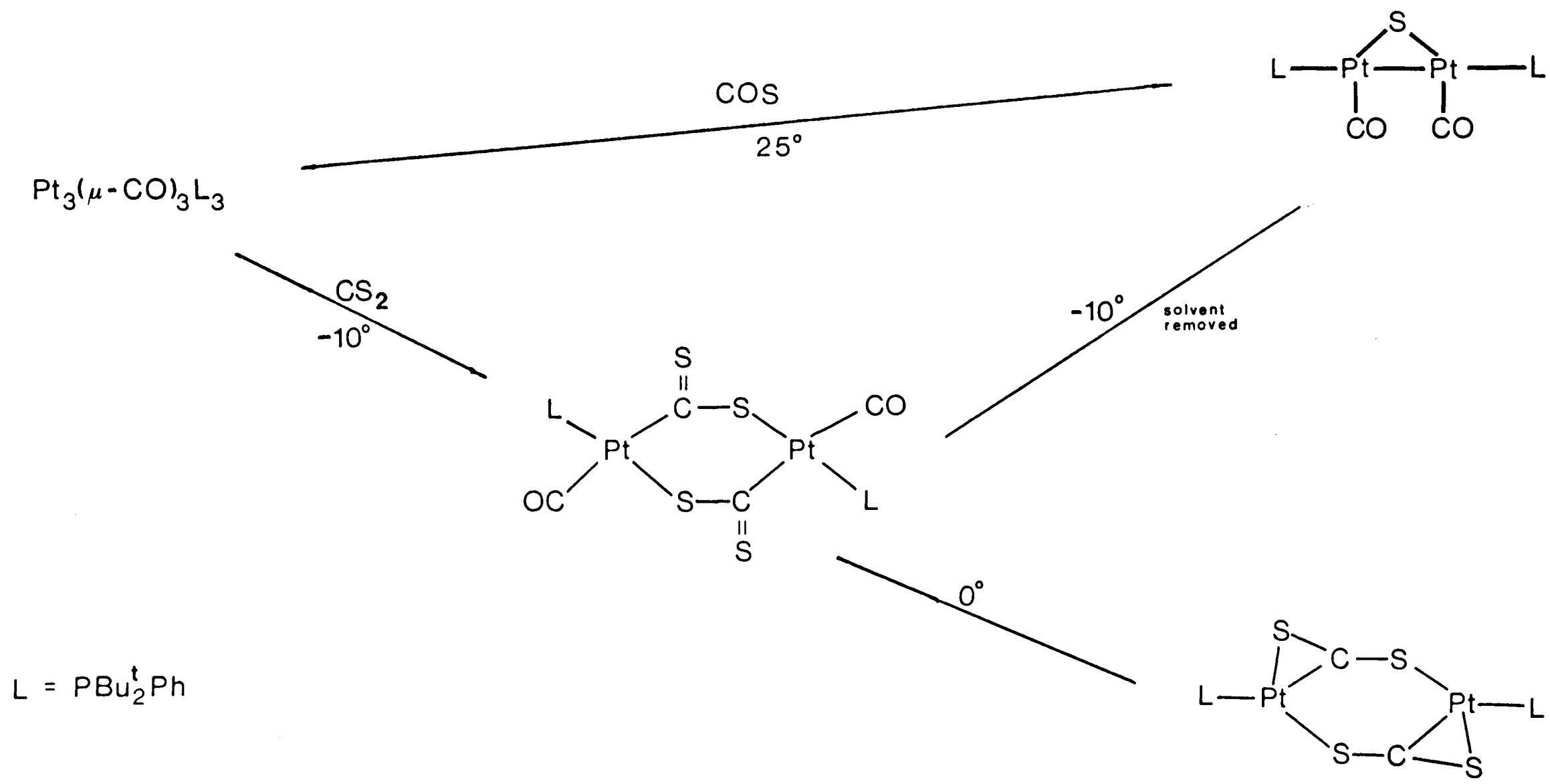

Figure 2.10 Fragmentation reactions of a Pt_3 triangular cluster

agreement with the observations of Farrar described above. This product, identified on the basis of infra red and $^{31}P\{^{1}H\}$ NMR evidence, has been made by another method and the significance of the compound is discussed in detail in Chapter 4. The $^{31}P\{^{1}H\}$ NMR spectrum is discussed in Chapter 5. The importance of the reaction with COS is that it gives an efficient synthetic route from the Pt_3 triangular clusters to the family of sulphur bridged binuclear compounds.

2.4 Amine oxide labilised ligand exchange

Much attention has been given to the interconversion of μ-CO and μ-SO_2 triangulo clusters of platinum as shown in reaction 2.18 below:

$$[Pt_3(\mu\text{-}CO)_3(PR_3)_3] \underset{\text{CO}}{\overset{SO_2}{\rightleftharpoons}} [Pt_3(\mu\text{-}SO_2)_3(PR_3)_3]$$

benzene, 60° (2.18)

The forward reaction is found to proceed to completion quite readily on passing SO_2 gas through the solution. However, as has been described above, the reverse reaction can not normally be achieved. Attempts in this direction produce mixed CO/SO_2 clusters and/or binuclear species.

It is known that trimethylamine N-oxide in some circumstances can labilise coordinated CO to substitution.[89,90] The main requirement is that the ligand be not too strongly bound to the metal and this is usually the case when the CO stretching frequency in the infra-red exceeds $2000cm^{-1}$. For example:

$$M(CO)_6 \xrightarrow[-30^\circ]{\text{xs } Me_3NO} M(CO)_5(NMe_3) \xrightarrow{PR_3} M(CO)_5(PR_3)$$

$$M = Cr, Mo, W \qquad (2.19)$$

It is also known that Me_3NO reacts with SO_2 to form the adduct Me_3NSO_3 which can be isolated as a white crystalline solid.[91] Therefore, it was thought that Me_3NO might also be able to labilise coordinated SO_2. The reaction of $[Pt_3(\mu\text{-}SO_2)_3(PCy_3)_3]$ with CO was carried out in the presence of varying amounts of Me_3NO and was monitored by UV spectroscopy. Three parallel reactions were carried out. CO gas was bubbled for one hour through hexane suspensions of $[Pt_3(\mu\text{-}SO_2)_3(PCy_3)_3]$ containing respectively 0, 3 and 20 mole equivalents of Me_3NO, after which time the suspensions were left stirring under an atmosphere of CO. The intended product of the reaction, $[Pt_3(\mu\text{-}CO)_3(PCy_3)_3]$, has a characteristic UV absorption band at 385nm and the course of the reaction was monitored by observing the growth of this band in the UV absorption spectra. Figure 2.11 shows the spectra obtained for these reactions. The first observation to be made is that the presence of Me_3NO is necessary for the total replacement of the bridging SO_2 ligands by CO. In the absence of Me_3NO the 385nm absorption band is not seen even after two days. The second observation is that a large excess of Me_3NO greatly increases the speed of the reaction.

The action of Me_3NO is not strictly catalytic since it is consumed in the reaction, presumably being converted, at least in the first instance, to Me_3NSO_3. Moreover, larger amounts of Me_3NO seem to give even greater acceleration in the reaction rate. It is clear that the Me_3NO does assist in labilising the bridging SO_2 ligands. Without it the reaction does not proceed to completion at all. Addition of 3

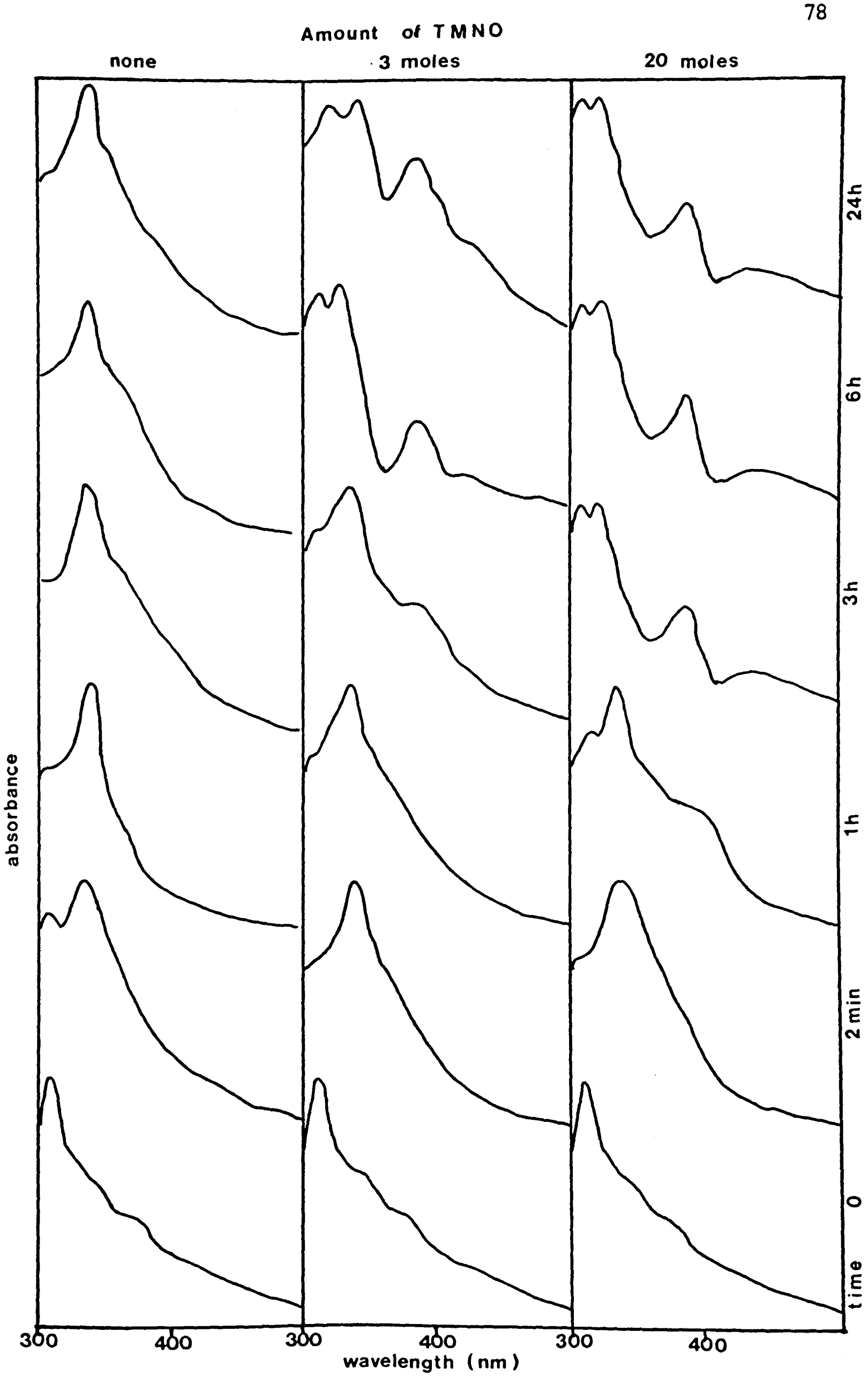

Figure 2.11 UV spectra monitoring the conversion of $[Pt_3(SO_2)_3(PCy_3)_3]$ to $[Pt_3(CO)_3(PCy_3)_3]$ in the presence of Me_3NO

mole equivalents of Me_3NO gives virtually complete reaction in about 6-8 hours and 20 equivalents will give complete reaction in about 2-3 hours.

The use of Me_3NO could turn out to be a useful general method for labilising the SO_2 ligand. Unlike CO, SO_2 can also be removed when in the bridging mode and this finds further application in the synthesis of the anionic Pt_3 clusters described below.

2.5 Synthesis of anionic triplatinum cluster compounds

All of the triangulo-Pt_3 clusters discussed so far are neutral compounds based on neutral ligands. An alternative route is available to the 44 electron species, involving the preparation of anionic clusters. Some high nuclearity anionic clusters of platinum have been known for some time. They are the chains of Pt_3 triangles of general formula $[Pt_3(\mu\text{-}CO)_3(CO)_3]_n^{2-}$ (n = 2,...,6,10).[39,71] Evidence for the existence of the single 44 electron triangle $[Pt_3(\mu\text{-}CO)_3(CO)_3]^{2-}$ has only been found in the ^{195}Pt solution NMR studies.[7] It has been predicted[60] that it should generally be possible to add an electron pair to the 42 electron cluster $[Pt_3(\mu\text{-}X)_3(PR_3)_3]$ if the a_2' cluster molecular orbital can be stabilised by a suitable bridging ligand. The a_2' orbital is an in plane orbital which is metal-metal antibonding:

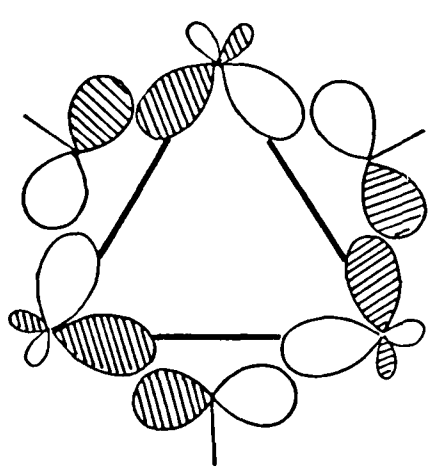

Bridging SO_2 stabilises the unoccupied a_2' orbital compared with CO since the single π-acceptor orbital of SO_2 lies in the Pt_3 plane. PR_2^+ and Cl^+ have a particularly low lying π-acceptor orbital and so can stabilise the a_2' orbital even further - to the extent that an extra electron pair can be accommodated. Thus it should be possible to generate a 44 electron anionic cluster by substituting one bridging SO_2 with PR_2^- or Cl^-.

The syntheses described below take the 42 electron $[Pt_3(\mu\text{-}SO_2)_3(PR_3)_3]$ clusters and replace one SO_2 ligand with a bridging halide ligand. These syntheses support the electronic arguments discussed above and the provision of the extra two electrons in this manner avoids any problem of overcrowding with the phosphine ligands at the metal centres.

A new type of 44-electron platinum phosphine cluster compound has been made by reacting the 42-electron $[Pt_3(\mu\text{-}SO_2)_3(PR_3)_3]$ (PR_3 = PPh_3, PCy_3) with free halide ion to give $[Pt_3(\mu\text{-}SO_2)_2(\mu\text{-}X)(PR_3)_3]^-$ (X = Cl, Br):

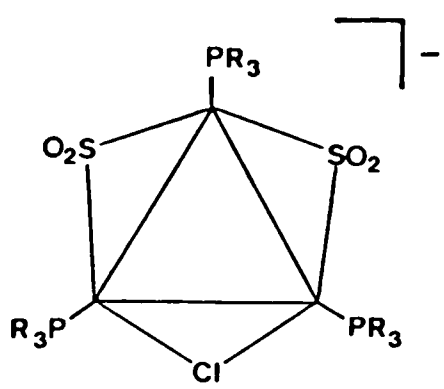

The reaction was carried out by adding an ethanol solution of the halide to a benzene solution of the parent cluster compound, the halide being chosen from a range of quaternary ammonium halides: PPNCl, $BzEt_3NCl$, Me_4NCl, Et_4NCl and Et_4NBr (Full experimental details are given in Chapter 6). In the case where PR_3 = PPh_3, the reaction

as given proceeds quickly and in good yield (84%) under ambient conditions. For PR_3 = PCy_3, the reaction is very slow and incomplete unless catalysed by the addition of Me_3NO which acts by labilising an SO_2 ligand to form Me_3NSO_3 as described in Section 2.4. In the absence of Me_3NO negligible reaction was observed in two days but Me_3NO was found to accelerate the reaction to good effect and a high yield of the anionic product was obtained after just 15 minutes. The apparent reactivity of the compounds $[Pt_3(\mu\text{-}SO_3)_3(PR_3)_3]$ towards the halide is in agreement with that found in Section 2.3 for reactivity towards CO. Characterisation of the products of these reactions has been achieved using analytical and infra-red data, but particularly by means of $^{31}P\{^1H\}$ NMR. The analysis of these NMR spectra is discussed in Chapter 5 along with structural information derived from them.

Further evidence for the structure of this anionic cluster was found from its reaction with the $[AuPR_3]^+$ cation. In Chapter 3 the synthesis of some mixed platinum - gold clusters is discussed. One particular example, shown below, is formed on reacting the neutral Pt_3 triangle $[Pt_3(\mu\text{-}SO_2)_3(PCy_3)_3]$ with $Au(PCy_3)Cl$:

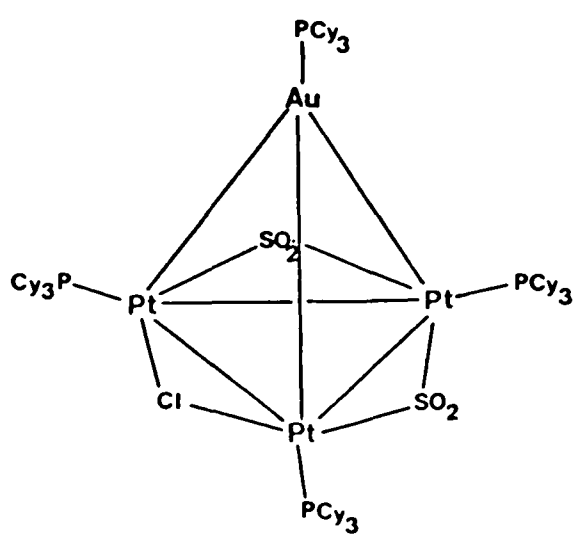

$^{31}P\{^1H\}$ NMR evidence showed that the analogous compound was formed when the anionic Pt_3 cluster, $[Pt_3(\mu\text{-}SO_2)_2(\mu\text{-}Cl)(PCy_3)_3]^-$, was reacted

with a solution containing $[AuP(p\text{-}FC_6H_4)_3]^+$. The gold-phosphine cation was prepared by pre-reacting $[Au\{P(p\text{-}FC_6H_4)_3\}Cl]$ with excess $TlPF_6$ in THF. In the presence of excess $[AuP(p\text{-}FC_6H_4)_3]^+$, the anionic cluster reacted further to give the bicapped cluster $[Pt_3Au_2(\mu\text{-}SO_2)_2(\mu\text{-}Cl)(PCy_3)_3\{P(p\text{-}FC_6H_4)\}_2]^+$. The structure of this product was also confirmed by its $^{31}P\{^1H\}$ NMR spectrum.

2.6 Summary

The homometallic cluster chemistry of platinum is dominated by 42 and 44 electron Pt_3 triangular clusters. Electronic and steric effects are responsible for discriminating between the two types and are influenced by variations in the terminal ligand (usually a phosphine) as well as the bridging ligand (typically CO, SO_2 and Cl^-). Under certain conditions the triangle can be made to fragment reversibly into binuclear species. Equally, higher nuclearity clusters can be formed which are still based on the triangular unit. In the case of cluster compounds containing PPh_3, it is is possible to relate all these types of reaction in the single scheme shown below.

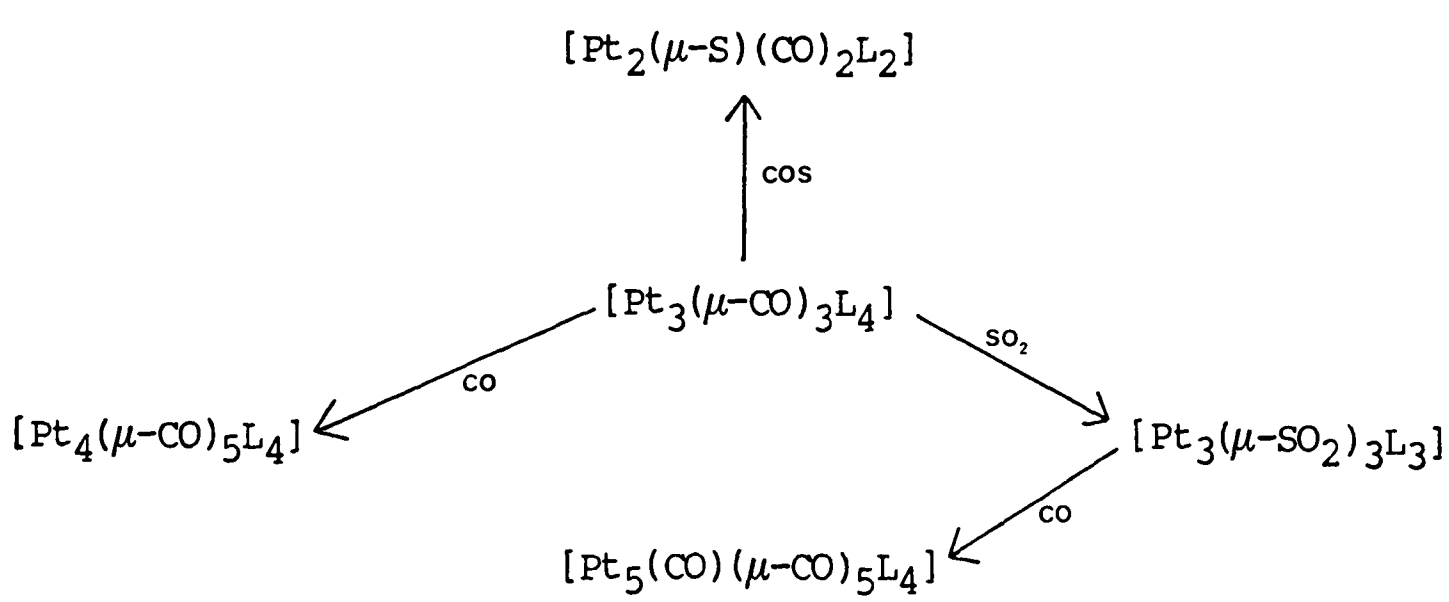

CHAPTER THREE

SYNTHESIS AND CHARACTERISATION OF SOME HETEROMETALLIC CLUSTER COMPOUNDS OF PLATINUM

3.1 Introduction

Triangular cluster compounds of platinum have been found to be convenient starting blocks from which to develop the syntheses of some mixed metal clusters. Chapter 1 described some recent examples in which gold has been added in capping fashion to one or both faces of a platinum triangle. Some clusters have also been reported in which hetero- atoms are sandwiched between a pair of platinum triangles. The "sandwich" type compounds will be discussed in detail later. All of these mixed metal clusters may also be considered as complexes of the hetero- metal atoms, in which the Pt_3 triangle acts as a bulky ligand. This Chapter describes some syntheses which use the platinum cluster $[Pt_3(\mu\text{-}CO)_3(PPh_3)_4]$ as a source of such a ligand. This compound is unusual among the platinum triangles in that it has a fourth terminal phosphine ligand and consequently 44 skeletal electrons. Therefore, a difference in reactivity might be be expected for both electronic and steric reasons.

3.2 The reaction of $[Pt_3(\mu\text{-}CO)_3(PPh_3)_4]$ with $[AuPPh_3]^+$

As discussed in Chapter 1, it has proved possible to cap some platinum clusters with the $[AuPR_3]^+$ fragment.[23,24] The reported examples all start from the 42 electron compounds $[Pt_3(\mu\text{-}X)_3(PR_3)_3]$ (X = CO or SO_2) and result in a symmetrically capped tetrahedral structure.

The compound $[Pt_3(\mu\text{-}CO)_3(PPh_3)_4]$ has been found to dissociate in solution according to the following equilibrium.[12]

$$[Pt_3(\mu\text{-}CO)_3(PPh_3)_4] \rightleftharpoons [Pt_3(\mu\text{-}CO)_3(PPh_3)_3] + PPh_3 \qquad (3.1)$$

Therefore, it was of interest to see whether this platinum cluster could be capped by $[AuPR_3]^+$ and, if so, whether the extra phosphine ligand on the platinum triangle would be lost. If it were lost, a tetrahedral cluster similar to those already reported would be expected.

No reaction was observed when $[Pt_3(\mu\text{-}CO)_3(PPh_3)_4]$ and $Au(PPh_3)Cl$ in 1:1 mole ratio were stirred together in benzene solution. On addition of excess $TlPF_6$, an orange-brown precipitate formed as the solution became almost colourless. Recrystallisation of the precipitate from acetone/benzene gave an orange crystalline solid for which elemental analyses were consistent with the formula $[Pt_3Au(\mu\text{-}CO)_3(PPh_3)_5(PF_6)]$. The infra-red spectrum of the product was similar to that of the starting compound $[Pt_3(\mu\text{-}CO)_3(PPh_3)_4]$ except that the absorption bands in the carbonyl region were shifted by $40cm^{-1}$ to higher frequency. This evidence suggests that the coordination of the ligands around the platinum triangle is essentially unchanged and that all the phosphine ligands are retained. In addition to any change in the elemental analysis, the loss of a phosphine ligand would have been expected to increase the symmetry of the platinum triangle by adding a C_3 axis. This would have been observed as a change in the infra-red spectrum from two strong carbonyl bands to one.

The solution $^{31}P\{^1H\}$ NMR spectrum of the product at ambient temperature indicates an equilibrium similar to that in Equation 3.1. An analysis of this NMR spectrum is included in Chapter 5. A series

of fairly sharp lines in the spectrum correspond to the structure $[Pt_3Au(\mu\text{-}CO)_3(PPh_3)_4]^+$ and there are also some broader lines, due to another structure, which are consistent with two pairs of phosphines coordinated to a platinum triangle as in the parent compound $[Pt_3(\mu\text{-}CO)_3(PPh_3)_4]$. The region of the $^{31}P\{^1H\}$ NMR spectrum corresponding to the $[AuPPh_3]$ moiety is particularly broad, suggesting that the coordination geometry of the gold changes significantly between the different structures. On steric grounds, it is likely that the platinum atom bearing two phosphine ligands is not bonded to the gold atom and a possible solid state structure for the product of the above reaction is as follows:

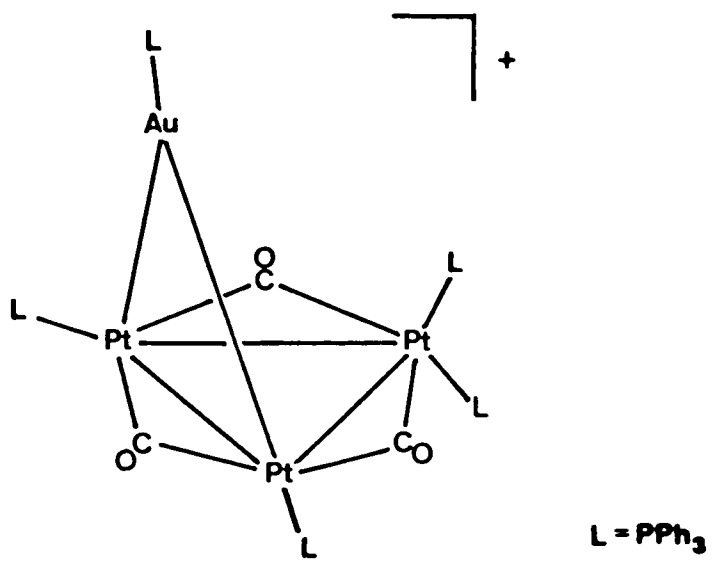

It has so far not proved possible to isolate crystals suitable for an X-ray crystallographic analysis and so a more detailed NMR study was made. The $^{31}Pt\{^1H\}$ NMR spectrum was recorded at lower temperatures in an attempt to freeze out the dissociation of the extra phosphine ligand on the NMR time scale. The best spectral resolution was obtained at -50°, although at this temperature it was still not possible to make any detailed analysis for the compound in question. The spectrum is shown in Figure 3.1. The sharp line at 40.4ppm is probably due to a small amount of $[Pt_3Au(\mu\text{-}CO)_3(PPh_3)_4]^+$ which was

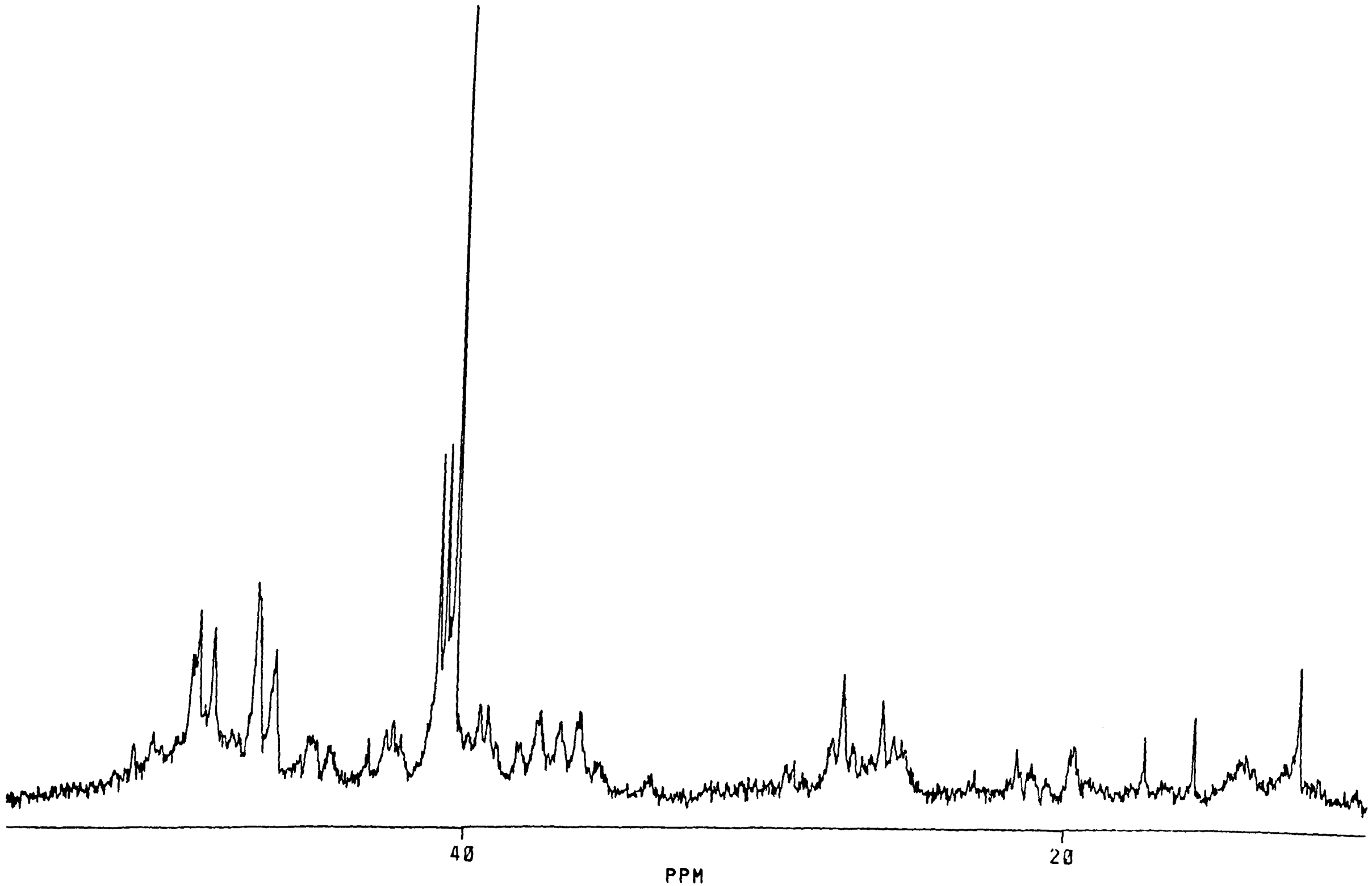

Figure 3.1 Low temperature (-50°) $^{31}P\{^{1}H\}$ NMR spectrum of the heterometallic cluster $[Pt_3Au(CO)_3(PPh_3)_5]^+$

observed more strongly at room temperature. The nearby doublet (40.8ppm) with ^{195}Pt triplet satellites may be tentatively assigned to the symmetric P-Pt-Pt-P unit in the above structure. The coupling constants within this system were measured as $^{2}J(Pt-P)$ = 290Hz, $^{3}J(P-P)$ = 24Hz. The two doublets may then be interpreted in terms of the two inequivalent geminal phosphines coordinated to the third platinum with a $^{2}J(P-P)$ value of 51Hz.

3.3 Gold capping reactions of $[Pt_3(\mu-SO_2)_3(PPh_3)_3]$

The reaction of $[Pt_3(\mu-CO)_3(PPh_3)_4]$ with SO_2 gives $[Pt_3(\mu-SO_2)_3(PPh_3)_3]$ which is a 42 electron cluster. The combination of PPh_3 and SO_2 ligands is exceptional since, according to the observations made in Chapter 2, the two ligands are known to stabilise different low-lying unoccupied molecular orbitals (the out of plane a_2'' and the in plane a_2' respectively). The reactivity of this compound towards gold capping has, therefore, been considered.

$[Pt_3(\mu-SO_2)_3(PPh_3)_3]$ was found to react with an equimolar amount of $[Au(PPh_3)Cl]$ on stirring in benzene. Recrystallisation of the product from CH_2Cl_2/hexane gave red microcrystals of $[Pt_3Au(\mu-SO_2)_2(\mu-Cl)(PPh_3)_4]$, shown below, which was characterised on the basis of analytical and spectroscopic evidence.

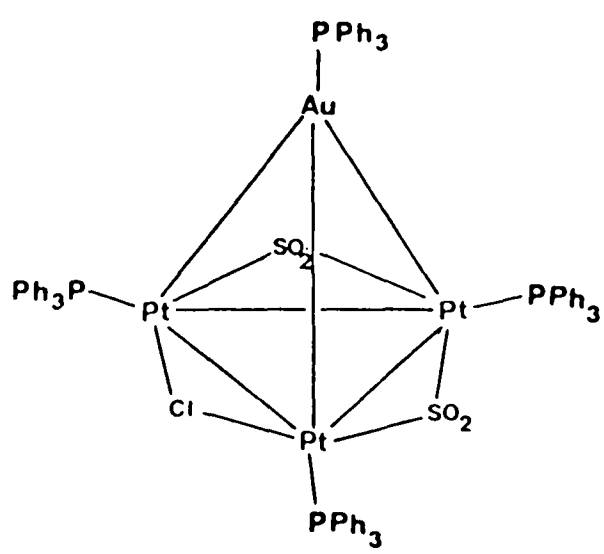

In particular, the characteristic $^{31}P\{^1H\}$ and $^{195}Pt\{^1H\}$ NMR spectra, which are described in detail in Chapter 5, served to identify the tetrahedral Pt_3Au structure which has already been observed in a similar reaction involving $[Pt_3(\mu\text{-}SO_2)_3(PCy_3)_3]$.[24] Thus it is possible to cap the triangular $[Pt_3(\mu\text{-}SO_2)_3(PPh_3)_3]$ using $[Au(PPh_3)Cl]$ to obtain the neutral tetrahedral cluster which incorporates a bridging chloride ligand.

$[Pt_3(\mu\text{-}SO_2)_3(PPh_3)_3]$ was then introduced into a solution containing $[AuPPh_3]^+$ in an attempt to synthesise the cationic gold-capped cluster $[Pt_3Au(\mu\text{-}SO_2)_3(PPh_3)_4]^+$. The $[AuPPh_3]^+$ moiety was generated by reacting $[Au(PPh_3)Cl]$ with $TlPF_6$ in THF solution and then filtering the solution to remove any chloride as TlCl. When a chlorinated solvent such as CH_2Cl_2 was used to work up the reaction mixture, the cluster product obtained was $[Pt_3Au(\mu\text{-}SO_2)_2(\mu\text{-}Cl)(PPh_3)_4]$. It was shown to be identical to that obtained from the reaction with $[Au(PPh_3)Cl]$ described above. When the reaction mixture was worked up with the rigorous exclusion of chlorinated solvents, the only platinum-containing material which could be identified was the starting compound $[Pt_3(\mu\text{-}SO_2)_3(PPh_3)_3]$. It seems that the simple capping reaction with $[AuPPh_3]^+$ can not be carried out on this platinum cluster. It is possible that without a bridging chloride ligand to act as a π-donor this particular Pt_3 cluster is not sufficiently nucleophilic to coordinate to the $[AuPPh_3]$ fragment.

3.4 Sandwich-type cluster compounds

A number of cluster compounds have been synthesised in which two platinum triangular units are coordinated to a hetero- metal atom in

"sandwich" fashion. Yamamoto et al[92] have characterised the compound $[Pt_3(\mu\text{-}CNC_8H_9)_3(CNC_8H_9)_3]_2Hg$ (I) which is a neutral complex, formed during the Na/Hg reduction of $[Pt(CNC_8H_9)_2Cl_2]$ in the presence of excess CNC_8H_9 (2,6 xylyl isocyanide). Another product formed in the same reaction was the homometallic cluster $[Pt_7(CNC_8H_9)_{12}]$,[93] the structure of which was described in Chapter 1. Both compounds are unusual in containing isocyanides as the only ligand. Venanzi et al[94] have synthesised the compound $[Pt_3(\mu\text{-}CO)_3(PPhPr^i{}_2)_3]_2Hg_2$ (II) which is also a neutral complex, formed from the triangular platinum cluster $[Pt_3(\mu\text{-}CO)_3(PPhPr^i{}_2)_3]$ by reaction with metallic mercury. This compound contains an Hg_2 moiety sandwiched between two platinum triangles and may also be considered as two $[Pt_3(\mu\text{-}CO)_3(PPhPr^i{}_2)_3]$ units each capped by a separate mercury atom, these two units being joined through the mercury atoms. Most recently, Venanzi et al[95] have reported the cationic complex $[Pt_3(\mu\text{-}CO)_3(PPr^i{}_3)_3]_2Ag^+$ (III) which they prepared by adding excess $AgCF_3SO_3$ to a solution of the triangular cluster $[Pt_3(\mu\text{-}CO)_3(PPr^i{}_3)_3]$, but they could not synthesise a related compound containing gold. The molecular stuctures of these three sandwich-type compounds are shown in Figure 3.2.

In compound (I) the six platinum atoms define a trigonal prism with the mercury atom approximately at the centre. There is a small rotational distortion of 11° from the eclipsed D_{3h} conformation. Bond lengths and angles within each of the Pt_3 triangles are similar to those found in homometallic platinum isocyanide complexes. Interactions between the two Pt_3 triangles are thought to be weak since the Hg-Pt bond distance (2.94Å) and the inter-triangle distance (4.95Å) are quite long. In compound (II) the two Pt_3 triangles are staggered and the cluster has a centre of symmetry between the mercury

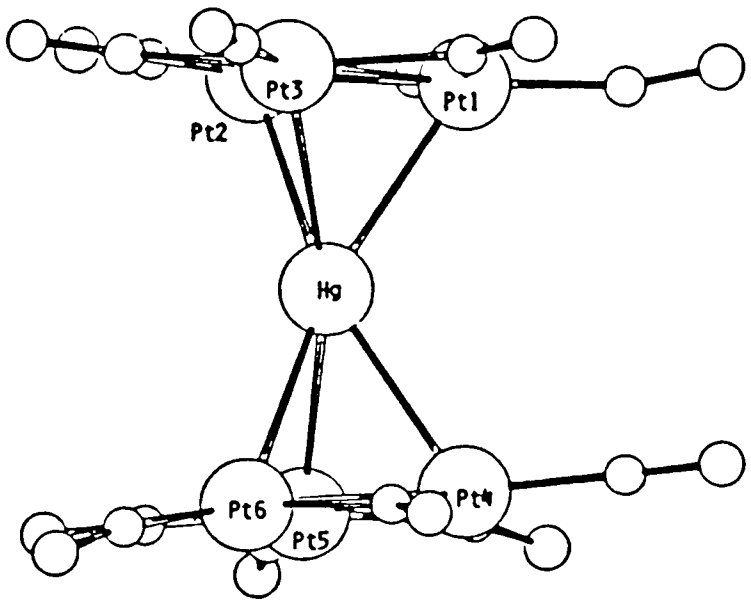

(I) $[Pt_3(CNC_8H_9)_6]_2Hg$[92]

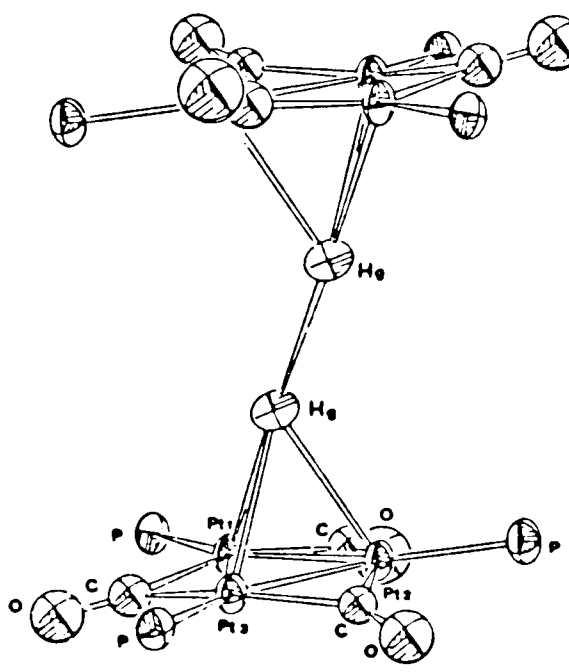

(II) $[Pt_3(CO)_3(PPhPr^i{}_2)_3]_2Hg_2$[94]

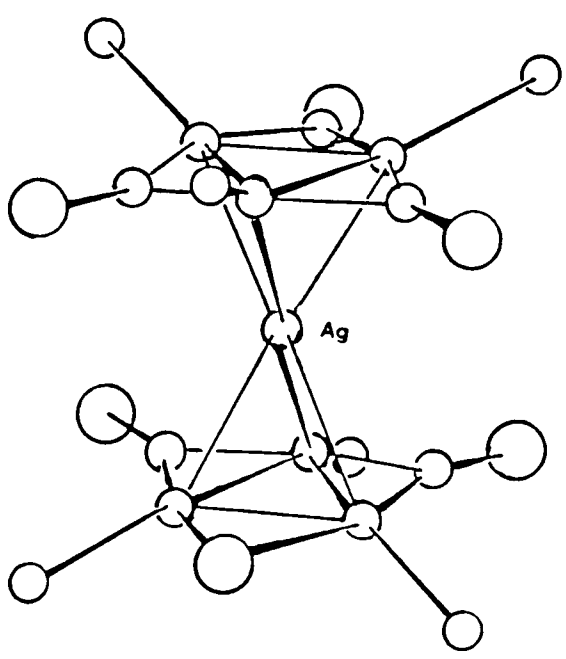

(III) $[Pt_3(CO)_3(PPr^i{}_3)_3]_2Ag^+$ [95]

Figure 3.2 Molecular structures of some sandwich cluster compounds

The R groups of the PR_3 and CNR ligands have been omitted for clarity

atoms. The Pt-Hg distances are quite long and varied (2.93 - 3.08Å) with one on each triangle significantly longer than the other two. The Hg-Hg separation is even longer (3.225Å) and suggests a weak interaction. Within each Pt_3 triangle there is a small inequivalence in the Pt-Pt bonds and the bridging CO ligands are bent out of the Pt_3 plane away from the Hg atoms. Compound (III) also has staggered Pt_3 triangles and a centre of symmetry at the silver atom. Similar distortions are found in the bond lengths with one Ag-Pt distance being longer than the other two and one Pt-Pt distance shorter than the other two. In contrast to compound (II), the bridging CO ligands are bent towards the silver atom but the phosphine ligands are bent out of the Pt_3 plane away from the silver atom. Some structural data for these sandwich compounds are given in Table 3.1.

The bonding in compounds (I) and (II) has been analysed by Hoffmann et al as part of their study of high nuclearity chains.[71] There are two ways of counting the cluster electrons in these sandwich compounds. If the mercury component is considered as Hg^{2+} (I) or Hg_2^{2+} (II) then the platinum triangles are, together, equivalent to $[Pt_3L_6]_2^{2-}$, which is analogous to the carbonyl anion $[Pt_3(CO)_6]_2^{2-}$. The sandwich compound may, therefore, be derived by insertion of an appropriate cation into a stacked triangular cluster anion. On the other hand, the sandwich may be considered as a combination of neutral Hg and neutral $[Pt_3L_6]$ fragments. In this case the Pt_3 triangles are separate entities which are capped by one shared or two separate Hg atoms. ESCA studies suggest that the oxidation state of Hg in compound (I) is close to neutral and that the latter interpretation is better. Molecular orbital calculations based on this interpretation show that the presence of ligands on the Pt_3 triangles such as CO,

	conformation	distances (Å)				
		Pt-Pt	Pt-M	M-M	between triangles	mean deviation of O atoms from Pt_3 plane
(I) $[Pt_3(CNC_8H_9)_6]_2Hg$	11° distortion from eclipsed	mean 2.643	mean 2.943	-	4.954	—
(II) $[Pt_3(CO)_3(PPhPr^i{}_2)_3]_2Hg_2$	staggered	2.661 2.651 2.662	2.968 2.931 3.084	3.225	6	0.54
(III) $[Pt_3(CO)_3(PPr^i{}_3)_3]_2Ag^+$	staggered	2.668 2.657 2.672	2.853 2.828 2.828	-	4.8	0.8

Table 3.1 Structural data for some sandwich cluster compounds

which have low lying π^* orbitals, favour the interaction of the Pt_3 triangles with Hg and, to a lesser degree, with Hg_2. The energy gain from such an intercalation reaction is not confined to a pair of platinum triangles and it is envisaged that long chain intercalates of this type could be synthesised.

3.5 Synthesis and structural characterisation of the sandwich compound $[Pt_3(\mu\text{-}CO)_3(PPh_3)_3]_2Au^+ PF_6^-$

It was found that the fourth phosphine ligand in $[Pt_3(\mu\text{-}CO)_3(PPh_3)_4]$ gave rise to complications in attempts to cap the platinum triangle with an $[AuPPh_3]$ fragment. It is known that this extra phosphine can dissociate in solution and so an attempt has been made to cap the platinum triangle with a gold reagent which is also a "phosphine scavenger". The reagents chosen were Au(CO)Cl and $Au(Me_2S)Cl$. The CO and Me_2S ligands in these compounds are labile and are easily displaced by phosphines.

When equimolar amounts of $[Pt_3(\mu\text{-}CO)_3(PPh_3)_4]$ and Au(CO)Cl were stirred together in benzene in the presence of excess $TlPF_6$, a dark red solid was precipitated as the solution became colourless. Slow recrystallisation of this solid from CH_2Cl_2/hexane gave deep red crystals, which analysed correctly for $[Pt_6(CO)_6(PPh_3)_6Au](PF_6)$, in 88% yield. The infra-red spectrum of these crystals (Nujol mull) showed a single carbonyl band at $1833cm^{-1}$ which indicated an increase in symmetry around the Pt_3 triangle compared with $[Pt_3(\mu\text{-}CO)_3(PPh_3)_4]$ to give a C_3 axis. This level of symmetry was supported by the $^{31}P\{^1H\}$ NMR spectrum of a CH_2Cl_2 solution of the product. All of the ^{31}P nuclei were found to be chemically equivalent within Pt_3L_3 triangles.

An identical product was obtained when the reaction was repeated with $Au(Me_2S)Cl$ in place of $Au(CO)Cl$. In both cases half of the gold used was accounted for in the cluster product and the other half appears to have scavenged the phosphine released by the $[Pt_3(\mu\text{-}CO)_3(PPh_3)_4]$, probably in forming the complex $Au(PPh_3)_2^+$.

An X-ray crystallographic analysis was carried out on a single crystal of the cluster product, obtained by slow diffusion of diethyl ether into an acetone solution. Details of this analysis are summarised in Table 3.2.

$C_{114}H_{90}AuF_6O_6P_7Pt_6$		M = 3254.1
Monoclinic,	space group $C_{2/c}$,	Z = 4
a = 26.637(6)Å,	b = 15.371(3)Å,	c = 27.821(6)Å
β = 108.73(2)°,	U = 10787.71Å^3,	D_c = 2.00 g cm^{-3}
F(000) = 7450,	μ(Mo-K_α) = 154.05cm^{-1},	Final R = 0.0485

Table 3.2 Crystal data for $[Pt_6(CO)_6(PPh_3)_6Au](PF_6)$

The cluster was found to be a sandwich-type compound, similar to those described in the previous Section and having the composition $[Pt_3(\mu\text{-}CO)_3(PPh_3)_3]_2Au^+\ PF_6^-$. Its molecular structure is shown in Figure 3.2 and a selection of bond data is given in Table 3.3. The cluster is cationic and may be described as two gold capped platinum triangles sharing a common Au^+ ion. The "sandwich" compound is comparable to the tetrahedral Pt_3Au clusters discussed earlier in this Chapter if one of the Pt_3 triangles is thought of as a ligand replacing the phosphine coordinated to the gold.

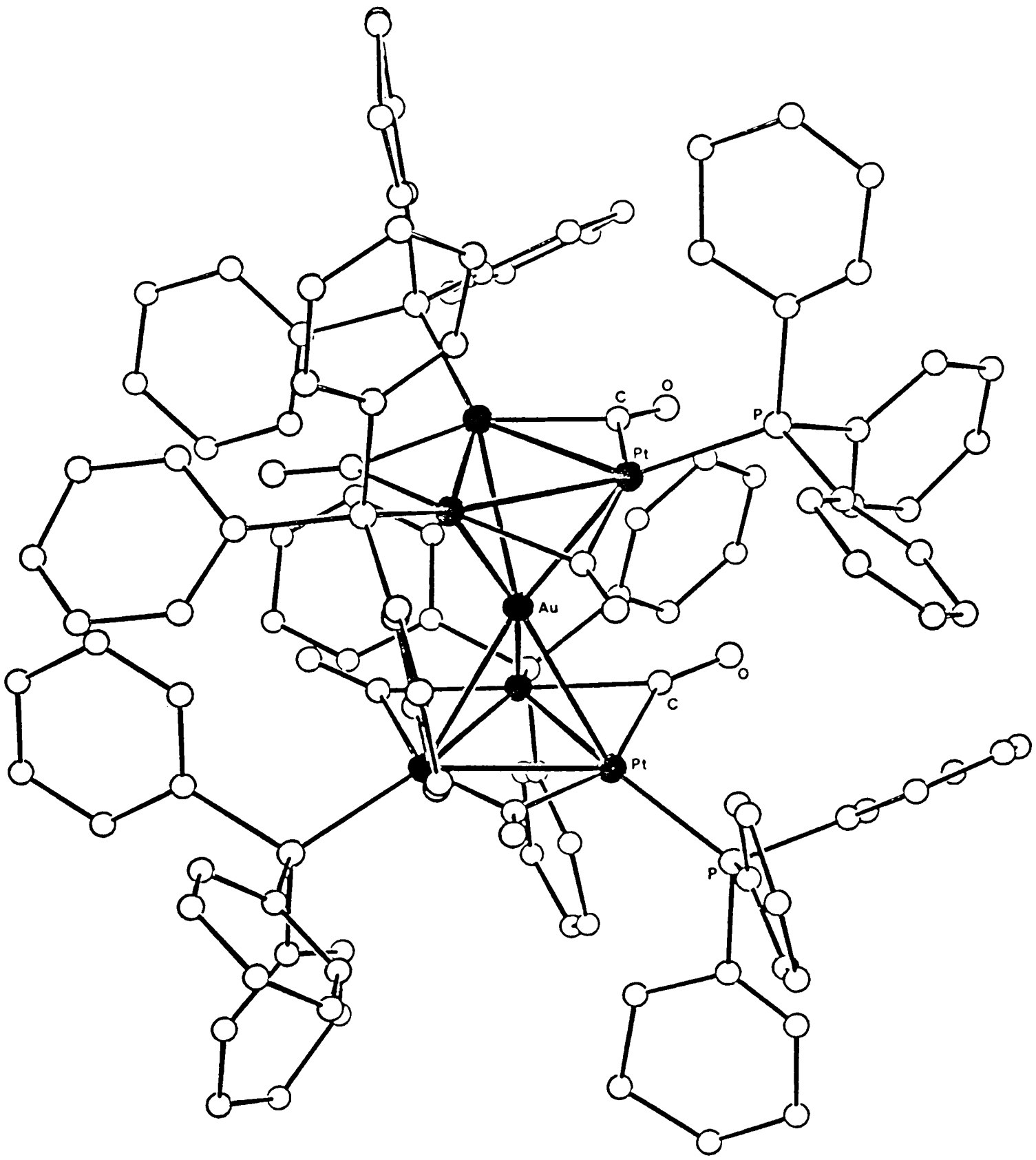

Figure 3.3 Molecular structure of $[Pt_3(\mu\text{-}CO)_3(PPh_3)_3]_2Au^+$

Intramolecular distances (Å)

Pt(1) - Pt(2)	2.683(1)
Pt(2) - Pt(3)	2.683(1)
Pt(1) - Pt(3)	2.683(1)
Pt(1) - Au	2.731(1)
Pt(2) - Au	2.728(1)
Pt(3) - Au	2.725(1)
Pt(1) - P(1)	2.249(5)
Pt(2) - P(2)	2.242(4)
Pt(3) - P(3)	2.250(4)
Pt(1) - C(1)	2.054(18)
Pt(1) - C(3)	2.087(16)

Bond angles (°)

Pt(1)-Pt(2)-Pt(3)	60.0(1)
Pt(3)-Pt(1)-Pt(2)	60.0(1)
Pt(2)-Pt(3)-Pt(1)	60.0(1)
Pt(1)-Pt(2)-Au	60.6(1)
Pt(1)-Pt(3)-Au	60.7(1)
Pt(1)-Au-Pt(3)	58.9(1)
Pt(1)-Au-Pt(2)	58.9(1)
Pt(3)-Au-Pt(3´)	136.1(1)
Pt(2)-Au-Pt(2´)	112.3(1)
Pt(1)-Pt(2)-P(2)	140.2(1)
Pt(1)-Pt(2)-C(2)	108.7(5)
Pt(1)-Pt(2)-C(3)	50.2(4)
Au-Pt(1)-P(1)	147.3(1)
Au-Pt(1)-C(1)	82.2(6)
Au-Pt(1)-C(3)	81.8(5)

Angle between Pt_3 planes: 0.06

Twist angle between planes: 22.31

Table 3.3 Selected molecular dimensions for $[Pt_3(\mu\text{-}CO)_3(PPh_3)_3]_2Au^+$

Estimated standard deviations in parentheses

The six platinum atoms in this structure define a trigonal prism, similar to that in $[Pt_3(\mu\text{-CNR})_3(CNR)_3]_2Hg$, but different from the cationic $[Pt_3(\mu\text{-CO})_3(PPr^i{}_3)_3]_2Ag^+$ which has a fully staggered conformation. The two Pt_3 planes are parallel to within 0.06° and there is a rotational distortion of 22.3° from the eclipsed D_{3h} conformation as can be seen in the diagram below.

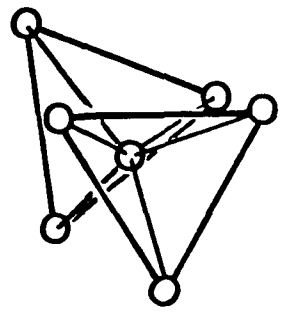

Each Pt_3Au unit is close to a regular tetrahedron with the Pt-Au distances quite similar (2.725 - 2.731Å) and not much longer than the Pt-Pt distances (2.683Å). As a result, the separation of the Pt_3 triangles is only 4.2Å and this suggests a stronger interaction between the platinum triangles and the intercalating atom than has been observed in the three previously reported sandwich compounds.

The bridging CO ligands, which are symmetrically coordinated around the platinum triangles, are distorted out of the plane of the triangle towards the central gold atom. The mean deviation of the O atoms from the Pt_3 plane is 0.8Å. The terminal phosphine ligands are also distorted out of the Pt_3 plane, but away from the gold atom. This arrangement of the ligands is similar to that reported by Venanzi[95] for the sandwich compound containing Ag^+. The sandwich compound containing Hg_2 was different in that only the carbonyl ligands were distorted and they were bent towards the centre of the cluster.

3.6 Synthesis and structural characterisation of the sandwich compound $[Pt_3(\mu\text{-}CO)_3(PPh_3)_4]_2Cu^+ PF_6^-$

The platinum triangular cluster unit has been used as the foundation of a number of heterometallic clusters containing gold as described earlier in this Chapter. Venanzi's sandwich cluster $[Pt_3(\mu\text{-}CO)_3(PPr^i{}_3)_3]_2Ag^+$ is a rare example of a silver containing cluster which also derives from a Pt_3 cluster. It was of interest, therefore, to see if the group IB triad could be completed by the synthesis of a mixed platinum-copper cluster.

When equimolar amounts of $[Pt_3(\mu\text{-}CO)_3(PPh_3)_4]$ and $[Cu(MeCN)_4(PF_6)]$ were stirred together in benzene, a dark red solid was precipitated slowly as the solution became almost colourless. Recrystallisation of this solid from CH_2Cl_2/diethyl ether gave deep red crystals, which analysed correctly as $[Pt_6(CO)_6(PPh_3)_6Cu](PF_6)$, in 80% yield. In particular, an X-ray microanalysis was performed on the crystals which established that the Pt:Cu ratio in the cluster was 6:1. The X-ray spectrum obtained from this analysis is shown in Figure 3.4. The infra-red spectrum of the crystals (Nujol mull) was similar to that observed for $[Pt_3(\mu\text{-}CO)_3(PPh_3)_3]_2Au^+ PF_6^-$. A single strong carbonyl band at $1833cm^{-1}$ indicated bridging carbonyl ligands on platinum triangles with a C_3 symmetry axis.

An X-ray crystallographic analysis was carried out on a single crystal of the cluster product, obtained by slow diffusion of diethyl ether into a CH_2Cl_2 solution, with the results given in Table 3.4.

PEAK LISTING

	ENERGY	AREA	EL. AND LINE
1	2.060	4369	P KA
2	8.044	257	CU KA
3	9.450	1556	PT LA

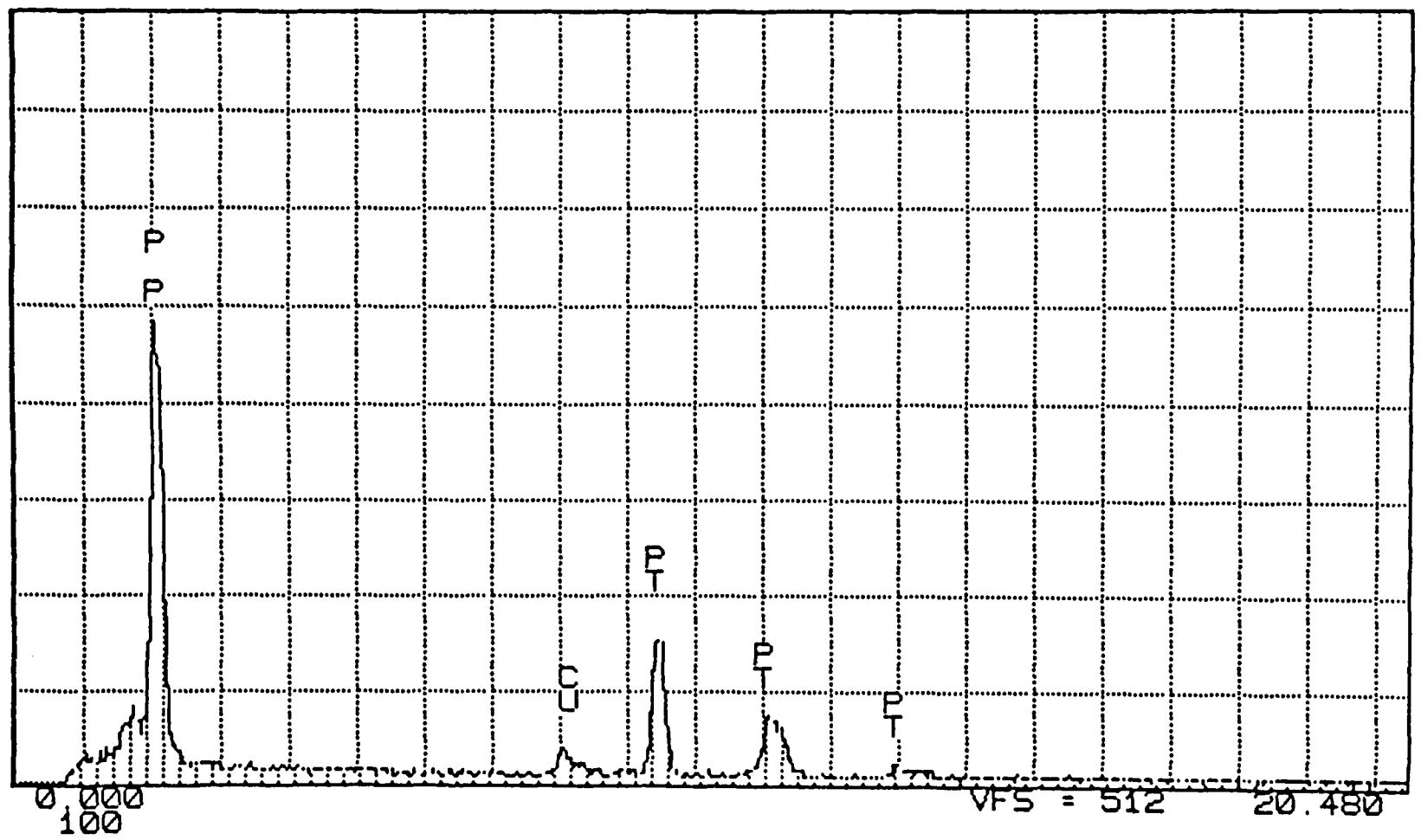

Figure 3.4 X-ray fluorescence spectrum of $[Pt_3(\mu\text{-}CO)_3(PPh_3)_3]_2Cu^+$ (Crystals mounted on nylon grid)

$C_{114}H_{90}CuF_6O_6P_7Pt_6$		M = 3120.7
Monoclinic,	space group $C_{2/c}$,	Z = 4
a = 26.583(6)Å,	b = 15.331(3)Å,	c = 27.366(6)Å
β = 108.56(2)°	U = 10554.06Å^3	D_c = 1.98 g cm^{-1}
F(000) = 5851	μ(Mo-K$_\alpha$) = 79.42cm^{-1}	Final R = 0.0481

Table 3.4 Crystal data for $[Pt_6(CO)_6(PPh_3)_6Cu](PF_6)$

The structure was found to be totally isomorphous with that of the cluster $[Pt_3(\mu\text{-}CO)_3(PPh_3)_3]_2Au^+ PF_6^-$ described in the previous Section. The molecular structure is shown in Figure 3.5 and a selection of bond length and angle data is given in Table 3.5. The two Pt_3 triangles sandwich the Cu atom, forming approximately regular Pt_3Cu tetrahedra. The bond angles in the metal framework are all about 60° and the Pt-Cu distances (2.60Å) are marginally shorter than the bonding Pt-Pt distances (2.65Å). The Pt_3 planes are parallel to within 0.12° and show a twist angle relative to each other of 21.5°. The separation of the Pt_3 planes is approximately 4.2Å which is the same as in the analogous gold sandwich compound. The ligands also show the same distortions from the Pt_3 planes, the CO ligands being bent towards the central Cu atom and the phosphines away from it.

3.7 Reaction of $[Pt_3(\mu\text{-}CO)_3(PCy_3)_3]$ with [Au(CO)Cl]

The sandwich compounds described in Sections 3.5 and 3.6 were synthesised from the platinum cluster $[Pt_3(\mu\text{-}CO)_3(PPh_3)_4]$ which has one more phosphine ligand on the Pt_3 triangle than does the product. Since the platinum triangle was reacted with [Au(L)Cl] (L = CO, Me_2S) in equimolar quantities and only half of the gold was found in the the

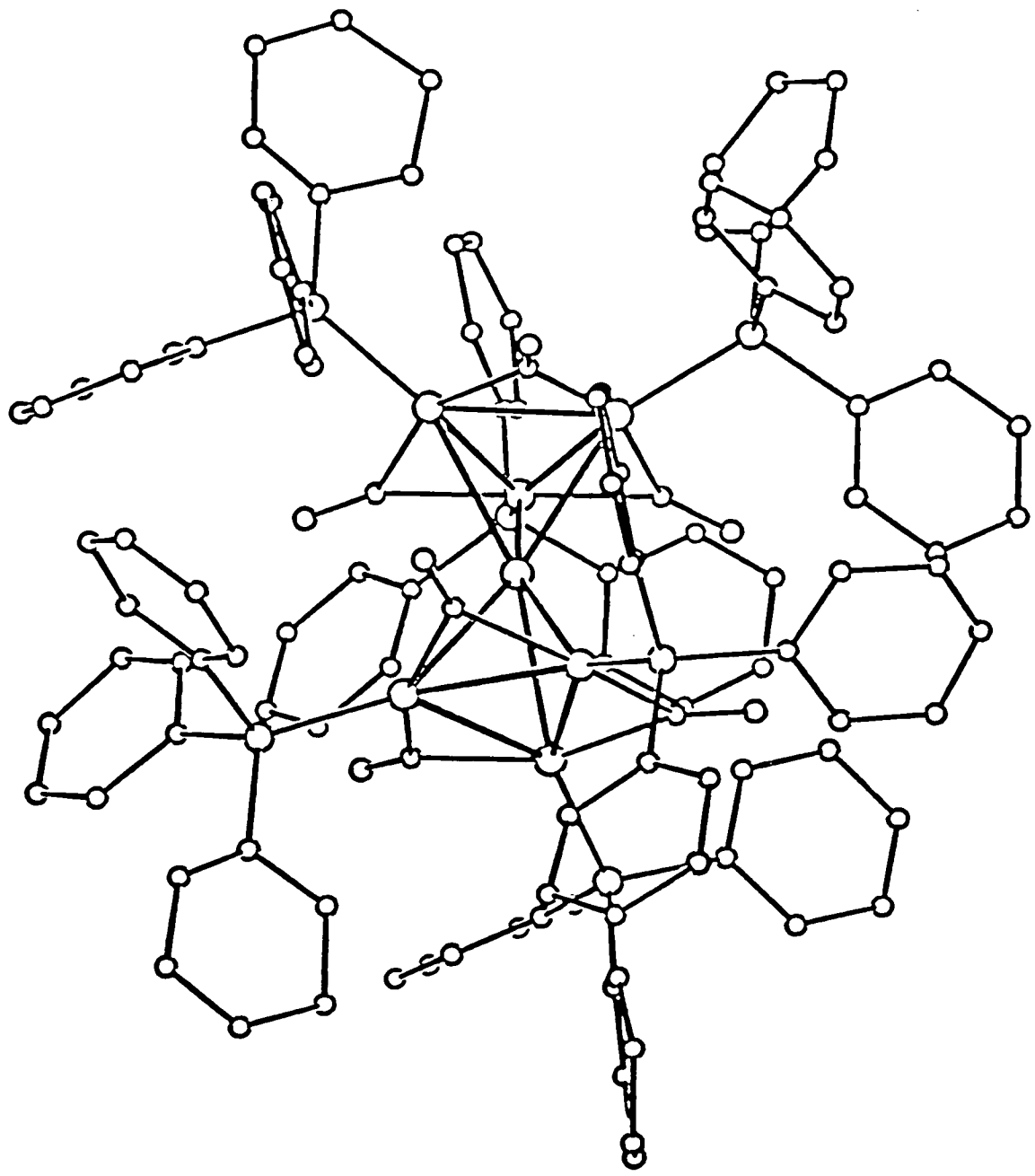

Figure 3.5 Molecular structure of $[Pt_3(\mu\text{-}CO)_3(PPh_3)_3]_2Cu^+$

Intramolecular distances (Å)

Pt(1) - Pt(2)	2.650(2)
Pt(2) - Pt(3)	2.648(2)
Pt(1) - Pt(3)	2.651(2)
Pt(1) - Cu	2.598(2)
Pt(2) - Cu	2.605(4)
Pt(3) - Cu	2.599(3)
Pt(1) - P(1)	2.234(10)
Pt(2) - P(2)	2.243(9)
Pt(3) - P(3)	2.241(8)
Pt(1) - C(1)	2.21(4)
Pt(1) - C(3)	2.052(23)

Bond angles (°)

Pt(1)-Pt(2)-Pt(3)	60.0(1)
Pt(3)-Pt(1)-Pt(2)	59.9(1)
Pt(2)-Pt(3)-Pt(1)	60.0(1)
Pt(1)-Pt(2)-Cu	59.3(1)
Pt(1)-Pt(3)-Cu	59.3(1)
Pt(1)-Cu-Pt(3)	61.3(1)
Pt(1)-Cu-Pt(2)	61.2(1)
Pt(3)-Cu-Pt(3´)	135.2(3)
Pt(2)-Cu-Pt(2´)	109.3(2)
Pt(1)-Pt(2)-P(2)	145.8(3)
Pt(1)-Pt(2)-C(2)	112(1)
Pt(1)-Pt(2)-C(3)	49.9(6)
Cu-Pt(1)-P(1)	149.2(2)
Cu-Pt(1)-C(1)	83(1)
Cu-Pt(1)-C(3)	82.5(7)

Angle between Pt_3 planes: 0.12

Twist angle between planes: 21.48

Table 3.5 Selected molecular dimensions for $[Pt_3(\mu\text{-}CO)_3(PPh_3)_3]_2Cu^+$

Estimated standard deviations in parentheses

cluster product, the extra phosphine was accounted for by the remainder of the gold.

In an attempt to synthesise a platinum-gold sandwich compound without this complication the tris-phosphine cluster $[Pt_3(\mu\text{-}CO)_3(PCy_3)_3]$ was reacted with a half mole-equivalent of [Au(CO)Cl]. The two reagents were stirred together in benzene in the presence of excess $TlPF_6$. The solution darkened and a red crystalline solid was precipitated. Bright red crystals were obtained on recrystallisation from acetone/benzene and were characterised on the basis of analytical and spectroscopic evidence as the tetrahedral cluster $[Pt_3Au(\mu\text{-}CO)_3(PCy_3)_4]^+ PF_6^-$. In particular, the $^{31}P\{^1H\}$ NMR spectrum was identical to that already reported[23] for this compound.

In this reaction, the gold cation has capped some of the platinum cluster compound but the sandwich compound has not been formed. Instead of taking a platinum triangle for its second ligand, the gold has abstracted a phosphine ligand from the remainder of the platinum cluster compound. This entails degradation of some of the platinum cluster and accounts for the darkening of the reaction solution. It is unlikely that formation of the sandwich compound is prevented for steric reasons since Venanzi was able to prepare such a compound using PPr^i_3, which is a fairly bulky ligand.

3.8 Summary

A number of recent syntheses have demonstrated that platinum cluster compounds of the type $[Pt_3(\mu\text{-}X)_3(PR_3)_3]$ are a versatile starting point for the preparation of some heterometallic clusters. The Pt_3 triangle can be capped on one or both sides by $[AuPR_3]$ fragments to give structures based on the tetrahedron or trigonal

bipyramid respectively. It has also proved possible to cap two Pt_3 triangles simultaneously with a shared gold atom to give a trigonal prismatic "sandwich" structure. As a result, there is now a family of platinum-gold clusters which demonstrates a systematic build-up from cluster fragments:

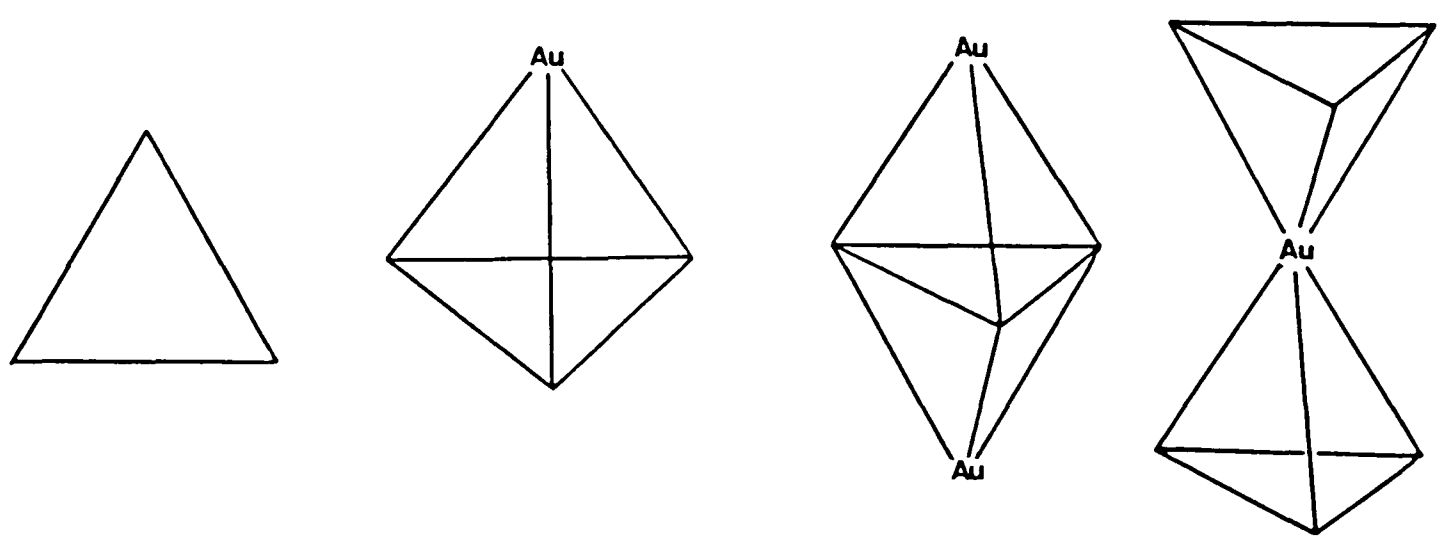

In principle, it should be possible to synthesise long chain clusters based on intercalation of hetero- metal atoms between platinum triangles. This idea is not limited to gold as the hetero- atom since clusters of the sandwich-type have also been synthesised with mercury, silver and copper in the centre.

CHAPTER FOUR

SYNTHETIC AND STRUCTURAL STUDIES OF $[Pt_2(\mu\text{-}S)(CO)(PPh_3)_3]$

4.1 Introduction

The compound $[Pt_2(\mu\text{-}S)(CO)(PPh_3)_3]$ is a potentially ligating platinum sulphido- complex which is known to contain a Pt-Pt bond. It was first synthesised by Wilkinson and Baird[27] by thermolysis of the complex $[Pt(PPh_3)_2(COS)]$. In Chapter 1 it was reported that the compound $[Pt_2(\mu\text{-}S)_2(PPh_3)_4\}$, a related sulphido- complex without a Pt-Pt bond, could function as a ligand towards other metals and thereby generate heterometallic aggregates. It was, therefore, of interest to investigate the ligating properties of the sulphido- group in $[Pt_2(\mu\text{-}S)(CO)(PPh_3)_3]$ since there was a possibility of using this complex to generate heterometallic cluster compounds.

Balch *et al*[96] have reported that $[Pt_2(\mu\text{-}S)(CO)(PPh_3)_3]$ has a robust Pt_2S triangular core in contrast to binuclear complexes of platinum(I) bridged by dppm which readily undergo insertion reactions.[97,98] For example, CO, SO_2 and isocyanides are found to cleave the metal-metal bond, placing a single atom between the metal atoms (4.1).

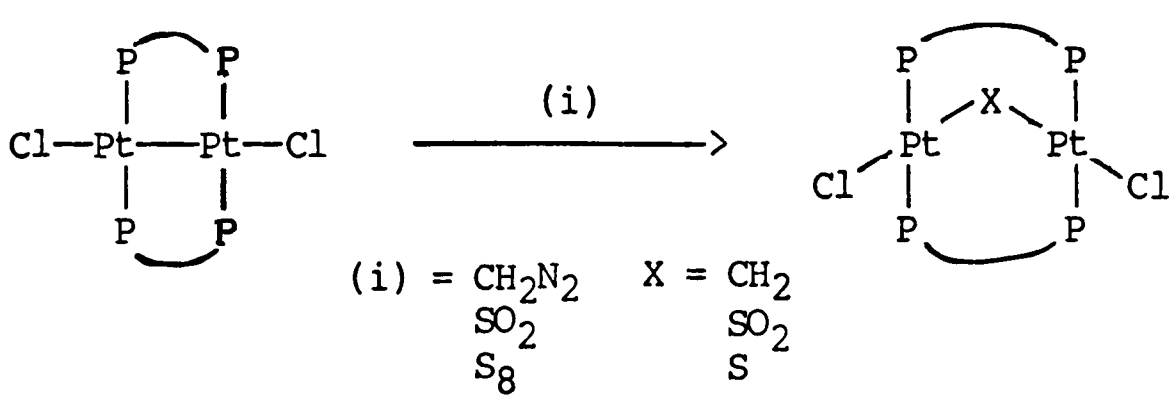

(4.1)

Attempts to insert CO or MeCN into the Pt-Pt bond of the sulphido-bridged complex have not succeeded. $[Pt_2(\mu\text{-}S)(CO)(PPh_3)_3]$ in solution

is not at all reactive towards CO or H_2 at 1 atm. pressure. Instead, its chemistry is found to involve reactions of the ligands. The CO ligand and the one labile phosphine ligand, which is coordinated to the adjacent platinum atom, are readily displaced by isocyanides and chelating diphosphines (e.g. 4.2).

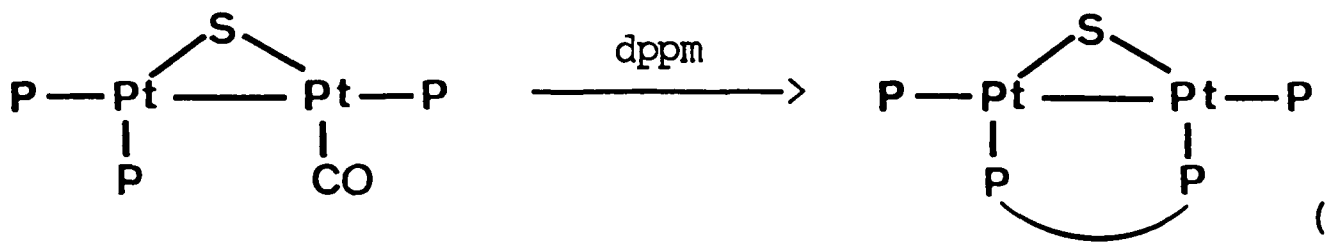

(4.2)

The CO ligand could not be replaced by reaction with excess PPh_3, even in the presence of excess Me_3NO, which is known to labilise terminal CO ligands (see Chapter 2).

The nucleophilic nature of the sulphur atom in the Pt_2S triangle is demonstrated by the methylation reaction with methyl iodide (4.3).

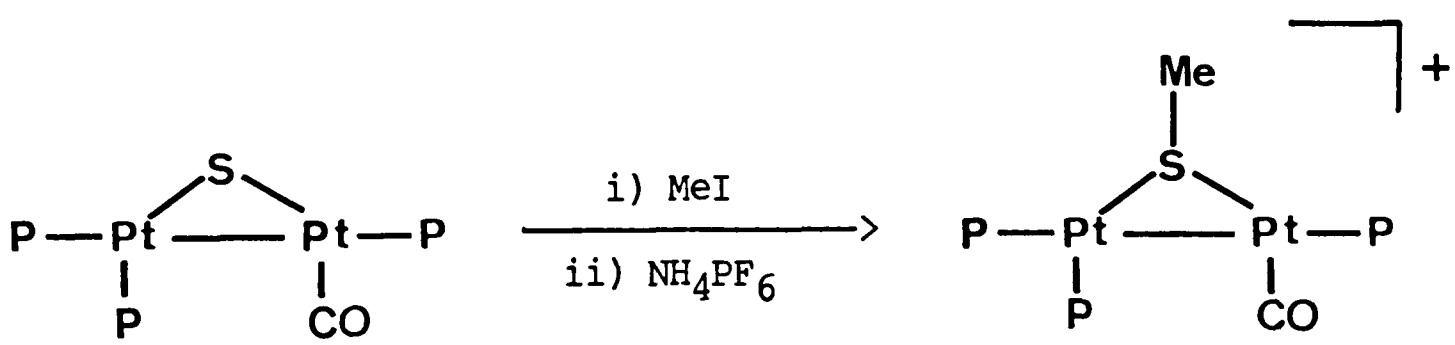

(4.3)

When SO_2 was passed through a suspension of $[Pt_2(\mu\text{-}S)(CO)(PPh_3)_3]$ in pentane, a bright orange complex was formed. Its infra-red spectrum showed absorption bands attributable to SO_2 at 1087s and 1283s cm^{-1}. These values are consistent with the the SO_2 ligand being S- bonded as shown in the following structure.

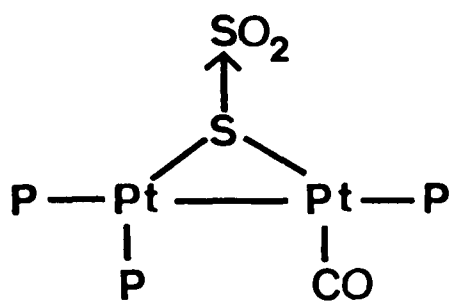

An analogous product has been reported for the reaction of $[Pt_2(\mu\text{-}S)_2(PPh_3)_4]$ with SO_2.[11] The SO_2 ligand is very weakly bound and is readily lost when the complex is allowed to stand in air.

4.2 Synthesis and structural characterisation of $[Pt_2(\mu\text{-}S)(CO)(PPh_3)_3]$

The procedure used to synthesise $[Pt_2(\mu\text{-}S)(CO)(PPh_3)_3]$ was based on the method of Balch[96], which itself was a modification of that originally reported by Wilkinson and Baird.[27] This method involved thermolysis in $CHCl_3$ solution of the complex $[Pt(PPh_3)_2(COS)]$ which was obtained by reacting $[Pt(PPh_3)_3]$ with carbonyl sulphide. A compound which analysed as $[Pt_2(\mu\text{-}S)(CO)(PPh_3)_3]$, which fitted the $^{31}P\{^1H\}$ NMR data reported by Balch and which showed a carbonyl absorption band at $2001cm^{-1}$ in the infra-red spectrum was obtained only if the complex $[Pt(PPh_3)_2(COS)]$ was stirred for a time in warm (50°) $CHCl_3$. If the synthesis was carried out at room temperature then another compound, also analysing as $[Pt_2(\mu\text{-}S)(CO)(PPh_3)_3]$, but with slightly different spectroscopic properties, was obtained. The infra-red spectrum of this alternative product showed a small shift in the carbonyl band to $1994cm^{-1}$. The $^{31}P\{^1H\}$ NMR spectrum showed the same pattern of lines, due to the same arrangement of ^{31}P and ^{195}Pt nuclei, but with different chemical shifts and slightly different coupling constants as shown in Table 4.1. This second form of $[Pt_2(\mu\text{-}S)(CO)(PPh_3)_3]$ was converted into the form characterised by Balch on

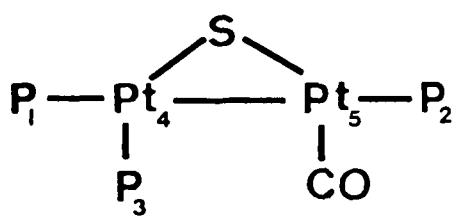

P = PPh_3

Reaction temperature in synthesis	20°	>50°
Infra-red ν(CO) (cm^{-1})	2001	1994
NMR (CD_2Cl_2 solution)		
$\delta(^{31}P)$ (ppm): P_1	19.5	20.9
	15.2	16.3
	19.1	19.5
J (Hz): $P_1 - P_2$	182	183
$P_1 - P_3$	-10	-9
$P_2 - P_3$	22	22
$P_1 - Pt_4$	3462	3510
$P_1 - Pt_5$	280	291
$P_2 - Pt_4$	204	193
$P_2 - Pt_5$	2663	2716
$P_3 - Pt_4$	3613	3600
$P_3 - Pt_5$	-117	-119

Table 4.1 ^{31}P NMR parameters for the two different samples of $[Pt_2(\mu\text{-}S)(CO)(PPh_3)_3]$

refluxing a suspension in ethanol.

4.2.1 X-ray structural analysis of $[Pt_2(\mu\text{-}S)(CO)(PPh_3)_3]$

An X-ray crystallographic analysis of $[Pt_2(\mu\text{-}S)(CO)(PPh_3)_3]$ was carried out by Skapski and Troughton in 1969.[29] The accuracy of the study was somewhat limited due to a disorder involving the carbonyl and the phosphine ligands coordinated to the same platinum atom. Two geometric isomers appeared to be present in the approximate ratio 63:37. In the course of this work single crystals of $[Pt_2(\mu\text{-}S)(CO)(PPh_3)_3]$ were obtained by slow diffusion of diethyl ether into an acetone solution and it was decided to measure the unit cell parameters as part of the characterisation of the compound. The cell parameters varied considerably from those reported previously and so a full structural redetermination was made. Table 4.2 gives a comparison of the crystallographic and structural parameters which were obtained from this determination with those reported by Skapski and Troughton. The large discrepancy in parameters can be attributed in part to alternative and arbitrary choices of triclinic unit cell. More significant is the difference in unit cell volumes and densities. In contrast to the original determination no crystallographic disorder was found on this occasion. In consequence the standard deviations on the bond lengths and angles are smaller.

The overall structural features are very similar for the two determinations. The platinum atoms with sulphur form a three membered ring. The Pt-Pt distance is 2.65Å and is typical for a Pt-Pt single bond. The slightly shorter of the two Pt-S bonds is observed trans to the carbonyl group although the Pt-P bond cis to the carbonyl group is longer than the other two. The molecular geometry of $[Pt_2(\mu\text{-}$

$C_{55}H_{45}OP_3Pt_2S$; M = 1236.9

Triclinic; space group $P\bar{1}$

Parameter	Original determination	This determination
Final R	0.069	0.044
D_c	1.72	1.65
a (Å)	10.687(3)	9.491(7)
b	25.240(7)	14.759(6)
c	9.307(3)	18.176(6)
α (°)	95.17(3)	79.79(3)
β	104.22(4)	85.74(5)
γ	97.67(5)	87.47(6)
U (Å^3)	2392.3	2497.5
Bond lengths (Å)		
Pt-Pt	2.647(2)	2.653(1)
Pt(1)-S	2.277(9)	2.273(4)
Pt(2)-S	2.218(8)	2.255(4)
Pt(1)-P(1)	2.318(9)	2.303(4)
Pt(2)-P(2)	2.267(9)	2.278(4)
Pt(2)-P(3)	2.226(9)	2.267(4)
Bond angles (°)		
Pt(1)-S-Pt(2)	73.1(1)	71.7(1)
Pt(1)-Pt(2)-S	53.5(3)	53.8(1)
Pt(2)-Pt(1)-S	53.6(3)	54.5(1)
S-Pt(2)-P(3)	106.8(4)	102.2(1)
S-Pt(1)-P(1)	104.5(4)	102.4(1)
P(3)-Pt(2)-P(2)	101.6(4)	104.6(1)

Table 4.2 Comparison of crystallographic parameters obtained for $[Pt_2(\mu\text{-}S)(CO)(PPh_3)_3]$

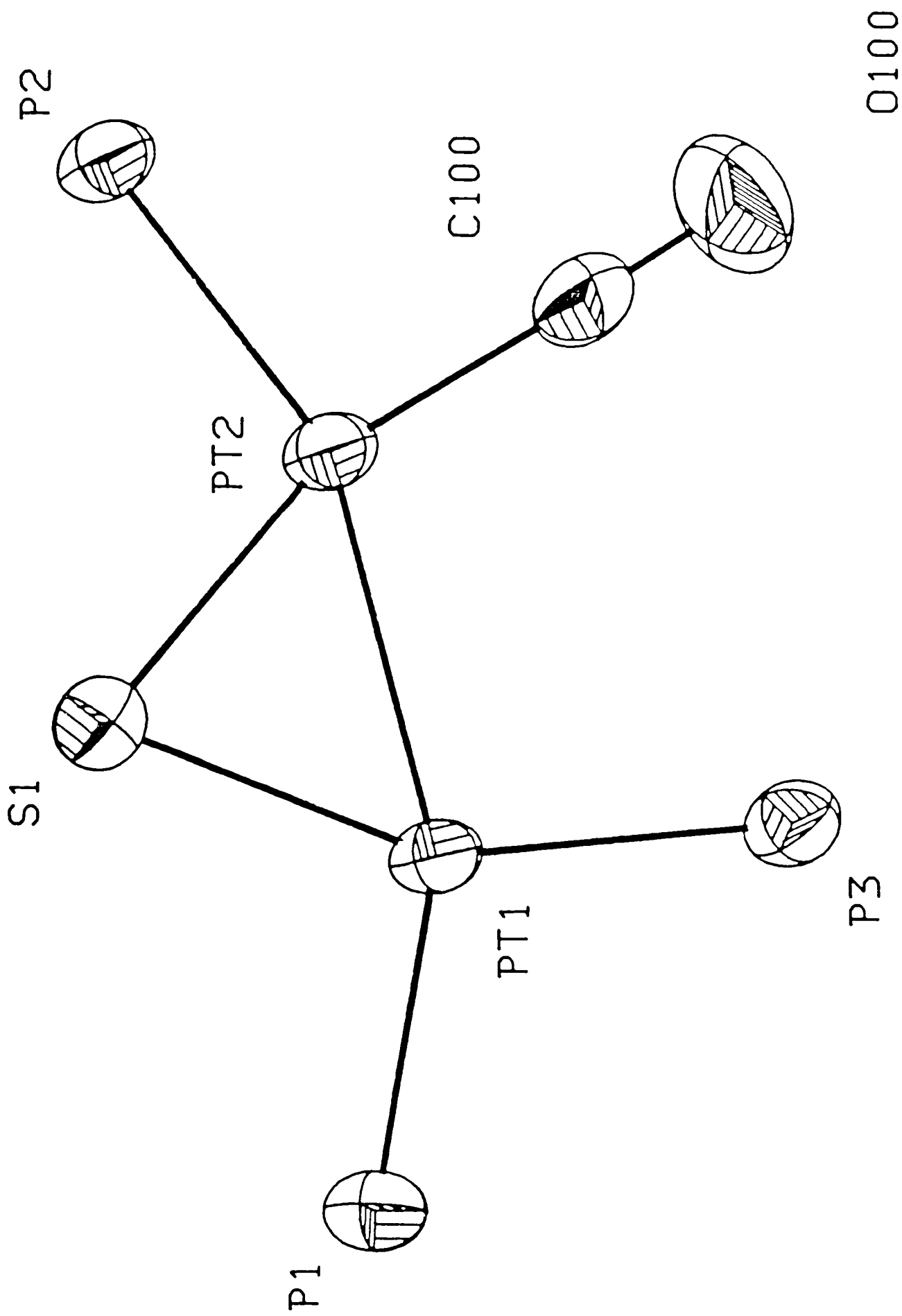

Figure 4.1 Molecular structure of $[Pt_2(\mu\text{-}S)(CO)(PPh_3)_3]$

S)(CO)$(PPh_3)_3$] is illustrated in Figure 4.1.

4.3 The reaction of $[Pt_2(\mu\text{-}S)(CO)(PPh_3)_3]$ with the olefin complex $[(\eta\text{-}C_5H_5)Fe(CO)_2(C_2H_4)]^+$

It has been found that olefin complexes of the type $[\eta\text{-}C_5H_5)Fe(CO)_2(olefin)]^+$ are suitable intermediates for some reactions of olefins with nucleophiles.[99] Such complexes have been reacted with a wide variety of nucleophiles, including amines, phosphines, alcohols and mercaptans as illustrated in (4.4) below.

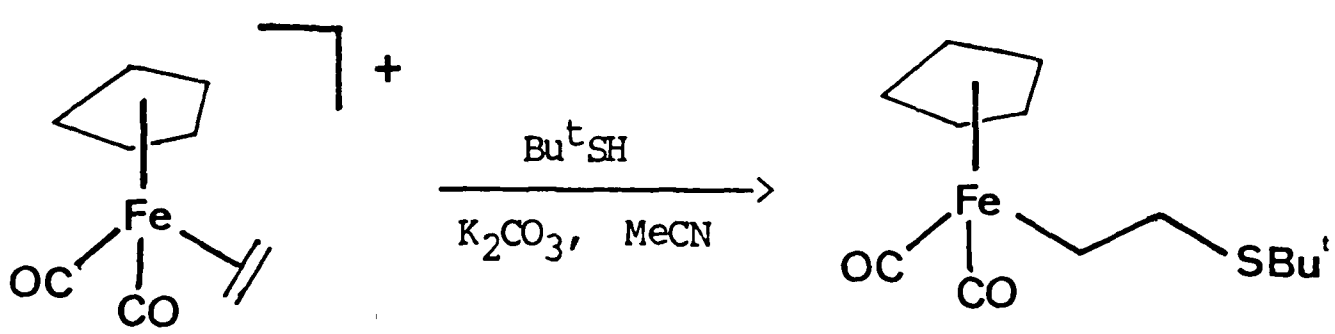

(4.4)

It was of interest to investigate whether the sulphido- ligand of $[Pt_2(\mu\text{-}S)(CO)(PPh_3)_3]$ was sufficiently nucleophilic to react with the olefin complex $[\eta\text{-}C_5H_5)Fe(CO)_2(C_2H_4)]^+$ in a similar way or whether the sulphur atom would coordinate directly to the iron centre.

When equimolar amounts of $[Pt_2(\mu\text{-}S)(CO)(PPh_3)_3]$ and the olefin complex $[\eta\text{-}C_5H_5)Fe(CO)_2(C_2H_4)]^+ BF_4^-$ were stirred together in acetone, a dirty green solid precipitated to leave a bright yellow solution. The solution was filtered, reduced in volume and left to stand whereupon a yellow crystalline precipitate formed. This product was found to contain platinum but not iron and elemental analysis suggested the composition $[Pt_2S(CO)_2(PPh_3)_2]$. The infra-red spectrum contained two strong bands attributable to carbonyl ligands at 2030 and 1990cm^{-1} but no band to suggest a BF_4^- counter ion. The $^{31}P\{^1H\}$ NMR spectrum (see Chapter 5) revealed that all the ^{31}P and ^{195}Pt

nuclei in the molecule were associated in near linear P-Pt-Pt-P units. A ^{13}C NMR spectrum confirmed the absence of η-C_5H_5 ligands in the product. The dirty green compound which was initially precipitated was not characterised but its infra-red spectrum showed it to contain PPh_3 and the BF_4^- anion but no CO ligands. The yellow crystalline compound was characterised as $[Pt_2S(CO)_2(PPh_3)_2]$ and the following structure is proposed.

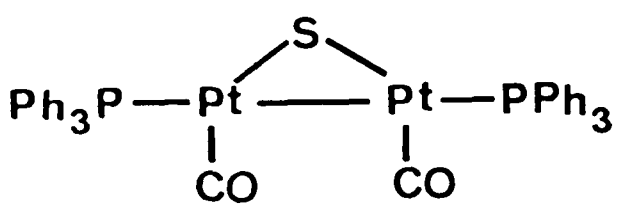

This compound is the same as the product reported in Chapter 2 for the reaction of the cluster $[Pt_3(\mu\text{-}CO)_3(PPh_3)_4]$ with COS. It appears that the iron complex has caused the exchange of a phosphine ligand in $[Pt_2(\mu\text{-}S)(CO)(PPh_3)_3]$ for CO. It is not clear whether the failure to obtain a reaction at the sulphur atom is for steric reasons or because the sulphur is not sufficiently nucleophilic.

The compound $[Pt_2(\mu\text{-}S)(CO)_2(PPh_3)_2]$, obtained from the above reaction, was stirred in benzene solution with an equimolar amount of PPh_3. Addition of cyclohexane to the solution yielded a yellow solid which was found to be the original starting compound $[Pt_2(\mu\text{-}S)(CO)(PPh_3)_3]$. This not only confirms the structure of $[Pt_2(\mu\text{-}S)(CO)_2(PPh_3)_2]$ but also reveals that it is possible to substitute one of the carbonyl ligands in this compound.

4.4 Heterometallic complexes derived from $[Pt_2(\mu\text{-}S)(CO)(PPh_3)_3]$

The ligating potential of the sulphido- group in $[Pt_2(\mu\text{-}$

S)(CO)$(PPh_3)_3$] has been demonstrated by its reactions with MeI and SO_2 described earlier. In view of the known reactions in which the complex [$Pt_2(\mu$-S$)_2(PPh_3)_4$] has been coordinated to other metals through the sulphido- groups, a number of reactions have been carried out in order to synthesise heterometallic complexes based on [$Pt_2(\mu$-S)(CO)$(PPh_3)_3$].

4.4.1 Synthesis and structural characterisation of the complex [$Pt_2(\mu$-S)(CO)$(PPh_3)_3Au(PPh_3)]^+$ PF_6^-

Equimolar amounts of [$Pt_2(\mu$-S)(CO)$(PPh_3)_3$] and [Au(PPh_3)Cl] were stirred together in THF at room temperature in the presence of excess $TlPF_6$ for several hours. Removal of the solvent *in vacuo* followed by recrystallisation from CH_2Cl_2/diethyl ether gave yellow microcrystals, which analysed correctly for [$AuPt_2S(CO)(PPh_3)_4$](PF_6), in good yield (86%). The infra-red spectrum of this compound contained a strong carbonyl absorption band at 2025cm^{-1} which represents a shift to higher frequency of 24cm^{-1} compared with the starting compound and can be attibuted to the positive charge of the complex.

The $^{31}P\{^1H\}$ and $^{195}Pt\{^1H\}$ solution NMR spectra of the compound were extremely complex due to the presence of several ^{31}P environments and a number of ^{195}Pt isotopomers. Analysis of these spectra has been possible and is described in detail in Chapter 5. The spectra have the same general form as for the parent compound [$Pt_2(\mu$-S)(CO)$(PPh_3)_3$] since there is no observable magnetic coupling to the phosphine which is coordinated to the gold atom.

The evidence so far suggests that the [$AuPPh_3]^+$ moiety has a perturbing influence on the [$Pt_2(\mu$-S)(CO)$(PPh_3)_3$] unit but little more can be said about the geometry of the complex. In order to define

more clearly the structure of $[Pt_2(\mu\text{-}S)(CO)(PPh_3)_3Au(PPh_3)]^+$ a single crystal X-ray analysis was carried out. Pale yellow, needle-like crystals were grown by slow diffusion of diethyl ether into a CH_2Cl_2 solution. During the X-ray analysis there were problems with repeated re-orientation of the crystal and so there are limitations on the accuracy of the structural determination. The crystal data obtained from this analysis are given in Table 4.3.

$C_{73}H_{60}AuF_6OP_5Pt_2S$		M = 1841.2
Triclinic,	space group $P\bar{1}$,	Z = 2
a = 11.065(22)Å,	b = 13.903(13)Å,	c = 26.439(13)Å
α = 89.81(6)°,	β = 79.31(8)°,	γ = 79.00(12)°
U = 3921 Å^3,	D_c = 1.56 g cm^{-1},	Final R = 0.081
crystal dimensions 0.1 x 0.05 x 0.1 mm		μ(Mo-K_α) = 58.5cm^{-1}

Table 4.3 Crystal data for $[Pt_2(\mu\text{-}S)(CO)(PPh_3)_3Au(PPh_3)]^+ PF_6^-$

The molecular structure of the complex is illustrated in Figure 4.2 and selected intramolecular bond lengths and angles are given in Table 4.4.

The three metal atoms in this structure define a triangle in which the gold atom is not symmetrically positioned between the two platinum atoms but is significantly closer to the platinum which has the CO ligand bound to it. This asymmetry is illustrated by the difference in the Pt-Au distances of 3.015 and 3.312Å. The latter distance is well out of the range of metal-metal bonding distances for Pt-Au bonds but the former is on the limit of those reported

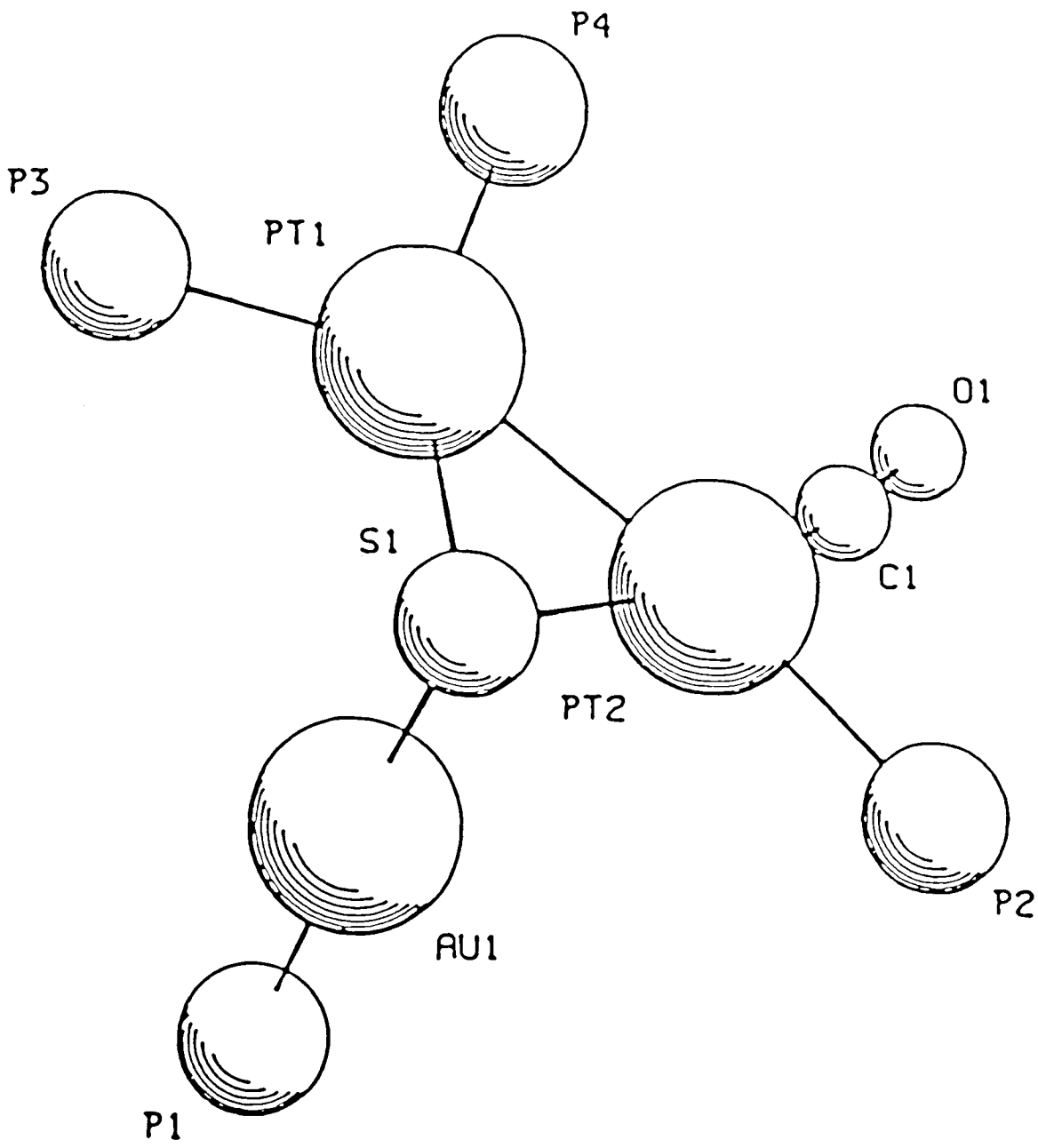

Figure 4.2 Molecular geometry of $[Pt_2(\mu\text{-}S)(CO)(PPh_3)_3Au(PPh_3)]^+ PF_6^-$

Intramolecular distances (Å)

Pt(1) - Au	3.312(2)
Pt(2) - Au	3.015(2)
Pt(1) - Pt(2)	2.650(2)
Pt(1) - S	2.303(9)
Pt(2) - S	2.30(1)
Au - S	2.33(1)
Pt(1) - P(3)	2.27(1)
Pt(1) - P(4)	2.28(1)
Pt(2) - P(2)	2.34(1)
Pt(2) - C(1)	1.87(5)
Au - P(1)	2.28(1)
C(1) - O	1.09(5)

Bond angles (°)

Pt(1)-S-Pt(2)	70.3(3)
Au-S-Pt(1)	91.3(3)
Au-S-Pt(2)	81.3(3)
S-Pt(1)-Pt(2)	54.9(3)
S-Pt(1)-P(3)	101.9(4)
S-Pt(1)-P(4)	153.8(4)
P(3)-Pt(1)-Pt(2)	155.4(3)
P(4)-Pt(1)-Pt(2)	100.1(3)
P(4)-Pt(1)-P(3)	103.9(4)
S-Pt(2)-Pt(1)	54.9(2)
S-Pt(2)-P(2)	105.5(3)
P(2)-Pt(2)-Pt(1)	159.1(3)
C(1)-Pt(2)-Pt(1)	105.6(15)
C(1)-Pt(2)-P(2)	94.6(15)
C(1)-Pt(2)-S	159.5(15)
S-Au-P(1)	177.1(4)

Table 4.4 Selected molecular dimensions for $[Pt_2(\mu\text{-}S)(CO)(PPh_3)_3Au(PPh_3)]^+ PF_6^-$ (see Figure 4.2)

(Estimated standard deviations in parentheses)

previously for Pt-Au bonding distances.[26,100] However, in such species as $[(PPh_3Au)_3S](PF_6)$, illustrated below, the Au-Au distances are as short as 3.0Å but no formal metal-metal bonds are invoked.[101]

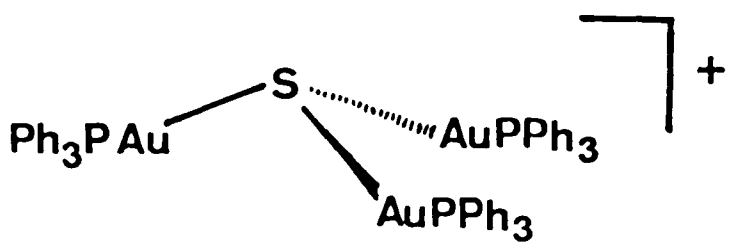

The Pt-S-Au bond angles of 91.3 and 81.3° in $[Pt_2(\mu\text{-}S)(CO)(PPh_3)_3Au(PPh_3)]^+$ are in good agreement with the angles found in $[(PPh_3Au)_3S]^+$, which are in the range 82.9 - 95.0°, although it would seem at first sight that the system would be subject to severe steric hindrance. Whether the distortion of the gold atom towards one platinum atom is due to steric or electronic factors is unsure. Molecular orbital calculations seem to suggest that there is no Pt-Au orbital overlap to stabilise the interaction and that the reason is purely steric.[11] The internal geometry of the $[Pt_2(\mu\text{-}S)(CO)(PPh_3)_3]$ unit is similar to that of the parent compound and it appears, therefore, that a localised Pt-Pt bond is retained.

4.4.2 Silver and copper analogues of $[Pt_2(\mu\text{-}S)(CO)(PPh_3)_3Au(PPh_3)]^+$

$[Pt_2(\mu\text{-}S)(CO)(PPh_3)_3]$ was stirred with excess $[Ag(PPh_3)Cl]_4$ and $TlPF_6$ in THF for three days. Light was excluded from the reaction to minimise decomposition of the silver compounds. On removal of the solvent *in vacuo* and recrystallisation from acetone/diethyl ether, a yellow crystalline solid was obtained. Elemental analysis of the solid suggested that the complex $[Pt_2(\mu\text{-}S)(CO)(PPh_3)_3Ag(PPh_3)]^+ PF_6^-$ had been formed in 71% yield. The infra-red spectrum contained a

strong carbonyl absorption band at $2022cm^{-1}$ which represented a shift to higher frequency of $21cm^{-1}$ compared with the starting compound. The $^{31}P\{^1H\}$ and $^{195}Pt\{^1H\}$ solution NMR spectra were recorded and a detailed analysis is given in Chapter 5. The spectra were particularly complicated by the presence of ^{107}Ag and ^{109}Ag nuclei which are almost equally abundant and both have a nuclear spin $I = \frac{1}{2}$. Nevertheless, it was possible to determine that the spectra had the same form as those of the complex $[Pt_2(\mu\text{-}S)(CO)(PPh_3)_3Au(PPh_3)]^+$ described in the previous Section. No magnetic coupling was observed between the $[Pt_2(\mu\text{-}S)(CO)(PPh_3)_3]$ unit and the phosphine coordinated to the silver but the $^{195}Pt\{^1H\}$ spectrum did reveal some coupling between the silver and the ^{195}Pt nuclei. The strong resemblance between these spectra and those obtained both for the gold complex and the parent compound suggests that the product of this reaction can be assigned the following molecular structure.

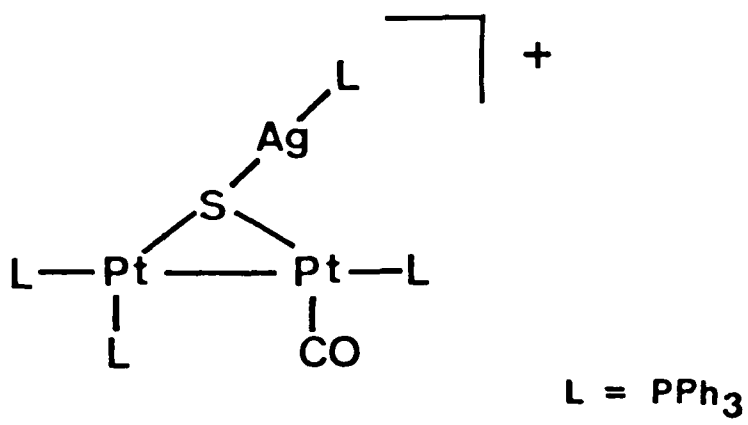

The above reaction was repeated with $[Cu(PPh_3)Cl]_4$ in place of $[Ag(PPh_3)Cl]_4$. Slow recrystallisation of the product from CH_2Cl_2/diethyl ether gave pale yellow crystals which satisfactorily analysed for $[Pt_2(\mu\text{-}S)(CO)(PPh_3)_3Cu(PPh_3)]^+ PF_6^-$ in 83% yield. The infra-red spectrum was similar to those recorded for the gold and silver complexes described above, with a strong carbonyl band at $2016cm^{-1}$. The $^{31}P\{^1H\}$ and $^{195}Pt\{^1H\}$ solution NMR spectra were

recorded and are analysed in detail in Chapter 5. They were found to be very similar to those for the gold complex $[Pt_2(\mu\text{-}S)(CO)(PPh_3)_3Au(PPh_3)]^+$ except that the ^{31}P chemical shift for the phosphine coordinated to the copper was at much higher field. It was concluded that the structure of the copper complex $[Pt_2(\mu\text{-}S)(CO)(PPh_3)_3Cu(PPh_3)]^+$ was analogous to those of the related silver and gold compounds.

The infra-red and NMR data emphasise the close resemblance between the three complexes $[Pt_2(\mu\text{-}S)(CO)(PPh_3)_3M(PPh_3)]^+$ (M = Au, Ag, Cu) and the platinum sulphido- complex $[Pt_2(\mu\text{-}S)(CO)(PPh_3)_3]$ from which they were derived. The $[Pt_2(\mu\text{-}S)(CO)(PPh_3)_3]$ unit appears to act as a ligand towards the $[MPPh_3]^+$ fragments and its internal structure is little changed by further coordination of the sulphur. In all of the heterometallic complexes the sulphur has a pyramidal geometry and the X-ray analysis of the one containing gold shows that the hetero-metal atom is brought quite close to the platinum atoms although metal-metal bonding is improbable.

4.4.3 The reaction of $[Pt_2(\mu\text{-}S)(CO)(PPh_3)_3]$ with $[Au(Me_2S)Cl]$

Gold in the univalent state is known to form linear complexes of the type AuL_2^+. In Chapter 3 a sandwich-type cluster compound was described which could also be considered as such a complex if the platinum triangle $[Pt_3(\mu\text{-}CO)_3(PPh_3)_3]$ was regarded as the ligand L. Thus the Pt_3 triangular cluster was used as a ligand towards Au^+ and $[AuPR_3]^+$:

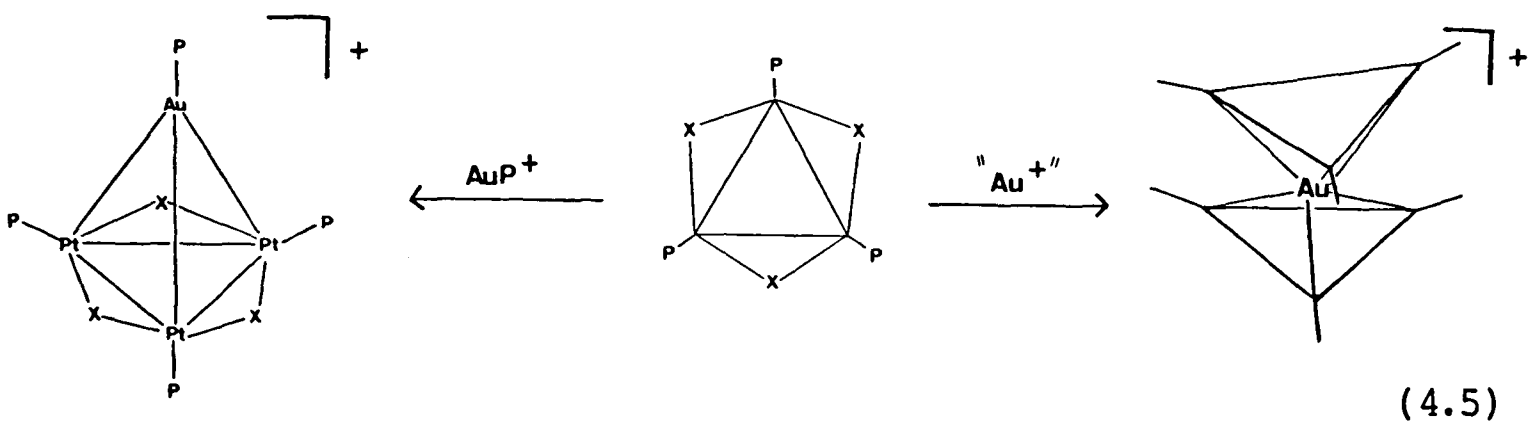

(4.5)

In the previous Section it was reported that the compound $[Pt_2(\mu\text{-}S)(CO)(PPh_3)_3]$ could function as a ligand towards $[AuPPh_3]^+$ and so it was decided to see whether it would also form a complex of the type AuL_2^+ as indicated below (4.6).

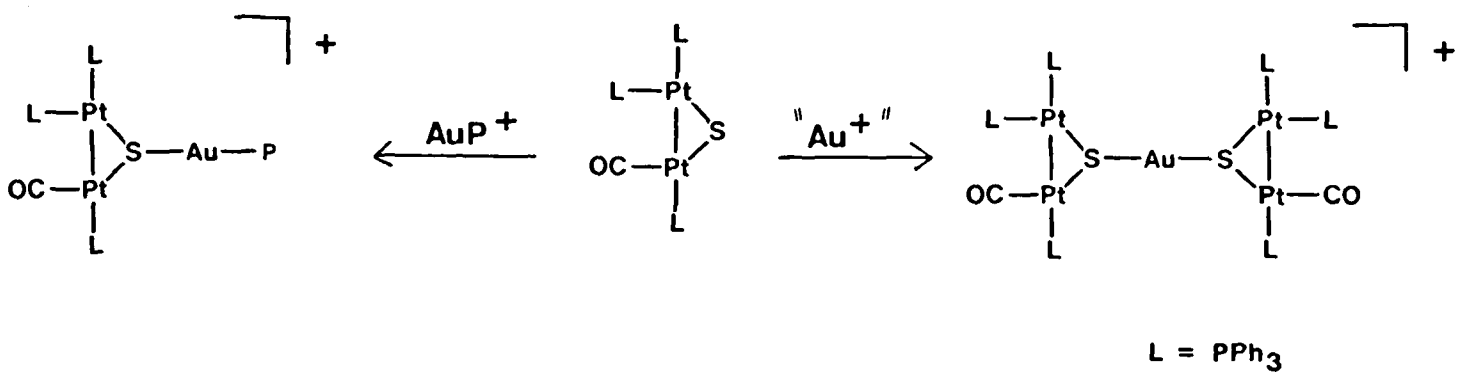

(4.6)

$[Pt_2(\mu\text{-}S)(CO)(PPh_3)_3]$ and $[Au(Me_2S)Cl]$ in 2:1 mole ratio were stirred together in benzene in the presence of excess $TlPF_6$ for one hour. An orange solid precipitate was formed. Recrystallisation of this product at -20° from CH_2Cl_2/hexane gave bright orange crystals which analysed correctly for $[Pt_2(\mu\text{-}S)(CO)(PPh_3)_3]_2Au^+ PF_6^-$ in 72% yield. The infra-red spectrum was similar to that of the starting compound except that there were two strong absorption bands in the carbonyl region at 2031 and 2019cm^{-1} and a further strong band at 839cm^{-1} due to the PF_6^- counter ion. The $^{31}P\{^1H\}$ solution NMR spectrum at -50° was similar to that of the parent compound $[Pt_2(\mu\text{-}S)(CO)(PPh_3)_3]$,

being derived from the same combination of ^{31}P and ^{195}Pt nuclei, except that the lines were broader and less well resolved. A partial analysis of this spectrum is included in Chapter 5. As with the heterometallic compounds described above, further coordination of the sulphur atom did not greatly influence the structure of the underlying $[Pt_2(\mu\text{-}S)(CO)(PPh_3)_3]$ unit. At room temperature the $^{31}P\{^1H\}$ spectrum was very broad and no structrural information could be determined. This can be attributed to the long range influence of one $[Pt_2(\mu\text{-}S)(CO)(PPh_3)_3]$ unit in the complex on the chemical shifts in the other.

The linearity of the ligand coordination in AuL_2^+ complexes is compatible with the steric requirements of such bulky ligands as $[Pt_2(\mu\text{-}S)(CO)(PPh_3)_3]$ and $[Pt_3(\mu\text{-}CO)_3(PPh_3)_3]$ and so presents no difficulty in synthesising the complexes. The preparation of these and similar AuL_2^+ complexes can, therefore, be envisaged as another way of generating higher nuclearity heterometallic clusters and aggregates.

4.5 Summary

The compound $[Pt_2(\mu\text{-}S)(CO)(PPh_3)_3]$ has proved to be a stable and chemically robust complex of Pt(I). It contains an undisputed Pt-Pt bond as part of a Pt_2S triangle which has so far proved inert to organic solvents, molecular species such as CO and SO_2 and a variety of reaction conditions. Substitution reactions have only been effected on the CO ligand and one of the phosphine ligands. Most attention has been given to the ligating properties of the sulphido-group and a number of heterometallic complexes have been prepared in which the suphur atom adopts μ_3 coordination between the two platinum

atoms and a third metal atom. However, it has not yet proved possible to synthesise new metal-metal bonded fragments by this means.

CHAPTER FIVE

$^{31}P\{^{1}H\}$ AND $^{195}Pt\{^{1}H\}$ NMR STUDIES ON PLATINUM CLUSTER COMPOUNDS

5.1 Introduction

In the course of this work it has proved possible to determine the solid state structures of some platinum cluster compounds by single crystal X-ray crystallography. It is often very difficult to obtain single crystals of new clusters and in any event the crystallographic process is time consuming. As an alternative method of probing structure, the technique of solution NMR has been used extensively. This technique is not a substitute for crystallography since the former is concerned with complexes in solution whereas the latter examines solid state structure. However, it is possible to derive much structural information from a combination of NMR spectra, often to the extent of unambiguously defining a structure. In many cases it is found that the solid state structure is retained in solution and in others there is the possibility of obtaining information about the dynamic behaviour of the cluster.

As discussed in Chapter 1, the cluster compounds of interest to this Thesis are amenable to $^{31}P\{^{1}H\}$ and $^{195}Pt\{^{1}H\}$ NMR spectroscopy. The spectra obtained are complicated by the presence of a mixture of isotopomers arising from the isotopic distribution of ^{195}Pt which has a natural abundance of 33.7%. The method for enumerating isotopomers of platinum cluster compounds is now well known[81,102,103] and will not be described here. It is important to point out, however, that for NMR purposes each isotopomer of a platinum cluster is effectively a separate compound and the observed NMR spectrum is the result of

superimposing the spectra associated with the different isotopomers. Satisfactory analyses of the $^{31}P\{^1H\}$ and $^{195}Pt\{^1H\}$ NMR spectra, which are generally second order, can be obtained, however, with the aid of computer simulation techniques (see Chapter 6).

5.2 NMR spectra of Pt_3 triangular clusters

The power of combined $^{31}P\{^1H\}$ and $^{195}Pt\{^1H\}$ NMR studies was demonstrated by the work by Pregosin and co-workers[81,102] on the cluster complexes $[Pt_3(\mu\text{-}CO)_3(PR_3)_n]$ (n = 3,4). The most important conclusion which they derived was that the triangular structures observed in the solid state were retained in solution. It was readily apparent that the nuclearity of such cluster compounds could be determined from the multiplicities of the ^{195}Pt satellites in the $^{31}P\{^1H\}$ spectra. The large values of the $^1J(Pt\text{-}P)$ coupling constants (typically about 4kHz) tended to simplify the observed spectra, making them fairly easy to analyse.

A number of the 42 electron clusters $[Pt_3(\mu\text{-}CO)_3(PR_3)_3]$ have been investigated and a series of analogous compounds containing bridging SO_2 ligands have also been studied. These compounds have yielded a substantial amount of NMR data, a selection of which are collected together in Tables 5.1 and 5.2. A number of trends are apparent from these data. The $^1J(Pt\text{-}P)$ values for the carbonyl clusters (around 4400Hz) are about 700Hz larger than for their SO_2 analogues. This is not surprising since the SO_2 ligand is known to be a better σ-donor and weaker π-acceptor than CO and this has a direct influence on one bond coupling constants, which mainly reflect s orbital contributions to bonding.[104] There is a similar pattern in the $^1J(Pt\text{-}Pt)$ values, which lie in the range 1500 - 1800Hz for carbonyl clusters but are

phosphine	$\delta(^{31}P)$	$\delta(^{195}Pt)$	$^{1}J(Pt-Pt)$	$^{1}J(Pt-P)$	$^{2}J(Pt-P)$	$^{3}J(P-P)$
[a]PBu^{n}_{3}	56.5	-3976	590	3673	361	49
[a]PCy_3	76.3	-4070	700	3760	330	49
[c]PPh_3	61.4	-4228	610	4104	426	52
[b]$P(CH_2CH_2CN)_3$	61.1			3785	367	51
[c]$P(p\text{-}Tol)_3$	60.9	-4125	540	4087	430	52

Table 5.1 ^{31}P and ^{195}Pt NMR data for the triangular clusters $[Pt_3(\mu\text{-}SO_2)_3(PR_3)_3]$

phosphine	$\delta(^{31}P)$	$\delta(^{195}Pt)$	$^{1}J(Pt-Pt)$	$^{1}J(Pt-P)$	$^{2}J(Pt-P)$	$^{3}J(P-P)$
[a]PBu^{n}_{3}	44.0	-4377	1580	4425	444	60
[a]PCy_3	68.8	-4392	1560	4410	426	60
[b]PPr^{i}_{3}	81.6	-4530	1607	4422	419	56
[b]$P(CH_2CH_2CN)_3$	52.9			4489	466	61
[c,d]$P(p\text{-}Tol)_3$	57.1				475	55

Table 5.2 ^{31}P and ^{195}Pt NMR data for the triangular clusters $[Pt_3(\mu\text{-}CO)_3(PR_3)_3]$

For both tables:

Chemical shifts in ppm; coupling constants in Hz

[a]solution in benzene
[b]solution in acetone
[c]solution in dichloromethane
[d]found in solution equilibrium with $[Pt_3(\mu\text{-}CO)_3(P\{p\text{-}Tol\}_3)_4]$

only 500 - 700Hz in their SO_2 analogues. It has not been possible to relate this coupling constant directly to metal-metal bonding. In a published comparison of ^1J(Pt-Pt) and d(Pt-Pt) values[105] a number of compounds have been found which have short Pt-Pt distances but small Pt-Pt coupling constants. One example of this is $[Pt_3(\mu\text{-}CNBu^t)_3(CNBu^t)_3]$[17] which has Pt-Pt bond distances of 2.63 - 2.64Å but a ^1J(Pt-Pt) value of only 188Hz. Despite the large difference in ^1J(Pt-Pt), the Pt-Pt bond distances[8] in the carbonyl and SO_2 bridged clusters are quite similar. Perhaps it is not surprising that the desired correlation does not exist since bond lengths are influenced by many more factors than s- orbital contributions. It should also be noted that measured coupling constants are the sum of coupling by all possible pathways. Nevertheless, it seems generally true that large ^1J(Pt-Pt) values (>1kHz) are indicative of metal-metal bonds, although the converse is not true. The data in Tables 5.1 and 5.2 include values for ^2J(Pt-P) and ^3J(P-P) which are larger than is usually found for compounds where metal-metal bonds are known not to exist. On the basis of studies on diphosphine bridged platinum dimers, Brown and others[106] have proposed a correlation between these coupling constants and the existence of platinum-platinum bonds and this is supported by the results for the Pt_3 clusters described above.

5.3 Pt_3 triangular clusters of lower symmetry

The triangular cluster compounds of the type $[Pt_3(\mu\text{-}X)_3(PR_3)_3]$ which were described in the previous Section have structures which approximate to D_{3h} symmetry. Variations on these compounds have been synthesised in the course of this work in which one of the bridging ligands is different from the other two:

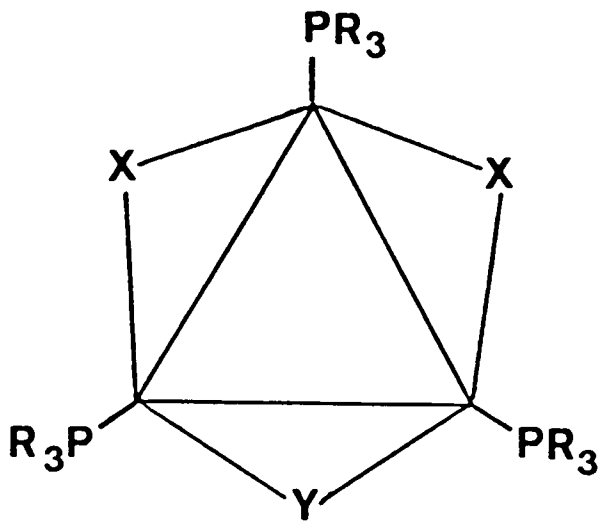

Such compounds approximate to C_{2v} symmetry, with the C_2 axis passing through the unique Y ligand and the phosphine which lies at the opposite vertex of the triangle. This reduction in symmetry introduces a chemical inequivalence among the ^{31}P and ^{195}Pt nuclei in addition to the existing magnetic inequivalence. In consequence, there are more isotopomers to consider in the analysis of the NMR spectra. The six isotopomers are illustrated in Figure 5.1. (I), which contains no ^{195}Pt, gives the strongest and simplest lines in the $^{31}P\{^1H\}$ spectrum. (II) and (III) dominate the $^{195}Pt\{^1H\}$ spectrum and are used to derive information from it and from the $^{31}P\{^1H\}$ spectrum concerning the ^{31}P-^{195}Pt coupling constants. (IV) and (V) give rise to many spectral lines of relatively low intensity. They are more easily seen in the $^{195}Pt\{^1H\}$ spectrum and are used to calculate ^{195}Pt-^{195}Pt coupling constants. It is usually not possible to observe spectral lines due to (VI) which, in any case, does not contribute any new information.

Two structures of this kind have been studied. $[Pt_3(\mu\text{-}CO)_2(\mu\text{-}SO_2)(PCy_3)_3]$ was obtained by reacting $[Pt_3(\mu\text{-}SO_2)_3(PCy_3)_3]$ with CO for a short period of time (see Section 2.3.3) and the anions $[Pt_3(\mu\text{-}SO_2)_2(\mu\text{-}Cl)(PR_3)_3]^-$ (R = Ph, Cy) were synthesised from $[Pt_3(\mu\text{-}SO_2)_3(PR_3)_3]$ and a quaternary ammonium chloride (see Section 2.5).

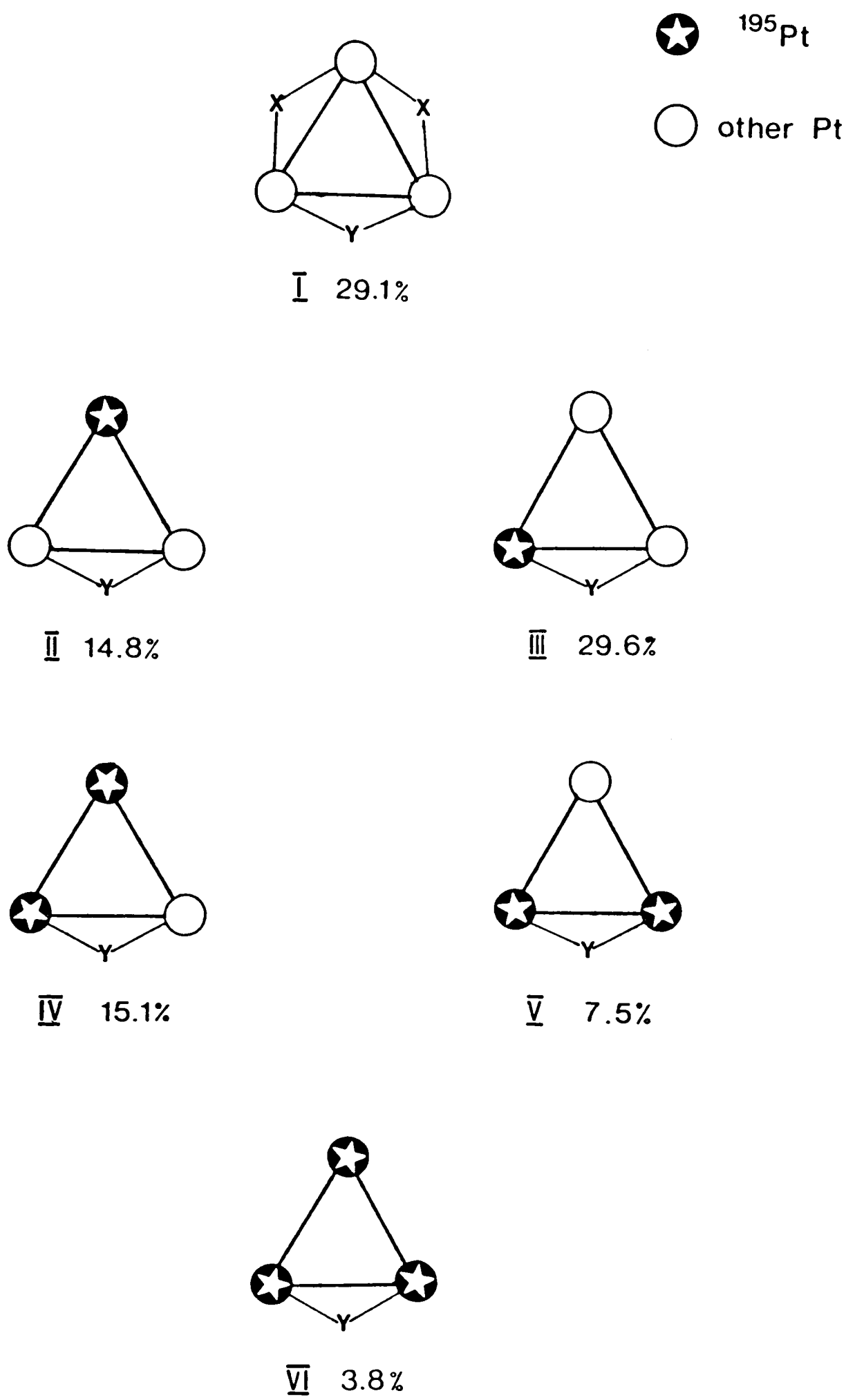

Figure 5.1 ^{195}Pt isotopomers of $[Pt_3(\mu\text{-}X)_2(\mu\text{-}Y)(PR_3)_3]$

The $^{31}P\{^1H\}$ NMR spectrum of $[Pt_3(\mu\text{-}CO)_2(\mu\text{-}SO_2)(PCy_3)_3]$ in CH_2Cl_2 solution is shown in Figure 5.2 together with its computer simulation. Two ^{31}P chemical shifts, in the ratio 2:1, are apparent at δ= 61.9 and 82.2ppm. The $^{31}P\{^1H\}$ NMR spectrum of $[Pt_3(\mu\text{-}SO_2)_2(\mu\text{-}Cl)(PR_3)_3]^-$ has the same form but with different chemical shifts. The $^{195}Pt\{^1H\}$ NMR spectrum of $[Pt_3(\mu\text{-}SO_2)_2(\mu\text{-}Cl)(PCy_3)_3]^-$ is shown in Figure 5.3 together with its computer simulation. As for ^{31}P, two ^{195}Pt chemical shifts, in the ratio 2:1, are apparent at δ= -4653 and -5977ppm. In this case the chemical shifts are a long way apart and separate accumulations were required to obtain both parts of the spectrum.

Data have been obtained for three compounds of the type $[Pt_3(\mu\text{-}X)_2(\mu\text{-}Y)(PR_3)_3]$ and are collected together in Table 5.3. The coupling constants are all similar to those observed for the compounds $[Pt_3(\mu\text{-}X)_3(PR_3)_3]$ described in Section 5.2 with the exception of $^1J(Pt\text{-}Pt)$ for the Pt-Pt bond bridged by chloride which has a particularly low value. It has not been possible to make an accurate measurement of $^1J(Pt\text{-}Pt)$ for the chloride bridged bond since the relevant lines in the $^{195}Pt\{^1H\}$ spectrum are obscurred by the main signals. An upper limit of about 400Hz can be placed on this coupling constant, however. In a related compound $[Pt_3Au(\mu\text{-}SO_2)_2(\mu\text{-}Cl)(PPh_3)_4]$, $^1J(Pt\text{-}Pt)$ for the chloride bridged bond has been measured at 190Hz (see next Section). The values for $^2J(Pt\text{-}P)$ and $^3J(P\text{-}P)$ are all consistent with the presence of metal-metal bonding.

The difference between the $^1J(Pt\text{-}Pt)$ values for SO_2 against CO bridged bonds contributed to the identification of the compound $[Pt_3(\mu\text{-}CO)_2(\mu\text{-}SO_2)(PCy_3)_3]$. Two of these coupling constants were 1830Hz and one was about700Hz. Comparison with the data of Tables 5.1 and 5.2 indicates that the 1830Hz coupling constants correspond to CO

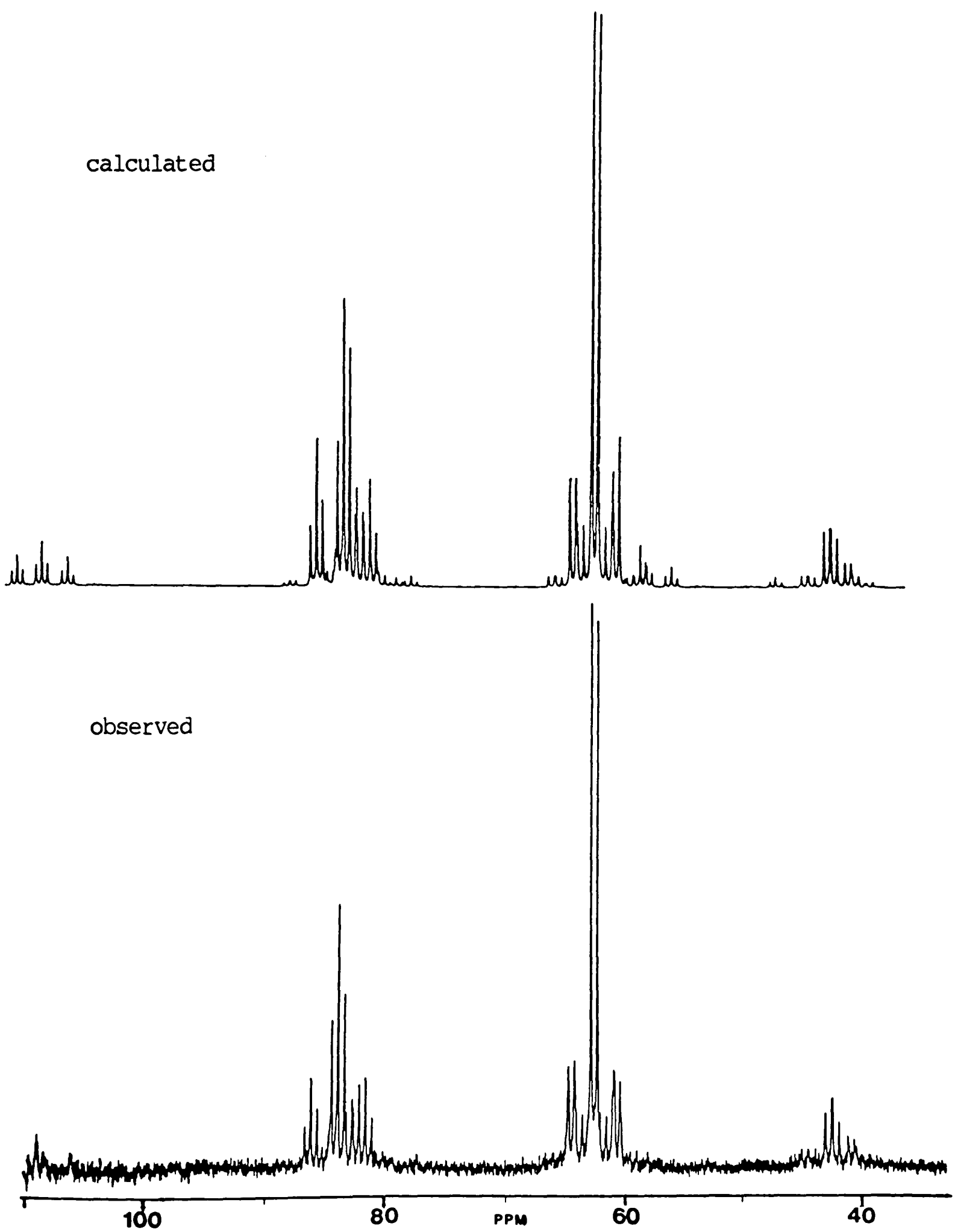

Figure 5.2 $^{31}P\{^{1}H\}$ NMR spectrum of $[Pt_3(\mu\text{-}CO)_2(\mu\text{-}SO_2)(PCy_3)_3]$

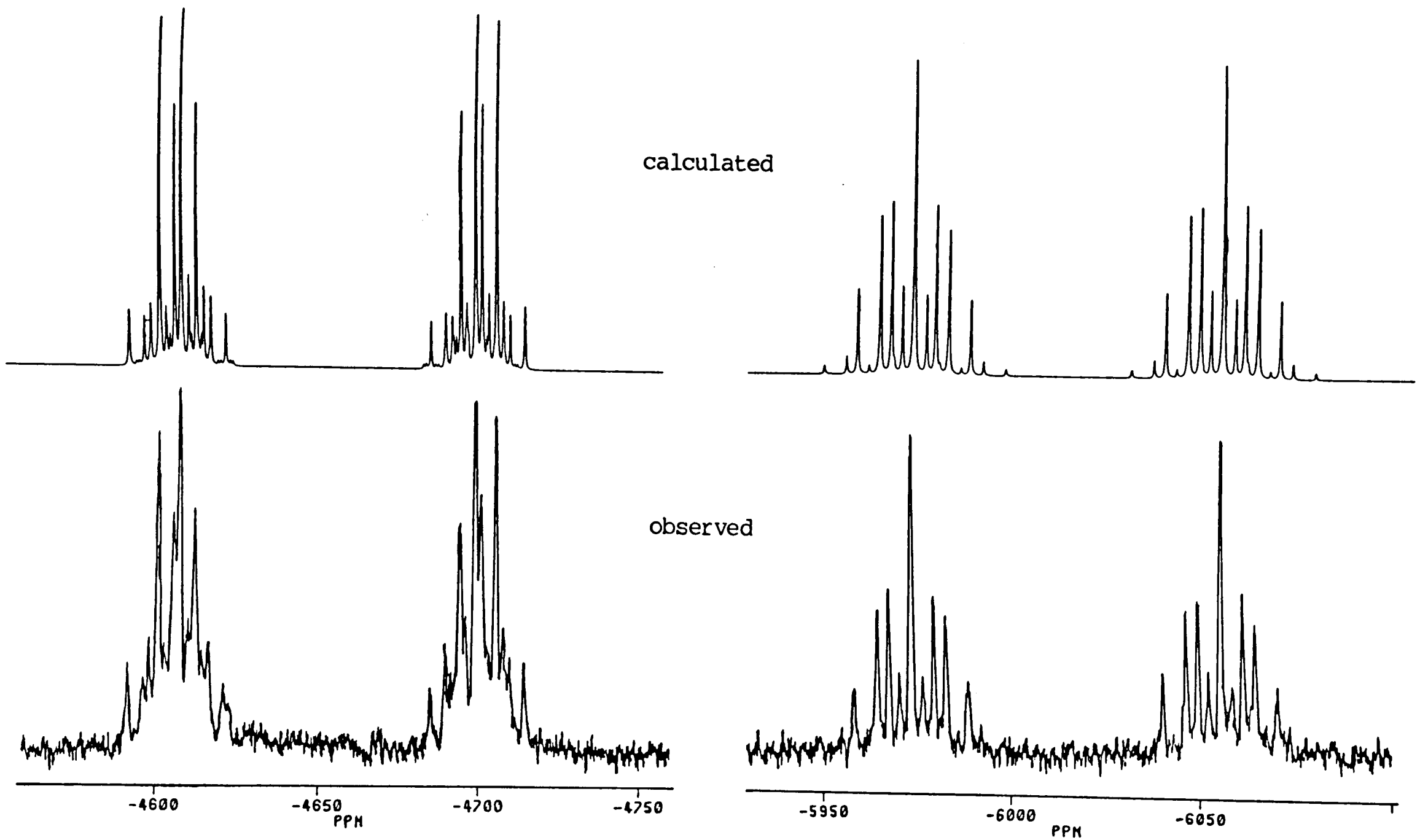

Figure 5.3 $^{195}Pt\{^{1}H\}$ NMR spectrum of $[Pt_3(\mu\text{-}SO_2)_2(\mu\text{-}Cl)(PCy_3)_3]^-$

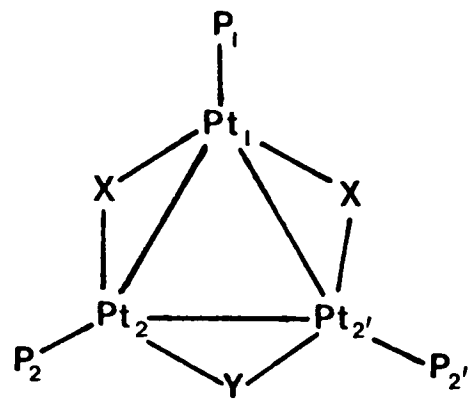

$[Pt_3(\mu\text{-}CO)_2(\mu\text{-}SO_2)(PCy_3)_3]$		P_1	P_2	$P_{2'}$	Pt_1	Pt_2	$Pt_{2'}$
δ(ppm)		82.2	61.9	61.9	-4011	-4515	-4515
J(Hz)	P_1		51	51	5134	449	449
	P_2			62	372	4055	301
	$P_{2'}$				372	301	4055
	Pt_1					1830	1830
	Pt_2						*

*could not be measured

$[Pt_3(\mu\text{-}SO_2)_2(\mu\text{-}Cl)(PPh_3)_3]^-$		P_1	P_2	$P_{2'}$	Pt_1	Pt_2	$Pt_{2'}$
δ(ppm)		4.0	17.3	17.3			
J(Hz)	P_1		62	62	4599	431	431
	P_2			46	300	5469	345
	$P_{2'}$				300	345	5469

$[Pt_3(\mu\text{-}SO_2)_2(\mu\text{-}Cl)(PCy_3)_3]^-$		P_1	P_2	$P_{2'}$	Pt_1	Pt_2	$Pt_{2'}$
δ(ppm)		12.9	28.9	28.9	-5977	-4653	-4653
J(Hz)	P_1		59	59	4341	352	352
	P_2			45	314	4963	245
	$P_{2'}$				314	245	4963
	Pt_1					968	968
	Pt_2						*

Table 5.3 NMR data for compounds of the type $[Pt_3(\mu\text{-}X)_2(\mu\text{-}Y)(PR_3)_3]$

bridging and the other value to SO_2 bridging. Otherwise it would have been impossible to decide whether the majority of the bridging ligands were CO or SO_2 without recourse to X-ray crystallography. Supporting evidence for the assignment made above is obtained by comparing the $^{31}P\{^1H\}$ spectrum with that of the compound $[Pt_3Au(\mu\text{-}CO)_2(\mu\text{-}SO_2)(PCy_3)_4]^+$, the structure of which has been determined crystallographically.[24] The differences between the spectra can all be attributed to the capping of the $[Pt_3(\mu\text{-}CO)_2(\mu\text{-}SO_2)(PCy_3)_3]$ triangular compound by an $[AuPCy_3]$ fragment as described in the following Section.

5.4 Heterometallic clusters from triangulo- Pt_3 compounds and gold

It was reported in Chapter 3 that a number of heterometallic platinum-gold clusters have been synthesised by capping a Pt_3 triangular cluster with an $[AuPR_3]$ fragment. Such compounds are of two types; one has approximate C_{3v} symmetry, in which the phosphines on the platinum triangle remain chemically equivalent, and another has approximate C_s symmetry, in which the substitution of one bridging ligand has introduced a chemical inequivalence among the phosphines on the platinum triangle. From the NMR point of view, these can be seen as deriving from the parent Pt_3 triangular compounds, $[Pt_3(\mu\text{-}X)_3(PR_3)_3]$ with D_{3h} symmetry and $[Pt_3(\mu\text{-}X)_2(\mu\text{-}Y)(PR_3)_3]$ with C_{2v} symmetry, by the addition of an extra ^{31}P nucleus. The effect on the shape of $^{31}P\{^1H\}$ NMR spectra is to add one degree of multiplicity to each of the signals from the parent compound. The chemical shifts are altered slightly and there is an additional group of lines associated with the phosphine of the $AuPR_3$ fragment but it remains apparent that the gold capping does not change the symmetry of the ligands around

the Pt_3 triangle. The cluster formed from bicapping of the Pt_3 triangle with $AuPR_3$ fragments shows the same effect but twice over for the two additional ^{31}P nuclei. Figure 5.4 shows the effect of capping a Pt_3 triangle with an $[AuPCy_3]^+$ fragment on the $^{31}P\{^1H\}$ spectrum of $[Pt_3(\mu\text{-}CO)_3(PCy_3)_3]$.

The $^{31}P\{^1H\}$ and $^{195}Pt\{^1H\}$ NMR spectra have been recorded for a number of gold capped platinum cluster compounds as part of this research and some others are reported in the published work of Wardle et al.[9,23,24] The chemical shift and coupling constant data obtained from these spectra are collected together in Tables 5.4(a) and 5.4(b). The data for the bicapped cluster $[Pt_3Au_2(\mu\text{-}SO_2)_2(\mu\text{-}Cl)(PCy_3)_3(P\{p\text{-}FC_6H_4\}_3)_2]^+$ are also included. The coupling constants in Table 5.4(b) generally have similar magnitudes to analogous values reported earlier in this Chapter for cluster compounds of Pt(0) but some are worthy of comment. The $^3J(P\text{-}P)$ and $^2J(Pt\text{-}P)$ values are slightly smaller than are found in the triangular clusters $[Pt_3(\mu\text{-}X)_3(PR_3)_3]$. In the case of the tetrahedral Pt_3Au clusters this can be attributed to the phosphines on the Pt_3 triangle being distorted out of the metal plane, away from the incoming $AuPR_3$ fragment. In the case of the trigonal bipyramidal Pt_3Au_2 cluster the smaller values are probably due to the longer Pt-Pt bonds. The two and three bond coupling constants involving gold as an intermediate nucleus are similar to those involving platinum in an equivalent environment except for the bicapped Pt_3Au_2 cluster in which the $^3J(P\text{-}P)$ values over Pt-Au bonds are approximately zero. In the absence of crystallographic information it could, therefore, still be deduced that the Pt-Au distances in these compounds were short enough for metal-metal bonding

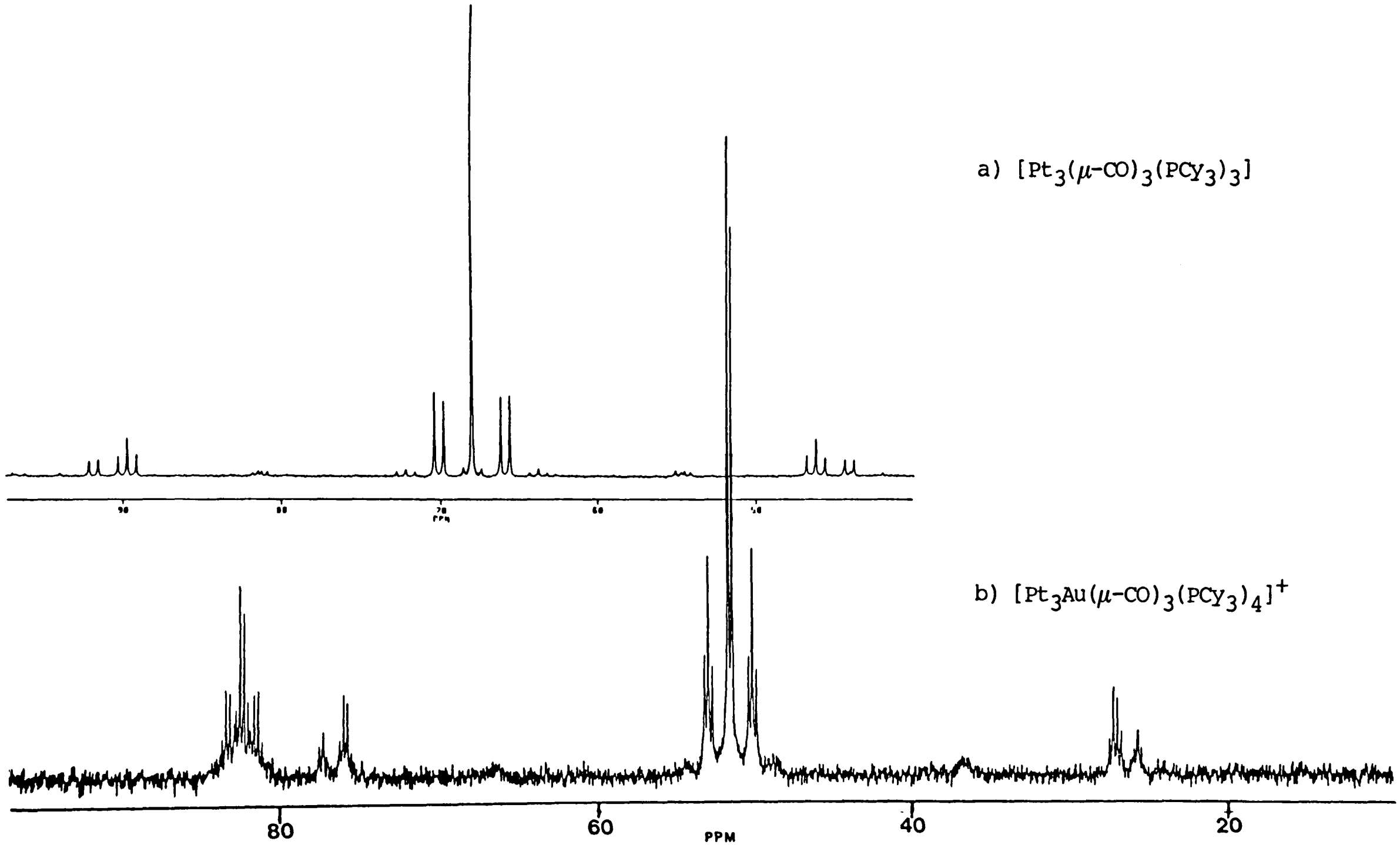

Figure 5.4 The effect of $[AuPCy_3]$ capping on the $^{31}P\{^1H\}$ spectrum of $[Pt_3(\mu\text{-}CO)_3(PCy_3)_3]$

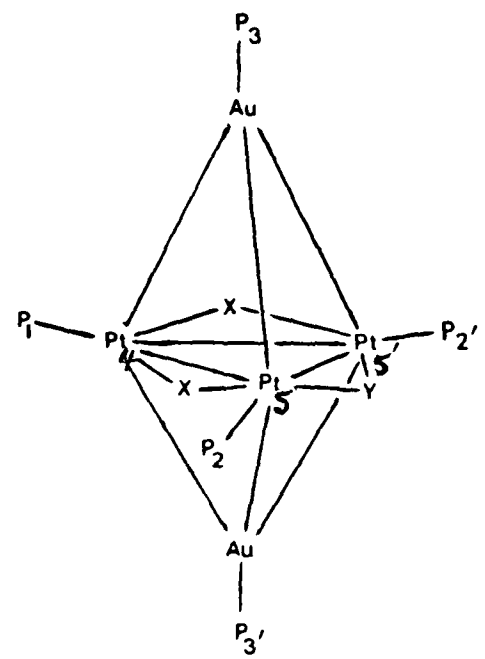

nucleus:	Ref.	$\delta(^{31}P)$ 1	2	3	$\delta(^{195}Pt)$ 4	5
$[Pt_3Au(CO)_3(PCy_3)_4]^+$	53	51.9		82.7	-4583	
$[Pt_3Au(SO_2)_3(PCy_3)_4]^+$	39	60.3		83.1	-4415	
$[Pt_3Au(CO)_2(SO_2)(PCy_3)_4]^+$	69	60.7	50.6	82.0	-4372	-4636
$[Pt_3Au(SO_2)_2(Cl)(PCy_3)_3P\{p\text{-}FC_6H_4\}_3]$	69	16.8	29.5	7.0	-5301	-4049
$[Pt_3Au(SO_2)_2(Cl)(PPh_3)_4]$		10.8	25.0	17.3	-5386	-4044
$[Pt_3Au(CO)_3(PPh_3)_4]^+$		40.8		49.6		
$[Pt_3Au_2(SO_2)_2(Cl)(PCy_3)_3(P\{p\text{-}FC_6H_4\}_3)_2]^+$		21.4	37.1	23.6		

Equivalent nuclei in each compound are bracketed together.

Table 5.4(a) Chemical shifts for gold capped clusters of platinum

coupling:	1-2	1-3	2-3	2-2′	3-3′	1-4	2-5	1-5	2-5′	2-4	3-4	3-5	4-5	5-5′
$[Pt_3Au(CO)_3(PCy_3)_4]^+$		25			-	4899			282		177		2100	
$[Pt_3Au(SO_2)_3(PCy_3)_4]^+$					-	4117								
$[Pt_3Au(CO)_2(SO_2)(PCy_3)_4]^+$		20		28	-	4705	4436	308	180	248	166	166	*	2167
$[Pt_3Au(SO_2)_2(Cl)(PCy_3)_3P\{p\text{-}FC_6H_4\}_3]$	37	20	20	25	-	4800	5450	220	197	197	250	250	*	1468
$[Pt_3Au(SO_2)_2(Cl)(PPh_3)_4]$	42	17	12	28	-	5079	5840	281	242	270	260	260	190	1560
$[Pt_3Au(CO)_3(PPh_3)_4]^+$		24			-	4138			324		235			
$[Pt_3Au_2(SO_2)_2(Cl)(PCy_3)_3(P\{p\text{-}FC_6H_4\}_3)_2]^+$	37	0	0	27	5	4640	5158	133	121	148	190	190		

Equivalent couplings in each compound are bracketed together.

*could not be measured

Table 5.4(b) Coupling constants (Hz) for gold capped clusters of platinum

For numbering of nuclei, see Table 5.4(a)

to be significant.

Particular attention was paid in Chapter 3 to the capping of the compound $[Pt_3(\mu\text{-}CO)_3(PPh_3)_4]$ since this was a 44 electron triangular cluster with a fourth terminal phosphine ligand. Solid state evidence indicated that the product from capping by $[AuPPh_3]^+$ retained the additional phosphine as shown below:

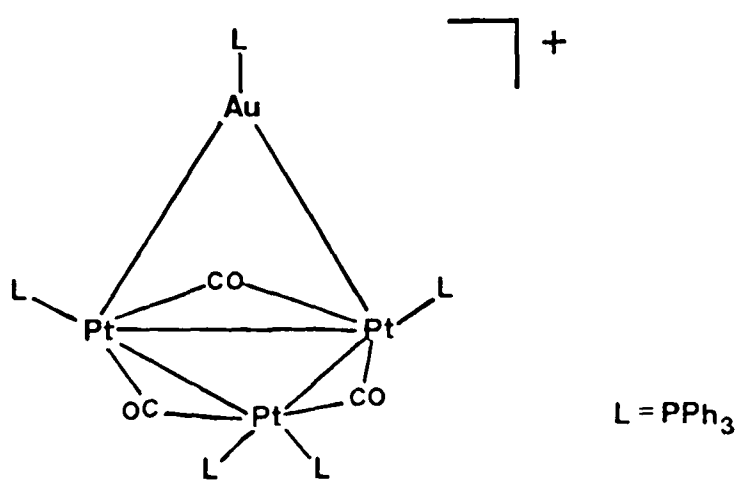

$^{31}P\{^1H\}$ studies on the product in solution revealed an equilibrium between the above structure which has five phosphines in C_s symmetry and a structure with four phosphines in C_{3v} symmetry. The latter structure gives a $^{31}P\{^1H\}$ spectrum similar in form to that shown in Figure 5.4 for $[Pt_3Au(\mu\text{-}CO)_3(PCy_3)_4]^+$ and seems likely, therefore, to have the same structure. Some NMR data for this structure are included in Tables 5.4(a) and 5.4(b). The lines of the $^{31}P\{^1H\}$ spectrum are broader for the structure with all five phosphines but it is still possible to determine two ^{31}P chemical shifts at 38.8 and 37.4ppm corresponding to the phosphines on the platinum triangle. These give rise to two overlapping groups of lines of roughly equal intensity from which can be determined approximate coupling constants of 125 and 164Hz for $^2J(Pt\text{-}P)$, 20Hz for $^3J(P\text{-}P)$ across a Pt-Pt bond and 10Hz for $^3J(P\text{-}P)$ across a Pt-Au bond. The region of the $^{31}\{^1H\}$ spectrum corresponding to the phosphine of the $AuPPh_3$ fragment (around

48ppm) is particularly broad, suggesting that the gold atom is not rigidly fixed in a tetrahedral position above the $[Pt_3(\mu\text{-}CO)_3(PPh_3)_4]$ triangle.

The $^{31}P\{^1H\}$ NMR spectrum has also been recorded for the "sandwich" compound $[Pt_3(\mu\text{-}CO)_3(PPh_3)_3]_2Au^+$, the solid state structure of which was described in Chapter 3. The form of this spectrum, which is shown in Figure 5.5, is quite simple but the lines are broad. In this compound long range coupling between the two platinum triangles is broken down by rotation of the triangles relative to each other. The effect is to present a simplified picture of a $[Pt_3(\mu\text{-}CO)_3(PPh_3)_3]$ triangle with C_{3v} symmetry. The NMR data obtained from the spectrum are as follows:

$\delta(^{31}P)$:	31.9ppm		
$^1J(Pt\text{-}P)$:	5727Hz,	$^2J(Pt\text{-}P)$:	342Hz
linewidth at half peak height:	32Hz		

The broadness of the lines obscures the $^3J(P\text{-}P)$ coupling.

5.5 Platinum μ-sulphido and related compounds

Chapter 4 described the synthesis of a range of compounds based on a $Pt_2(\mu\text{-}S)$ triangular unit illustrated below:

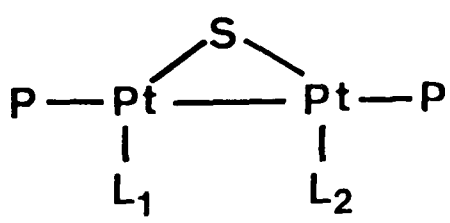

P = tertiary phosphine

L_1, L_2 = tertiary phosphine or CO

In some compounds the sulphur was further coordinated to a different metal. For all of these compounds a substantial investigation by

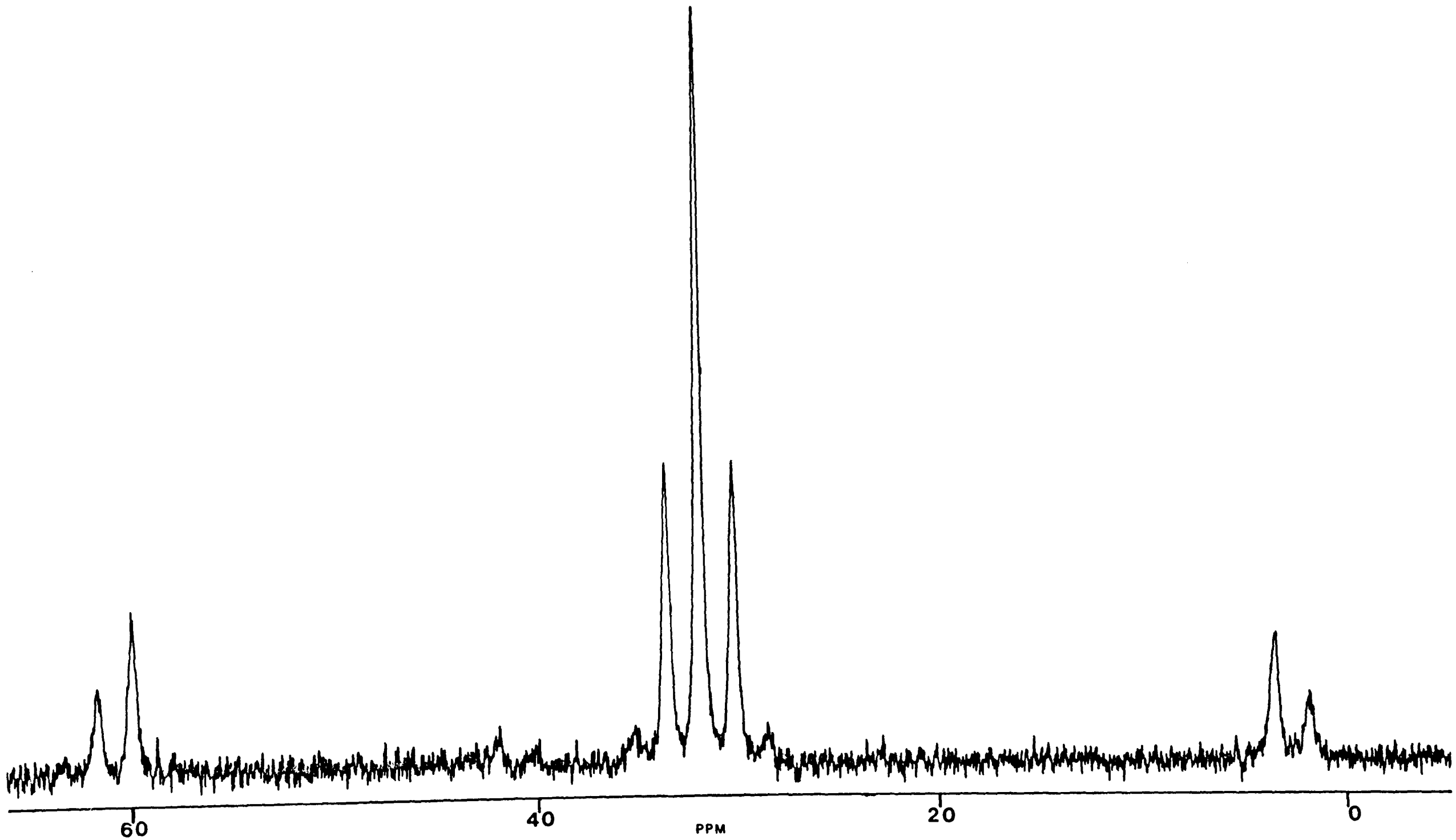

Figure 5.5 $^{31}P\{^{1}H\}$ NMR spectrum of $[Pt_3(\mu\text{-}CO)_3(PPh_3)_3]_2Au^+$ ("sandwich" compound)

$^{31}P\{^1H\}$ and $^{195}Pt\{^1H\}$ NMR has been carried out. This has produced a large collection of data from which could be deduced the structures of the compounds in solution and, by comparison with known structures, an idea of the solid state structures also.

5.5.1 Structures with chemically equivalent phosphines

The compound $[Pt_2(\mu\text{-}S)(CO)_2(PPh_3)_2]$ was synthesised by reacting the trinuclear cluster $[Pt_3(\mu\text{-}CO)_3(PPh_3)_4]$ with COS (see Section 2.3.4). The same product, as suggested by the NMR spectra, was also formed by the reaction of $[Pt_2(\mu\text{-}S)(CO)(PPh_3)_3]$ with $[(\eta\text{-}C_5H_5)Fe(CO)_2(C_2H_4]^+$ (see Section 4.3). This compound contains only two chemically equivalent phosphines, each coordinated to one of two platinum atoms and the $^{31}P\{^1H\}$ NMR spectrum of this system is particularly simple, being made up by the superposition of only three isotopomers. Table 5.5 shows the isotopomers found in this structure and the contributions that they make to the total $^{31}P\{^1H\}$ spectrum. The observed and calculated $^{31}P\{^1H\}$ spectra for $[Pt_2(\mu\text{-}S)(CO)_2(PPh_3)_2]$ are shown in Figure 5.6. The clear separation of the lines in the spectrum meant that calculation of the coupling constants was straightforward and these are given in Table 5.6, together with data for a related SO_2 compound.

		abundance	spin system	form of spectrum
I	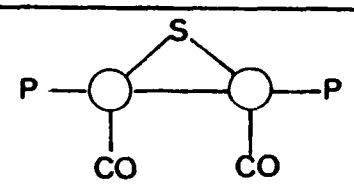	44.0%	A_2	singlet
II	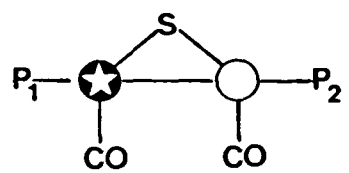	44.7%	AA´X	P_1: doublet [$^1J(Pt,P)$] of doublets [$^3J(P,P)$] P_2: doublet [$^2J(Pt,P)$] of doublets [$^3J(P,P)$]
III	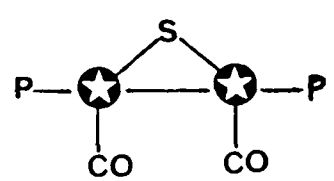	11.4%	AA´XX´	complex second order based on doublet [$^1J(Pt,P)$ + $^2J(Pt,P)$]

✪ = ^{195}Pt

Table 5.5 ^{195}Pt isotopomers of $[Pt_2(\mu\text{-}S)(CO)_2(PR_3)_2]$

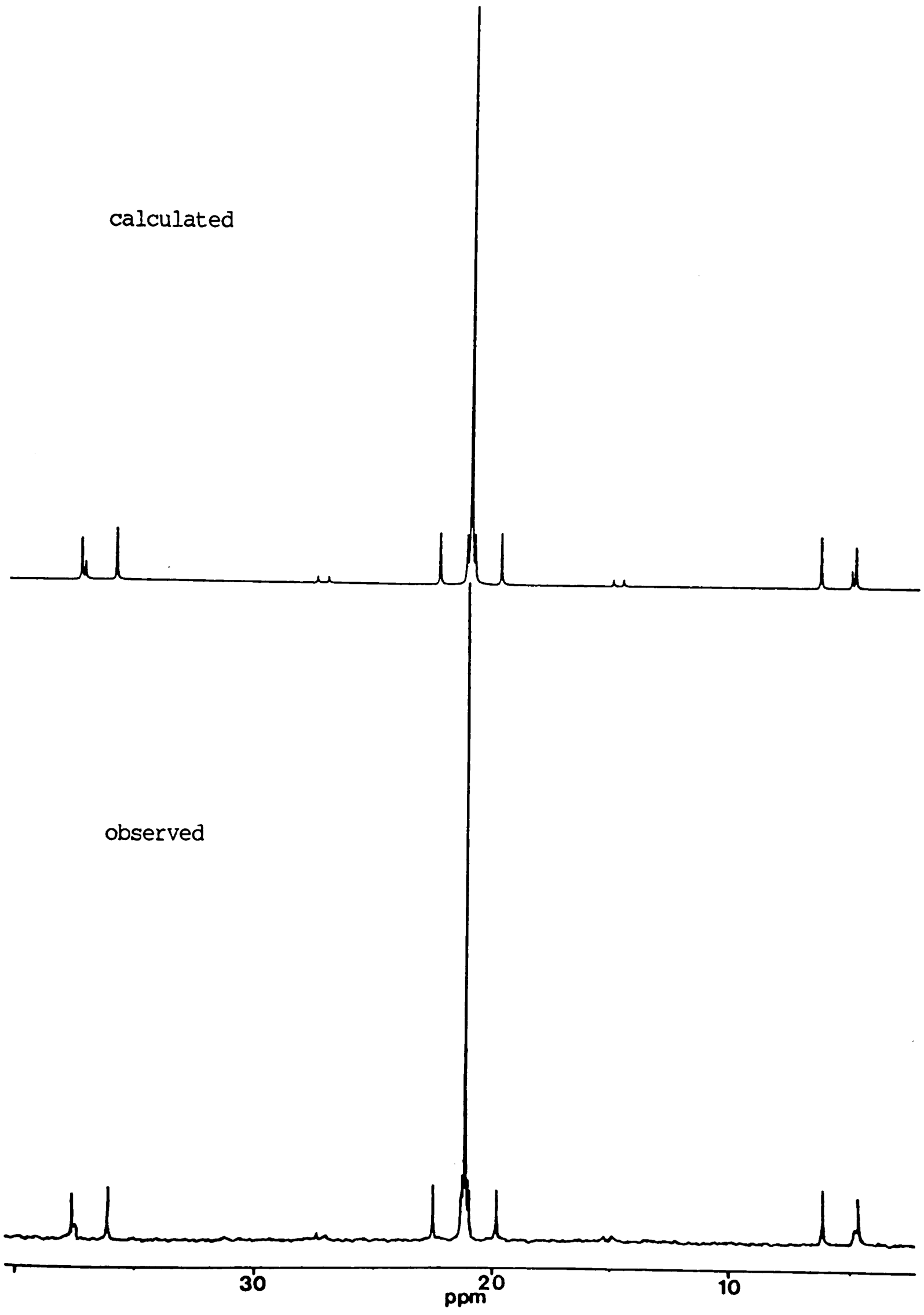

Figure 5.6 $^{31}P\{^{1}H\}$ NMR spectrum of $[Pt_2(\mu\text{-}S)(CO)_2(PPh_3)_2]$

	$Pt_2(\mu\text{-}S)(CO)_2(PPh_3)_2]$	$Pt_2(\mu\text{-}SO_2)(CO)_2(PCy_3)_2]$
$\delta(^{31}P)$ (ppm)	21.1	29.2
$\delta(^{195}Pt)$ (ppm)	-4838	
$^1J(Pt,P)$ (Hz)	3161	3854
$^2J(Pt,P)$ (Hz)	122	297
$^3J(P,P)$ (Hz)	149	67
$^1J(Pt,Pt)$ (Hz)	3000	

(solution in CH_2Cl_2)

Table 5.6 NMR data for compounds $Pt_2(\mu\text{-}X)(CO)_2(PR_3)_2]$

The $^1J(Pt\text{-}Pt)$ value was measured from the $^{195}Pt\{^1H\}$ NMR spectrum which was also quite simple because it only contained contributions from isotopomers (II) and (III) of Figure 5.6. The observed and calculated $^{195}Pt\{^1H\}$ NMR spectra of $[Pt_2(\mu\text{-}S)(CO)_2(PPh_3)_2]$ are shown in Figure 5.7. Of the measured coupling constants, $^1J(Pt\text{-}Pt)$ is large (3kHz) although by no means the largest seen for a platinum-platinum bond. Values as high as 9kHz have been reported for some compounds based on the $Pt_2(\mu\text{-dppm})_2$ unit.[105] $^1J(Pt\text{-}P)$ at close to 4kHz is typical for the cluster compounds of platinum encountered in this work but $^2J(Pt\text{-}P)$ is smaller than is found in the Pt_3 triangular clusters discussed in Section 5.2. $^3J(P\text{-}P)$ is large (149Hz) and is an indication that the P-Pt-Pt-P unit is close to linear.

The compound $[Pt_2(\mu\text{-}SO_2)(CO)_2(PCy_3)_2]$ was detected in the reaction of $[Pt_3(\mu\text{-}SO_2)_3(PCy_3)_3]$ with CO. The form of the $^{31}P\{^1H\}$ NMR spectrum is similar to that of $[Pt_2(\mu\text{-}S)(CO)_2(PPh_3)_2]$ but the coupling constants show some differences. $^2J(Pt\text{-}P)$ and $^3J(P\text{-}P)$ are similar to

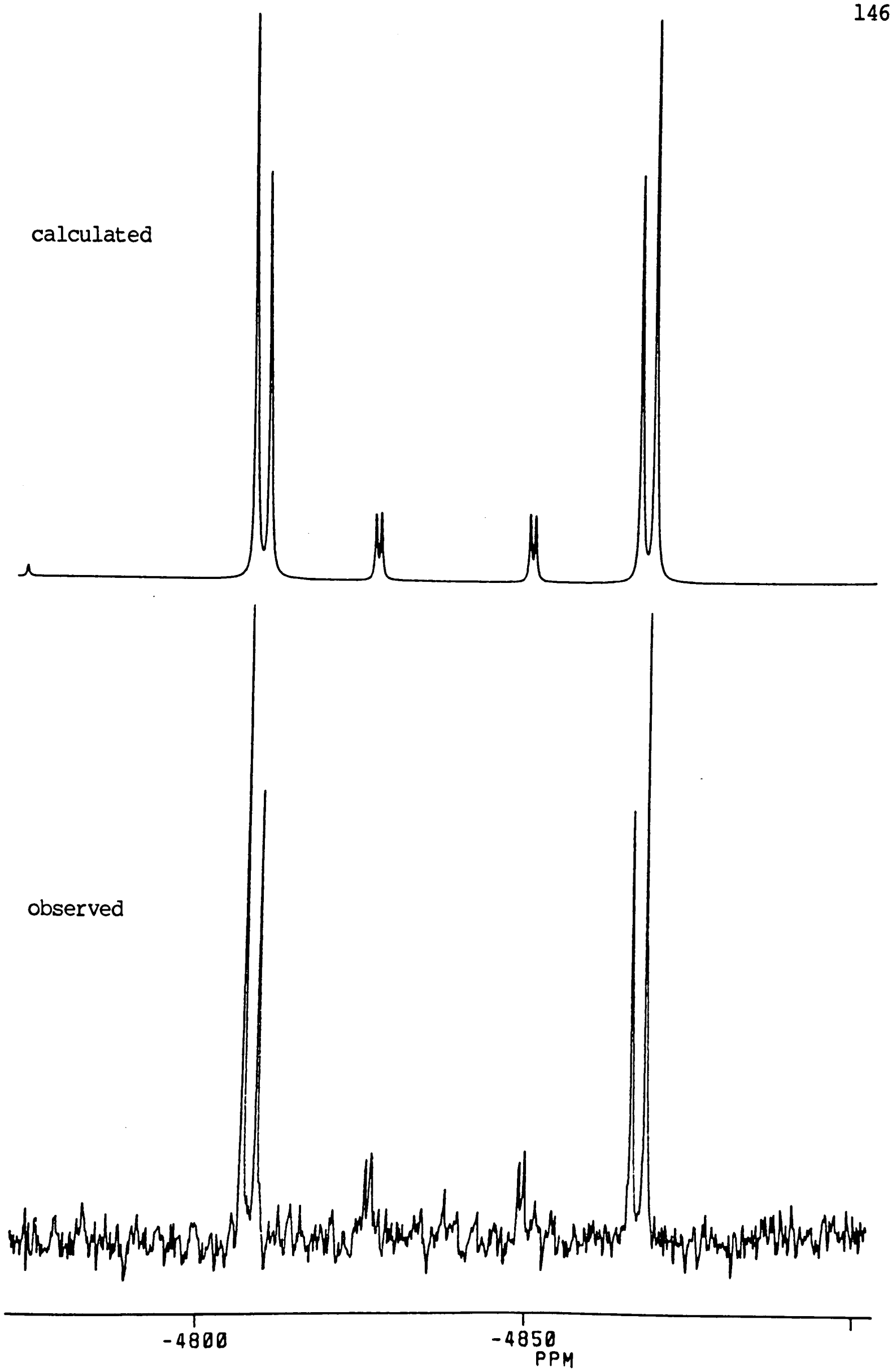

Figure 5.7 $^{195}Pt\{^{1}H\}$ NMR spectrum of $[Pt_2(\mu\text{-}S)(CO)_2(PPh_3)_2]$

the values found for the Pt_3 triangular clusters. In the case of $^3J(P-P)$ this could suggest that the P-Pt-Pt-P unit is not strictly linear.

5.5.2 Structures based on $[Pt_2(\mu\text{-}S)(CO)(PPh_3)_3]$

The syntheses of a number of compounds based on $[Pt_2(\mu\text{-}S)(CO)(PPh_3)_3]$ were described in Chapter 4. Three such compounds involved coordination of the sulphur atom to a $[MPR_3]^+$ moiety (M = Au, Ag, Cu) as shown below.

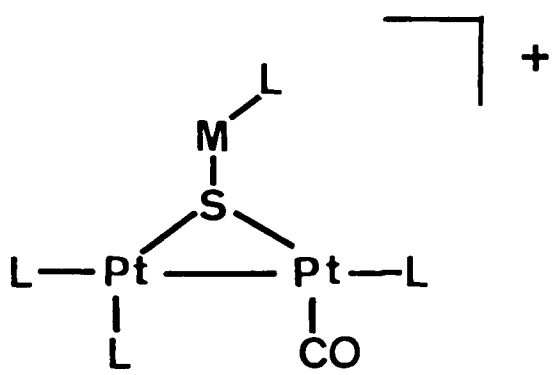

L = PPh_3

M = (I) Au
(II) Ag
(III) Cu

Another compound was synthesised in which two $[Pt_2(\mu\text{-}S)(CO)(PPh_3)_3]$ units were coordinated via their sulphur atoms across a single gold atom to give the following:

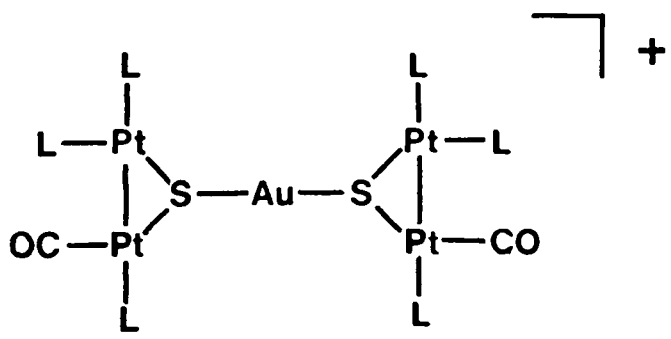

L = PPh_3

The solid state structures of the parent compound, $[Pt_2(\mu\text{-}S)(CO)(PPh_3)_3]$, and the $[AuPPh_3]^+$ adduct (I) are known from X-ray crystallographic studies (see Chapter 4). The $^{31}P\{^1H\}$ and $^{195}Pt\{^1H\}$ NMR spectra indicate that the same structures, as shown above, are retained in solution. Analogous structures for the $[AgPPh_3]^+$ and

$[CuPPh_3]^+$ adducts [(II) and (III)] may be inferred from the very similar NMR spectra obtained for these compounds.

Balch et al carried out an analysis of the $^{31}P\{^1H\}$ NMR spectrum of $[Pt_2(\mu\text{-}S)(CO)(PPh_3)_3]$ involving complex Selective Population Transfer (SPT) experiments and they have reported values for all of the coupling constants involving ^{31}P nuclei.[96] In the field of platinum-phosphine cluster chemistry it is usually difficult or impossible to determine the signs of the coupling constants but in this case the SPT experiments have revealed relative signs within groups of the coupling constants. These results are shown below in Table 5.7.

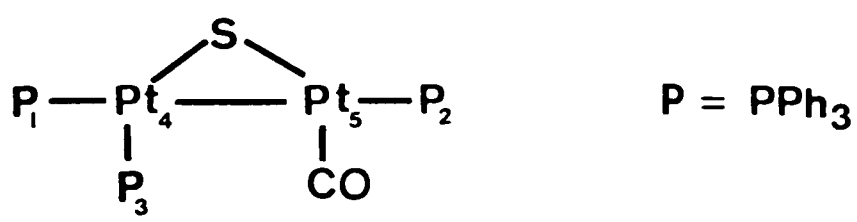

(i)		(ii)		(iii)	
$^3J(P_1\text{-}P_2)$	180	$^1J(P_1\text{-}Pt_4)$	3462	$^2J(P_1\text{-}Pt_5)$	280
$^2J(P_1\text{-}P_3)$	-11	$^2J(P_2\text{-}Pt_4)$	204	$^1J(P_2\text{-}Pt_5)$	2663
$^3J(P_2\text{-}P_3)$	22	$^1J(P_3\text{-}Pt_4)$	3613	$^2J(P_3\text{-}Pt_5)$	-117

Coupling constants within a group have correlated signs.

Table 5.7 Coupling constants (Hz) for $[Pt_2(\mu\text{-}S)(CO)(PPh_3)_3]$

The observation of coupling constants with differing signs emphasises the existence of multiple coupling pathways and the care that must be taken in relating magnitudes of one bond coupling constants to bond lengths.

The object of Balch's SPT experiments was to distinguish the spectral lines due to the various isotopomers of the compound so that the coupling constants could be assigned. In this work it has been found that coupling constants can be assigned if the $^{31}P\{^{1}H\}$ spectrum is examined in conjunction with the $^{195}Pt\{^{1}H\}$ spectrum. The latter has a reasonably straightforward form owing to the wide separation of the ^{195}Pt chemical shifts and the large values of the $^{1}J(Pt-P)$ coupling constants. Relative signs of coupling constants can not be assigned by this means, except that computer simulation of the $^{195}Pt\{^{1}H\}$ spectrum shows up an anomaly in the intensities of some minor lines which may be resolved by correcting $^{2}J(P_3-Pt_5)$ (see Table 5.7) to a negative value. For the purposes of the spectral analysis which follows, advantage has been taken of Balch's SPT results in assigning $^{2}J(P_3-Pt_5)$ and $^{3}J(P_1-P_3)$ negative values relative to the others.

The parent compound $[Pt_2(\mu-S)(CO)(PPh_3)_3]$ and the three $[MPR_3]^+$ adducts [(I) -(III)] all give similar $^{31}P\{^{1}H\}$ and $^{195}Pt\{^{1}H\}$ NMR spectra. The only significant difference between the compounds is in the signal due to the phosphine of the $[MPR_3]$ fragment. Since the ^{31}P nucleus of this fragment shows no perceptible coupling to platinum, this extra ^{31}P signal affects the form only of the $^{31}P\{^{1}H\}$ spectra. Examples of the NMR spectra obtained for these compounds are given in Figure 5.8, which shows the observed and calculated $^{31}P\{^{1}H\}$ spectra for $[Pt_2(\mu-S)(CO)(PPh_3)_3AuPPh_3]^+$, and Figure 5.9, which shows the observed and calculated $^{195}Pt\{^{1}H\}$ spectra for $[Pt_2(\mu-S)(CO)(PPh_3)_3]$. For compound (I) (M = Au), the $^{31}P\{^{1}H\}$ spectrum was recorded at an observation frequency of 162MHz instead of the usual 101MHz. This had

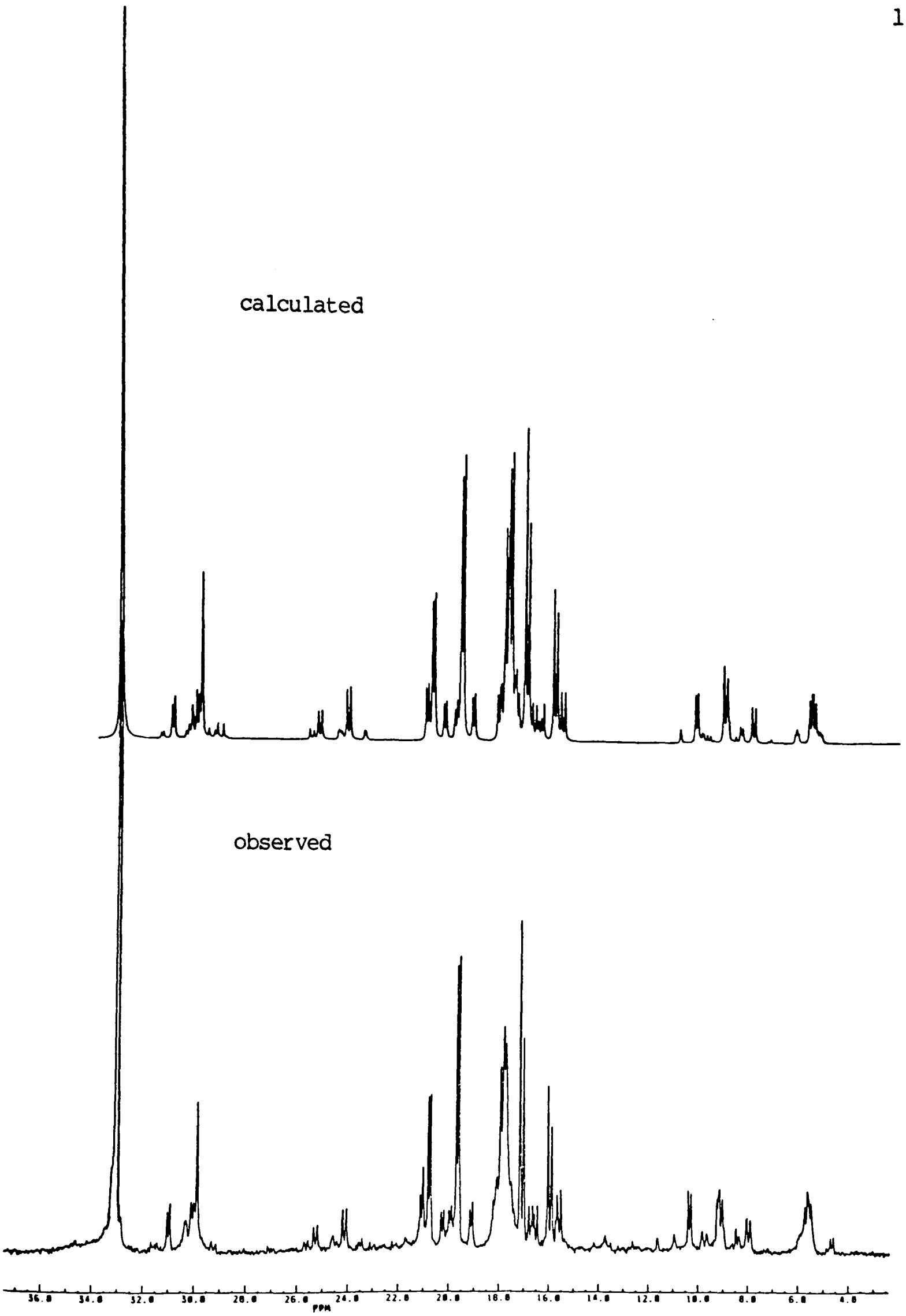

Figure 5.8 162MHz $^{31}P\{^{1}H\}$ NMR spectrum of $[Pt_2(\mu\text{-}S)(CO)(PPh_3)_3AuPPh_3]^+$

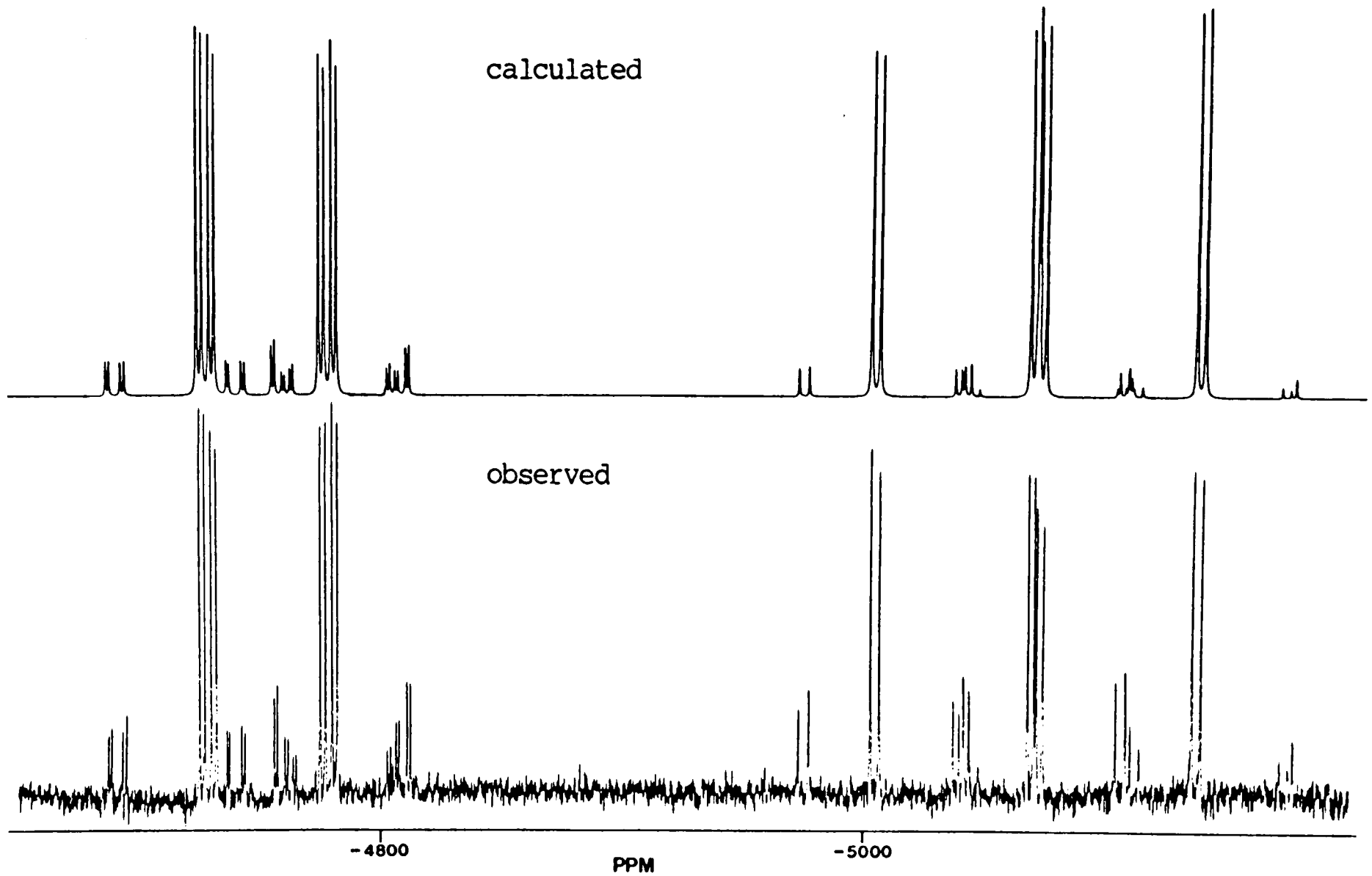

Figure 5.9 $^{195}Pt\{^{1}H\}$ NMR spectrum of $[Pt_2(\mu\text{-}S)(CO)(PPh_3)_3]$

the effect of spreading out the ^{31}P chemical shifts and so simplifying the spectrum slightly. Consequently it was easier to measure the NMR parameters. The $^{31}P\{^{1}H\}$ signals for the phosphines of the coordinated MPR_3 fragments are found as very strong singlets in the cases M = Cu [$\delta(^{31}P)$ = -3.5ppm] and M = Au [$\delta(^{31}P)$ = 33.1ppm]. For M = Ag, this phosphine is observed as a pair of doublets due to slightly different coupling to ^{109}Ag (48%) and ^{107}Ag (52%) (both I = $\frac{1}{2}$). The signals in this case are broad due to the slow relaxation of the silver nuclei (see Figure 5.10). The chemical shifts for all of these compounds are given in Table 5.8 and the coupling constants are collected together in Table 5.9.

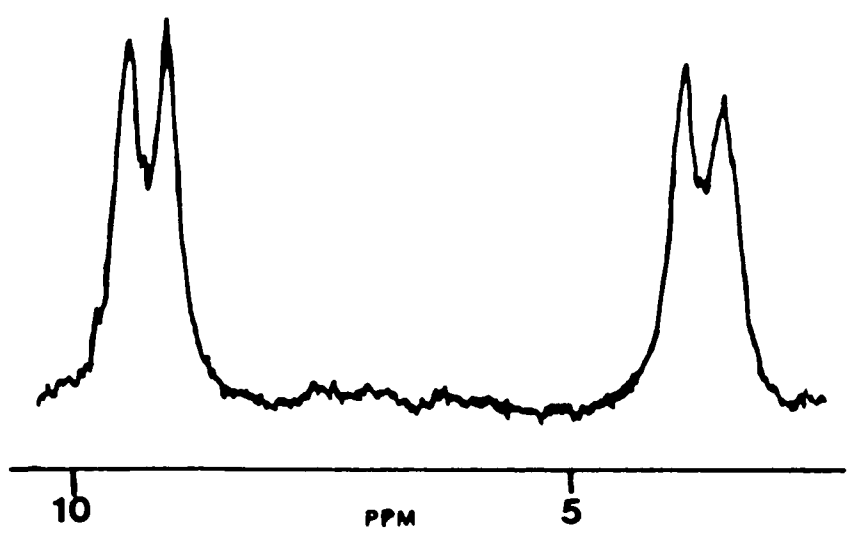

Figure 5.10 ^{31}P signals for the $AgPPh_3$ fragment in complex (II): $[Pt_2(\mu\text{-}S)(CO)(PPh_3)_3AgPPh_3]^+$

The $^{31}P\{^{1}H\}$ NMR spectra are very complex and the relative proximity of the chemical shifts for the ^{31}P nuclei attached to the $Pt_2(\mu\text{-}S)$ triangle causes severe second order distortions. Therefore, chemical shifts and coupling constants have to be calculated by iteration from estimates. Good estimates of the coupling constants involving ^{195}Pt nuclei are obtained from the $^{195}Pt\{^{1}H\}$ NMR spectra

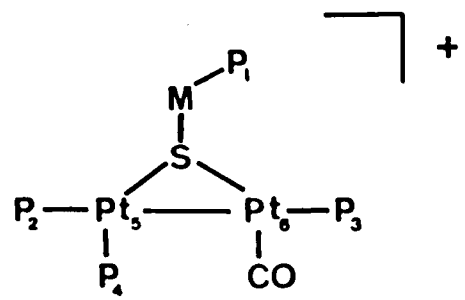

P = PPh_3

		$\delta(^{31}P)$				$\delta(^{195}Pt)$	
		1	2	3	4	5	6
	$[Pt_2(\mu\text{-}S)(CO)(PPh_3)_3]$	-	19.5	15.2	19.1	-5072	-4753
I	$[Pt_2(\mu\text{-}S)(CO)(PPh_3)_3AuPPh_3]^+$	33.1	20.1	16.6	17.8	-4841	-4629
II	$[Pt_2(\mu\text{-}S)(CO)(PPh_3)_3AgPPh_3]^+$	6.3[a]	17.7	14.1	16.0	-4857	-4661
III	$[Pt_2(\mu\text{-}S)(CO)(PPh_3)_3CuPPh_3]^+$	-3.5	18.6	15.1	16.4	-4864	-4670
	$[Pt_2(\mu\text{-}S)(CO)(PPh_3)_3]_2Au^+$ [b]	-	22.6	12.6	12.9		

[a] average of ^{31}P - ^{107}Ag and ^{31}P - ^{109}Ag

[b] approximate values

Table 5.8 ^{31}P and ^{195}Pt chemical shifts (ppm) for $[Pt_2(\mu\text{-}S)(CO)(PPh_3)_3]$ and its $[MPR_3]^+$ adducts

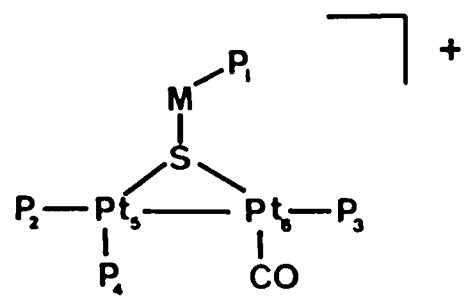

P = PPh_3

		^1J(Pt-P)			^2J(Pt-P)			^2J(P-P)	^3J(P-P)		^1J(Pt-Pt)
		(2-5)	(4-5)	(3-6)	(2-6)	(4-6)	(3-5)	(2-4)	(3-4)	(2-3)	(5-6)
	$[Pt_2(\mu\text{-}S)(CO)(PPh_3)_3]$	3462	3613	2663	280	-117	204	-11	22	180	3628
I	$[Pt_2(\mu\text{-}S)(CO)(PPh_3)_3AuPPh_3]^+$	3352	3953	2617	131	-96	148	-17	24	184	2567
II	$[Pt_2(\mu\text{-}S)(CO)(PPh_3)_3AgPPh_3]^+$	3299	3832	2586	167	-99	188	-15	23	183	2850
III	$[Pt_2(\mu\text{-}S)(CO)(PPh_3)_3CuPPh_3]^+$	3308	3878	2600	150	-98	144	-24	31	182	2630
	$[Pt_2(\mu\text{-}S)(CO)(PPh_3)_3]_2Au^+$	3435	3960				160	(-)16	25	192	

also (II): $^1J(^{107}Ag,P)$ and $^1(^{109}Ag,P)$
one of 615Hz and one of 536Hz

[a] approximate values

Table 5.9 Coupling constants (Hz) for $[Pt_2(\mu\text{-}S)(CO)(PPh_3)_3]$ and derived compounds

which are very much simpler. Since these compounds have only two isotopomers which contain ^{195}Pt (see Table 5.5), calculation of $^{1}J(Pt-Pt)$ is also quite easy.

The ^{195}Pt chemical shifts are consistently to higher field for the platinum which is coordinated to two PPh_3 ligands than for the platinum which is coordinated to PPh_3 and CO ligands - by about 300ppm in $[Pt_2(\mu-S)(CO)(PPh_3)_3]$ and by about 200ppm in the $[MPR_3]^+$ adducts. The ^{31}P chemical shift for the phosphine cis to CO is also found to higher field than the other two (by about 4ppm).

The coupling constants in Table 5.9 show only small variations between the four compounds except that $^{2}J(Pt-P)$ and $^{1}J(Pt-Pt)$ are noticeably smaller in the $[MPR_3]^+$ adducts than in the parent compound. The values for the (3-6) coupling are the smallest encountered in this work for $^{1}J(Pt-P)$ and are smaller than is found in Pt(0) compounds.[107] This $^{1}J(Pt-P)$ is for the phosphine which is cis to CO and its value being smaller than for the two mutually cis phosphines is in agreement with the "cis effect" observed by Pregosin[108] in some Pt(II) complexes. Within each compound, the difference between $^{2}J(Pt-P)$ for (2-6) and (4-6), typically +200 and -100Hz respectively emphasises the need to consider coupling pathways since both values involve the same Pt-Pt bond.

The $^{31}P\{^{1}H\}$ NMR spectrum at ambient temperature of the complex $[Pt_2(\mu-S)(CO)(PPh_3)_3]_2Au^+$ gave broad and poorly resolved lines. Therefore, this spectrum was recorded at -50° and the result is shown in Figure 5.11. Although the lines are still moderately broad and the ^{195}Pt satellites are not well resolved, it is possible to identify the resemblance between this spectrum and that of the parent compound $[Pt_2(\mu-S)(CO)(PPh_3)_3]$. There is an extra single line at 28.1ppm which

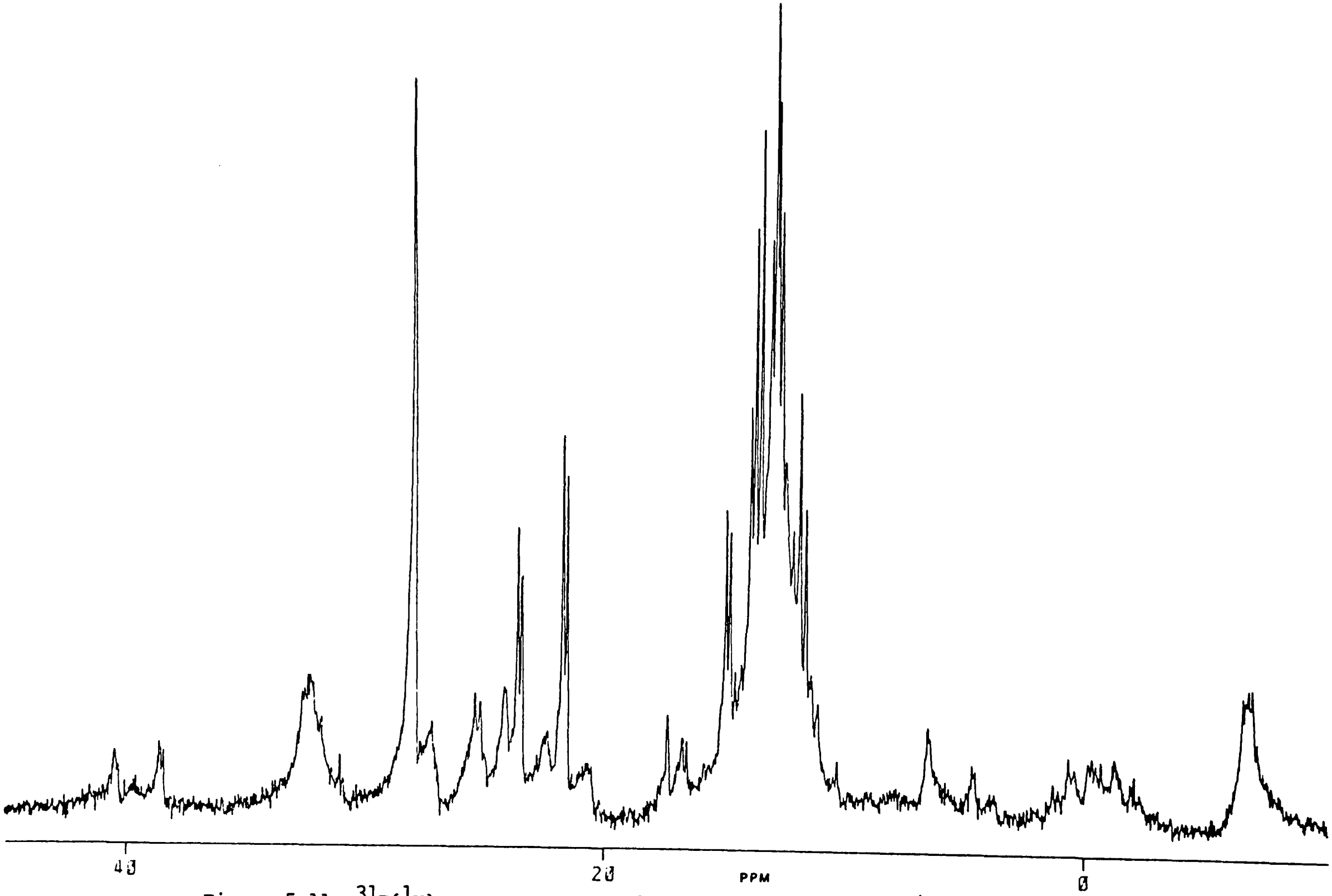

Figure 5.11 $^{31}P\{^{1}H\}$ NMR spectrum of $[Pt_2(\mu\text{-}S)(CO)(PPh_3)_3]_2Au^+$; recorded at -50°

is possibly due to the presence of excess $[AuPPh_3]^+$, but otherwise the spectrum can be interpreted in terms of the same arrangement of ^{31}P and ^{195}Pt nuclei. Some of the NMR parameters were measured approximately and are included in Tables 5.8 and 5.9. The coupling constants have similar magnitudes to those of the parent compound but the chemical shifts show a significant change. In $[Pt_2(\mu\text{-}S)(CO)(PPh_3)_3]$, P_2 and P_4 are close together and about 4ppm to low field of P_3. However, in $[Pt_2(\mu\text{-}S)(CO)(PPh_3)_3]_2Au^+$, P_3 and P_4 are close together and about 10ppm to high field of P_2. The ^{195}Pt satellites which were sufficiently resolved for coupling constants to be measured are all associated with Pt_5, that is the Pt coordinated to two phosphines.

5.6 Summary

It has proved possible to observe the $^{31}P\{^1H\}$ and $^{195}Pt\{^1H\}$ NMR spectra of a large number of cluster compounds of platinum and, with the assistance of computer simulation techniques, to determine from them most of the chemical shifts and coupling constants. A substantial collection of NMR data for spectra of compounds with known solid state structures have allowed the structures of related compounds to be determined. Starting with the relatively simple and well documented spectra of the triangular clusters $[Pt_3(\mu\text{-}X)_3(PR_3)_3]$, it was possible to deduce the structures of the less symmetrical compounds $[Pt_3(\mu\text{-}X)_2(\mu\text{-}Y)(PR_3)_3]$ from the chemical inequivalence that resulted in the ^{31}P and ^{195}Pt nuclei. It was also possible to deduce the structures of the gold capped tetrahedral clusters $[Pt_3Au(\mu\text{-}X)_3(PR_3)_4]^+$ and $[Pt_3Au(\mu\text{-}X)_2(\mu\text{-}Y)(PR_3)_4]$ from the extra multiplicity in the observed spectral lines compared with the parent platinum

cluster compounds. The marked similarity of the NMR spectra of the complexes $[Pt_2(\mu\text{-}S)(CO)(PPh_3)_3MPPh_3]^+$ (M = Au, Ag and Cu) implied that they were isostructural and that the $Pt_2(\mu\text{-}S)$ triangle was essentially unchanged from the parent compound $[Pt_2(\mu\text{-}S)(CO)(PPh_3)_3]$.

Some trends have been observed in the coupling constant data. $^1J(Pt\text{-}P)$ values are always large (2 - 5kHz) and are moderately sensitive to the electronic properties of other nearby ligands in <u>cis</u> and <u>trans</u> positions. $^1J(Pt\text{-}Pt)$ can be large (e.g. 3kHz) for Pt-Pt bonds but a direct correlation with the Pt-Pt bond length does not exist. Some undisputed Pt-Pt bonds have $^1J(Pt\text{-}Pt)$ less than 200Hz. $^2J(Pt\text{-}P)$ and $^3J(P\text{-}P)$ seem to be better indicators of the presence of Pt-Pt and Pt-Au bonds and particularly large $^3J(P\text{-}P)$ values (150Hz +) suggest an almost linear P-Pt-Pt-P unit.

CHAPTER SIX

EXPERIMENTAL DETAILS

6.1 General

Reactions were routinely carried out in Schlenk tubes under an atmosphere of nitrogen unless otherwise stated. All solvents were chemically dried and degassed before use. Chemicals were used as supplied. Microanalyses were performed by Mr. M. Gascoyne and his staff of these laboratories. Infra-red spectra were recorded on a Perkin Elmer 1710 FT-IR spectrometer as Nujol mulls between KBr discs and calibrated using polystyrene film. Ultra-violet spectra were recorded on a Perkin Elmer 552 UV-VIS spectrophotometer. X-ray microanalyses were carried out by Mrs Ann Stoker of the Oxford University Chemical Crystallography department. X-ray diffraction data relevant to Chapter 3 were collected on a Phillips PW1100 diffractometer and processed by Dr Mary McPartlin of the Chemistry Department at the Polytechnic of North London. X-ray diffraction data relevant to Chapter 4 were collected on an Enraf-Nonius CAD4 diffractometer and processed by Michael A. Luke in the Oxford University Chemical Crystallography department.

Unless otherwise stated, proton decoupled ^{13}C, ^{31}P and ^{195}Pt NMR spectra were recorded in deuteriated solvents on a Bruker AM250 spectrometer operating at 62.90 MHz, 101.26MHz and 53.77MHz respectively. The 162MHz $^{31}P\{^{1}H\}$ NMR spectrum described in Chapter 5 was recorded on the University of London Bruker WH400 spectrometer at Queen Mary College.Chemical shifts were referenced externally to aqueous solutions of TMP in the case of ^{31}P and Na_2PtCl_6 in the case

of ^{195}Pt. ^{13}C spectra were referenced internally to the solvent used. Chemical shifts were taken as positive to high frequency of the reference. Computer simulations of NMR spectra were carried out using a program developed by Prof. R.K. Harris, then of the University of East Anglia, and adapted for use on the Oxford University VAX system by Dr A.E. Derome. Simulation of a spectrum was performed in the following way. From the observed spectrum chemical shifts of nuclei and coupling constants were estimated in frequency units. The program was then used to calculate a spectrum from these parameters. The calculated frequencies and intensities of the lines were then compared with the observed spectrum, adjustments made to the parameter set and the spectrum recalculated using the new parameters. This process was repeated until a close fit of the calculated and observed spectra was obtained. If a reasonable fit did not occur after several cycles of refinement, then a new spectral assignment was made to obtain a closer fit. The resulting spectrum was then plotted graphically. At this stage it was assumed that the refined parameters were the optimum values for the chemical system under study.

The following compounds were prepared by standard literature methods:

$[Au(CO)Cl]$[109]

$[Au(Me_2S)Cl]$[110]

$[Au\{P(p\text{-}FC_6H_4)_3\}Cl]$[43]

$[Ag(PPh_3)Cl]_4$[111]

$[Cu(PPh_3)Cl]_4$[112]

$[Cu(MeCN)_4(PF_6)]$[113]

$[Pt(cod)Cl_2]$[114]

$[Pt(PPh_3)_3]$[115]

<u>cis</u>-$[Pt(PPh_3)(CO)Cl_2]$[74]

<u>cis</u>-$[Pt(PMe_2Ph)(CO)Cl_2]$[74]

<u>cis</u>-$[Pt(PCy_3)(CO)Cl_2]$[74]

<u>cis</u>-$[Pt(PBu^n{}_3)(CO)Cl_2]$[75]

$[Fe(\eta\text{-}C_5H_5)(CO)_2(C_2H_4)](BF_4)$[116]

6.2 Experimental Details Relevant to Chapter 2

6.2.1 Synthesis of cis-$[Pt\{P(CH_2CH_2CN)_3\}(CO)Cl_2]$

This compound was prepared by a modification of the published[74] synthesis of <u>cis</u>-$[Pt(PR_3)(CO)Cl_2]$. $[Pt(cod)Cl_2]$ (0.32g,0.86mmol) was dissolved in chloroform (40cm^3) and CO bubbled through for one hour to give a pinkish solution. A solution of $P(CH_2CH_2CN)_3$ (0.16g,0.83mmol) in hot chloroform (30cm^3) was added dropwise over 30 minutes with stirring. A yellow solid was precipitated. The solid was washed with fresh chloroform and then recrystallised from acetone/propan-2-ol. Yield: 0.34g(81%). Melting point: 202-3°. Elemental analyses: Found C,24.2%; H,2.7%; N,7.6%. $C_{10}H_{12}Cl_2N_3OPPt$ requires C,24.6%; H,2.5%; N,8.6%. Infra-red spectrum (cm^{-1}): ν(CN) 2240m, ν(CO) 2100s.

6.2.2 Synthesis of $[dppmAuCl]_2$

Bis(1,2-diphenylphosphino)methane (dppm) (0.26g,0.68mmol) was added with stirring to a solution of $[Au(Me_2S)Cl]$ (0.20g,0.68mmol) in CH_2Cl_2 (20cm^3). After 15 minutes, the solution was filtered and concentrated to low volume. Addition of hexane gave $[dppmAuCl]_2$ as a white precipitate which was then filtered and dried <u>in vacuo</u>. Yield 0.33g(79%) Elemental analyses: Found C,48.5%; H,3.5%; Cl,5.9%.

$C_{50}H_{44}Au_2Cl_2P_4$ requires C,48.7%; H,3.6%; Cl,5.8%. ^{31}P NMR in CD_2Cl_2 solution: $\delta(^{31}P)$ 29.6ppm.

6.2.3 Reaction of $[dppmAuCl]_2$ with $[Pt(cod)Cl_2]$

This reaction was based on the published[74] method for synthesising compounds of the type $[Pt(PR_3)(CO)Cl_2]$. $[Pt(cod)Cl_2]$ (0.16g,0.43mmol) was dissolved in chloroform (25cm^3) and CO bubbled through for one hour to give a pink solution. $[dppmAuCl]_2$ (0.26g,0.21mmol) was added slowly under CO and the solution stirred for 30 minutes. The solution was concentrated, giving a small amount of a fine white precipitate which was found to be unreacted $[Pt(cod)Cl_2]$. The solution was filtered and diethyl ether added to precipitate a second white solid which was dried *in vacuo* and characterised as $[Pt(dppmAuCl)_2Cl_2]$. Yield: 0.22g(70% based on Au). Elemental analyses: Found C,39.8%; H,3.1%; Cl,9.8%. $C_{50}H_{44}Au_2Cl_4Pt$ requires C,40.0%; H,2.9%; Cl,9.5%. Infra-red spectrum: no ν(CO) present. NMR in CD_2Cl_2 solution: $\delta(^{31}P)$ 21.9(s), -67.9(t,1:4:1) ppm - shifts in 1:1 ratio; $\delta(^{195}Pt)$ -3801ppm(t,1:2:1).

6.2.4 Synthesis of $[Pt_3(\mu\text{-}CO)_3(PBu^n{}_3)_3]$

A suspension of *cis*-$[Pt(PBu^n{}_3)(CO)Cl_2]$ (0.4g,0.81mmol) in methanol (30cm^3) was saturated with CO. A solution of $NaBH_4$ (0.16g,4.2mmol) in methanol (20cm^3), also saturated with CO, was added under CO, giving a deep red solution. The mixture was brought to boiling and filtered under CO. Reduction of the volume under vacuum, followed by standing at -40° resulted in the precipitation of red microcrystals of $[Pt_3(\mu\text{-}CO)_3(PBu^n{}_3)_3]$. The solid was washed with water

and a little cold methanol. Yield: 0.22g(64%). Elemental analyses: Found C,36.4%; H,6.6%. $C_{39}H_{81}O_3P_3Pt_3$ requires C,36.7%; H,6.4%. Infra-red spectrum (cm^{-1}): ν(CO) 1800sh, 1788vs. $^{31}P\{^1H\}$ NMR in benzene solution: $\delta(^{31}P)$ 24.4ppm.

6.2.5 Synthesis of $[Pt_3(\mu\text{-}CO)_3\{P(CH_2CH_2CN)_3\}_3]$

A solution of cis-$[Pt\{P(CH_2CH_2CN)_3\}(CO)Cl_2]$ (0.32g,0.66mmol) in acetone ($30cm^3$) was saturated with CO and zinc dust (0.21g,3.2mmol) was then added. The solution was stirred under CO for 18 hours during which time it became first green then red. The excess zinc dust was then filtered off and the filtrate evaporated to dryness in vacuo. The resulting orange solid was washed well with dichloromethane and methanol and then dissolved in acetone. Addition of ethanol to this solution gave, on standing, red crystals of $[Pt_3(\mu\text{-}CO)_3\{P(CH_2CH_2CN)_3\}_3]$. Yield: 0.20g(73%). Elemental analyses: Found C,29.4%; H,2.9%; N,9.4%. $C_{30}H_{36}N_9O_3P_3Pt_3$ requires C,28.8%; H,2.9%; N,10.1%. Infra-red spectrum (cm^{-1}): ν(CO) 1790br,s. $^{31}P\{^1H\}$ NMR in acetone solution: $\delta(^{31}P)$ 16.1ppm.

6.2.6 Synthesis of $[Pt_3(\mu\text{-}CO)_3(PCy_3)_3]$

a) by zinc dust reduction

A solution of cis-$[Pt(PCy_3)(CO)Cl_2]$ (0.32g,0.56mmol) in THF ($30cm^3$) was saturated with CO and zinc dust (0.32g,4.9mmol) was then added. The solution was stirred under CO for four days during which time it became first green then red. The excess zinc dust was filtered off and the filtrate evaporated to dryness in vacuo. The resulting orange solid was extracted into benzene and filtered. Addition of ethanol to this solution gave, on standing, red crystals of $[Pt_3(\mu\text{-}$

$CO)_3(PCy_3)_3]$.PhH. Yield: 0.18g(63%).

b) by $NaBH_4$ reduction

A suspension of cis-$[Pt(PCy_3)(CO)Cl_2]$ (0.32g,0.56mmol) in methanol was saturated with CO. $NaBH_4$ (0.15g,3.9mmol) was added under CO to give a dark brown suspension. The mixture was brought to boiling and then filtered. The brown residue was extracted into benzene to give a red solution which was filtered. Addition of ethanol to this solution gave, on standing, red crystals of $[Pt_3(\mu\text{-}CO)_3(PCy_3)_3]$.PhH. Yield: 0.17g(60%).

Elemental analyses: Found C,47.9%; H,6.7%. $C_{63}H_{105}O_3P_3Pt_3$ requires C,47.6%; H,6.6%. Infra-red spectrum (cm^{-1}): ν(CO) 1769s. (Lit.[81] 1770s) NMR in benzene solution: $\delta(^{31}P)$ 66.9ppm. (Lit.[81] 69.8ppm from H_3PO_4); $\delta(^{195}Pt)$ -4392ppm (Lit.[81] -4392ppm)

6.2.7 Synthesis of $[Pt_4(\mu\text{-}CO)_5(PMe_2Ph)_4]$

A suspension of cis-$[Pt(PMe_2Ph)(CO)Cl_2]$ (0.79g,1.8mmol) in methanol ($60cm^3$) was saturated with CO. A solution of vacuum dried $NaBH_4$ (0.7g,18mmol) in methanol ($40cm^3$), also saturated with CO, was added rapidly under CO giving a red solution and a brown precipitate. The mixture was stirred under CO for 30 minutes, then brought to boiling to give a red solution which was filtered, while hot, under CO. On cooling and standing, $[Pt_4(\mu\text{-}CO)_5(PMe_2Ph)_4]$ was deposited as red, needle-like crystals which were washed well with water, then a little methanol and dried in vacuo. Yield: 0.54g(80%). Elemental analyses: Found C,30.5%; H,3.0%. $C_{37}H_{44}O_5P_4Pt_4$ requires C,30.2%; H,3.0%. Infra-red spectrum (cm^{-1}): ν(CO) 1800s, 1775s. (Lit.[12] 1800s, 1779s) $^{31}P\{^1H\}$ NMR in CD_2Cl_2 solution: $\delta(^{31}P)$ 6.7ppm. (Lit.[40] 10.3ppm

from H_3PO_4)

6.2.8 Synthesis of $[Pt_5(CO)(\mu\text{-}CO)_5(PPh_3)_4]$

A solution of cis-$[Pt(PPh_3)(CO)Cl_2]$ (0.20g,0.36mmol) in THF ($50cm^3$) was saturated with CO. Excess zinc dust (0.47g,7.2mmol) was added and the reaction mixture stirred under CO at room temperature for 6 hours. The colour of the solution changed to green and finally deep red. The excess zinc dust was filtered off and the solution was evaporated to dryness in vacuo. The residue was extracted with benzene ($30cm^3$). Concentration of this solution followed by addition of methanol gave $[Pt_5(CO)(\mu\text{-}CO)_5(PPh_3)_4]$ as reddish-brown microcrystals. Yield: 0.12g(76%). Elemental analyses: Found C,42.1%; H,2.6%. $C_{78}H_{60}O_6P_4Pt_5$ requires C,42.7%; H,2.7%. Infra-red spectrum (cm^{-1}): ν(CO) 1998vs, 1895w, 1860s, 1812s, 1787vs. (Lit.[65] 1998vs, 1899m, 1858s, 1812s, 1788vs.)

6.2.9 Synthesis of $[Pt_3(\mu\text{-}CO)_3(PPh_3)_4]$

To a stirred solution of cis-$[Pt(PPh_3)(CO)Cl_2]$ (0.20g,0.36mmol) in THF ($50cm^3$), triphenylphosphine (0.03g,0.12mmol) was added. The reaction mixture was saturated with CO and excess zinc dust (0.30g,4.6mmol) was added. This mixture was stirred under an atmosphere of CO for four hours during which period the colour of the solution changed to pale green and finally to red. The excess zinc dust was filtered off and the solvent removed in vacuo. The residue was extracted with acetone and concentration of this solution to low volume gave red crystals of $[Pt_3(\mu\text{-}CO)_3(PPh_3)_4]$. A second crop of this product was obtained on addition of methanol to the filtered acetone solution. Yield: 0.17g(80%). Elemental analyses: Found

C,51.6%; H,3.4%. $C_{75}H_{60}O_3P_4Pt_3$ requires C, 52.4%; H,3.5%. Infra-red spectrum (cm^{-1}): ν(CO) 1860mw, 1800s, 1790s. (Lit.[12] 1854w, 1803s, 1788s.)

6.2.10 Synthesis of $[Pt_3(\mu\text{-}SO_2)_3(PCy_3)_3]$

This compound was prepared using a method developed in this laboratory by Evans.[46] $[Pt_3(\mu\text{-}CO)_3(PCy_3)_3]$.PhH (0.20g,0.13mmol) was dissolved in benzene ($30cm^3$) and the solution warmed to 60°. SO_2 gas was bubbled through this solution for 45 minutes. Concentration of the solution followed by addition of hexane precipitated $[Pt_3(\mu\text{-}SO_2)_3(PCy_3)_3]$.PhH as an orange microcrystalline solid. Yield: 0.14g(65%). Elemental analyses: Found C,40.2%; H,6.2%. $C_{60}H_{105}O_6P_3Pt_3S_3$ requires C,40.0%; H,6.1%. Infra-red spectrum (cm^{-1}): $\nu(SO_2)$ 1248mw, 1081vs, 1072s. NMR in benzene solution: $\delta(^{31}P)$ 76.3ppm; $\delta(^{195}Pt)$ -4070ppm.

6.2.11 Synthesis of $[Pt_3(\mu\text{-}SO_2)_3(PPh_3)_3]$

A slightly different method was used for this compound, taking advantage of the poor solubility of the product in toluene. $[Pt_3(\mu\text{-}CO)_3(PPh_3)_4]$.PhH (0.20g,0.11mmol) was dissolved in the minimum necessary volume of toluene ($20cm^3$) and the solution warmed to 60°. SO_2 gas was bubbled through the solution for 30 minutes during which time an orange crystalline solid was deposited. This solid was filtered, dried *in vacuo* and identified as $[Pt_3(\mu\text{-}SO_2)_3(PPh_3)_3]$. PhMe.$SO_2$. Yield: 0.16g(84%). Elemental analysis: Found C,42.7%; H,3.1%. $C_{61}H_{53}O_8P_3Pt_3S_4$ requires C,42.6%; H,3.1%. Infra-red spectrum (cm^{-1}): $\nu(SO_2)$ 1275s, 1260m, 1084vs (bound); 1325m, 1140m (solvation).

NMR in CD_2Cl_2 solution: $\delta(^{31}P)$ 61.4ppm; $\delta(^{195}Pt)$ -4228ppm.

6.2.12 Substitution by CO of SO_2 in $[Pt_3(\mu\text{-}SO_2)_3(PPh_3)_3]$

$[Pt_3(\mu\text{-}SO_2)_3(PPh_3)_3]$.PhMe.$SO_2$ (0.23g,0.13mmol) was dissolved in benzene (25cm^3) to give an orange solution. On addition of PPh_3 (12mg,0.04mmol) the colour darkened to red. CO was then bubbled through the solution which immediately became yellow then orange again. The solvent was removed *in vacuo* and the solid recrystallised from diethyl ether/methanol to give $[Pt_3(\mu\text{-}CO)_2(\mu\text{-}SO_2)(PPh_3)_3]$.PhH as orange microcrystals. Yield 0.16g(76%). Elemental analysis: Found C,47.9%; H,3.5%. $C_{62}H_{51}O_2P_3Pt_3S$ requires C,47.4%; H,3.3%. Infra-red spectrum (cm^{-1}): ν(CO) 1790vs, 1850w; $\nu(SO_2)$ 1094s, 1263m.

6.2.13 Reaction of $[Pt_3(\mu\text{-}SO_2)_3(PCy_3)_3]$ with CO

$[Pt_3(\mu\text{-}SO_2)_3(PCy_3)_3]$.PhH (0.12g,0.07mmol) was dissolved in benzene (20cm^3) and CO bubbled through the solution for two minutes during which time the colour changed from orange to yellow. The solvent was removed *in vacuo* and the solid recrystallised from diethyl ether/methanol to give $[Pt_3(\mu\text{-}CO)_2(\mu\text{-}SO_2)(PCy_3)_3]$.PhH. Yield 0.08g(70%). Elemental analysis: Found C,46.0%; H,6.5%. $C_{62}H_{105}O_2P_3Pt_3S$ requires C,45.8%; H,6.5%. Infra-red spectrum (cm^{-1}): ν(CO) 1785vs, 1842s; $\nu(SO_2)$ 1070s, 1087w. NMR in CD_2Cl_2 solution: $\delta(^{31}P)$ 82.2 (1P), 61.9 (2P) ppm; $\delta(^{195}Pt)$ -4515 (2Pt), -4011 (1Pt) ppm.

6.2.14 Conversion of $[Pt_3(\mu\text{-}SO_2)_3(PCy_3)_3]$ to $[Pt_3(\mu\text{-}CO)_3(PCy_3)_3]$

$Me_3NO.2H_2O$ (0.10g,0.90mmol) was added to a solution of $[Pt_3(\mu\text{-}SO_2)_3(PCy_3)_3]$.PhH (0.30g,0.18mmol) in benzene (25cm^3). The mixture

was saturated with CO and then stirred under an atmosphere of CO for 12 hours. The solvent was removed *in vacuo* and the residue washed well with water. The product was extracted into benzene ($10cm^3$) and ethanol added to precipitate $[Pt_3(\mu\text{-}CO)_3(PCy_3)_3]$.PhH as a crystalline solid. Yield 0.26g(93%) Analytical and spectroscopic characterisation was the same as in Section 6.2.6.

Found C, 48.0 %; H, 6.5%.

6.2.15 Reaction of $[Pt_3(\mu\text{-}CO)_3(PPh_3)_4]$ with CS_2

$[Pt_3(\mu\text{-}CO)_3(PPh_3)_4]$ (0.10g,0.06mmol) was dissolved in CH_2Cl_2 ($15cm^3$) and cooled to -15°. CS_2 (5 drops) was added with stirring whereupon the solution darkened from orange to deep red. The solvent was removed *in vacuo* and the residue allowed to warm to room temperature. Recrystallisation from CH_2Cl_2/hexane gave $[Pt_5(CO)(\mu\text{-}CO)_3(PPh_3)_4]$ as a brown powder. Yield 0.04g(55% based on Pt). Analytical and spectroscopic characterisation was the same as in Section 6.2.8. Found C, 42.4% ; H 2.6%

6.2.16 Reaction of $[Pt_3(\mu\text{-}CO)_3(PPh_3)_4]$ with COS

$[Pt_3(\mu\text{-}CO)_3(PPh_3)_4]$ (0.10g,0.06mmol) was dissolved in CH_2Cl_2 ($20cm^3$) and COS bubbled through for 10 minutes. The solution was then stirred under an atmosphere of COS for 24 hours. The solution was concentrated to low volume under reduced pressure and ethanol added to precipitate a yellow solid. $[Pt_2(\mu\text{-}S)(CO)_2(PPh_3)_2]$ was obtained on recrystallisation from CH_2Cl_2/hexane. Yield 0.06g(72% based on Pt) Elemental analysis: Found C,45.1%; H,3.1%. $C_{38}H_{30}O_2P_2Pt_2S$ requires C,45.5%; H,3.0%. Infra-red spectrum (cm^{-1}): ν(CO) 2030s, 1990s. NMR in CD_2Cl_2 solution: $\delta(^{31}P)$ 21.1ppm; $\delta(^{195}Pt)$ -4838ppm.

6.2.17 Synthesis of $[Pt_3(\mu\text{-}SO_2)_2(\mu\text{-}Cl)(PPh_3)_3]^-$ $BzEt_3N^+$

$[Pt_3(\mu\text{-}SO_2)_3(PPh_3)_3.SO_2.PhMe$ (65mg,0.04mmol) was dissolved in a 4:1 mixture of benzene and ethanol ($30cm^3$). $BzEt_3NCl$ (26mg,0.12mmol) was added with stirring. During the course of two hours, the colour of the solution lightened from orange to yellow. The solution was then evaporated under reduced pressure to a small volume ($10cm^3$) and hexane added to give a bright yellow precipitate. Recrystallisation from acetone and diethyl ether gave yellow crystals of $[Pt_3(\mu\text{-}SO_2)_2(\mu\text{-}Cl)(PPh_3)_3]^-$ $BzEt_3N^+$. Yield: 55mg(84%). Elemental analysis: Found C,46.6%; H,3.9%; N,0.8%; Cl,2.0%. $C_{67}H_{67}ClO_4NP_3S_2Pt_3$ requires C,46.6%; H,3.9%; N,0.8%; Cl,2.1%. Infra-red spectrum (cm^{-1}): $\nu(SO_2)$ 1154, 1046sh, 1027. $^{31}P\{^1H\}$ NMR in CD_2Cl_2 solution: $\delta(^{31}P)$ 4.0 (1P), 17.3 (2P) ppm.

6.2.18 Synthesis of $[Pt_3(\mu\text{-}SO_2)_2(\mu\text{-}Cl)(PCy_3)_3]^-$ PPN^+

To a stirred solution of $[Pt_3(\mu\text{-}SO_2)_3(PCy_3)_3].PhH$ (0.14g,0.09mmol) in benzene ($30cm^3$) was added a solution of PPNCl (0.05g,0.09mmol) in ethanol ($10cm^3$) followed by a solution of $Me_3NO.2H_2O$ (0.01g,0.09mmol) in ethanol ($5cm^3$). After about ten minutes the colour of the solution changed from orange to yellow. The solvent was removed in vacuo and the residue washed well with water and diethyl ether. The yellow product was extracted into CH_2Cl_2, the solution filtered and hexane added to give $[Pt_3(\mu\text{-}SO_2)_2(\mu\text{-}Cl)(PCy_3)_3]^-$ PPN^+ as a crystalline solid. Yield 0.15g(85%). Elemental analysis: Found C,50.6%; H,6.0%; N,0.7%; Cl,1.7%. $C_{90}H_{129}ClO_4NP_5Pt_3S_2$ requires C,50.8%; H,6.1%; N,0.7%; Cl,1.7%. Infra-red spectrum (cm^{-1}): $\nu(SO_2)$ 1007s, 1226s; ν(PPN) 1115m. NMR in CD_2Cl_2 solution: $\delta(^{31}P)$ 12.9 (1P),

28.9 (2P) ppm; $\delta(^{195}Pt)$ -5977 (1Pt), -4653 (2Pt) ppm.

6.2.19 Synthesis of $[Pt_3(\mu\text{-}SO_2)_2(\mu\text{-}Br)(PCy_3)_3]^-$ Et_4N^+

To a stirred solution of $[Pt_3(\mu\text{-}SO_2)_3(PCy_3)_3.PhH$ (0.10g,0.06mmol) in benzene (25cm^3) was added a solution of Et_4NBr (0.04g,0.19mmol) in ethanol (5cm^3) followed by a solution of $Me_3NO.2H_2O$ (0.02g,0.18mmol) in ethanol (5cm^3). The solution was stirred for one hour during which time the colour of the solution changed from orange to pale yellow. The solution was then evaporated under reduced pressure to a small volume (10cm^3) and hexane added to give a yellow precipitate. Recrystallisation from CH_2Cl_2/hexane gave small crystals of $[Pt_3(\mu\text{-}SO_2)_2(\mu\text{-}Br)(PCy_3)_3]^-$ Et_4N^+. Yield 0.10g(96%). Elemental analysis: Found C,41.9%; H,6.5%; N,0.9%. $C_{62}H_{119}BrO_4NP_3Pt_3S_2$ requires C,42.2%; H,6.7%; N,0.8%. Infra-red spectrum (cm^{-1}): $\nu(SO_2)$ 1018s, 1152m.

6.2.20 Reactions of $[Pt_3(\mu\text{-}SO_2)_2(\mu\text{-}Cl)(PCy_3)_3]^-$ PPN^+ with different amounts of $[Au\{P(p\text{-}FC_6H_4)_3\}]^+$

a) Reaction of equimolar amounts

$[Au\{P(p\text{-}FC_6H_4)_3\}Cl]$ (0.05g,0.09mmol) and $TlPF_6$ (0.10g,0.29mmol) were stirred together in THF (10cm^3) for one hour. A white precipitate was allowed to settle before the solution was filtered and added to a solution of $[Pt_3(\mu\text{-}SO_2)_2(\mu\text{-}Cl)(PCy_3)_3]^-$ PPN^+ (0.20g,0.09mmol) in THF (15cm^3). The solution was stirred for 30 minutes, filtered and the solvent removed *in vacuo*. The residue was recrystallised from CH_2Cl_2/hexane to obtain $[Pt_3Au(\mu\text{-}SO_2)_2(\mu\text{-}Cl)(PCy_3)_3\{P(p\text{-}FC_6H_4)_3\}].PhH$ as an orange crystalline solid. Yield: 0.15g(76%) Elemental analysis: Found C,43.8%; H,5.8%; Cl 1.7%. $C_{78}H_{117}AuClF_3O_4P_4Pt_3S_2$

requires C,42.9%; H,5.4%; Cl,1.6%. Infra-red spectrum (cm^{-1}): $\nu(SO_2)$ 1185s, 1052s. $^{31}P\{^1H\}$ NMR in CD_2Cl_2 solution: $\delta(^{31}P)$ 29.5 (2P), 16.8 (1P), 7.0 (1P) ppm.

b) Reaction of two mole equivalents of gold species with one mole equivalent of platinum cluster species.

The above reaction was repeated with the quantities of $[Au\{P(p\text{-}FC_6H_4\}_3\}Cl]$ and $TlPF_6$ doubled. The orange crystalline solid isolated in this case was $[Pt_3Au_2(\mu\text{-}SO_2)_2(\mu\text{-}Cl)(PCy_3)_3\{P(p\text{-}FC_6H_4)_3\}_2]^+ PF_6^-$. Yield: 0.20g(77%) Elemental analysis: Found C,39.7%; H,4.7%; Cl 1.1%. $C_{90}H_{123}Au_2ClF_{12}O_4P_6Pt_3S_2$ requires C,39.1%; H,4.4%; Cl,1.3%. Infra-red spectrum (cm^{-1}): $\nu(SO_2)$ 1162s, 1058s. $^{31}P\{^1H\}$ NMR in CD_2Cl_2 solution: $\delta(^{31}P)$ 37.1 (2P), 23.6 (2P), 21.4 (1P) ppm.

6.3 Experimental Details Relevant to Chapter 3

6.3.1 Synthesis of $[Au(PPh_3)Cl]$

This compound was prepared using a method devised in this laboratory by Hall.[43] To a stirred solution of $[Au(Me_2S)Cl]$ (0.21g,0.71mmol) in CH_2Cl_2 ($20cm^3$) was added triphenylphosphine (0.19g,0.73mmol). The solution was concentrated and hexane added to precipitate $[Au(PPh_3)Cl]$ as a white solid. The product was filtered, washed with ether and dried *in vacuo*. Yield: 0.33g(94%). Elemental analysis: found C,43.7%; H,3.1%; Cl,7.4%. $C_{18}H_{15}AuClP$ requires C,43.7%; H,3.0%; Cl,7.2%. $^{31}P\{^1H\}$ NMR in CD_2Cl_2 solution: $\delta(^{31}P)$ 30.0ppm.

6.3.2 Synthesis of $[Pt_3Au(\mu\text{-}CO)_3(PPh_3)_5]^+ PF_6^-$

$[Pt_3(\mu\text{-}CO)_3(PPh_3)_4]$.PhH (0.29g,0.16mmol) was dissolved in benzene ($25cm^3$) together with $Au(PPh_3)Cl$ (0.08g,0.16mmol). Finely ground $TlPF_6$ (0.27g,0.80mmol) was added with stirring. A fine brown precipitate was immediately observed and the mixture was left stirring for two hours to complete the reaction at the end of which time the solution was virtually colourless. The brown precipitate was filtered off, washed with benzene and extracted into acetone. Addition of benzene to this solution gave orange-brown crystals of $[Pt_3Au(\mu\text{-}CO)_3(PPh_3)_5]^+ PF_6^-$. Yield: 0.29g(77%) Elemental analysis: Found C,48.7%; H,3.2%. $C_{93}H_{75}AuF_6O_3P_6Pt_3$ requires C,48.1%; H,3.2%. Infra-red spectrum (cm^{-1}): ν(CO) 1893m, 1844s, 1829s; $\nu(PF_6)$ 841s.

6.3.3 Synthesis of $[Pt_3Au(\mu\text{-}SO_2)_2(\mu\text{-}Cl)(PPh_3)_4]$

$[Pt_3(\mu\text{-}SO_2)_3(PPh_3)_3.SO_2$.PhMe (0.12g,0.08mmol) was dissolved in benzene. $Au(PPh_3)Cl$ (0.04g,0.08mmol) was added and the mixture stirred for 30 minutes. The benzene was removed *in vacuo* and the residue extracted with CH_2Cl_2. Addition of hexane followed by standing at -20° gave red microcrystals of $[Pt_3Au(\mu\text{-}SO_2)_2(\mu\text{-}Cl)(PPh_3)_4]$. Yield: 0.13g(81%). Elemental analysis: Found C,43.2%; H,3.2%; Cl,2.0%. $C_{72}H_{60}AuClO_4P_4S_2Pt_3$ requires C,43.3%; H,3.0%; Cl,1.8%. Infra-red spectrum (cm^{-1}): $\nu(SO_2)$ 1199m, 1053s. $^{31}P\{^1H\}$ NMR in CD_2Cl_2 solution $\delta(^{31}P)$ 10.8 (1P), 17.3 (1P), 25.0 (2P) ppm. $^{195}Pt\{^1H\}$ NMR $\delta(^{195}Pt)$ -4044 (2P), -5386 (1P) ppm.

6.3.4 Synthesis of $[Pt_3(\mu\text{-}CO)_3(PPh_3)_3]_2Au^+$ PF_6^-

a) using $Au(Me_2S)Cl$

$[Pt_3(\mu\text{-}CO)_3(PPh_3)_4]$.PhH (0.24g,0.13mmol) was dissolved in benzene ($30cm^3$) and $TlPF_6$ (0.15g,0.43mmol) added with stirring followed by $Au(Me_2S)Cl$ (0.04g,0.14mmol). After 15 minutes, a dark red solid gradually precipitated as the solution became colourless. The solid was filtered off and extracted with CH_2Cl_2. Addition of hexane gave, on standing, deep red crystals of $[Pt_3(\mu\text{-}CO)_3(PPh_3)_3]_2Au^+$ PF_6^-. Yield: 0.20g(88%).

b) using Au(CO)Cl

The same product was obtained on reacting $[Pt_3(\mu\text{-}CO)_3(PPh_3)_4]$ (0.23g,0.13mmol) with Au(CO)Cl (0.04g,0.13mmol) in the presence of $TlPF_6$ (0.14g,0.40mmol) according to the same procedure as above. Yield: 0.18g(82%).

Elemental analysis: Found C,41.6%; H,2.9%; Au,6.3%; Pt,34.0%. $C_{114}H_{90}AuF_6O_6P_7Pt_6$ requires C,42.1%; H,2.8%; Au,6.1%; Pt,36.0%. Infra-red spectrum (cm^{-1}): ν(CO) 1833vs; $\nu(PF_6)$ 838s. $^{31}P\{^1H\}$ NMR in CD_2Cl_2 solution: $\delta(^{31}P)$ 31.9ppm. Single crystals were grown for X-ray diffraction by slow diffusion of diethyl ether into an acetone solution.

6.3.5 Synthesis of $[Pt_3(\mu\text{-}CO)_3(PPh_3)_3]_2Cu^+$ PF_6^-

Contact between the product and metal implements (e.g. spatula) was avoided in this synthesis since decomposition had been a problem in early attempts. $[Pt_3(\mu\text{-}CO)_3(PPh_3)_4]$.PhH (0.40g,0.22mmol) was dissolved in benzene ($30cm^3$) and $Cu(MeCN)_4(PF_6)$ (0.08g,0.21mmol) added with stirring. During the course of an hour a deep red precipitate was formed as the solution became almost colourless. The solid was

filtered off and extracted into CH_2Cl_2. Slow addition of diethyl ether gave deep red crystals of $[Pt_3(\mu\text{-}CO)_3(PPh_3)_3]_2Cu^+ PF_6^-$. Yield 0.28g(81%). Elemental analysis: Found C,43.6%; H,3.0%; Cu,2.1%. $C_{114}H_{90}CuF_6O_6P_7Pt_6$ requires C,43.9%; H,2.8%; Cu,2.0%. X-ray microanalysis confirmed that the Pt:Cu atom ratio was 6:1. Infra-red spectrum (cm^{-1}): ν(CO) 1837vs; $\nu(PF_6)$ 839s. Single crystals were grown for X-ray diffraction by slow diffusion of diethyl ether into a CH_2CL_2 solution.

6.3.6 Reaction of $[Pt_3(\mu\text{-}CO)_3(PCy_3)_3]$ with [Au(CO)Cl]

$[Pt_3(\mu\text{-}CO)_3(PCy_3)_3]PhH$ (0.30g,0.19mmol) was dissolved in benzene. $TlPF_6$ (0.10g,0.29mmol) and [Au(CO)Cl] (25mg,0.10mmol) were added and the solution stirred for 12 hours during which time it darkened considerably. The solvent was removed *in vacuo* and the residue extracted into CH_2Cl_2. Addition of ethanol gave, on standing at -20°, bright red crystals of $[Pt_3Au(\mu\text{-}CO)_3(PCy_3)_4]^+ PF_6^-$. Yield: 0.14g(35% based on Pt). Elemental analysis: Found C,42.6%; H,5.9%. $C_{75}H_{132}AuF_6O_3P_5Pt_3$ requires C,42.2%; H,6.2%. $^{31}P\{^1H\}$ NMR in CD_2Cl_2 solution: $\delta(^{31}P)$ 51.8 (3P), 82.4 (1P) ppm. (Lit.[23] 51.9, 82.7 ppm)

6.4 Experimental Details Relevant to Chapter 4

6.4.1 Synthesis of $[Pt_2(\mu\text{-}S)(CO)(PPh_3)_3]$

This compound was prepared by a modification of the method of Balch *et al.*[96] $Pt(PPh_3)_3$ (6.0g,4.9mmol) was suspended in pentane ($40cm^3$). COS gas was bubbled through for about 20 minutes until the suspension was almost white. The solid was then filtered off and

dissolved in the minimum volume of $CHCl_3$. Pentane was added to precipitate a yellow powder which was then suspended in ethanol and refluxed under nitrogen. A bright yellow solid, $[Pt_2(\mu\text{-}S)(CO)(PPh_3)_3].\frac{1}{2}PhH$, was filtered off and dried *in vacuo*. Yield 3.5g(90%). Elemental analysis: Found C,54.6%; H,4.0%. $C_{58}H_{48}OP_3Pt_2S$ requires C,54.6%; H,3.8%. Infra-red spectrum (cm^{-1}): ν(CO) 2001s. $^{31}P\{^1H\}$ NMR in CD_2Cl_2 solution: $\delta(^{31}P)$ 15.2, 19.1, 19.5ppm (Lit.[96] 18.7, 23.1, 23.3ppm from H_3PO_4); $\delta(^{195}Pt)$ -5072, -4753ppm. Single crystals for X-ray diffraction were grown by slow diffusion of diethyl ether into an acetone solution.

6.4.2 Reaction of $[Pt_2(\mu\text{-}S)(CO)(PPh_3)_3]$ with $[Fe(\eta\text{-}C_5H_5)(CO)_2(C_2H_4)]^+ BF_4^-$

$[Pt_2(\mu\text{-}S)(CO)(PPh_3)_3]$ (0.74g,0.60mmol) was dissolved in acetone ($30cm^3$) and $[Fe(\eta\text{-}C_5H_5)(CO)_2(C_2H_4)]^+ BF_4^-$ (0.18g,0.60mmol) added with stirring. After 15 hours the solution was filtered and concentrated under reduced pressure to about $5cm^3$. On standing at -20° a yellow crystalline precipitate formed which was found to be $[Pt_2(\mu\text{-}S)(CO)_2(PPh_3)_2]$. Yield: 0.39g(65%). Analytical and spectroscopic characterisation was the same as in Section 6.2.16, with the additional elemental analysis: Found Fe,0.0%

Found C, 45.5%; H, 3.2%.

6.4.3 Synthesis of $[Pt_2(\mu\text{-}S)(CO)(PPh_3)_3Au(PPh_3)]^+ PF_6^-$

To a solution of $[Pt_2(\mu\text{-}S)(CO)(PPh_3)_3]$ (0.17g,0.14mmol) in THF ($30cm^3$) were added, with stirring, $[Au(PPh_3)Cl]$ (0.07g,0.14mmol) and $TlPF_6$ (0.05g,0.14mmol). After six hours the solvent was removed *in vacuo* and the residue extracted into CH_2Cl_2. Addition of diethyl ether

to the filtered solution gave, on standing, yellow needle-like crystals of $[Pt_2(\mu\text{-}S)(CO)(PPh_3)_3Au(PPh_3)]^+ PF_6^-$. Yield: 0.21g(83%). Elemental analysis: Found C,47.2%; H,3.7%. $C_{73}H_{60}AuF_6OP_5Pt_2S$ requires C,47.6%; H,3.3%. Infra-red spectrum (cm^{-1}): ν(CO) 2025s; $\nu(PF_6)$ 838s. NMR in CD_2Cl_2 solution: $\delta(^{31}P)$ 33.1, 20.1, 17.8, 16.6 ppm; $\delta(^{195}Pt)$ -4841, -4629 ppm. Single crystals for X-ray diffraction were grown by slow diffusion of diethyl ether into a CH_2Cl_2 solution.

6.4.4 Synthesis of $[Pt_2(\mu\text{-}S)(CO)(PPh_3)_3Ag(PPh_3)]^+ PF_6^-$

$[Pt_2(\mu\text{-}S)(CO)(PPh_3)_3Ag(PPh_3)]^+ PF_6^-$ was prepared by the same method as the Au analogue (Section 6.4.3), using $[Ag(PPh_3)Cl]_4$ in four-fold excess and allowing three days for the reaction to be complete. Quantities used were: $[Pt_2(\mu\text{-}S)(CO)(PPh_3)_3]$ (0.13g,0.11mmol), $[Ag(PPh_3)Cl]_4$ (0.18g,0.11mmol) and $TlPF_6$ (0.19g,0.54mmol) in THF ($25cm^3$). The product was recrystallised from CH_2Cl_2/hexane. Yield: 0.13g(71%). Elemental analysis: Found C,49.9%; H,3.0%; Ag,6.6%. $C_{73}H_{60}AgF_6OP_5Pt_2S$ requires C,50.0%; H,3.4%; Ag,6.2%. Infra-red spectrum (cm^{-1}): ν(CO) 2022s; $\nu(PF_6)$ 835s. $^{31}P\{^1H\}$ NMR in CD_2Cl_2 solution: $\delta(^{31}P)$ 6.3, 17.7, 16.0, 14.1 ppm; $\delta(^{195}Pt)$ -4857, -4661 ppm.

6.4.5 Synthesis of $[Pt_2(\mu\text{-}S)(CO)(PPh_3)_3Cu(PPh_3)]^+ PF_6^-$

The procedure described in Section 6.4.3 was used, with the following reagents: $[Pt_2(\mu\text{-}S)(CO)(PPh_3)_3]$ (0.27g,0.22mmol), $[Cu(PPh_3)Cl]_4$ (0.08g,0.06mmol) and $TlPF_6$ (0.08g,0.23mmol) in THF ($25cm^3$). The product was obtained as pale yellow crystals from CH_2Cl_2/diethyl ether. Yield: 0.31g(83%) Elemental analysis: Found C,51.0%; H,3.5%. $C_{73}H_{60}CuF_6OP_5Pt_2S$ requires C,51.3%; H,3.5%. Infra-

red spectrum (cm^{-1}): ν(CO) 2016s. NMR in CD_2Cl_2 solution: $\delta(^{31}P)$ -3.4, 18.6, 16.4 15.1 ppm; $\delta(^{195}Pt)$ -4864, -4670 ppm.

6.4.6 Synthesis of $[Pt_2(\mu\text{-}S)(CO)(PPh_3)_3]_2Au^+ PF_6^-$

$[Pt_2(\mu\text{-}S)(CO)(PPh_3)_3]$ (0.22g,0.18mmol) was dissolved in benzene ($30cm^3$) and $TlPF_6$ (0.07g,0.20mmol) added with stirring followed by $[Au(Me_2S)Cl]$ (0.03g,0.10mmol). The mixture was stirred for one hour during which time the solution became colourless and an orange solid was precipitated. This product was filtered off, washed with a little benzene and then extracted into CH_2Cl_2. Addition of hexane gave, on standing overnight at -20° , orange microcrystals of $[Pt_2(\mu\text{-}S)(CO)(PPh_3)_3]_2Au^+ PF_6^-$. Yield: 0.21g(84%). Elemental analysis: Found C,47.2%; H,3.6%; Au,6.5%; Pt,26.4%. $C_{110}H_{90}AuF_6O_2P_7Pt_4S_2$ requires C,46.9%; H,3.2%; Au,7.0%; Pt,27.7%. Infra-red spectrum (cm^{-1}): ν(CO) 2031s, 2019s; $\nu(PF_6)$ 839s. $^{31}P\{^1H\}$ NMR in CD_2Cl_2 solution: $\delta(^{31}P)$ 22.6, 12.9, 12.6ppm.

REFERENCES

1. C.E. Briant, B.R.C. Theobald, J.W. White, L.K. Bell, D.M.P. Mingos and A.J. Welch, J. Chem. Soc., Chem. Commun., 1981, 201.
2. D.M.P. Mingos, J. Chem. Soc., Dalton Trans., 1976, 1163.
3. E.L. Muetterties and R.M. Wexler, Survey of Prog. in Chem., 1983, 10, 61.
4. E.L. Muetterties, Chem. and Eng. News, 1982, 60:No.35, 28.
5. P. Chini, J. Organomet. Chem., 1980, 200, 37.
6. O. Zahraa, F. Garin and G. Maire, Faraday Discuss. Chem. Soc., 1982, 72, 45.
7. G. Longoni and P. Chini, J. Amer. Chem. Soc., 1976, 98, 7225.
8. D.M.P. Mingos and R.W.M. Wardle, Trans. Met. Chem., 1985, 10, 441.
9. R.W.M. Wardle, D.Phil. Thesis, University of Oxford, 1985.
10. M.H. Chisholm and F.A. Cotton, Acc. Chem. Res., 1978, 11, 356.
11. M.A. Luke, D.Phil. Thesis, University of Oxford, 1985.
12. J. Chatt and P. Chini, J. Chem. Soc. (A), 1970, 1538.
13. N.J. Taylor, P.C. Chieh and A.J. Carty, J. Chem. Soc., Chem. Commun., 1980, 1255.
14. H.C. Clark, A.B. Goel and C.S. Wong, Inorg. Chim. Acta, 1979, 34, 159.
15. G.K. Anderson, H.C. Clark and J.A. Davies, Organometallics, 1982, 1, 550.
16. P.L. Bellon, A. Ceriotti, F. Demartin, G. Longoni and B.T. Heaton, J. Chem. Soc., Dalton Trans., 1982, 1671.
17. M. Green, J.A.K. Howard, M. Murray, J.L. Spencer and F.G.A. Stone, J. Chem. Soc., Dalton Trans., 1977, 1509.
18. J.M. Ritchey and D.C. Moody, Inorg. Chim. Acta, 1983, 74, 271.

19. D.G. Evans and D.M.P. Mingos, J. Organomet. Chem., 1982, 232, 171.

20. K.P. Hall and D.M.P. Mingos, Prog. Inorg. Chem., 1984, 32, 237.

21. B.F.G. Johnson, J. Lewis, W.J.H. Nelson, M.D. Vargas, D. Braga and M. McPartlin, J. Organomet. Chem., 1983, 246, C69.

22. M. Green, K.A. Mead, R.M. Mills, I.D. Salter, F.G.A. Stone and P. Woodward, J. Chem. Soc., Chem. Commun., 1982, 51.

23. C.E. Briant, R.W.M. Wardle and D.M.P. Mingos, J. Organomet. Chem., 1984, 267, C49.

24. D.M.P. Mingos and R.W.M. Wardle, J. Chem. Soc., Dalton Trans., 1986, 73.

25. P. Braunstein, H. Lenner, D. Matt, A. Tiripicchio and M. Tiripicchio-Camellini, Angew. Chem., Int. Ed. Engl., 1984, 24, 304.

26. C.E. Briant, D.I. Gilmour and D.M.P. Mingos, J. Organomet. Chem., 1984, 267, C52.

27. M.C. Baird and G. Wilkinson, J. Chem. Soc. (A), 1967, 865.

28. M.C. Baird and G. Wilkinson, J. Chem. Soc., Chem. Commun., 1966, 514.

29. A.C. Skapski and P.G.H. Troughton, J. Chem. Soc. (A), 1969, 2772.

30. W.M. Hawling, A. Walker and M.A. Woitzik, J. Chem. Soc., Chem. Commun., 1983, 11.

31. J. Chatt and D.M.P. Mingos, J. Chem. Soc. (A), 1970, 1243.

32. R. Ugo, G. La Monica, S. Cenini, A Segre and F. Conti, J. Chem. Soc. (A), 1971, 522.

33. C.E. Briant, T.S.A. Hor, N.D. Howells and D.M.P. Mingos, J. Organomet. Chem., 1983, 256, C15.

34. C.E. Briant, T.S.A. Hor, N.D. Howells and D.M.P. Mingos, J. Chem. Soc., Chem. Commun., 1983, 1118.

35. R.R. Ryan, G.J. Kubas, D.C. Moody and P.G. Eller, Structure and Bonding (Berlin), 1981, 46, 47.

36. D.M.P. Mingos, Trans. Met. Chem., 1978, 3, 1.

37. P.W. Frost, J.A.K. Howard, J.L. Spencer, D.G. Turner and D. Gregson, J. Chem. Soc., Chem. Commun., 1981, 1104.

38. D. Gregson, J.A.K. Howard, M. Murray and J.L. Spencer, J. Chem. Soc., Chem. Commun., 1981, 716.

39. C. Brown, B.T. Heaton, A.D.C. Towl, P. Chini, A. Fumagalli and G. Longoni, J. Organomet. Chem., 1979, 181, 233.

40. A. Moor, P.S. Pregosin, L.M. Venanzi and A.J. Welch, Inorg. Chim. Acta, 1984, 85, 103.

41. R.G. Vranka, L.F. Dahl, P. Chini and J. Chatt, J. Amer. Chem. Soc., 1969, 91, 1574.

42. G. Longoni and F. Morazzoni, J. Chem. Soc., Dalton Trans., 1981, 1735.

43. K.P. Hall, D.Phil. Thesis, University of Oxford, 1983.

44. R.J. Goodfellow, E.M. Hamon, J.A.K. Howard, J.L. Spencer and D.G. Turner, J. Chem. Soc., Chem. Commun., 1984, 1604.

45. D.G. Evans and D.M.P. Mingos, J. Organomet. Chem., 1982, 240, 321.

46. D.G. Evans, D.Phil. Thesis, University of Oxford, 1984.

47. J.C. Calabrese, L.F. Dahl, P. Chini, G. Longoni and S. Martinengo, J. Amer. Chem. Soc., 1974, 96, 2614.

48. A.Albinati, Inorg. Chim. Acta, 1977, 22, L31.

49. D.C. Moody and R.R. Ryan, Inorg. Chem., 1977, 16, 1052.

50. D.G. Evans, G.R. Hughes, D.M.P. Mingos, J-M. Bassett and A.J. Welch, J. Chem. Soc., Chem. Commun., 1980, 1255.

51. G. Longoni, M. Manassero, and M. Sansoni, J. Amer. Chem. Soc., 1980, 102, 7973.

52. A.Albinati, G. Carturan and A. Musco, Inorg. Chim. Acta, 1976, 16, L3.

53. L.J. Guggenberger, J. Chem. Soc., Chem. Commun., 1968, 512.

54. N.J. Taylor, P.C. Chieh and A.J. Carty, J. Chem. Soc., Chem. Commun., 1975, 448.

55. M.F. Hallam, N.D. Howells, D.M.P. Mingos and R.M.W. Wardle, J. Chem. Soc., Dalton. Trans., 1985, 845.

56. Y. Yamamoto, K. Takahashi and H. Yamazaki, J. Amer. Chem. Soc., 1986, 108, 2458.

57. C.E. Briant, D.I. Gilmour and D.M.P. Mingos, J. Organomet. Chem., 1986, in press.

58. C.E. Briant, D.G. Evans and D.M.P. Mingos, J. Chem. Soc., Chem. Commun., 1982, 1144.

59. C.E. Briant, D.I. Gilmour, D.M.P. Mingos and R.W.M. Wardle, J. Chem. Soc., Dalton Trans., 1985, 1693.

60. D.I. Gilmour and D.M.P. Mingos, J. Organomet. Chem., 1986, 302, 127.

61. P.E. Jones and L. Katz, J. Chem. Soc., Chem. Commun., 1967, 842.

62. C.E. Briant, M.J. Calhorda, T.S.A. Hor, N.D. Howells and D.M.P. Mingos, J. Chem. Soc., Dalton Trans., 1983, 1325.

63. Y. Yamamoto and H. Yamazaki, J. Chem. Soc., Dalton Trans., 1986, 677.

64. A.A. Frew, R.H. Hill, L. Manojlović-Muir, K.W. Muir and R.J. Puddephatt, J. Chem. Soc., Chem. Commun., 1982, 198.

65. J-P. Barbier, R. Bender, P. Braunstein, J. Fischer and L. Ricard, J. Chem. Res. (S), 1978, 230; (M), 1978, 2913.

66. R. Bender, P. Braunstein, J. Fischer, L. Ricard and A. Mitschler, Nouv. J. de Chimie, 1981, 5, 81.

67. R. Bender and P. Braunstein, J. Chem. Soc., Chem. Commun., 1983, 334.

68. A.B. Goel and S. Goel, Inorg. Chim. Acta, 1982, 65, L77.

69. J. Evans, J. Chem. Soc., Dalton Trans., 1980, 1005.

70. J.W. Lauher, J. Amer. Chem. Soc., 1978, 100, 5305.

71. D.J. Underwood, R. Hoffmann, K. Tatsumi, A. Nakamura and Y. Yamamoto, J. Amer. Chem. Soc., 1985, 107, 5968.

72. P. Giannocarro, A. Sacco and G. Vasapollo, Inorg. Chim. Acta, 1979, 37, L455.

73. F.R. Hartley, The Coordination Chemistry of Platinum and Palladium, Applied Science, London, 1973.

74. G.K. Anderson, H.C. Clark and J.A. Davies, Inorg. Chem., 1981, 20, 1636.

75. A.C. Smithies, M. Rycheck and M. Orchin, J. Organomet. Chem., 1968, 12, 199.

76. J. Chatt, N.P. Johnson, and B.L. Shaw, J. Chem. Soc., 1964, 1662.

77. D.B. Dell'Amico, F. Calderazzo and G. Dell'Amico, Gazz. Chim. Ital., 1977, 107, 101.

78. D.G. Evans, M.F. Hallam, D.M.P. Mingos and R.W.M. Wardle, Inorg. Chim. Acta, to be submitted.

79. C.A. Tolman, Chem. Rev., 1977, 77, 313.

80. H. Schmidbaur, A. Wohlleben, H. Schubert, A. Frank and G. Huttner, Chem. Ber., 1977, 110, 2751.

81. A. Moor, P.S. Pregosin and L.M. Venanzi, Inorg. Chim. Acta, 1981, 48, 153.

82. T. Yoshida and S.Otsuka, J. Amer. Chem. Soc., 1977, 99, 2134.

83. D.M.P. Mingos, Inorg. Chem., 1982, 21, 464.

84. L.S. Meriwether, E.C. Colthup, M.L. Fiene and F.A. Cotton, J.

Inorg. Nucl. Chem., 1959, 11, 181.

85. M. Green, R.M. Mills, G.N. Pain, F.G.A. Stone and P. Woodward, J. Chem. Soc., Dalton Trans., 1982, 1309.

86. C.S. Browning, D.H. Farrar, R.R. Gukathasan and S.A. Morris, Organometallics, 1985, 4, 1750.

87. O.J. Ezomo, Unpublished results.

88. M.J. Watson, Unpublished results.

89. T-Y Luh, Coord. Chem. Rev., 1984, 60, 255.

90. U. Koelle, J. Organomet. Chem., 1977, 133, 53.

91. J.R. Malpass in Comprehensive Org. Chem., Vol. 2, p40; Ed. I.O. Sutherland, 1979, Pergamon, Oxford.

92. Y. Yamamoto, H. Yamazaki and T. Sakurai, J. Amer. Chem. Soc., 1982, 104, 2329.

93. Y. Yamamoto, K. Aoki and H. Yamazaki, Chem. Lett., 1979, 391.

94. A. Albinati, A. Moor, P.S. Pregosin and L.M. Venanzi, J. Amer. Chem. Soc., 1982, 104, 7672.

95. A. Albinati, K-H. Dahmen, A. Togni and L.M. Venanzi, Angew. Chem., Int. Ed. Engl., 1985, 24, 766.

96. C.T. Hunt, G.B. Matson and A.L. Balch, Inorg. Chem., 1981, 20, 2270.

97. M.P. Brown, J.R. Fisher, R.J. Puddephatt and K.R. Seddon, Inorg. Chem., 1979, 18, 2808.

98. M.P. Brown, R.J. Puddephatt, M. Rashidi and K.R. Seddon, J. Chem. Soc., Dalton Trans., 1978, 1540.

99. P. Lennon, M. Madhavarao, A. Rosan and M. Rosenblum, J. Organomet. Chem., 1976, 108, 93 and references therein.

100. C.E. Briant, D.I. Gilmour and D.M.P. Mingos, J. Chem. Soc., Dalton Trans., 1986, 835.

101. P.G. Jones, G.M. Sheldrick and E. Hädicke, Acta Cryst., 1980, B36, 2777.

102. A. Moor, P.S. Pregosin and L.M. Venanzi, Inorg. Chim. Acta, 1982, 61, 135.

103. M.F. Hallam, Part II Thesis, University of Oxford, 1983.

104. P.S. Pregosin, Coord. Chem. Rev., 1982, 44, 247.

105. N.M. Boag, J. Browning, C. Crocker, P.L. Goggin, R.J. Goodfellow, M. Murray and J.L. Spencer, J. Chem. Res. (S), 1978, 228; (M), 1978, 2962.

106. M.P. Brown, J.R. Fisher, S.J. Franklin and K.R. Seddon, J. Organomet. Chem., 1978, 161, C46.

107. J. Chatt, R. Mason and D.W. Meek, J. Amer. Chem. Soc., 1975, 97, 3826.

108. P.S. Pregosin, R. Favez, R. Roulet, T. Boschi, A. Michelin and R. Ros, Inorg. Chim. Acta, 1980, 45, L7.

109. D.B. Dell'Amico and F. Calderazzo, Gazz. Chim. Ital., 1973, 103, 1099.

110. F. Bonati and G. Minghetti, Gazz. Chim. Ital., 1973, 103, 373.

111. B.K. Teo and J.C. Calabrese, Inorg. Chem., 1976, 15, 2467.

112. M.R. Churchill, S.A. Bezman, J.A. Osborn and J. Wormald, Inorg. Chem., 1972, 11, 1818.

113. G.J. Kubas, Inorg. Syn., 1979, 19, 90.

114. D. Drew and J.R. Doyle, Inorg. Synth., 1972, 13, 47.

115. R. Ugo, F. Cariati and G. La Monica, Inorg. Syn., 1968, 11, 105.

116. W.P. Giering, M. Rosenblum and J. Tancrede, J. Amer. Chem. Soc., 1972, 94, 7170.

APPENDIX A

Final fractional atomic coordinates and isotropic temperature factors ($Å^2$) for $[Pt_3(\mu\text{-}CO)_3(PPh_3)_3]_2Au(PF_6)$ with estimated Standard Deviations in parentheses.

Atom	x/a	y/b	z/c	U(iso)
Pt(1)	0.02663(3)	0.28254(4)	0.16475(3)	0.0277(4)
Pt(2)	-0.03965(3)	0.15108(4)	0.16473(3)	0.0271(4)
Pt(3)	-0.07217(3)	0.31624(4)	0.16480(3)	0.0270(4)
Au	0.00000	0.24998(7)	0.2500	0.0286(6)
P(1)	-0.0701(2)	0.0211(3)	0.1315(2)	0.028(3)
P(2)	0.0907(2)	0.3180(3)	0.1317(2)	0.030(3)
P(3)	-0.1387(2)	0.4110(3)	0.1315(2)	0.030(3)
P(4)	0.7500	0.2500	0.5000	0.0452(46)
F(1)	0.7706(6)	0.3090(11)	0.4662(7)	0.159(13)
F(2)	0.8069(5)	0.2282(11)	0.5351(6)	0.138(12)
F(3)	0.7535(6)	0.1728(10)	0.4662(7)	0.146(13)
C(1)	-0.0075(7)	0.4007(12)	0.1693(7)	0.035(4)
O(1)	0.0017(5)	0.4717(9)	0.1769(6)	0.055(4)
C(2)	-0.1093(7)	0.2019(11)	0.1694(7)	0.032(4)
O(2)	-0.1485(5)	0.1776(9)	0.1767(6)	0.056(4)
C(3)	0.0384(6)	0.1482(10)	0.1681(6)	0.022(4)
O(3)	0.0738(5)	0.0986(9)	0.1780(5)	0.050(4)
C(112)	-0.1625(4)	-0.0725(8)	0.1275(4)	0.039(5)
C(113)	-0.1970(4)	-0.1114(8)	0.1496(4)	0.049(5)
C(114)	-0.1886(4)	-0.1018(8)	0.2014(4)	0.076(7)
C(115)	-0.1456(4)	-0.0533(8)	0.2312(4)	0.056(6)
C(116)	-0.1110(4)	-0.0144(8)	0.2092(4)	0.044(5)
C(111)	-0.1195(4)	-0.0240(8)	0.1573(4)	0.026(4)
C(122)	-0.1169(6)	0.1029(8)	0.0404(6)	0.064(7)
C(123)	-0.1407(6)	0.1065(8)	-0.0121(6)	0.086(8)
C(124)	-0.1478(6)	0.0304(8)	-0.0409(6)	0.085(8)
C(125)	-0.1311(6)	-0.0492(8)	-0.0171(6)	0.086(8)
C(126)	-0.1073(6)	-0.0528(8)	0.0354(6)	0.069(8)
C(121)	-0.1002(6)	0.0233(8)	0.0642(6)	0.042(5)
C(132)	0.0180(5)	-0.0578(7)	0.1185(5)	0.052(6)
C(133)	0.0577(5)	-0.1207(7)	0.1277(5)	0.055(6)
C(134)	0.0582(5)	-0.1903(7)	0.1601(5)	0.058(6)
C(135)	0.0191(5)	-0.1968(7)	0.1833(5)	0.071(7)
C(136)	-0.0206(5)	-0.1339(7)	0.1741(5)	0.056(6)
C(131	-0.0211(5)	-0.0643(7)	0.1417(5)	0.035(4)
C(212)	0.1671(4)	0.2377(8)	0.2094(4)	0.041(5)
C(213)	0.2144(4)	0.1928(8)	0.2317(4)	0.053(6)
C(214)	0.2449(4)	0.1656(8)	0.2021(4)	0.056(6)
C(215)	0.2281(4)	0.1833(8)	0.1502(4)	0.055(6)
C(216)	0.1808(4)	0.2281(8)	0.1279(4)	0.039(5)
C(211)	0.1503(4)	0.2553(8)	0.1575(4)	0.030(4)
C(222)	0.1643(4)	0.4495(8)	0.1735(5)	0.055(6)
C(223)	0.1806(4)	0.5359(8)	0.1827(5)	0.070(7)

C(224)	0.1459(4)	0.6031(8)	0.1599(5)	0.060(6)
C(225)	0.0950(4)	0.5839(8)	0.1279(5)	0.057(6)
C(226)	0.0787(4)	0.4975(8)	0.1187(5)	0.044(5)
C(221)	0.1134(4)	0.4303(8)	0.1415(5)	0.034(4)
C(232)	0.0280(5)	0.2503(9)	0.0405(6)	0.072(7)
C(233)	0.0117(5)	0.2379(9)	-0.0119(6)	0.091(9)
C(234)	0.0377(5)	0.2809(9)	-0.0412(6)	0.115(11)
C(235)	0.0802(5)	0.3361(9)	-0.0181(6)	0.084(8)
C(236)	0.0965(5)	0.3485(9)	0.0343(6)	0.057(6)
C(231)	0.0704(5)	0.3056(9)	0.0636(6)	0.037(5)
C(312)	-0.2281(5)	0.3108(7)	0.1191(5)	0.043(5)
C(313)	-0.2744(5)	0.2857(7)	0.1285(5)	0.058(6)
C(314)	-0.2938(5)	0.3355(7)	0.1606(5)	0.059(6)
C(315)	-0.2669(5)	0.4105(7)	0.1833(5)	0.060(6)
C(316)	-0.2206(5)	0.4355(7)	0.1739(5)	0.050(5)
C(311)	-0.2012(5)	0.3857(7)	0.1418(5)	0.028(4)
C(322)	-0.1403(4)	0.5938(8)	0.1279(3)	0.043(5)
C(323)	-0.1308(4)	0.6758(8)	0.1505(3)	0.051(6)
C(324)	-0.1043(4)	0.6834(8)	0.2024(3)	0.060(6)
C(325)	-0.0875(4)	0.6089(8)	0.2319(3)	0.042(5)
C(326)	-0.0971(4)	0.5269(8)	0.2093(3)	0.041(5)
C(321)	-0.1235(4)	0.5193(8)	0.1573(3)	0.034(4)
C(332)	-0.1199(4)	0.3945(9)	0.0395(6)	0.067(7)
C(333)	-0.1326(4)	0.4026(9)	-0.0130(6)	0.101(10)
C(334)	-0.1815(4)	0.4372(9)	-0.0415(6)	0.107(10)
C(335)	-0.2176(4)	0.4556(9)	0.0349(6)	0.051(6)
C(331)	-0.1560(4)	0.4210(9)	0.0635(6)	0.031(4)

Final anisotropic temperature factors ($Å^2$) with estimated Standard Deviations in parentheses

Atom	U11	U22	U33	U23	U13	U12
Pt(1)	0.0204(3)	0.0284(4)	0.0342(5)	0.0008(3)	0.0115(3)	-0.0009(3)
Pt(2)	0.0226(3)	0.0250(4)	0.0335(5)	-0.0015(3)	0.0088(3)	-0.0018(3)
Pt(3)	0.0201(3)	0.0268(4)	0.0340(5)	0.0015(3)	0.0083(3)	0.0030(3)
Au	0.0259(5)	0.0338(5)	0.0261(6)	0.0000(1)	0.0067(4)	0.0000(1)
P(1)	0.029(2)	0.024(2)	0.031(3)	0.002(2)	0.007(2)	0.000(2)
P(2)	0.022(2)	0.036(3)	0.033(3)	-0.003(2)	0.009(2)	-0.004(2)
P(3)	0.025(2)	0.030(2)	0.033(3)	0.003(2)	0.010(2)	0.003(2)
P(4)	0.046(4)	0.058(5)	0.032(4)	0.004(4)	0.010(4)	0.000(4)
F(1)	0.171(13)	0.144(13)	0.161(15)	0.062(11)	0.091(11)	-0.007(10)
F(2)	0.079(9)	0.185(13)	0.149(13)	0.021(11)	-0.026(9)	0.019(9)
F(3)	0.164(12)	0.125(12)	0.150(14)	-0.067(10)	0.060(10)	0.004(10)

APPENDIX B

Final fractional atomic coordinates and isotropic temperature factors ($Å^2$) for $[Pt_3(\mu\text{-}CO)_3(PPh_3)_3]_2Cu(PF_6)$ with estimated Standard Deviations in parentheses.

Atom	x/a	y/b	z/c	U(iso)
Pt(1)	0.02731(5)	0.28300(9)	0.16885(5)	0.0275(7)
Pt(2)	-0.03780(5)	0.15207(8)	0.16872(6)	0.0275(7)
Pt(3)	-0.07070(5)	0.31509(9)	0.16878(6)	0.0270(7)
Cu	0.00000	0.25043(40)	0.25000	0.0310(31)
P(2)	-0.0682(3)	0.0213(6)	0.1353(4)	0.029(5)
P(1)	0.0903(3)	0.3189(5)	0.1347(3)	0.026(4)
P(3)	-0.1375(3)	0.4092(5)	0.1351(3)	0.028(5)
P(4)	0.75000	0.25000	0.50000	0.0523(94)
C(1)	-0.0102(15)	0.4100(27)	0.1725(15)	0.046(10)
O(1)	0.0035(10)	0.4767(17)	0.1810(10)	0.050(7)
C(2)	-0.1106(15)	0.1946(24)	0.1739(14)	0.030(9)
O(2)	-0.1491(10)	0.1746(16)	0.1790(9)	0.045(6)
C(3)	0.0397(8)	0.1507(15)	0.1712(8)	0.016(4)
O(3)	0.0755(9)	0.1003(16)	0.1787(9)	0.042(6)
C(112)	-0.1629(9)	-0.0685(16)	0.1286(6)	0.050(10)
C(113)	-0.1975(9)	-0.1082(16)	0.1506(6)	0.053(11)
C(114)	-0.1882(9)	-0.1017(16)	0.2037(6)	0.049(10)
C(115)	-0.1443(9)	-0.0555(16)	0.2346(6)	0.043(10)
C(116)	-0.1096(9)	-0.0158(16)	0.2125(6)	0.049(11)
C(111)	-0.1189(9)	-0.0223(16)	0.1595(6)	0.028(8)
C(122)	-0.1167(11)	0.1056(14)	0.0441(10)	0.068(13)
C(123)	-0.1415(11)	0.1109(14)	-0.0091(10)	0.078(14)
C(124)	-0.1478(11)	0.0361(14)	-0.0395(10)	0.087(15)
C(125)	-0.1292(11)	-0.0441(14)	-0.0166(10)	0.081(14)
C(126)	-0.1045(11)	-0.0494(14)	0.0366(10)	0.057(11)
C(121)	-0.0981(11)	0.0254(14)	0.0670(10)	0.039(9)
C(132)	0.0175(10)	-0.0567(14)	0.1194(9)	0.043(9)
C(133)	0.0565(10)	-0.1207(14)	0.1266(9)	0.052(11)
C(134)	0.0578(10)	-0.1912(14)	0.1592(9)	0.083(15)
C(135)	0.0202(10)	-0.1976(14)	0.1847(9)	0.079(15)
C(136)	-0.188(10)	-0.1336(14)	0.1775(9)	0.049(10)
C(131)	-0.0202(10)	-0.0631(14)	0.1449(9)	0.034(8)
C(212)	0.1696(8)	0.2409(15)	0.2132(7)	0.035(8)
C(213)	0.2171(8)	0.1958(15)	0.2353(7)	0.049(10)
C(214)	0.2467(8)	0.1675(15)	0.2045(7)	0.055(11)
C(215)	0.2288(8)	0.1843(15)	0.1516(7)	0.055(11)
C(216)	0.1813(8)	0.2294(15)	0.1294(7)	0.046(10)
C(211)	0.1517(8)	0.2577(15)	0.1602(7)	0.033(8)
C(222)	0.1645(9)	0.4507(16)	0.1778(10)	0.063(12)
C(223)	0.1810(9)	0.5374(16)	0.1858(10)	0.086(16)
C(224)	0.1467(9)	0.6042(16)	0.1608(10)	0.070(14)
C(225)	0.0959(9)	0.5843(16)	0.1278(10)	0.058(11)
C(226)	0.0793(9)	0.4976(16)	0.1198(10)	0.056(11)

C(221)	0.1136(9)	0.4308(16)	0.1449(10)	0.032(8)
C(232)	0.0289(10)	0.2498(18)	0.0458(10)	0.057(11)
C(233)	0.0127(10)	0.2316(18)	-0.0070(10)	0.092(16)
C(234)	0.0377(10)	0.2725(18)	-0.0384(10)	0.106(17)
C(235)	0.0789(10)	0.3316(18)	-0.0171(10)	0.072(14)
C(236)	0.0951(10)	0.3497(18)	0.0356(10)	0.070(14)
C(231)	0.0702(10)	0.3088(18)	0.0671(10)	0.036(8)
C(312)	-0.2285(10)	0.3088(14)	0.1211(9)	0.049(10)
C(313)	-0.2752(10)	0.2849(14)	0.1305(9)	0.062(12)
C(314)	-0.2945(10)	0.3358(14)	0.1627(9)	0.070(13)
C(315)	-0.2671(10)	0.4107(14)	0.1856(9)	0.072(13)
C(316)	-0.2204(10)	0.4346(14)	0.1762(9)	0.044(9)
C(311)	-0.2011(10)	0.3837(14)	0.1440(9)	0.025(7)
C(322)	-0.1398(8)	0.5919(15)	0.1294(6)	0.046(10)
C(323)	-0.1306(8)	0.6747(15)	0.1517(6)	0.046(10)
C(324)	-0.1045(8)	0.6834(15)	0.2046(6)	0.056(11)
C(325)	-0.0875(8)	0.6094(15)	0.2352(6)	0.050(10)
C(326)	-0.0966(8)	0.5267(15)	0.2128(6)	0.047(10)
C(321)	-0.1228(8)	0.5179(15)	0.1599(6)	0.033(8)
C(332)	-0.1158(8)	0.3978(18)	0.0437(10)	0.064(12)
C(333)	-0.1273(8)	0.4065(18)	-0.0096(10)	0.073(14)
C(334)	-0.1774(8)	0.4352(18)	-0.0400(10)	0.101(17)
C(335)	-0.2160(8)	0.4551(18)	-0.0173(10)	0.083(14)
C(336)	-0.2045(8)	0.4464(18)	0.0350(10)	0.057(11)
C(331)	-0.1543(8)	0.4177(18)	0.0664(10)	0.040(9)
F(1)	0.6915(17)	0.2759(31)	0.4668(17)	0.170(17)
F(2)	0.7491(17)	0.1621(28)	0.4667(17)	0.164(17)
F(3)	0.7745(18)	0.3062(32)	0.4631(18)	0.184(18)

Final anisotropic temperature factors ($Å^2$) with estimated Standard Deviations in parentheses

Atom	U11	U22	U33	U23	U13	U12
Pt(1)	0.012(1)	0.022(1)	0.049(1)	0.001(1)	0.011(1)	0.000(1)
Pt(2)	0.015(1)	0.019(1)	0.049(1)	-0.001(1)	0.009(1)	-0.001(1)
Pt(3)	0.012(1)	0.020(1)	0.049(1)	0.001(1)	0.008(1)	0.002(1)
Cu(1)	0.020(3)	0.027(3)	0.046(3)	0.000(1)	0.009(3)	0.000(1)
P(2)	0.023(4)	0.023(5)	0.041(5)	0.000(4)	0.008(4)	-0.001(4)
P(1)	0.014(4)	0.017(4)	0.046(5)	-0.004(4)	0.008(4)	0.001(3)
P(3)	0.019(4)	0.016(4)	0.049(5)	0.004(4)	0.012(4)	-0.007(3)
P(4)	0.037(8)	0.065(11)	0.055(9)	0.000(1)	0.006(7)	0.000(1)

APPENDIX C

Final fractional atomic coordinates and isotropic temperature factors ($Å^2$) for $[Pt_2(\mu\text{-}S)(CO)(PPh_3)_3]$ with estimated Standard Deviations in parentheses.

Atom	x/a	y/b	z/c	U(iso)
Pt(1)	0.21668(5)	0.24240(4)	0.24072(3)	0.0297
Pt(2)	0.18730(6)	0.39319(4)	0.30180(3)	0.0338
S(1)	0.1070(4)	0.3371(3)	0.1913(2)	0.0436
P(1)	0.2214(4)	0.1613(3)	0.1449(2)	0.0352
P(2)	0.1308(4)	0.5454(2)	0.3071(2)	0.0349
P(3)	0.3373(4)	0.1511(3)	0.3303(2)	0.0361
C(100)	0.2741(20)	0.3675(11)	0.3921(10)	0.0539
O(100)	0.3242(20)	0.3533(10)	0.4472(9)	0.0892
C(111)	0.1614(13)	0.2259(7)	0.0567(7)	0.0411(38)
C(112)	0.0246(14)	0.2639(7)	0.0577(8)	0.0600(47)
C(113)	-0.0287(17)	0.3134(8)	-0.0084(9)	0.0870(63)
C(114)	0.0558(17)	0.3242(8)	-0.0747(9)	0.0850(62)
C(115)	0.1918(17)	0.2865(8)	-0.0760(9)	0.0864(63)
C(116)	0.2459(15)	0.2367(7)	-0.0099(8)	0.0646(50)
C(121)	0.1157(11)	0.0597(7)	0.1541(6)	0.0377(36)
C(122)	0.1061(11)	0.0119(8)	0.0949(7)	0.0474(41)
C(123)	0.0197(12)	-0.0636(8)	0.1025(8)	0.0600(47)
C(124)	-0.0589(13)	-0.0911(9)	0.1691(8)	0.0769(57)
C(125)	-0.0524(13)	-0.0444(9)	0.2282(9)	0.0814(60)
C(126)	0.0362(12)	0.0318(9)	0.2213(8)	0.0661(51)
C(131)	0.4010(13)	0.1257(8)	0.1177(5)	0.0398(37)
C(132)	0.4439(15)	0.0393(9)	0.1014(5)	0.0585(46)
C(133)	0.5878(16)	0.0203(11)	0.0833(5)	0.0765(57)
C(134)	0.6869(17)	0.0873(11)	0.0817(5)	0.0764(57)
C(135)	0.6460(16)	0.1763(11)	0.0975(5)	0.0760(56)
C(136)	0.5021(15)	0.1922(9)	0.1154(5)	0.0593(47)
C(211)	-0.0547(13)	0.5814(8)	0.2993(5)	0.0387(37)
C(212)	-0.1052(16)	0.6668(10)	0.3126(5)	0.0749(56)
C(213)	-0.2469(17)	0.6946(11)	0.3023(6)	0.0850(62)
C(214)	-0.3369(16)	0.6376(10)	0.2783(5)	0.0677(51)
C(215)	-0.2879(16)	0.5517(10)	0.2646(5)	0.0752(56)
C(216)	-0.1453(14)	0.5242(9)	0.2757(5)	0.0573(46)
C(221)	0.1830(13)	0.5802(6)	0.3931(7)	0.0433(39)
C(222)	0.3284(15)	0.5853(6)	0.3996(8)	0.0602(47)
C(223)	0.3785(17)	0.6059(6)	0.4658(9)	0.0796(58)
C(224)	0.2822(18)	0.6211(7)	0.5245(9)	0.0902(65)
C(225)	0.1371(18)	0.6158(6)	0.5182(9)	0.0819(60)
C(226)	0.0864(16)	0.5952(6)	0.4518(8)	0.0646(50)
C(231)	0.2225(10)	0.6267(8)	0.2338(6)	0.0387(37)
C(232)	0.2944(11)	0.5967(10)	0.1729(7)	0.0580(46)
C(233)	0.3628(12)	0.6622(11)	0.1168(8)	0.0810(59)
C(234)	0.3596(12)	0.7544(10)	0.1211(8)	0.0656(50)
C(235)	0.2879(12)	0.7847(10)	0.1819(8)	0.0719(54)

C(236)	0.2195(12)	0.7207(10)	0.2387(8)	0.0684(52)
C(311)	0.3698(11)	0.0271(8)	0.3306(6)	0.0370(36)
C(312)	0.4746(12)	-0.0016(9)	0.2820(6)	0.0547(44)
C(313)	0.5027(13)	-0.0958(10)	0.2834(7)	0.0616(48)
C(314)	0.4262(14)	-0.1613(11)	0.3328(7)	0.0737(55)
C(315)	0.3211(15)	-0.1332(11)	0.3818(8)	0.0843(61)
C(316)	0.2930(13)	-0.0382(10)	0.3804(7)	0.0675(51)
C(321)	0.5199(14)	0.1869(8)	0.3317(6)	0.0489(41)
C(322)	0.5624(15)	0.2682(9)	0.2855(6)	0.0554(45)
C(323)	0.7053(15)	0.2913(10)	0.2779(7)	0.0698(53)
C(324)	0.8033(17)	0.2332(10)	0.3167(7)	0.0762(56)
C(325)	0.7636(17)	0.1519(10)	0.3632(7)	0.0791(58)
C(326)	0.6205(15)	0.1285(9)	0.3708(6)	0.0618(48)
C(331)	0.2546(13)	0.1490(6)	0.4239(7)	0.0426(38)
C(332)	0.1087(15)	0.1592(6)	0.4295(8)	0.0612(48)
C(333)	0.0351(18)	0.1498(6)	0.4995(9)	0.0861(63)
C(334)	0.1067(19)	0.1313(7)	0.5647(10)	0.0982(71)
C(335)	0.2530(19)	0.1216(7)	0.5601(9)	0.0903(65)
C(336)	0.3284(16)	0.1306(6)	0.4896(8)	0.0690(52)

Final anisotropic temperature factors ($Å^2$ x 10^4) with estimated Standard Deviations in parentheses.

Atom	U(11)	U(22)	U(33)	U(23)	U(13)	U(12)
Pt(1)	271(3)	292(3)	348(3)	-89(3)	-6(3)	11(3)
Pt(2)	344(3)	296(3)	404(4)	-97(3)	-39(3)	33(3)
S(1)	496(25)	400(24)	433(24)	-48(19)	-70(19)	93(19)
P(1)	346(22)	365(23)	358(22)	-96(18)	1(18)	-21(18)
P(2)	366(23)	270(22)	438(24)	-79(18)	-11(18)	15(17)
P(3)	303(22)	341(23)	475(25)	-91(19)	-65(18)	13(18)
C(100)	916(144)	330(100)	698(128)	-145(92)	-361(110)	128(93)
O(100)	1886(176)	688(99)	1070(123)	-88(88)	-1003(124)	-1(101)

APPENDIX D

Final fractional atomic coordinates and isotropic temperature factors ($Å^2$) for $[Pt_2(\mu\text{-}S)(CO)(PPh_3)_3Au(PPh_3)]PF_6$ with estimated Standard Deviations in parentheses

Atom	x/a	y/b	x/c	U(iso)
Pt(1)	0.1852(1)	0.4772(1)	0.28427(6)	0.0437
Pt(2)	0.1699(1)	0.5122(1)	0.18683(6)	0.0417
Au(1)	-0.0088(2)	0.6721(1)	0.25449(7)	0.0577
P(1)	-0.0274(13)	0.8384(9)	0.2545(6)	0.0803
P(2)	0.0890(9)	0.5224(8)	0.1110(4)	0.0459
P(3)	0.1113(9)	0.4781(9)	0.3704(4)	0.0503
P(4)	0.3972(10)	0.4378(8)	0.2772(4)	0.0539
S(1)	0.0027(8)	0.5032(7)	0.2529(4)	0.0379
P(6)	0.5000	0.0000	1.0000	0.1134(75)
O(1)	0.4259(34)	0.5352(23)	0.1380(13)	0.0917(100)
F(1)	0.3626(44)	0.0101(34)	1.0298(19)	0.1939(173)
F(2)	0.4216(69)	0.0727(55)	0.9669(30)	0.2889(297)
F(3)	0.4792(67)	0.8915(52)	0.0044(28)	0.2816(288)
F(4)	0.5058(62)	0.0428(53)	1.0542(27)	0.2742(276)
C(1)	0.3305(48)	0.5266(34)	0.1544(19)	0.0797(147)
C(110)	0.0986(53)	0.8732(42)	0.2102(22)	0.1015(172)
C(111)	0.1988(57)	0.8091(43)	0.1976(23)	0.1102(185)
C(112)	0.3125(61)	0.8246(50)	0.1580(26)	0.1306(218)
C(113)	0.3084(64)	0.9180(54)	0.1436(25)	0.1285(219)
C(114)	0.2181(72)	0.9810(52)	0.1496(27)	0.1397(237)
C(115)	0.0921(74)	0.9666(58)	0.1857(31)	0.1646(278)
C(120)	-0.0421(72)	0.8943(48)	0.3164(28)	0.1350(227)
C(121)	0.0799(146)	0.9032(106)	0.3302(62)	0.3160(665)
C(122)	0.0969(140)	0.9401(100)	0.3885(62)	0.2998(615)
C(123)	-0.0529(134)	0.9670(87)	0.4195(47)	0.2368(506)
C(124)	-0.1229(145)	0.9373(113)	0.4057(62)	0.2947(703)
C(125)	-0.1279(84)	0.8705(64)	0.3533(38)	0.1807(314)
C(130)	-0.1558(64)	0.8952(53)	0.2285(28)	0.1309(223)
C(131)	-0.2024(54)	0.8550(41)	0.1914(23)	0.1069(181)
C(132)	-0.3094(57)	0.9027(46)	0.1704(23)	0.1136(191)
C(133)	-0.3603(128)	0.9998(110)	0.1893(55)	0.2861(591)
C(134)	-0.3039(187	1.0574(146)	0.2214(60)	0.3927(940)
C(135)	-0.2197(142)	0.9720(120)	0.2496(56)	0.2987(628)
C(210)	0.1933(20)	0.5715(23)	0.0596(11)	0.0678(129)
C(211)	0.2232(24)	0.6624(23)	0.0682(11)	0.0965(165)
C(212)	0.3104(26)	0.6989(20)	0.0324(14)	0.0985(169)
C(213)	0.3678(22)	0.6443(25)	-0.0120(13)	0.1008(173)
C(214)	0.3388(23)	0.5542(24)	-0.0206(11)	0.0897(157)
C(215)	0.2519(24)	0.5168(19)	0.0150(12)	0.0776(142)
C(220)	-0.0639(24)	0.5898(14)	0.1109(9)	0.0512(111)
C(221)	-0.1630(29)	0.5689(14)	0.1476(9)	0.0584(118)

C(222)	-0.2866(28)	0.6135(17)	0.1446(10)	0.0859(151)
C(223)	-0.3096(28)	0.6779(17)	0.1054(12)	0.0898(157)
C(224)	-0.2100(33)	0.6985(15)	0.0692(10)	0.1067(181)
C(225)	-0.0869(28)	0.6544(15)	0.0720(9)	0.0574(118)
C(230)	0.0830(29)	0.4002(21)	0.0911(5)	0.0605(121)
C(231)	-0.0190(25)	0.3750(24)	0.0740(6)	0.0726(136)
C(232)	-0.0173(30)	0.2783(27)	0.0592(5)	0.0996(170)
C(233)	0.0866(37)	0.2049(23)	0.0613(6)	0.1095(184)
C(234)	0.1891(31)	0.2291(26)	0.0782(7)	0.1210(202)
C(235)	0.1870(27)	0.3261(28)	0.0930(6)	0.0961(166)
C(310)	0.1140(28)	0.3628(21)	0.4032(11)	0.0651(126)
C(311)	0.0260(25)	0.3523(26)	0.4470(12)	0.1020(174)
C(312)	0.033(3)	0.2621(31)	0.4707(11)	0.1374(229)
C(313)	0.1275(34)	0.1833(25)	0.4509(13)	0.1008(171)
C(314)	0.2153(28)	0.1938(24)	0.4073(14)	0.1204(200)
C(315)	0.2088(25)	0.2836(27)	0.3832(10)	0.0894(156)
C(320)	-0.0546(29)	0.5394(24)	0.3902(8)	0.0791(143)
C(321)	-0.0893(39)	0.6287(25)	0.4178(8)	0.1121(188)
C(322)	-0.2154(45)	0.6717(23)	0.4309(8)	0.1436(239)
C(323)	-0.3058(34)	0.6256(29)	0.4168(9)	0.1352(224)
C(324)	-0.2721(34)	0.5366(29)	0.3895(9)	0.1188(199)
C(325)	-0.1453(35)	0.4934(20)	0.3761(7)	0.0746(137)
C(330)	0.1912(15)	0.5475(19)	0.4085(11)	0.0531(113)
C(331)	0.2263(18)	0.6323(21)	0.3867(10)	0.0815(146)
C(332)	0.2927(19)	0.6873(19)	0.4114(14)	0.0981(169)
C(333)	0.3243(17)	0.6578(24)	0.4583(14)	0.1207(201)
C(334)	0.2900(19)	0.5737(25)	0.4803(11)	0.1053(177)
C(335)	0.2236(19)	0.5194(19)	0.4556(12)	0.0864(152)
C(410)	0.4690(11)	0.3623(22)	0.3237(10)	0.0534(113)
C(411)	0.4734(12)	0.4094(21)	0.3696(12)	0.0662(126)
C(412)	0.5091(14)	0.3558(27)	0.4106(11)	0.0879(155)
C(413)	0.5408(13)	0.2546(27)	0.4058(12)	0.1155(193)
C(414)	0.5365(12)	0.2074(21)	0.3599(13)	0.0805(144)
C(415)	0.5006(12)	0.2611(22)	0.3184(11)	0.0614(122)
C(420)	0.4725(30)	0.3578(17)	0.2181(9)	0.0638(125)
C(421)	0.5904(30)	0.3603(19)	0.1899(12)	0.0955(165)
C(422)	0.6393(28)	0.2969(24)	0.1479(12)	0.1083(182)
C(423)	0.5705(35)	0.2314(20)	0.1338(10)	0.1226(203)
C(424)	0.4530(33)	0.2280(18)	0.1613(12)	0.0929(160)
C(425)	0.4046(25)	0.2921(20)	0.2036(11)	0.0748(138)
C(430)	0.4763(28)	0.5390(21)	0.2712(4)	0.0667(128)
C(431)	0.4059(25)	0.6302(25)	0.2637(4)	0.0735(136)
C(432)	0.4542(32)	0.7160(23)	0.2656(4)	0.1054(178)
C(433)	0.5748(33)	0.7102(24)	0.2750(5)	0.0938(163)
C(434)	0.6453(27)	0.6197(27)	0.2824(4)	0.0946(163)
C(435)	0.5967(27)	0.5348(22)	0.2806(4)	0.0690(131)